8-2016

Surface Modifications of Capillary-Channeled Polymer (C-CP) Fiber Stationary Phases for Protein Separations

Liuwei Jiang
Clemson University

SURFACE MODIFICATIONS OF CAPILLARY-CHANNELED POLYMER (C-CP) FIBER STATIONARY PHASES FOR PROTEIN SEPARATIONS

A Dissertation
Presented to
the Graduate School of
Clemson University

In Partial Fulfillment
of the Requirements for the Degree
Doctor of Philosophy
Chemistry

---

by
Liuwei Jiang
August 2016

Accepted by:
R. Kenneth Marcus, Committee Chair
Jeffrey N. Anker
George Chumanov
Philip J. Brown

ABSTRACT

High performance liquid chromatography (HPLC) is one of the most important and commonly used techniques for protein separation and purification. Stationary phase is the most important component of HPLC since it is where the separation takes place. Traditional HPLC columns that are packed with highly porous micro-particular silica beads suffered from several drawbacks, including high column pressure, low stability of stationary phase, peak broadening and tailing. Large amount of research has been done to develop new HPLC stationary phase for protein separation. Capillary-channeled Polymer (C-CP) fibers have been studied as HPLC stationary phase for protein separation in the Marcus research group for years. C-CP fibers are made from melting extrusion of commonly used polymers such as polypropylene (PP), polyester (PET) and polyamide (Nylon). C-CP fibers are 30 – 50 μm in diameter, with 8 capillary channeled running axially along the whole length of the fibers. These capillary channels largely increase the surface area of C-CP fibers for protein interaction. In this dissertation, different surface modification methods, including physical adsorption of lipid tethered ligands on PP fiber, and chemical modifications of PET and nylon fibers, are studied to enhance the protein separation characteristics of C-CP fiber columns, in terms of protein binding selectivity, capacity, recovery yield as well as the resolution of separation.

DEDICATION

I dedicate my dissertation work to my father, who taught me science when I was young and led me to the world of chemistry. I also dedicate this dissertation to my mother for her endless love, support and encouragement.

To all my friends at Clemson, thank you for your friendship and supporting me throughout my graduate school years. I will always appreciate what you have done, especially Yi Jin for helping me learn how to conduct independent scientific research, and Lynn X. Zhang for helping me solving on all kinds of troubles in the lab.

ACKNOWLEDGMENTS

I would like to express my special appreciation and thanks to my current research advisor, Dr. R. Kenneth Marcus, for pulling me out from my darkest days in graduate school, providing me the opportunity to be part of this research group and letting me continue pursuing Ph.D. degree. Since my first day in this group, I have enough freedom to conduct research on the ideas I like and want to try. Thank you for providing me research assistantship and scientific advice during these years.

I would also like to thank my research committee professors, Dr. Jeffrey N. Anker, Dr. George Chumanov and Dr. Philip J. Brown for providing invaluable guidance in my research career.

I would like to acknowledge National Science Foundation, Division of Chemistry for funding support (Grant No. CHE-1307078).

TABLE OF CONTENTS

Page

Table of Contents (Continued) Page

Table of Contents (Continued) Page

LIST OF TABLES

LIST OF FIGURES

List of Figures (Continued)

Figure Page

List of Figures (Continued)

Figure Page

List of Figures (Continued)

Figure Page

List of Figures (Continued)

Figure Page

List of Figures (Continued)

Figure Page

List of Figures (Continued)

Figure Page

CHAPTER I

INTRODUCTION

Introduction to Liquid Chromatography

Chromatography separation is one the most important and commonly used techniques in analytical chemistry. Chromatography was firstly introduced by Russian botanist Mikhail Tswett in the early 1900's to separate the pigments in leaf extracts[1]. Since then, the theory, technique and applications of chromatography have been under tremendous development. As one of the chromatography technique, high performance liquid chromatography (HPLC) was developed from traditional liquid chromatography (LC) and gas chromatography (GC) after 1960's.[2] During that time period, as the applications of GC were limited by the volatility of organic molecules, LC started to draw more and more attention from scientist and instrumentation industry.[3] After the 1970's, with the development of micro particular beads packed columns, high-pressure liquid pumps and highly sensitive detectors, HPLC became the most important separation technique for organic molecules and biomolecules (such as proteins) in pharmaceutical and biotechnology industry.

Protein purification is to isolate one or more than one specific proteins from very complex biological mixture, such as the crude lysis product of cell cultures. Protein purification has been performed for over 200 years.[4] In the

early years of protein purification, the available techniques were very limited. Scientist separated different proteins based on their differences on solubility. Alternating solvent condition, such as adding salts or organic solvents, changing pH of solvents and changing temperature of the solvent system, causes protein precipitating from mixture and leads to isolating of proteins from complex. Nowadays, fractional precipitation methods are still being using in large scale protein purifications for separating gross impurities in cell lysate.

Due to the high resolving power of liquid chromatography, it has become a dominant method for protein purification. In different types of liquid chromatography, column chromatography is the most commonly used chromatography format. In column chromatography, the stationary phase, to which proteins absorb, is packed into a tube. Mobile phases are pumped through stationary phase packed tubing for protein loading and separation.

Liquid Chromatography Modes for Protein Purification

Liquid chromatography separates proteins by taking advantages of their differences in bio-specificity, charges, sizes, hydrophobicity or isoelectric points. Table 1.1 shows examples of properties of proteins and the corresponding chromatography methods.[5]

Table 1.1 Commonly used Liquid chromatography methods

Chromatography methods	Protein property
Hydrophobicity	Reversed phase chromatography (RPC) Hydrophobicity interaction chromatography (HIC)
Charge/Isoelectric point	Ion exchange chromatography (IEX) / Chromatofocusing
Size	Size exclusion chromatography (SEC)
Bio-specificity	Affinity chromatography (AC)
Metal ion binding	Immobilized metal ion affinity chromatography (IMAC)

Ion exchange chromatography (IEX) / Chromatofocusing

Ion exchange chromatography and chromatofocusing separate proteins based on their net charge in a specific environmental condition which is related to the isoelectric point of the protein. Proteins are very complex molecules that have both positive and negative charges due to different amino acid side chains. Positive charges coming from the lysines, histidines, arginines and N-terminal amine group, while negative charges are provided by aspartate acid, glutamic acid and C-terminal carboxylic acid group, depending on the pH of the solvent. Buffer solution are used in ion exchange chromatography to keep a constant pH (or to a specific pH gradient for chromatofocusing) during separation process. The charged amino acid site chains which are exposed on protein surface interact with the charged ligand, ion-exchanger, on stationary phase, leading to

protein retention. The most commonly used elution strategy in ion exchange chromatography is increasing the ionic strength of the buffer by adding salt such as NaCl. The Na^+ (in cation-exchange) or Cl^- (in anion-exchange) ions compete with protein on binding sites on stationary phases. As the concentration of the salt increases, the more weakly charged protein elutes at lower ionic strength and the more strongly charged protein elutes at higher ionic strength, which results in protein separation. Another elution strategy that is used in ion exchange chromatography is by changing the pH of the buffer solution. This method is named “chromatofocusing”. In anion exchange, as pH of buffer decreases, the net charge of the proteins decreases which leads to weaker ionic interaction with stationary phase. The protein with higher pI gets eluted earlier at higher buffer pH and the protein with lower pI gets eluted later at lower buffer pH. In cation exchange, as pH of buffer increases, the net chanrge of the protein decreases. The protein with lower pI gets eluted earlier at lower buffer pH while the protein with higher pI gets eluted later at higher buffer pH. However, real world does not always goes as planned. When buffer pH is close to the pI of a protein, the largely decrease of the protein solubility often cause protein precipitation. What’s more, the elution of proteins results in large change of the buffer pH, which leads to poor separation of proteins. Research has shown that by employing a carefully selected buffer system, with maximum buffering capacity and good linear gradient of pH, higher resolution can be achieved in chromatofocusing, in comparasion to salt gradient separation.

The properties of the ion exchangers on stationary phases largely influence protein separations. Based on the pKa of the ion exchangers, they are divided into 4 categories. They are weak anion exchanger, strong anion exchanger, weak cation exchanger and strong cation exchanger. Strong anion exchangers (quatery ammonium) and strong cation exchangers (such as sulphonate) are the functional groups with pKa values outside of the buffering range of protein separation. The charges of strong anion or cation exchangers do not change as buffer pH changes. To the contrary, weak anion exchangers and weak cation exchangers are the functional groups with pKa inside of the pH buffering ranger of protein separations. Hence, their uses are limited by the pH range of the buffer solutions. The most commonly used weak anion exchanger is tertiary amine and the most commonly used weak cation exchanger is carboxylate. For proteins having very high or very low pI, they can only be separated on strong ion exchangers. On the other hand, weak ion exchange is superior for proteins having high net charges. Due to the decreased ionic interaction, proteins are less likely denatured on weak ion exchangers. Weakly charged impurities can also be easily separated from protein matrix which enhances the separation resolution.

Table 1.2 Common ion exchanger types

Ion exchanger*	Type of exchange	Functional Group	pH range
DEAE	Weak anion	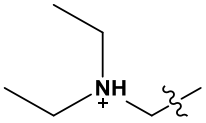	5 – 9
Q	Strong anion	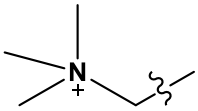	0 – 14
CM	Weak cation	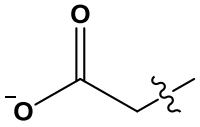	5 – 9
S	Strong cation	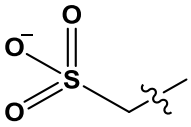	0 – 14

* DEAE: Diethyl-aminoethyl
Q: Quatery ammonium
CM: Carboxymethyl
S: Sulfonate

Proteins interact with ion exchange chromatography stationary phase by ionic interaction. Unwanted hydrophobic interactions between proteins and stationary phase result in mixed-mode interaction, which causes peak tailing and broadening as well as low protein recovery from the stationary phase. Hence, if the supporting material of the stationary phase is hydrophobic, such as polystyrene, sufficient ion exchange ligand coverage on the supporting material is required for high resolution and high recovery protein separation.[6]

Ion exchange chromatography is one of the most powerful techniques for protein separation. It is also the most commonly used chromatography technique

for protein, peptide, nucleic acid and many other biomolecules. Ion exchange is capable of high resolution separation and its capacity for protein binding is very high, comparing to other chromatography methods. Due to the mild conditions used from protein adoption and elution, ion exchange chromatography is considered as a non-denaturing separation where protein retains its native conformation during the separation.

Reversed phase chromatography

Among all kinds of chromatography modes, reversed phase chromatography is the most extensively separation method. Reversed phase separation is used in small organic molecule, amino acids, peptide nucleic acids and protein separations. In reversed phase chromatography, proteins are separated based on the differences of their hydrophobicity. The name “reversed phase” is corresponding to normal phase chromatography in which the analytes are absorbed on stationary phase in an organic solvents and the elution of the analytes is caused by introducing aqueous mobile phase on to stationary phase. In reversed phase chromatography, analytes absorb onto stationary phase in aqueous mobile phase and the elution was performed using organic solvents. Revered phase chromatography was originally developed for small organic molecule separations. Due to its high revolving power, reversed phase separation achieved lots of interest industry and academia.

The most commonly used stationary support is surface modified porous silica beads. Silica based materials are mechanically strong in high pressure

conditions in HPLC and chemically stable in organic solvents. To achieve strong hydrophobic interaction with molecules, the Si-OH in silica surface is usually modified with hydrocarbon chains. The surface modification must cover most of the surface Si-OH groups since any exposed Si-OH group may lead to ionic interaction which may result in peak broadening and tailing. While long hydrocarbon chain (C18) is usually used for small molecule separation, shorter chains (C4 and C8) are used for proteins to avoid too strong hydrophobic interaction between proteins and stationary phase. Polymeric stationary phase such as cross-linked polystyrene (PS), due to its surface hydrophobicity, has also been used for stationary phase in reversed phase protein separation.

Adding organic solvents in mobile phase is used for protein elution in reversed phase. However, the added organic solvents disrupt the inter-peptide chain hydrophobic interactions and the hydrogen binding of amino acid side chains in protein molecule, leading to denaturation of the proteins.[7] Due to this reason, reversed phase chromatography is mainly used for analytical scale protein separation other than large scale protein purification.

Hydrophobicity interaction chromatography

Hydrophobic interaction chromatography separates proteins based reversible interaction of a protein surface and hydrophobic surface of stationary phase surface.[8] Proteins are separated based on the differences of the surface exposed hydrophobic amino acids. Unlike reversed phase chromatography, in hydrophobic interaction chromatography, proteins are loaded on stationary phase

in a buffer solution with high concentration of salts to facilitate the hydrophobic interaction. Protein elution was performed by decreasing the concentration of the salts. As salt concentration decreased, less hydrophobic protein elutes earlier and more hydrophobic protein is more retained.[9]

Normally, amino acid with hydrophobic side chains (such as leucine, isoleucine, valine and phenylalanine) tend to be buried in hydrophobic core of the native protein structure. However, only a small fraction of hydrophobic amino acids can be resided in the core, some of them will also be presented near the protein structure surface. The hydrophobicity of a protein is a result of all surface exposed hydrophobic amino acids. In aqueous environment, the hydrophobic region on a protein surface is covered by an ordered water molecules. These ordered water molecule films result in a decrease in entropy. The hydrophobic region of a protein will associate with the hydrophobic surface of stationary phase in an aqueous solution, in order to minimize the hydrophobic region that is exposed to water molecules. During this process, the ordered water molecules will be released in to bulk water, resulting in an increase of entropy. Hence, this association process is spontaneous and thermodynamically favorable. High concentration of salt ions in aqueous solution associates with the ordered water molecules, and then facilitate the hydrophobic interaction. Ammonium sulfate and sodium sulfate are the most commonly used salts in HIC.[10] The tendency of hydrophobic interaction will decrease as the salt concentration decreases.

The conditions for hydrophobic interaction chromatography are usually the opposite to those in ion exchange chromatography. Hydrophobic interaction chromatography can be performed after proteins are separated from ion exchange chromatography since they are eluted in high salt concentration buffers. The proteins are then eluted from hydrophobic interaction chromatography by decreasing salt concentration, resulting to proteins in low salt concentration buffer which is ready for next purification without further buffer exchange. Just like ion exchange chromatography, hydrophobic interaction chromatography is considered as a mild, non-denaturing method for protein separation. During the separation, the native conformation of the protein structure is mostly retained. In summary, hydrophobic interaction is a very powerful separation technique with high recovery yield in protein purification.

Affinity chromatography

Proteins are the macromolecules that have biological functions. Due to the biological function and the structural complexity of proteins, they often show very specific interaction with other molecules. These molecules, named protein ligands, can be small molecules such as inhibitors and substrates of proteins. Macromolecular ligands, such as peptides and other proteins, can also be ligands for proteins. The specific binding is contributed from a combination of different types of inter molecular interaction, such as hydrophobic interaction, electrostatic interaction, hydrogen bond and Van der Waals forces. In affinity chromatography, the target protein in a matrix is specifically captured by the

affinity ligand on stationary phase, leave impurity molecules passing through. Changing buffer condition results in reduced specific binding which causes the target protein being eluted from stationary phase.[11]

The ideal supporting material for affinity chromatography stationary phase should have several characteristics. First of all, the supporting material should have appropriate reactive sites on its surface that allows the affinity ligand being covalently (or non-covalently) attached. Secondly, the base material should be chemically and mechanically stable during ligand attaching reaction and affinity separation process. Thirdly, the supporting material should be relatively hydrophilic and neutral charged to minimize non-specific protein interactions, such as hydrophobic interaction and ionic interaction, during the separation. At last, the supporting material should have large surface area for maximum protein binding capacity but with larges pores for fast protein mass transfer. Commonly used base material for affinity stationary phases are agarose, dextrans, polyacrylamide, cellulose and porous silica. Some of the surface modified hydrophobic polymers, such as polystyrene and polyamide, are also used for affinity stationary phase if their surfaces are fully covered by hydrophilic spacers and ligands.

The ligand for affinity separation must be able to form a specific but reversible binding with target proteins. The binding should be strong enough during the separation process. However, the binding should also be easy to be disassociated in the elution process without irreversible affecting the ligand and

target protein. Synthetic small molecular ligands are chemically stable and inexpensive. However, the problem for small molecular ligand is lack of specificity. Macromolecular ligands such as proteins usually provide higher selectivity but they are less stable and more expensive than small molecular ligand. Protein ligand may be irreversibly denatured during the separation by elution solution which could further increase the cost of the separation. Hence, there is a need to develop low-cost affinity stationary phases with protein ligands

A hydrophilic spacer arm/linker is usually used for connecting ligand with stationary phase surface. The spacer arms not only decrease non-specific protein binding by hydrophilic blocking, but also reduce the steric hindrance for protein binding to ligands. Spacer arms are usually indispensable for small molecular ligands, but not always necessary for macromolecular ligands. Attaching spacer arms must not affect either binding affinity or specificity of the ligands. Affinity ligands are attached with reactive groups on stationary surface or on spacer arms through chemical reactions. The residue unreacted groups are then capped with small molecules such as ethanolamine. The primary groups of ethanolamine has good reactivity toward the reactive groups while leaving free hydroxyl group of ethanolamine as hydrophilic barrier, reducing the non-specific interaction to target proteins. Commonly used strategy for coupling affinity ligands are showed in table 1.3.

Table 1.3 Commonly used chemistry for affinity ligand coupling

Reagent Name	Reactive group on stationary phase or spacer	Reactive group on ligand	Coupled ligand
CNBr	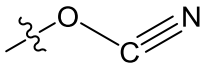	Ligand – NH_2	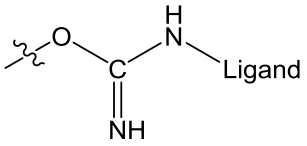
Epoxide	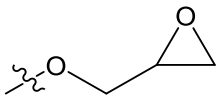	Ligand – NH_2	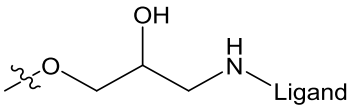
N-hydroxy succinimide ester (NHS-ester)	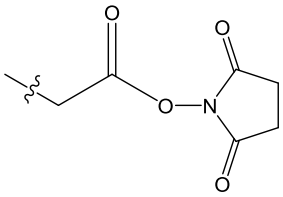	Ligand – NH_2	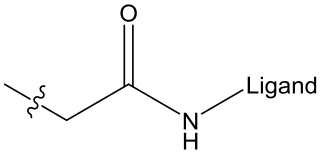
N, N'-carbonyl diimidazole (CDI)	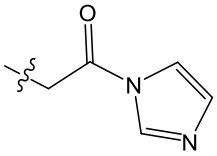	Ligand – NH_2	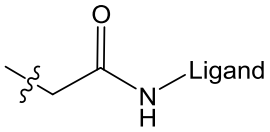

Affinity chromatography is a simple isolation step to capture target protein from matrix. Due to the high specificity, affinity chromatography is capable of separating a desired protein that is presented at a very low concentration in a very complex matrix. Affinity chromatography is a very important technique for large scale protein purification. In Immunoglobulin G (IgG) downstream processing, the first chromatography purification is using protein A column as the affinity stationary phase to selectively capture IgG from complex cell lysate.

Immobilized metal affinity chromatography

Immobilized metal affinity chromatography (IMAC) takes advantage of the weak coordinate bonds between some amino acids (mainly histidine residues) on proteins and the immobilized metal on stationary phases.[12] It is considered as a pseudo-affinity chromatography since it is not based on bio-specific interactions.

The interaction in IMAC is formed between metal ions and electron donor groups on protein surface. Histidine residue, with electron donors on imidazole ring form coordinate bonds with transitional metal, shows the strongest interaction among all amino acids. Hence, the interaction in IMAC is based on the availability of the surface histidine residues on protein surface. The most commonly used chelators for immobilizing metal ions are imino diacetate (IDA) and nitrotriacetate acid (NTA). The most commonly used metal ions in IMAC are divalent ions such as Fe^{2+}, Co^{2+}, Ni^{2+} and Cu^{2+}. Some trivalent ions are sometimes used, such as Fe^{3+} and Al^{3+}.

The buffer used for protein adsorption in IMAC is always contains relatively high concentration of salt such as 0.1 – 1 M NaCl to minimized the non-specific ionic interaction between proteins and chelators. Proteins are eluted by decreasing buffer pH to 4 -5 to protonate the imidazole of histidine residue. For proteins that are not stable at low pH, buffers with high concentration of imidazole are used to displace proteins from immobilized metal ions. Buffers with ethylenediaminetetraacetic acid (EDTA) can also be used to disrupt the binding between metal ions and chelaters to release proteins from stationary phase. However, IMAC column must be recharged with metal ions after EDTA elution.

Compares to affinity separation, IMAC is not considered as highly specific, but only moderately specific. However, high protein loading capacity, mild elution condition and low cost make IMAC a very useful technique in protein purifications.

Size exclusion chromatography

Size exclusion chromatography (SEC) is sometimes also referred to gel permeation chromatography (GPC) or gel filtration. It is a different process than all chromatography previously discussed. All previously discussed chromatography relies on the interaction of protein and stationary phases and the different retention degree of proteins based on some of their properties. However, proteins are separated in size exclusion chromatography according to their sizes and shapes. The stationary phases for size exclusion chromatography are highly porous material that has different sizes of pores. Protein mixture enter size exclusion chromatography will need to pass through the porous material. The smaller proteins have higher chance to enter more pores or channels while larger sized protein, for steric reasons, will morel likely be excluded from the pores and then rapidly pass through size exclusion chromatography column. The sizes of proteins refer to their hydrodynamic volumes. Molecular weight and shape of proteins together determine the hydrodynamic volumes of proteins. More linear proteins have larger hydrodynamic volumes than more globular proteins.[13]

The buffers that are used in size exclusion chromatography is changing during the separation process. Appropriate buffers should be chosen to minimized any interactions between proteins and stationary phases so that the

separation is only dominated by protein sizes. The buffer also needs to have a pH and ionic strength which keeps proteins in their native conformation.

Compares to other chromatography method, size exclusion chromatography is the one with the lowest capacity, the least resolution and the most dilution of the samples. However, size exclusion chromatography is frequently used since it provides different selectivity from other chromatography methods. In IgG purification, size exclusion chromatography is used to separate the protein fragments, native state and aggregations.

Separation Theory

The goal of chromatography is to separate all the components in a sample mixture. A good separation refers to each components are completely separated in a short time. When a mixture sample is injected into a chromatography column at t = 0 min, some components do not have any interaction with the stationary phase so that they just pass through the column and being detected by detector. Due to the volume of injection valve, tubing and column void volumes, non-retained component will be eluted and detected at t_0, corresponding to the flow rate and mobile phase. Component A and B are retained in the column and eluted from the column at retention time t_R(A) and t_R(B), respectively. The peak width, W, refers to the distance between intersections of two peak side tangents with baseline. $W_{0.5}$ is the peak width at the half peak height.

The capacity factor k' is the ratio of the time that an analyte stays in stationary phase to the time that it stays in mobile phase (equation 1.1). Capacity factor of zero means this analyte is non-retained on stationary phase. Different analytes have different strength of interaction with stationary phase thus they stay on stationary phase for different time. If two analytes have larger different capacity factor, they can be distinguished by the chromatography column better. The selectivity factor α describes the relative capacity factor of two analytes (equation 1.2).

Capacity factor $$k' = \frac{t_R - t_0}{t_0}$$ (equation 1.1)

Selectivity factor $$\alpha = \frac{k'_B}{k'_A} = \frac{t_R(A) - t_0}{t_R(B) - t_0}$$ (equation 1.2)

A large selectivity does not always result in two analytes being completely separated. The resolution of a separation describes how well the two analytes are separated (equation 1.3)

Resolution $$R = \frac{2[t_R(A) - t_R(B)]}{W_A + W_B} = \frac{1.18[t_R(A) - t_R(B)]}{W_{0.5}(A) + W_{0.5}(B)}$$ (equation 1.3)

If R = 1.5, the two peaks only overlapped by 0.3%. If R = 1 the two peaks overlapped by 4%. A high resolution is desired and can be optimized by improving the selectivity and minimizing peak broadening.

Peak broadening during chromatography process is unavoidable. The efficiency of a separation is the key factor on peak broadening. If peaks have

large selectivity factor but they are too broad, the overlapping of them will result in low resolution. The efficiency or the peak broadening of a column is described as a concept of plate height equivalent to a theoretical plate, H (equation 1.4). For a column with length of L, the efficiency can also be expressed by plate number, N (equation 1.5). Smaller plate height equivalent to a theoretical plate (H) or larger plate number (N) mean the column has higher efficiency and less peak broadening.

Plate height $\mathrm{H} = 16(\frac{t_R}{W})^2 = 5.54(\frac{t_R}{W_{0.5}})^2$ (equation 1.4)

Plate number $\mathrm{N} = \frac{L}{N}$ (equation 1.5)

In 1956, J. J. Van Deemter described an equation with three parameters that affects peak broadening.[14] This equation is later named van Deemter Equation (equation 1.6) which is also valid for gas chromatography and capillary electrophoresis.

Van Deemter Equation $H = A + {}^{B}/_{u} + Cu$ (equation 1.6)

In van Deemter equation, the height of theoretical plate is depended on three terms: A, B/u and Cu. The first term related to band broadening is Eddy Diffusion. This term describes the variations of mobile phase or analyte flow path in stationary phase. The variations are due to inhomogeneous column packing or the irregular shape of the packing material. A term is independent from the flow

rate and constant for a given column. The second term, Bu, describes diffusion of the analytes in every direction due to the concentration variances at the edges of the peak band. Bu is called longitudinal diffusion and it is reversely proportional to the flow rate. The third term, Cu, describes the resistance of the mass transfer between mobile phase and stationary phase. Cu term is proportional to the flow rate.

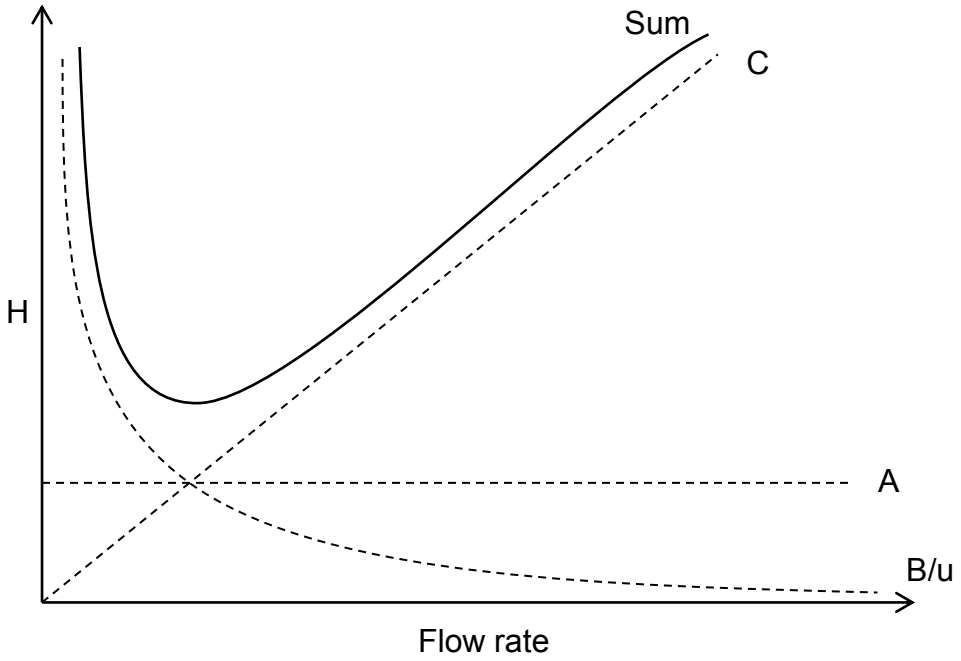

Figure 1.1 Van Deemter plot

By plotting H as a function of u results in van Deemter plot. Running separation at too low or too high flow rate will both result in increased H and decreased column efficiency. For a given column and a molecule, there is an optimum flow rate that gives the lowest H on van Deemter plot.

Stationary Phases for Protein Separations

Stationary phase is probably the most important component in HPLC. Stationary phase is where the separation takes place. Traditional HPLC columns are packed with highly porous micro-particular bead with extremely large surface area for interaction with analytes. Silica is a material that has high mechanical stability that can withstand high pressure, highly controllable size and porosity that gives uniform packing, and the ease of surface chemistry for ligand attaching. Silica based porous bead packed column are excellent for small organic molecule separation. However, their applications on protein separations are suffered by several drawbacks.

The major disadvantages of using porous silica for protein separation include low chemical stability, limited pH range and slow mass transfer. Silica material is not stable under slightly high pH or very low pH conditions. The normal working pH range for silica beads is between 2 to 8.[15] Some of the chromatography conditions used for protein separation, such as ion exchange chromatography, affinity chromatography, require high or low pH buffer for optimized separation or protein elution. When mobile phase pH is lower than 2 or higher than 8, silica material will be deteriorated by losing surface ligand and the column performance will be decreased (figure 1.2).

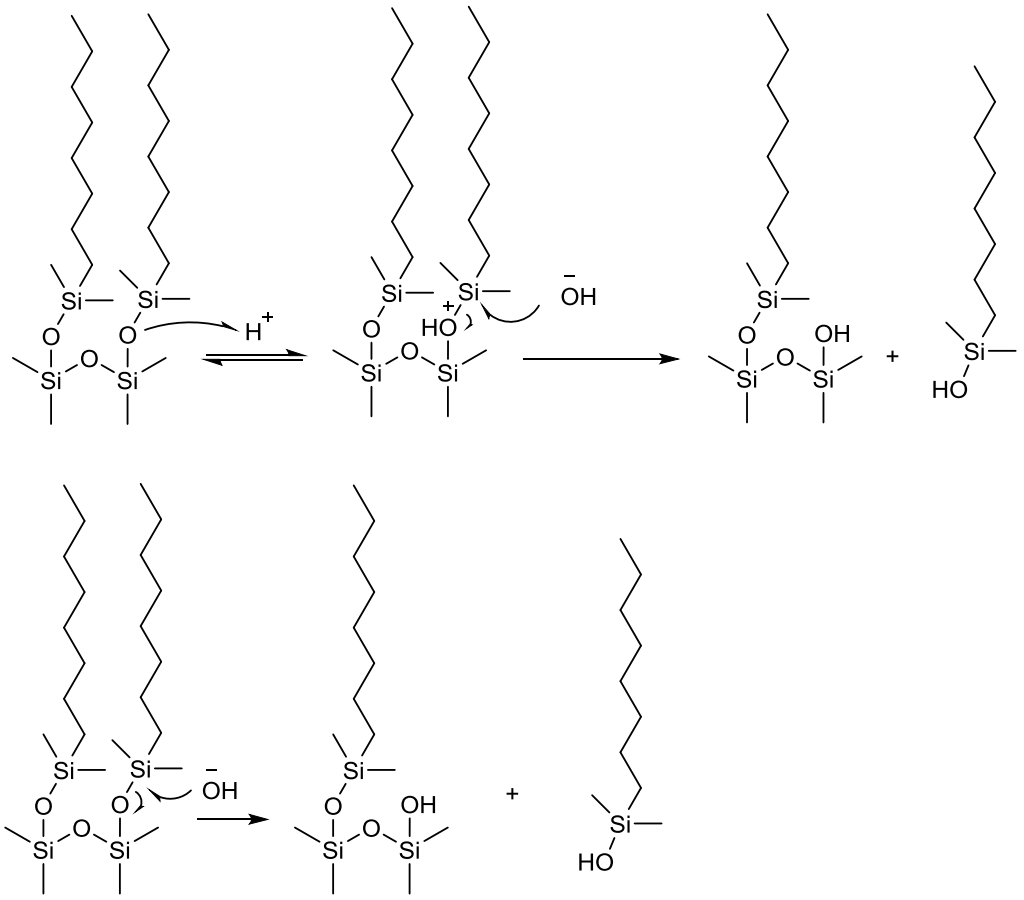

Figure 1.2 C8 silica hydrolysis in acidic and basic conditions

The other disadvantage of using porous silica for protein separation is the slow mass transfer (C term in van Deemter plot). Due to the large size of protein molecule, they diffuse in and out of the pores very slowly, resulting in peak tailing and broadening (figure 1.3).

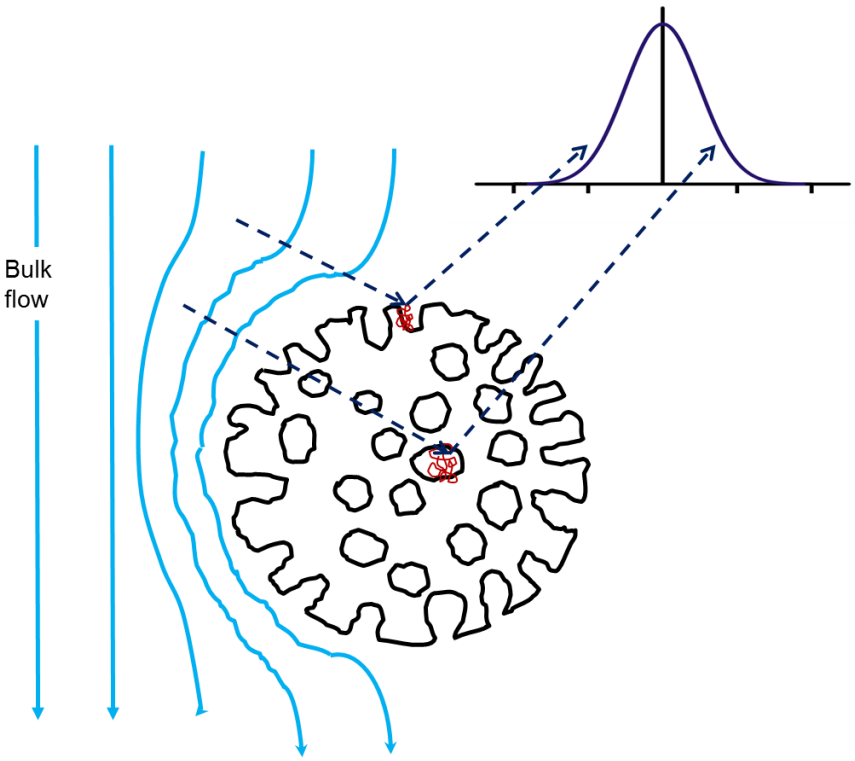

Figure 1.3 Peak broadening due to diffusing of proteins into and out of pores

New technologies, such as using high purity silica and extensive end-capping of the silica surface, have been developed to improve the stability of silica stationary phase in acidic and basic condition.[16] New types of silica stationary phase can be used at pH 1 – 11 for prolonged time.[17] Research has been focused on reducing the diffusing distance of protein to improve the column efficiency. Poroshell silica particle which has a non-porous core and a thin porous shell (5 – 10 nm) has been developed for fast protein separations.[18,19]

Non-porous silica bead has also been used for protein separation due to its non-porous surface.[20-22]

Polymer based stationary phases, such as cross-linked polystyrene and polyacrylamide, are chemically stable that can withstand the whole pH range used in protein separations.[23,24] They can also be surface modified with ligands to affect the surface chemistry for different types of chromatography uses. Polymer bead with large pores and non-porous beads have been used for protein separation. Monolithic column which has large through pores and channels are shown to be capable of fast protein separation with low column pressure.

Capillary-Channeled Polymer (C-CP) fibers have been studied as stationary phase for HPLC and solid phase extraction in the Marcus laboratory for year.[25-31] C-CP fibers are made from melt-extrusion of commonly used polymers, such as polypropylene (PP), polyamide (Nylon) and polyester (PET). They have nominal diameters of 30 – 50 μm, with 8 capillary channels running axially along the entire length of the fibers. Due to these capillary channels, C-CP fibers have 3 × surface areas comparing to the circular shaped fibers with the same diameter. C-CP columns are packed by pulling C-CP fibers through tubing. When C-CP fibers are packed, the capillary channels allow efficient liquid transportation. C-CP columns are highly permeable. A 20 cm long, 2.1 mm I.D. C-CP column can be run at 10 mL min^{-1} with column pressure less than 1500 psi. The surfaces of C-CP fibers are non-porous comparing to the size of proteins. As a result, C-CP fibers have very low mass transfer resistance of proteins. Fast

protein separation can be realized on C-CP columns under high flow rates and low column pressure.

Summary

Capillary-channeled polymer (C-CP) fibers have been studied as a stationary phase for liquid chromatography in recent years. The low-cost of these materials bodes well for preparative-scale protein separation. C-CP fiber-packed columns show other advantages over traditional microsphere packed columns toward macromolecule separations, including high permeability, low mass transfer resistance and very high protein throughput and yield in preparative scenarios. However, low equilibrium protein binding capacity may limit the potential application of the C-CP fibers.

In chapter II, lipid tethered ligand (LTL) was synthesized for PP C-CP fiber surface modification. PP C-CP fibers have been used in this laboratory as stationary phases for high performance liquid chromatography and solid phase extraction of proteins. Greater selectivity has been realized through the functionalization of the PP fibers through the physical adsorption of commercially available head group-modified poly(ethylene glycol) lipids (PEG-lipids), where the head group is chosen to affect affinity separations. We refer to this general surface modification methodology as *lipid tethered ligands* (LTLs). In this study, LTLs were synthesized by solid phase synthesis. In comparison to the

commercial PEG-lipids, the synthesized LTLs contain no chemically labile phosphate groups. Instead of an ester linkage in the commercial lipids, amide functionality was used in the synthesized LTLs to attach the lipids and ligands. By use of fluorescent imaging of FITC-labeled LTLs, the synthesized LTL was shown to be superior to the commercial LTL in terms of the adsorption efficiency to PP C-CP fibers, the resistance to solvent wash from the PP C-CP fibers, and their chemical stability under acidic, neutral and basic conditions. The PP C-CP fibers functionalized with a synthesized LTL that was biotinylated at the head group are shown to be capable of capturing streptavidin from *E. coli* cell lysate more efficiently than the PP C-CP fibers functionalized with the commercial biotinylated PEG-lipid. The functionalization of PP C-CP fibers with the synthesized LTLs is a simple, but highly efficient, method to generate novel stationary phases with a variety of functionalities for solid phase extraction and liquid chromatography. Results were published in the Analyst (Jiang, L.; Schadock-Hewitt, A. J.; Zhang, L. X.; Marcus, R. K. *Analyst* **2015**, *140*, 1523.), and reproduced with permission from The Royal Society of Chemistry.

In chapter III, native PET fibers were treated with ethylenediamine (EDA) to generate primary amine groups on the fiber surface, allowing for the subsequent covalent attachment of ligands. The ninhydrin test for primary amines revealed surface densities of 13.9 – 60.0 mol m^{-2} for PET fibers exposed for periods of 3 – 12 minutes. Here, 8-amino-3,6-dioxaoctanoic acid was linked to the EDA treated PET fiber surface as a hydrophilic spacer and then D-biotin was

attached on the end of the spacer as an affinity ligand. The streptavidin binding capacity and binding homogeneity were studied on the biotin functionalized PET C-CP fiber microbore column. The selectivity of the biotin surface functionalization was assessed by spiking lysate with Texas Red-labeled streptavidin and enhanced green fluorescent protein. Greater than 99% of selectivity was realized. This ligand coupling strategy from standard solid phase peptide synthesis applied in stationary phase functionalization creates great potential for PET C-CP fiber packed HPLC columns to perform various chromatographic separations. Results were published in the Analytical and Bioanalytical Chemistry (Jiang, L.; Marcus, R. K. *Anal. Bioanal. Chem.* **2015**, *407*, 939.), and reprinted with permission from Springer-Verlag GmbH.

In chapter IV, surface modified PET C-CP fibers were evaluated for the anion exchange separation of proteins. The native PET C-CP fiber were aminated using polyethylenimine (PEI) followed by a 1,4-butanediol diglycidyl ether (BUDGE) cross-linking step. Subsequent PEI/BUDGE treatments can be employed to further develop the polyamine layer on the fiber surfaces. The PEI densities of the modified fibers were quantified through the ninhydrin reaction, yielding values of 0.43 – 0.89 μmol g^{-1}. The surface modification impact on column permeability was found to be 0.66×10^{-11} – 1.33×10^{-11} m^2, depending on the modification time and conditions. The dynamic binding capacities of the modified fiber media were determined to be 1.99 – 8.54 mg mL^{-1} bed volume, at linear velocities of 88 – 438 cm min^{-1} using bovine serum albumin as the model

protein. It was found that increasing the mobile phase linear velocity (up to 438 cm min^{-1}) had no effect on the separation quality for a synthetic protein mixture, reflecting the lack of van Deemter C-term effects for the C-CP fiber phase. The low-cost, easy modification method and the capability of fast protein separation illustrate great potential in the use of PEI/BUDGE-modified PET C-CP fibers for high-throughput protein separation and downstream processing. Results were published in the Journal of Chromatography A (Jiang, L.; Jin, Y.; Marcus, R. K. *J. Chromatogr. A* **2015**, *1410*, 200.), and reprinted with permission from Elsevier B.V.

In chapter V, the three amine-based C-CP fiber phases (native nylon 6, PEI modified PET, PEI/BUDGE modified PET) are compared in terms of protein separation characteristics. Each phase was shown to be able to separate a BSA/hemoglobin/lysozyme mixture at high mobile phase linear velocity (~70 mm s^{-1}) but with different elution characteristics. This study provides important fundamental understanding for the development of surface-modified C-CP fiber media for protein separation. Results were published in the Analytical and Bioanalytical Chemistry (Jiang, L.; Marcus, R. K. *Anal. Bioanal. Chem.* **2016**, *408*, 1373.), and reprinted with permission from Springer-Verlag GmbH.

In chapter VI, a weak cation exchange liquid chromatography stationary phase (nylon-COOH) was prepared by grafting polyacrylic acid on to native nylon 6 capillary-channeled polymer (C-CP) fibers via a microwave-assisted radical polymerization. The C-CP fiber surfaces were characterized by attenuated total

reflection (ATR) infrared spectroscopy and scanning electron microscope (SEM). The anticipated carbonyl peak at 1722.9 cm^{-1} was found on the nylon-COOH fibers, but was not found on the native fiber, indicating the presence of the polyacrylic acid on nylon fibers after grafting. The nylon-COOH phase showed a ~12X increase in lysozyme dynamic binding capacity (~12 mg mL^{-1}) when compared to the native fiber phase (~1 mg mL^{-1}). The loading capacity of the nylon-COOH phase is nearly independent of the lysozyme loading concentration (0.05 – 1 mg mL^{-1}) and the mobile phase linear velocity (7.3 – 73 mm s^{-1}). The reproducibility of the lysozyme recovery from the nylon-COOH (RSD = 0.3 %, n = 10) and the batch-to-batch variability in the functionalization (RSD = 3%, n = 5) were also investigated, revealing very high levels of consistency. Fast baseline separations of myoglobin, α-chymotrypsinogen A, cytochrome c and lysozyme were achieved using the nylon-COOH column. It was found that a 5X increase in the mobile phase linear velocity (7.3-to-36.5 mm s^{-1}) had little effect on the separation resolution. In totality, the results suggest that this nylon-COOH fiber phase holds promise towards high-throughput preparative and analytical-scale protein separations. The microwave-assisted grafting polymerization has great potential as a generalized surface modification methodology across the applications of C-CP fibers.

In chapter VII, native nylon C-CP fibers were modified with 2-acrylamido-2-methylpropanesulfonic acid (AMPS) via the microwave-assisted grafting polymerization to affect a strong cation exchange stationary phase. Various

concentrations of AMPS and the initiator potassium persulfate (KPS) were used in the modifications, with the resultant nylon-SO_3H fiber columns characterized by attenuated total reflection-Fourier transform infrared spectroscopy (ATR-FTIR), scanning electron microscopy (SEM) and acid-base titrations. The cation exchange ligand densities on the modified fibers (-SO_3H) were determined to be 50 – 317 μmol g^{-1}, in comparison to the cation (-COOH) density of 28 μmol g^{-1} on native fibers. The modified fiber phase showed increased lysozyme dynamic loading capacities (up to ~13 mg mL^{-1} bed volume) at a linear velocity of ~90 cm min^{-1}, while native fiber phase showed only ~1 mg mL^{-1} lysozyme loading capacity. Fast (30 s to 3 min) gradient separations of α-chymotrypsinogen A and lysozyme were achieved on nylon-SO_3H columns, with the separation resolution and peak capacity characterized. The efficiency of surface re-equilibration was probed with an eye toward using the phase as the second dimension in comprehensive two-dimensional liquid chromatography (2D-LC). The results indicate that this nylon-SO_3H fiber phase has a good deal of potential for use in high-throughput analytical and preparative protein separations.

References

[1] TSWETT, M. **1906**.

[2] Karger, B. L. *Journal of chemical education* **1997**, *74*, 45.

[3] Henry, R. A. **2009**.

[4] Scopes, R. K. *Protein purification: principles and practice*; Springer Science & Business Media, 2013.

[5] Janson, J.-C. *Protein purification: principles, high resolution methods, and applications*; John Wiley & Sons, 2012; Vol. 151.

[6] Regnier, F. E. *Analytical biochemistry* **1982**, *126*, 1-7.

[7] Benedek, K.; Dong, S.; Karger, B. *Journal of Chromatography A* **1984**, *317*, 227-243.

[8] Queiroz, J.; Tomaz, C.; Cabral, J. *Journal of Biotechnology* **2001**, *87*, 143-159.

[9] Machold, C.; Deinhofer, K.; Hahn, R.; Jungbauer, A. *Journal of Chromatography A* **2002**, *972*, 3-19.

[10] Hahn, R.; Deinhofer, K.; Machold, C.; Jungbauer, A. *Journal of Chromatography B* **2003**, *790*, 99-114.

[11] Lee, W.-C.; Lee, K. H. *Analytical biochemistry* **2004**, *324*, 1-10.

[12] Porath, J. *TrAC Trends in Analytical Chemistry* **1988**, *7*, 254-259.

[13] Štulík, K.; Pacáková, V.; Tichá, M. *Journal of biochemical and biophysical methods* **2003**, *56*, 1-13.

[14] Van Deemter, J. J.; Zuiderweg, F.; Klinkenberg, A. v. *Chemical Engineering Science* **1956**, *5*, 271-289.

[15] Kirkland, J. *Journal of chromatographic science* **1996**, *34*, 309-313.

[16] Kirkland, J.; Henderson, J.; DeStefano, J.; Van Straten, M.; Claessens, H. *Journal of Chromatography A* **1997**, *762*, 97-112.

[17] Kirkland, J. J.; Henderson, J. W.; DeStefano, J. J.; van Straten, M. A.; Claessens, H. A. *Journal of Chromatography A* **1997**, *762*, 97-112.

[18] Kirkland, J. *Analytical chemistry* **1992**, *64*, 1239-1245.

[19] Kirkland, J.; Truszkowski, F.; Dilks, C.; Engel, G. *Journal of Chromatography A* **2000**, *890*, 3-13.

[20] MacNair, J. E.; Opiteck, G. J.; Jorgenson, J. W.; Moseley, M. A. *Rapid communications in mass spectrometry* **1997**, *11*, 1279-1285.

[21] Jungbauer, A. *Journal of Chromatography A* **2005**, *1065*, 3-12.

[22] Lee, W.-C. *Journal of Chromatography B: Biomedical Sciences and Applications* **1997**, *699*, 29-45.

[23] Svec, F. *Journal of separation science* **2004**, *27*, 1419-1430.

[24] Hemström, P.; Nordborg, A.; Irgum, K.; Svec, F.; Fréchet, J. M. *Journal of separation science* **2006**, *29*, 25-32.

[25] Marcus, R. K.; Davis, W. C.; Knippel, B. C.; LaMotte, L.; Hill, T. A.; Perahia, D.; Jenkins, J. D. *J. Chromatogr. A* **2003**, *986*, 17-31.

[26] Nelson, D. K.; Marcus, R. K. *J. Chromatogr. Sci.* **2003**, *41*, 475-479.

[27] Nelson, D. M.; Marcus, R. K. *Anal. Chem.* **2006**, *78*, 8462-8471.

[28] Marcus, R. K. *J. Sep. Sci.* **2008**, *31*, 1923-1935.

[29] Marcus, R. K. *J. Sep. Sci.* **2009**, *32*, 695-705.

[30] Burdette, C. Q.; Marcus, R. K. *Analyst* **2013**, *138*, 1098-1106.

[31] Jiang, L.; Schadock-Hewitt, A. J.; Zhang, L. X.; Marcus, R. K. *Analyst* **2015**, *140*, 1523-1534.

CHAPTER II

EVALUATION OF SYNTHESIZED LIPID TETHERED LIGANDS FOR SURFACE FUNCTIONALIZATION OF POLYPROPYLENE CAPILLARY-CHANNELED POLYMER FIBER STATIONARY PHASES

Introduction

High performance liquid chromatography (HPLC) is one of the most often used techniques in chemical and biological analysis for the separation of desired analytes, including small molecules to large proteins, from complex media. Ultimately, the most essential part of an HPLC system is the support/stationary phase, determining what can be separated, the mechanism by which the separation occurs, and the efficiency of the process.[1-4] The kinetic and thermodynamic aspects of a separation are controlled by the physical (i.e., support) and chemical (i.e., stationary phase) attributes of the phase, respectively. The principle differences between the support phases employed for small molecule or bio-macromolecule separations lies in the diffusional characteristics of the solutes, where the large radii and low mobile phase diffusivities of proteins and the like preclude the use of the high porosity, small diameter particles now common in small molecule separations. For this reason, there is a great deal of effort directed at the use of silica-based materials that have a certain level of porosity in the near surface region of the particles.[5-7] In such systems, higher throughputs can be achieved, though naturally at some sacrifice to loading capacities.

Monolithic materials are employed in bio-macromolecule separations as a means of improving throughput, as the macroporous/mesoporous structures act in concert to affect systems that are under convective diffusion transport conditions.[8,9] Monoliths based on silica and polymer materials are employed, with the latter providing a level of greater synthetic flexibility in terms of phase chemistry and reduced non-specific binding.[10] Indeed, as one considers preparative protein separations, polymeric stationary/support phases are the predominant column packing materials based on their material costs, chemical and physical robustness, and overall throughput and yield characteristics.[11,12] In this regard, the most common phases are either carbohydrate (e.g. agarose-based) or synthetic polymer (e.g. polystyrene-based) beads or a variety of membrane formats. To this list of formats, one can include natural and synthetic polymer fibers, a format that has a long history of investigation. Fibrous phases have a number of interesting attributes that could be used to advantage in high speed and preparative protein separation scenarios,[13,14] and so continue to be of interest as new technologies evolve.

This laboratory is developing capillary-channeled polymer (C-CP) fibers as stationary/support phases for HPLC and solid phase extraction (SPE) separations of proteins.[15-20] C-CP fibers are melt-extruded from commodity polymers, such as polypropylene (PP), polyamide (nylon 6), and poly (ethylene terephthalate) (PET).[21] They have eight capillary channels extending the entire length of the fibers. When packed in a column, C-CP fibers self-align and yield a

monolith like structure with 1-5 μm capillary channels for fluidic flow. As a result, C-CP fiber packed columns exhibit excellent fluid transport properties. The fibers have a limited porosity (~4 nm) on the size scale of proteins,[22] hence high speed (>100 mm s^{-1}) protein separations can be realized without suffering from van Deemter C-term broadening.[23,24] C-CP fiber-packed HPLC columns are believed to be a particular promising choice for preparative protein purification, exhibiting throughput and yield characteristics that rival more traditional formats.[25]

The three base polymers used in C-CP fibers used to date provide a good deal of flexibility in terms of their native surface chemistries and the modes of separation that can be affected. Polypropylene is least chemically versatile, as its entirely aliphatic structure is only amenable to hydrophobicity-based (e.g. reversed phase) separations, which are not ideal in the preparative realm. That said, PP C-CP fibers have shown excellent performance as SPE media for proteins in complex media including buffers, urine, and saliva, with detection via UV absorbance, and electrospray and matrix-assisted laser desorption/ionization mass spectrometries (ESI and MALDI-MS).[18,19,26,27] In process terms, though, it is stable at a wide range of chemical conditions, including strong acidic and strong basic conditions.[28] To further expand the potential of PP C-CP fiber columns in protein separations, surface functionalization of the fibers is necessary. Chemical modification usually results in physical damage of polymer fibers,[29-35] which make the fibers easily breakable in the column or during the

column packing process. On the other hand, a physical modification method, taking advantage of the highly hydrophobic nature of PP would not compromise the integrity of the fibers and the column transport characteristics. To this end, recombinant protein A has been simply adsorbed on PP C-CP fiber to affect the affinity capture and recovery of immunoglobulin G (IgG) with high specificity and yield.[36] The protein A-PP fiber interaction was found to be quite robust towards typical affinity column regeneration methods, including exposure to 10 mM NaOH/1 M NaCl solutions. Those initial studies are being extended to preparative scale columns for the isolation of IgG from *E. coli* fermentation broths.

Recently, PP C-CP fibers were functionalized by the physical adsorption of commercial head group-functionalized PEG-lipids, an approach termed lipid tethered ligands (LTLs), to yield an analyte-specific polymer surface.[37] The adsorption is driven by the strong hydrophobic interaction between the lipid tail of LTLs (Fig. 1) and the PP surface. The poly(ethylene glycol) (PEG) chain in the LTL is a spacer that extends the functional ligand from the hydrophobic PP surface to the hydrophilic mobile phase. After functionalization with a biotinylated PEG-lipid, the PP C-CP fiber packed SPE tips were shown to be capable of affinity capture of Texas Red labeled streptavidin (SAv-TR) from mCitrine-spiked *E. coli* cell lysate with high specificity. The PEG-lipids are commercially available with a variety of functional ligands (R-groups in Fig. 1), which could be used to offer PP C-CP fiber surfaces of different functionality. Subsequent studies have shown that the surface loading of the PEG-lipids is very efficient and very robust

towards any solvents imaginable in biomacromolecule separations.[38] This simple LTL functionalization method opens the door for the use of PP C-CP fibers as stationary phase for affinity separations. Indeed, it is believed that this methodology could be practically applied to virtually any hydrophobic surface.

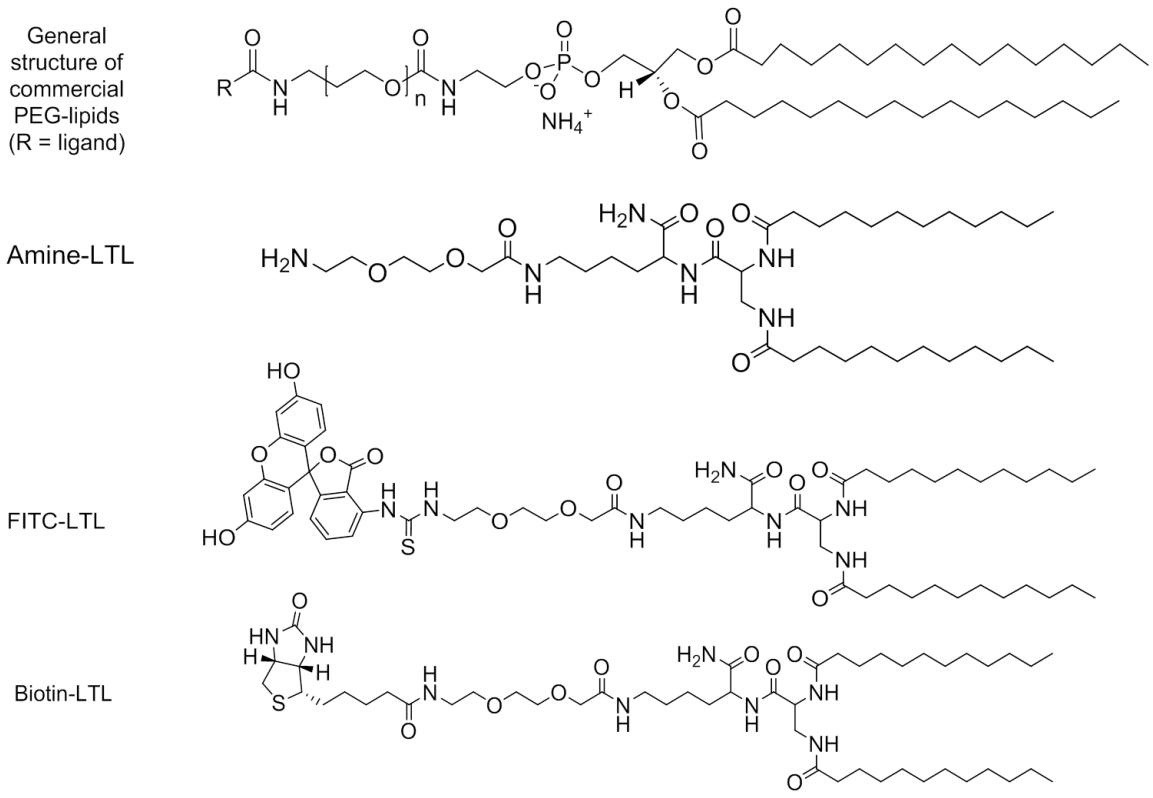

Figure 2.1 Structures of the commercial (PEG-lipid) and synthesized LTLs. R group represents the ligand of the commercial PEG-Lipids. The MW of the commercial FITC-PEG-Lipid is 5000. The MW of the commercial Biotin-PEG-Lipid is 2000.

In this study, LTLs were synthesized using a straightforward solid phase synthesis approach. In comparison to the commercial PEG-lipids, the synthesized LTLs contain no phosphate groups. Organic phosphate groups are usually labile towards hydrolysis in aqueous conditions,[39-41] decoupling the

PEG-R group from the lipid tail, and thus the LTL would lose its functionality. The lipid tails and the spacers in the synthesized LTLs are connected via an amide group that is more chemically stable than the ester groups used in commercial LTLs. Using a FITC-labeled LTL (FITC-LTL) as a model system, the synthesized version showed far greater surface adsorption densities and greater resistance to chemical washes than the commercial LTL (PEG-lipid). In solution, the synthesized LTL was more chemically stable than the commercial LTL across acidic, neutral, and basic conditions. Synthesized biotin-LTL functionalized PP C-CP fibers were shown to be capable of selectively capturing SAv-TR from an *E. coli* cell lysate with higher efficiency than fibers that were functionalized with the commercial biotin-PEG-lipid. It is believed that the use of the phosphate group-free lipid offers a number of advantages over the commercial PEG-lipids, with the general synthetic strategy allowing for a high degree of flexibility in choice of lipid tail, the ability to insert linker (e.g., PEG) groups of various lengths and composition, and the potential R-group entities. Furthermore, it is envisioned that the LTL methodology may hold potential in the modification of any number of hydrophobic surfaces, such as the polystyrene-divinylbenzene (PS-DVB) media commonly used as chromatographic supports.

Experimental Methods

Chemicals and materials

Unless otherwise specified, chemicals were purchased from commercially available sources and used without further purification. The commercial biotin-PEG-lipid, 1,2-distearoyl-sn-glycero-3-phosphoethanolamine-N-[biotinyl (polyethylene glycol)-2000], was purchased from Avanti Polar Lipids, Inc. (Alabaster, AL). The commercial FITC-PEG-lipid, 1,2-distearoyl-sn-glycero-3-phosphoethanolamine-N-[fluorescein isothiocyanate (polyethylene glycol)-5000], was purchased from Nanocs Inc. (Boston, MA). Rink Amide MBHA resins (100-200 mesh, 0.59 mmol/g loading) were obtained from AnaSpec (Fremont, CA). Dichloromethane (DCM), methanol, hydrazine (65%), trifluoroacetic acid (TFA), diethyl ether, dimethylformamide (DMF), dimethyl sulfoxide (DMSO), N,N-diisopropylethylamine (DIPEA), and piperidine were purchased from VWR (Atlanta, GA). Lauric acid, fluorescein isothiocyanate isomer I (FITC, purity ≥90%) was purchased from Sigma-Aldrich (St. Louis, MO). Fmoc-lys(ivDde)-OH, Fmoc-Dap(Fmoc)-OH, Fmoc-8-amino-3,6-dioxaoctanoic acid, 1-[bis-(dimethylamino)-methylene]-5-chloro-1H-benzotriazolium hexafluorophosphate 3-oxide (HCTU) and D-biotin were purchased from Chem-Impex International, Inc. (Wood Dale, IL). Ethanol was purchased from EMD (HPLC grade, 190 proof, Billerica, MA). Streptavidin-Texas Red (SAv-TR) was obtained from SouthernBiotech (Birmingham, AL). Enhanced green fluorescent protein (sequence for EGFP found in p3051 retrovirus vector was amplified by PCR) was provided by the group of G. Chumanov (Dept. of Chemistry, Clemson University, Clemson, SC). The cell lysate of *E. coli* (NEB 5-alpha E. coli) was obtained from

the group of K. Christensen (Dept. of Chemistry, Clemson University, Clemson, SC). *E.coli* was grown in 1 L of Luria-Bertani broth at 37 ºC to an O.D. of 0.8. The cells were pelletized at 13,000x g for 10 min. The cell pellet was then re-suspended in PBS buffer. This cell slurry was then disrupted and centrifuged at 30,000x g for 30 minutes to pellet out cell debris and produce a cleared lysate. Deionized water (DI-H_2O) was prepared by a Milli-Q water system. PBS buffer was prepared by dissolving NaCl (8.0g), KCl (0.2g), Na_2HPO_4 (1.44g) and KH_2PO_4 (0.24g) in DI-H_2O to a final volume of 1.0 L. The pH of PBS buffer was adjusted to 7.4. PBST buffer was prepared by adding 1.0 mL of Tween-20 in 1.0 L of PBS buffer (pH 7.4).

Preparation of PP C-CP fiber SPE tips

The method for packing C-CP fiber microbore columns and creation of micropipette tips for solid phase extraction was previously described by Marcus and co-workers.[18,19] PP C-CP fibers were obtained from Clemson University, School of Materials Science and Engineering on spools measuring more than 1000 m in length,[21] with fiber sizes equivalent to 3 denier per filament (dpf). In this study, 470 PP fibers were pulled through 0.8 mm i.d. fluorinated ethylene propylene (FEP, Cole Palmer, Vernon Hills, IL) tubing to form the microbore columns. After packing, the columns were connected to a Dionex Ultimate 3000 HPLC system (LPG-3400SD pump, WPS-3000TSL autosampler, VWD-3400 RS UV–Vis absorbance detector, Thermo Fisher Scientific Inc., Sunnyvale, CA), washed with ACN and then DI-H_2O until a stable baseline was observed on the

UV-Vis absorbance detector (216 nm). Once assembled and cleaned, columns could be stored under ambient conditions until being converted to tip format. After cleaning, the column was cut into segments with 10 mm of fibers and additional 4-6 mm empty gap. The end with empty gap of column segment was press-fit on to the end of the commercial low-retention micropipette tip (Redi-tip, Fisher Scientific, Pittsburgh, PA) to make into an SPE tip as described previously.

Solid phase synthesis of lipid tethered ligands

As depicted in Figure 2, the LTLs were synthesized via standard solid phase peptide synthesis (SPPS) protocol with fluorenylmethyloxycarbonyl (Fmoc) and 1-(4,4-dimethyl-2,6-dioxocyclohex-1-ylidene)isovalery (ivDde) as the orthogonal protecting groups.[42,43] Developed more than half of a century ago, SPPS is capable of assembling a large number of different ligand moieties via the amide linkage.[42-48] All raw materials used in the synthesis of LTLs are commercially available. Choosing SPPS as the synthesis strategy makes the synthesis and the purification process much easier, thus reducing the cost associated with LTL production. O-(1H-6-Chlorobenzotriazole-1-yl)-1,1,3,3-tetramethyluronium hexafluorophosphate (HCTU) was used as the coupling reagent as it has been reported to be nontoxic, nonirritating, noncorrosive, and capable of fast coupling in SPPS in comparison to other coupling reagents.[49] The multifunctional Fmoc-NH-PEG_2-COOH was chosen as a spacer due to its inexpensiveness. This hydrophilic spacer between the lipid tails and the functional ligands of the LTLs facilitates the ligand-analyte interactions in

solvents. While the present system uses two PEG groups, this number can be tailored for specific applications. Lauric acid was used as the lipid tail because longer lipid acids were insoluble in the reaction solvent or crashed out of solution after HCTU activation. The basic structure of the LTLs, with a primary amine as the ligand (amine-LTL), was synthesized and characterized by ESI-MS and ^{1}H NMR. (The relevant spectra are included in Electronic Supplementary Information.) The amine-LTL is readily converted into other R-group species. A FITC labeled LTL (FITC-LTL) was synthesized and used as a model LTL to study the adsorption of LTLs on PP C-CP fibers. A biotinylated LTL (biotin-LTL) was synthesized and used to functionalize PP C-CP fibers as a demonstration of affinity capture, in this case of streptavidin.

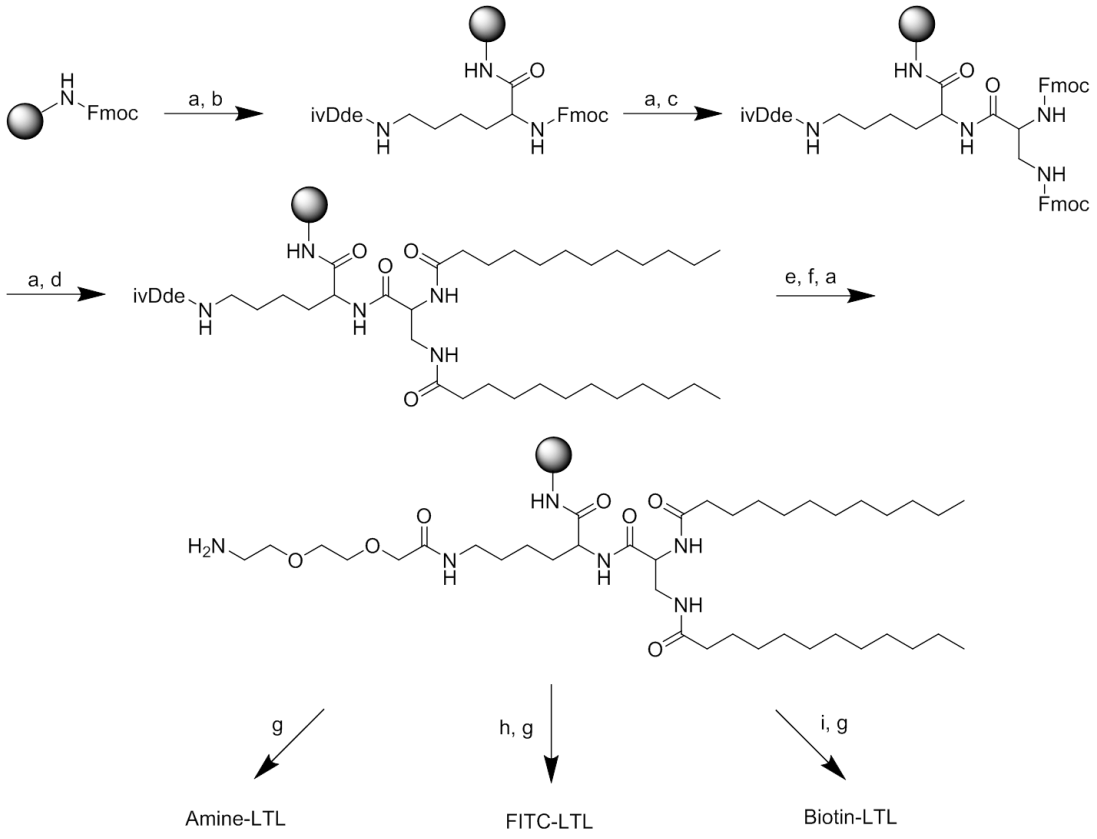

Figure 2.2 Solid phase synthesis scheme of LTLs. Reagents and conditions: (a) 25% piperidine in DMF, 10 min × 2; (b) Fmoc-lys(ivDde)-OH, HCTU, DIPEA, DMF, 1h; (c) Fmoc-Dap(Fmoc)-OH, HCTU, DIPEA, DMF, 1h; (d) Lauric acid, HCTU, DIPEA, DMF, 1h; (e) 2% hydrazine in DMF, 15 min × 5; (f) Fmoc-8-amino-3,6-dioxaoctanoic acid, HCTU, DIPEA, DMF, 1h; (g) 88/5/5/2 TFA/H_2O/phenol/TIPS, 2h; (h) FITC, DIPEA, DMF, 12h; (i) D-biotin, HCTU, DIPEA, DMF, 12h.

Synthesis of amine-LTL

Rink amide MBHA resins (19.9 mg) with 0.51 mmol g^{-1} of loading were swollen in DMF (2 mL, 2 × 10 min.) with stirring. The resins were de-protected by stirring with 25% piperidine in DMF (2 mL, 2 × 10 min). Fmoc-Lys(ivDde)-OH (0.4 M in DMF, 5 equiv., in comparison to the loading of the resins) were then

coupled to the resins in DMF in the presence of HCTU (5 equiv.) and DIPEA (10 equiv.) for 2 h. The resins were washed extensively with DMF (1 mL × 4) between reactions. After coupling, the resins were treated with 25% piperidine in DMF (2 mL, 2 × 10 min) to remove Fmoc protection. Fmoc-Dap(Fmoc)-OH (0.4 M in DMF, 5 equiv.) were then coupled to the resins in DMF in the presence of HCTU (5 equiv.) and DIPEA (10 equiv.) for 2 h followed by treatment with 25% piperidine in DMF (2 mL, 2 × 10 min). A DMF solution of lauric acid (0.4 M, 5 equiv.), HCTU (5 equiv.) and DIPEA (10 equiv.) was then stirred with the resins for 2 h to introduce the lipid tail moieties. The 1-(4,4-Dimethyl-2,6-dioxocyclohex-1-ylidene)-3-methylbutyl (ivDde) group on the side chain of lysine was removed by treatment with 2% hydrazine in DMF (2 mL, 5 × 15 min). A DMF solution of Fmoc-8-amino-3,6-dioxaoctanoic acid (0.4 M, 5 equiv) and HCTU (5 equiv.) and DIPEA (10 equiv.) was mixed with the resins for 2h. The Fmoc on the amine group of spacer was removed by 25% piperidine treatment (2 mL, 2 × 10 min) to yield the desired amine-LTL, on-resin.

The resins with the amine-LTL attached to the surface were washed extensively with DMF (1 mL × 4), methanol (1 mL × 4) and DCM (1 mL × 4). After drying in vacuum for 2h, the resin was stirred in 1 mL of 90/10 TFA/DI-H_2O for 2h. The mixture was filtered to remove the resins. The filtrate was mixed with 10 mL of ice-cold diethyl ether, forming a white precipitate. The mixture suspensions were kept in ice for 10 min to maximize the precipitation. The white precipitates were collected after centrifugation and dried in vacuum for 6h to

afford the amine-LTL as a white, wax like solid with 60% overall yield. NMR spectra were recorded on a Bruker Avance-500 spectrometer. FT-IR (cm^{-1}): 3398, 3283 (N–H stretch), 2919, 2849 (C–H stretch, alkane), 1675, 1649, 1622 (C=O stretch), 1547 (N–H bend), 835, 800 (N–H wag), 720 (C–H rock). ^{1}H NMR (500 MHz, DMSO) δ 7.87 (t, *J* = 8.4 Hz, 3H), 7.83 – 7.73 (m, 3H), 7.32 (s, 1H), 7.11 (s, 1H), 4.32 – 4.25 (m, 1H), 4.13 – 4.08 (m, 1H), 3.88 (s, 2H), 3.60 (s, 6H), 3.43 – 3.35 (m, 1H), 3.24 – 3.15 (m, 1H), 3.12 – 3.03 (m, 2H), 3.03 – 2.93 (m, 2H), 2.16 – 1.99 (m, 4H), 1.66 (s, 1H), 1.55 – 1.43 (m, 5H), 1.42 – 1.36 (m, 2H), 1.23 (s, 34H), 0.85 (t, *J* = 6.8 Hz, 6H). Electrospray ionization (ESI) mass spectra were recorded using a Thermo Finnigan LCQ Advantage Max Mass Spectrometer. The resulting mass spectrum displayed a base peak at m/z = 741.57 Da, which compares very well with the calculated protonated molecule weight ($[M+H]^{+}$) of the desired product ($C_{39}H_{77}N_6O_7$) of m/z = 741.58.

Synthesis of biotin-LTL

5 equiv. of D-biotin (in comparison to the loading of the resins) were dissolved in a minimal volume of 50/50 DMF/DMSO to form a saturated D-biotin solution. 5 equiv. of HCTU and 10 equiv. of DIPEA were then added into the solution and mixed. The solution was added to the amine-LTL resins and was stirred for 12h to yield the biotin-LTL on-resin. The product was then cleaved from the resin as described above. The biotin-LTL was obtained as white, wax like solid with 50% yield. FT-IR (cm^{-1}): 3282 (N–H stretch), 2923, 2853 (C–H stretch, alkane), 1675, 1649, 1624 (C=O stretch), 1549 (N–H bend). ^{1}H NMR

(500 MHz, DMSO) δ 7.94 – 7.79 (m, 4H), 7.69 (t, *J* = 5.5 Hz, 1H), 7.35 (s, 1H), 7.11 (s, 1H), 6.45 (s, 1H), 4.37 – 4.21 (m, 2H), 4.18 – 4.05 (m, 2H), 3.86 (s, 2H), 3.56 (d, *J* = 3.1 Hz, 4H), 3.45 – 3.36 (m, 3H), 3.27 – 3.14 (m, 3H), 3.14 – 3.02 (m, 3H), 2.82 (dd, *J* = 12.4, 4.9 Hz, 1H), 2.62 – 2.55 (m, 1H), 2.19 – 1.96 (m, 6H), 1.71 – 1.56 (m, 2H), 1.55 – 1.43 (m, 8H), 1.42 – 1.36 (m, 2H), 1.33 – 1.17 (m, 36H), 0.86 (t, *J* = 6.6 Hz, 6H). The resulting ESI mass spectrum displayed a base peak at m/z = 967.55 Da, which compares very well with the calculated protonated molecule weight ($[M+H]^+$) of the desired product ($C_{49}H_{91}N_8O_9S$) of m/z = 967.66 Da.

Synthesis of FITC-LTL

3 equiv. of FITC (purity 90%) (in comparison to the loading of the resins), were dissolved in a minimal volume of DMF to form a saturated FITC solution. 6 equiv. of DIPEA were then added into the solution and mixed. The solution was mixed with the amine-LTL resins and stirred for 12h to afford the FITC-LTL on-resin. The product was then cleaved from the resin as described above. After cleavage, a wax like solid was isolated with 42% yield. Due to the impurities present in the commercial FITC (~10 %), NMR characterization of FITC-LTL was not attempted. FT-IR (cm^{-1}): 3280 (N–H stretch), 2922, 2854 (C–H stretch, alkane), 1674, 1645, 1625 (C=O stretch), 1541 (N–H bend), 850 (=C–H oop bending). The resulting ESI mass spectrum displayed a base peak at m/z = 1130.51 Da, which compares very well with the calculated protonated molecule weight ($[M+H]^+$) of the desired product ($C_{60}H_{88}N_7O_{12}S$) of m/z = 1130.62 Da.

LTL functionalization and fluorescence imaging of PP C-CP fiber SPE tips

The synthesized and commercial (PEG-lipid) LTL solutions were prepared in 50% ethanol to the desired concentrations (5 g mL^{-1} or 30 g mL^{-1}). Each PP C-CP fiber SPE tip was washed with 1.0 mL of 50% ethanol (~200 x column volume) at 3000 rpm for 5 min on a centrifuge (Symphony 4417, VWR international, Radnor, PA). 1.0 mL of the LTL solutions were then passed through the tips at the same centrifuge speed. After LTL functionalization, all tips were washed with 1.0 mL of 50% ethanol to remove un-adsorbed LTL prior to further experiments. Fluorescence data and images were generated on an Olympus IX71, 2×/0.08 UPlanFI (infinity corrected) objective (Olympus, Center Valley, PA). Fluorescence excitation was achieved by a Xe arc lamp with filters (excitation/emission: 494 nm/525 nm for FITC-LTL, 575 nm/624 nm for SAv-TR, Chroma, Bellows Falls, VT). The fluorescence images were captured by an Ocra-ER (Hamamatsu) CCD camera. The fluorescence data was processed using Slidebook 5.0 (Denver, CO).

Robustness of LTL-modified surfaces

After functionalization with synthesized or commercial FITC-LTL, PP C-CP fiber SPE tips were washed with 3.0 mL (600 column volumes) of “wash solvents” (PBS buffer solution, 0.1% Tween-20 solution or 50% acetonitrile solution). After washing, all tips were conditioned with 1.0 mL of 50% ethanol solution containing 0.2% triethylamine, as this was shown to minimize changes in the FITC fluorescence yields due to “wash solvent” residues on the tips (*i. e.*, inorganic

salts, Tween-20 or acetonitrile). Fluorescence imaging was performed on the solvent-washed tips, and for tips through which FITC was passed and native un-functionalized tips, which were used as controls. The fluorescence intensity of the challenged tips was normalized to the native tips and the percentage of fluorescence retention reported. All experiments were performed in triplicate.

Chemical stability of LTLs

The synthesized and commercial FITC-LTL were prepared in 50% ethanol solutions containing 100 mM HCl, 10 µM HCl, 10 µM NaOH, 100 mM NaOH, to final LTL concentrations of 4.4 µM. A 4.4 µM solution of each LTL in 50% aqueous ethanol was also prepared as a test solution. The test solutions were stored in a dark box at room temperature. Fluorescence measurements were made of each test solution during the course of the incubation as a monitor of the possible degradation of the FITC tags. The LTL functionalization of C-CP fiber SPE tips was performed with each test solution after 1h, 4h, 8h, 16h, 24h and 48h incubation times. Fluorescence imaging was subsequently performed using freshly-made synthesized and commercial FITC-LTL-functionalized tips as controls. The fluorescence intensity of the challenged-LTL tips was normalized to tips created from fresh LTLs in the challenge solvents and the percentage of fluorescence retention reported. All experiments were performed in triplicate.

Capture of streptavidin using biotin-LTL functionalized PP C-CP fiber tips.

The PP C-CP fiber tips were functionalized with the synthesized or the commercial biotin-LTL following the general functionalization procedure described above. After the functionalization, each tip was washed with 1.0 mL of PBST buffer. 1.0 mL of SAv-Tr (5.0 μg mL^{-1}) in PBST buffer or SAv-TR (0.5 μg mL^{-1}) and EGFP (0.5 μg mL^{-1}) -spiked *E. coli* cell lysate was then passed through each tip. Before fluorescence imaging, the tips were washed with 1.0 mL of PBST buffer to remove loosely adsorbed (non-captured) SAv-TR or EGFP from the fiber surfaces.

Results and Discussions

The studies described here probe a number of different aspects between the commercially available PEG-lipid LTLs and the LTLs synthesized in this laboratory. As described above, the predominate driving force for this effort was to generate LTLs which would presumably be more robust than PEG-lipids, eliminating the phosphate group as a potential source of chemical instability and degradation. Thus, use of the same R-groups, yet having or not having the phosphate group is investigated. A secondary, yet very important aspect is the ability to choose the length of the PEG linker unit between the adsorbed lipid portion of the LTL and the reactive R-group. In this particular study, the length of the linker in the synthesized version of the LTLs is set at two ethylene oxide units, while the commercial versions extend up to weight equivalents of ~5000 Da. While it is well known that tether lengths are very important in providing efficient ligand-target coupling, with surface-bound ligands usually being poor performers,

long tethers limit the overall ligand densities that can be created due to crowding effects. Use of the short linkers for the synthetic LTLs versus the long ones of the commercial PEG-lipids provides contrast in terms of surface loading and capture efficiency.

Adsorption of FITC-LTLs on to PP C-CP fibers

PP C-CP fibers were functionalized with the FITC-LTLs, the commercial PEG-lipid and the synthesized lipid, respectively, in an SPE tip format to reduce the amount of LTL used in the experiments and to be suitable for fluorescence imaging. Figure 3 depicts representative fluorescent images of the two LTLS at initial solute concentrations of 5 and 30 g mL^{-1}. The associated bar graphs provide quantitative figures as well as the relative responses for FITC exposed to native PP fibers and the amine-LTL without FITC labeling, which are used as control specimens. It is clear from the images that the synthesized FITC-LTL functionalized PP C-CP fibers yields a stronger fluorescence response (~17X) than the commercial FITC-LTL functionalized PP C-CP fibers when the concentrations of the LTL solutions were 5 g mL^{-1}. (The synthesized amine-LTL showed no fluorescence response (as expected), while the exposure of FITC to bare PP C-CP fibers reflects some degree of dye molecule adsorption.) Of course, the more relevant point of comparison is on an equimolar basis. To that end, an increase in the commercial LTL solution concentration to 30 g mL^{-1} allows a direct comparison to the 5 g mL^{-1} synthetic LTL, at a value of 4.4 M. On this basis, the relative fluorescence yield of the synthesized LTL is still ~9X

greater. Given the fact that the fluorescent quantum yield between the two LTLs is equivalent, this implies that an approximately one order of magnitude greater ligand density is achieved with the synthetic LTL. As the lipid tails of the two LTLs are very similar, one would expect no real difference in the binding affinities or crowding at the fiber surface level.[38,50] Therefore, the differences in the densities observed here are attributed to crowding of the PEG linker units in the near surface regions for the commercial LTL. An approach to some level of surface saturation is evident when increasing the concentrations of both LTL solutions by a factor of 6, where the fluorescence on the synthetic FITC-LTL fibers only increased by ~3X, while the fluorescence on the commercial FITC-LTL fibers increased by less than 2X. It cannot be denied that there may also be kinetic limitations to the surface adsorption in the flow-through micropipette tip loading. As the surface densities increase, the mass transport of the hydrophobic tails toward the surface will become impeded, limiting the amount of adsorption in the ~1 min transient of the solution through the fiber tips.

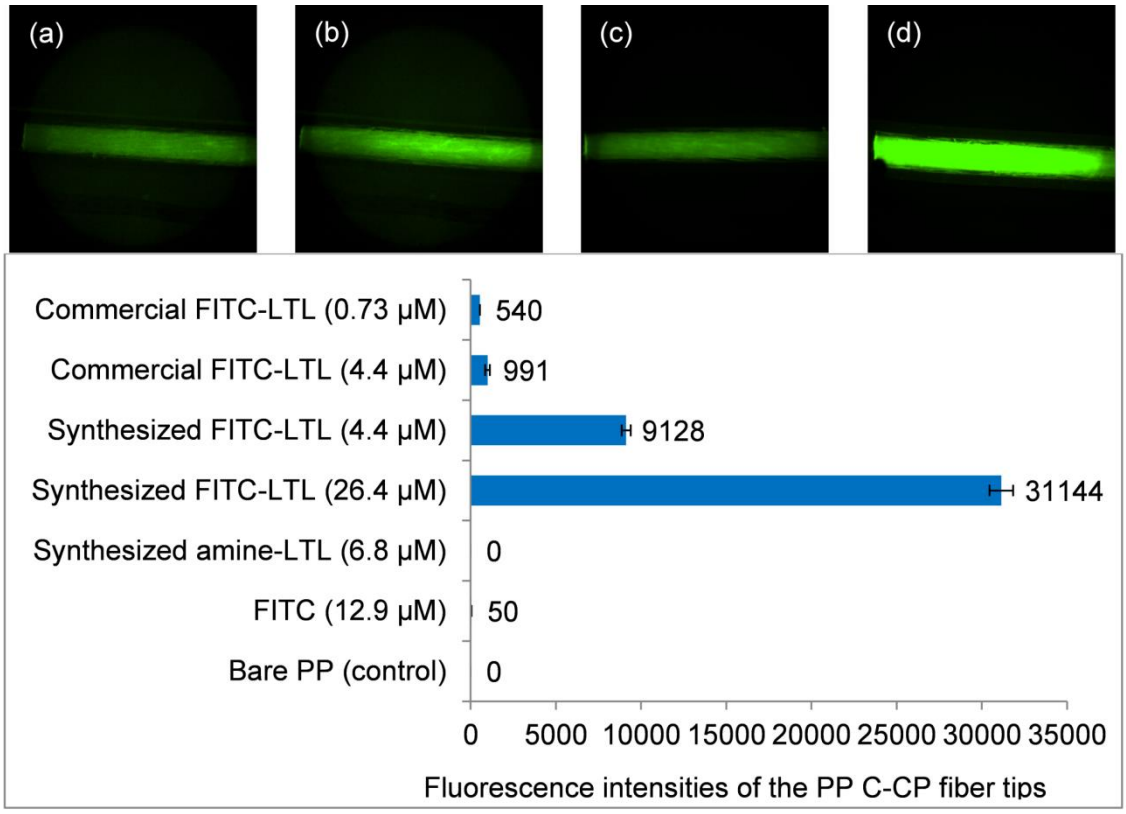

Figure 2.3 Fluorescence images of PP C-CP fiber tips functionalized with: (a) commercial FITC-LTL (5 g mL^{-1}, 0.73 M); (b) commercial FITC-LTL (30 g mL^{-1}, 4.4 M); (c) synthesized FITC-LTL (5 g mL^{-1}, 4.4 M). (d) synthesized FITC-LTL (30 g mL^{-1}, 26.4 M); All images were normalized to fluorescence counts of (a) and (b), 500-2000; (c) and (d) 500-20000 for display.

Robustness of LTL-modified surfaces

One of the primary concerns for any sort of surface modification proposed for stationary phases in SPE or HPLC applications is the lifetime of the ligand under conditions that would be typical of practical applications, i.e. exposure to common mobile phase and column regeneration media. Previous studies had shown that the commercial PEG-lipid LTL was quite robust with respect to

exposure to a wide variety of chromatographic solvents, ranging from the aqueous to mixed-organic phases.[38] Following fiber functionalization with the commercial and synthesized FITC-LTLs at the same molar concentration (4.4 μM), the PP C-CP SPE tips were washed with approximately 600 tip (bed) volumes (i.e., 3 mL) of either PBS buffer or 0.1% Tween-20 solution, and then fluorescently imaged to assess the overall retention of the FITC-labeled ligands (Fig. 4). This number of bed volumes would be the equivalent of between 50 – 100 separation cycles in an HPLC column application. PBS buffer is representative of a very common matrix employed in the processing of biomacromolecules, while Tween-20 is often employed in the course of affinity-based separations to minimize non-specific binding. After the PBS buffer wash, the fluorescence on the commercial FITC-LTL-modified fibers was reduced by about 40%, while the fluorescence on the synthetic FITC-LTL fibers remained mostly un-changed (< 10% lost). The 0.1% Tween-20 solution wash more challenging, removing about 60% of the commercial FITC-LTL and about 20% of the synthesized FITC-LTL from the PP C-CP fiber surfaces. The increased loss of the PEG-lipid (and to a lesser extent the synthetic LTL) may be a result of the structural similarity to the Tween-20 detergent molecule, making them particularly soluble or causing a competitive binding situation. The final test of robustness, exposure to 50:50 ACN: H_2O, results in the loss of approximately half of the synthesized and commercial FITC-LTLs from the PP C-CP fiber surfaces. To be clear, this is an extreme test as this solvent would not be used in biomolecule

separations. In this case, though, it is clear that solubilization of the lipid from the PP matrix is affected. The results of these tests suggest that the synthesized LTL presents a more robust situation in comparison to the commercial LTL-functionalized PP C-CP fibers.

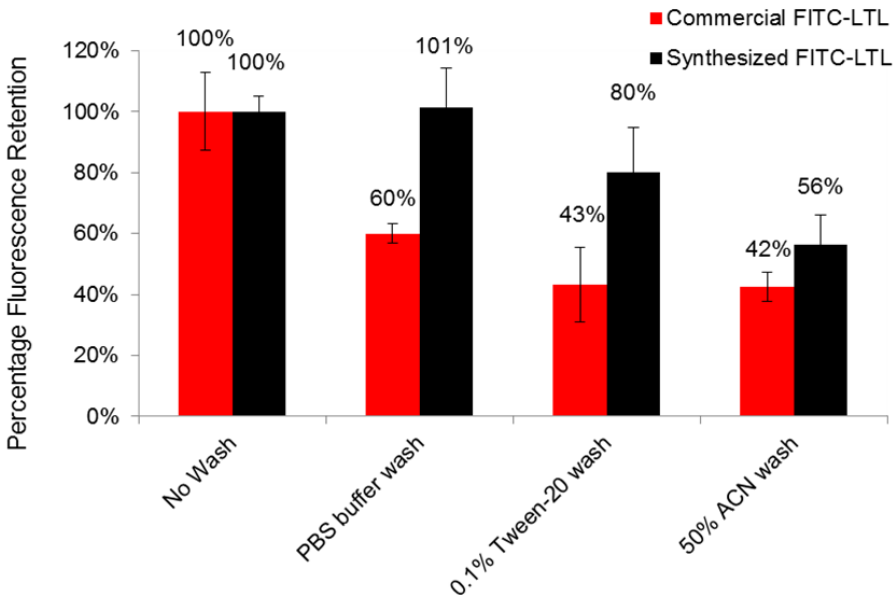

Figure 2.4 Average percentile fluorescence of the FITC-LTL functionalized PP C-CP fiber tips after solvent wash. LTL solutions used for functionalization: commercial FITC-LTL (30 g mL^{-1}, 4.4 M); synthesized FITC-LTL (5 g mL^{-1}, 4.4 M).

Chemical stability of LTLs

While LTLs are usually stored as solid at –20 °C, their chemical stabilities in the solution phase at room temperature (i.e., normal LC operation conditions) must be evaluated. Different from the previous section, the experiments here are designed to assess the robustness of the molecules themselves. Using the generic PEG-lipid in Fig. 1 as a reference, chemical degradation, resulting in loss

of function as a ligand system, can occur at a few key parts of the molecule. Specifically, there can be loss of the active R-group though the decomposition of the thiourea bond of the FITC to the terminus of the tether,[51] hydrolysis occurring at the phosphate group[39-41], and decomposition at the ester linkages to the lipid tails. In the case of the synthetic LTLs, there is no phosphate group and the ester linkages are replaced by more robust amides, which should pay benefits in terms of chemical stability. The FITC-LTL test solutions were prepared in neutral, acidic and basic solvent conditions to a final LTL concentration of 4.4 μM. The test solutions were stored in a dark box at room temperature. After 1h, 4h, 16h, 24h and 48h, PP C-CP fiber SPE tips were functionalized with the test solutions and the fluorescence from the fibers imaged. For each fluorescence image, PP C-CP fibers were functionalized with freshly-made FITC-LTL solutions containing the same LTL and solvent, were used as controls. All tips (test tips and control tips) were conditioned with 0.2% triethylamine prior to fluorescence imaging. The fluorescence intensity of the challenged tips was normalized to the fresh-solution tips and the percentage of fluorescence retention reported.

The on-fiber FITC-LTL fluorescence responses are presented in Fig. 5 for each of the challenge solution compositions. Although the fluorescence intensities of each test solution were different, they did not change significantly (< 10% change) for a given solution composition during the 48 h incubation period. Thus the decomposition of the FITC ligand itself would not contribute to any

fluorescence changes observed on the FITC-LTL functionalized fibers. Instead, any decreases in on-fiber fluorescence responses are due to the decomposition of the LTLs during the incubation period; specifically, the loss of the ligand, hydrolysis of the phosphate group, or decomposition of the ester/amide linkers. In the strongly acidic (100 mM HCl, pH 1) and the weakly acidic (10 μM HCl, pH 5) conditions, the average fluorescence of the commercial FITC-LTL-modified fibers decreased by about 50% after 48h, while the fluorescence on synthetic FITC-LTL fibers only decreased by about 20% (Figs. 5a and b, respectively). In the case of the phosphate-containing LTL, the reduced fluorescence is likely due to hydrolysis, resulting in the loss of the PEG and FITC label from the lipid base. For the synthetic LTL, there are no acid-labile functionalities, other than the FITC fluorescence yield. It may be that the triethylamine wash is not sufficient to remove the latent acid, lowering the fiber fluorescence. In the case of neutral conditions (simply 50:50 EtOH:H_2O), the fluorescence of the commercial FITC-LTL-functionalized fibers decreases by about 90% after 48h, while the fluorescence of the synthetic FITC-LTL fibers showed no significant change (Fig. 5c). In this case, the synthetic LTL behaves exactly as expected, while the commercial version suffers from phosphate hydrolysis, even under neutral conditions.[40] Thus, the synthesized LTL shows supreme stability advantages under those conditions most anticipated in biomacromolecule separations. The final challenge, under basic solution conditions (10 M, pH 9 and 100 mM NaOH, pH 14), is seen in Figs. 5d and e to effect the greatest changes in the

apparent loading for both LTL-types. Under these conditions, the loss of fluorescence is most surely due to the decomposition of the thiourea linkage between the tether and the FITC head group, which is common to both LTLs.[51] That said, the extent of depression is appreciably greater for the commercial version as the phosphate group is also susceptible to hydrolysis under basic conditions.[39-41] Based on its superior chemical stability, the synthesized LTL would appear to be a far better choice than the commercial, phosphate-containing LTL for the functionalization of PP C-CP fibers.

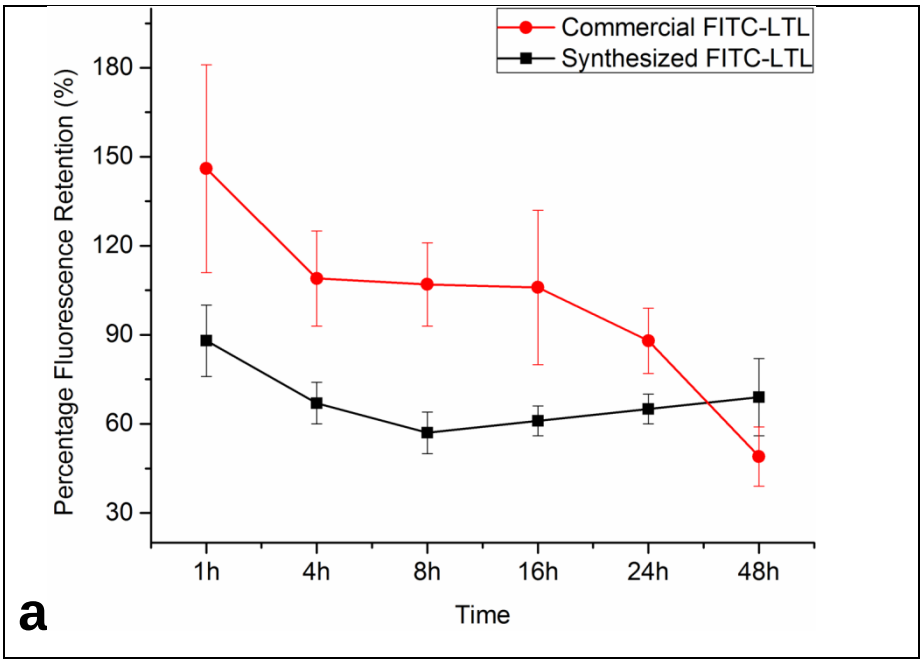

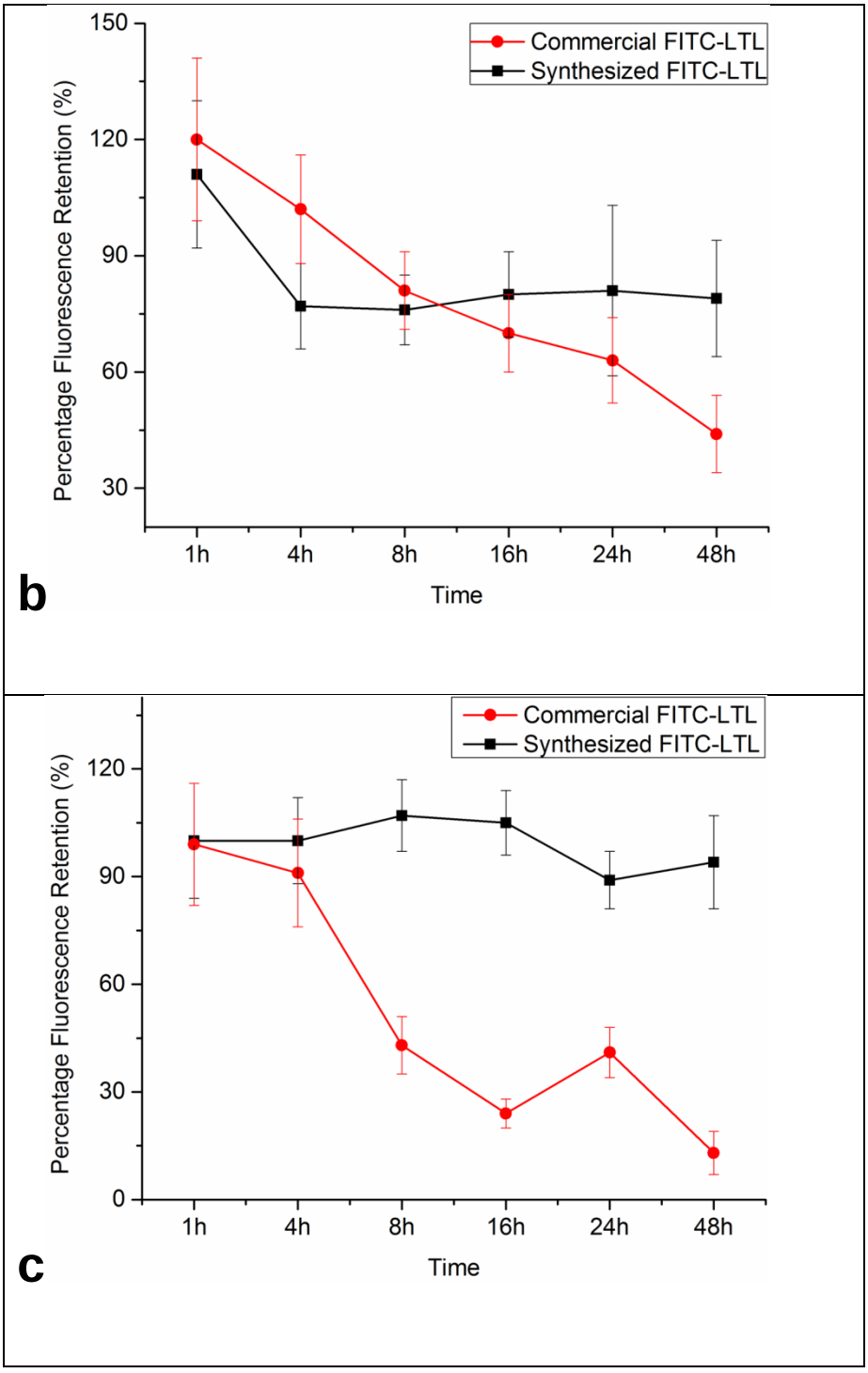
Commercial FITC-LTL
Synthesized FITC-LTL
Percentage Fluorescence Retention (%)
150
120
90
60
30
1h
4h
8h
16h
24h
48h
Time
b
Commercial FITC-LTL
Synthesized FITC-LTL
Percentage Fluorescence Retention (%)
120
90
60
30
0
1h
4h
8h
16h
24h
48h
Time
c

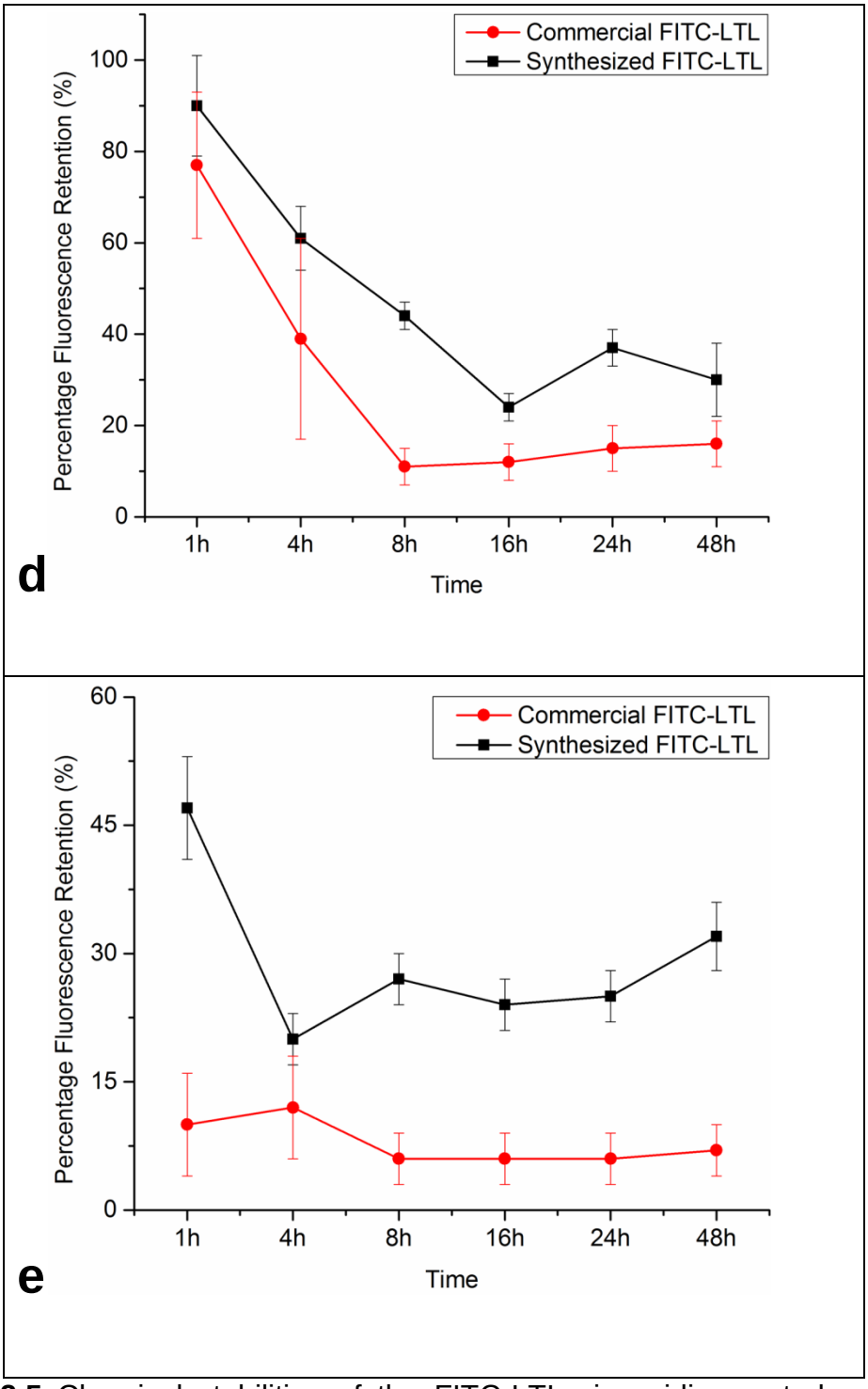

Figure 2.5 Chemical stabilities of the FITC-LTLs in acidic, neutral and basic solvent conditions. Acid or base concentration: (a) 100 mM HCl; (b) 10 µM HCl; (c) neutral conditions; (d) 10 µM NaOH; (e) 100 mM NaOH.

Biotin-LTL-functionalized PP C-CP fibers for the affinity capture of streptavidin-Texas Red.

Previously we have reported that functionalization of PP C-CP fibers with a commercial biotin-LTL (biotin-PEG-lipid) yielded a suitable surface for the affinity capture of SAv-TR from cell lysate material.[37] In Fig. 6, the commercial and the synthesized biotin-LTL-functionalized PP C-CP fiber SPE tips are shown to be capable of selective capture of SAv-TR from PBST buffer (note that a bare PP fiber tips was used as the control to assess non-specific binding). In each case, a 1.0 mL aliquot of 83 nM M SAv-TR is passed through the tip under microcentrifugation. As suggested in the FITC-LTL loading studies (Fig. 3), the use of different load concentrations allows assessment of factors that might limit the surface ligand concentrations. Comparing first the response of the commercial biotin-LTL applied at the two LTL load concentrations, it is seen that the 2X increase in ligand concentration only results in a fluorescence increase of 27%. There are two mechanisms that would lead to this sort of response; either the increased solute concentration did not proportionally increase the surface ligand density, or those ligands were not effectively accessed by the passing SAv-TR. The response observed in Fig. 3 for the commercial FITC-LTL suggests that the former is likely the limiting factor. The fluorescence responses for the equimolar applications of the synthesized biotin-LTL are markedly improved over the commercial biotin-PEG lipid. In the case of the 5 M load concentration, the improvement is ~3X. More impressively, the response for the

10 M loading increased by another ~3X, yielding intensities that are 7.6X greater than the same load concentration of the commercial LTL. The relative increase between the two synthesized LTL load concentrations is perhaps surprising as overcrowding of surface ligands can often be a limitation in affinity capture of proteins. It appears here that the increased load concentration improved the kinetics of the initial LTL adsorption process, increasing the surface coverage without creating deleterious effects in the protein capture step. The relative agreement between the results displayed in Figs. 3 and 6 seems to suggest that the presence of the long PEG chains in the commercial LTL does indeed inhibit the overall surface loading versus the shorter tether lengths of the synthesized version.

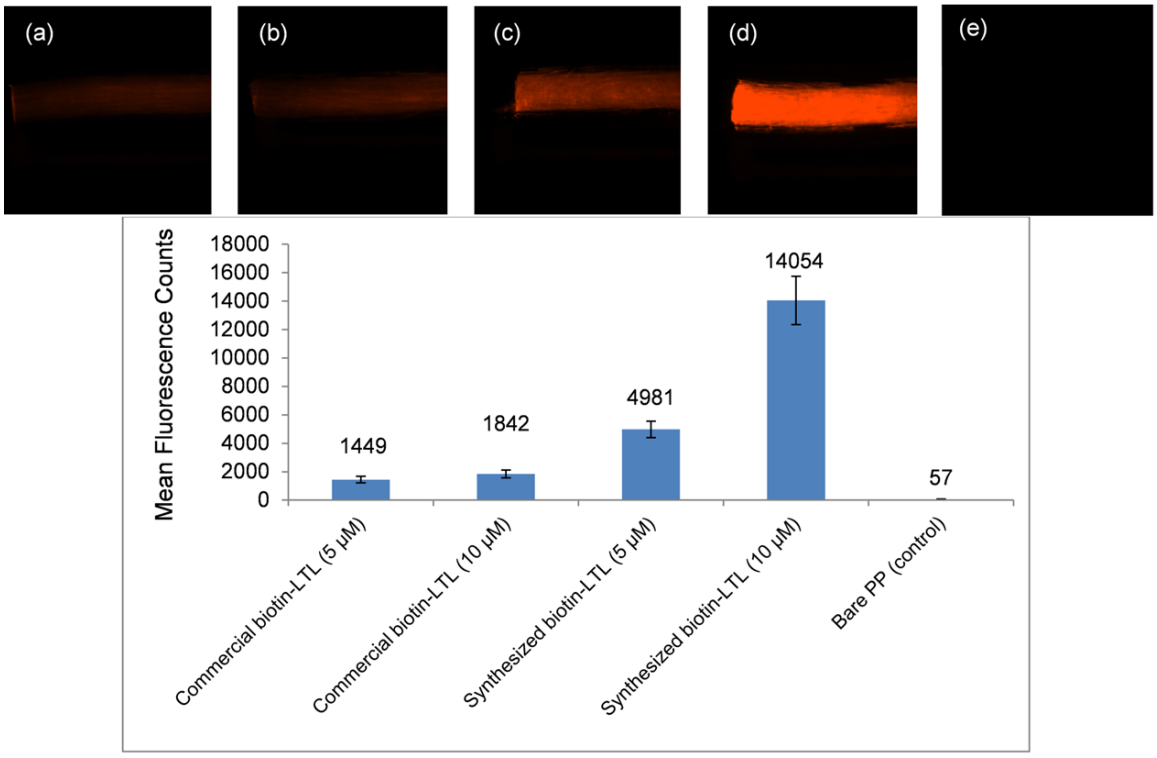

Figure 2.6 Fluorescence images of (a) commercial biotin-LTL (15 g mL^{-1}, 5 M), (b) commercial biotin-LTL (30 g mL^{-1}, 10 M) (c) synthesized biotin-LTL (5 g mL^{-1}, 5 M), (d) synthesized biotin-LTL (10 g mL^{-1}, 10 M) functionalized PP C-CP fiber tips and (e) no functionalized PP C-CP fiber tips after the passage of SAv-TR in PBST buffer solution (5.0 g mL^{-1} (83 nM), 1.0 mL). All images were normalized to fluorescence counts of 100-10000 for display.

In affinity separations, the target species are present in a matrix containing non-desirable species that can inhibit selective capture or foul the process through non-specific binding. To further study the streptavidin binding specificity of biotin-LTL functionalized PP C-CP fibers, SAV-TXR was captured from an *E. coli* cell lysate spiked with SAv-TR and EGFP, both at concentrations of 0.5 g mL^{-1}. An equimolar load concentration 5 M of each LTL was employed. As in the previous example, 1.0 mL of the test solutions were passed through the

functionalized tips as well as ones composed of bare PP C-CP fibers. Spiking of the solution with the EGFP allows for assessment of non-specific protein binding by simply changing the monitored emission wavelength. As expected based on the responses depicted in Fig. 7, the synthetic LTL was indeed more effective in capture of the spiked SAv-TR, by a factor of 2X, with neither of the fibers showing statistically significant amounts of EGFP retention. It is important to note that while both proteins have high affinity to the PP fiber surfaces in simple PBS solution, in the presence of PBST the PP C-CP fibers are relatively immune to non-specific binding.

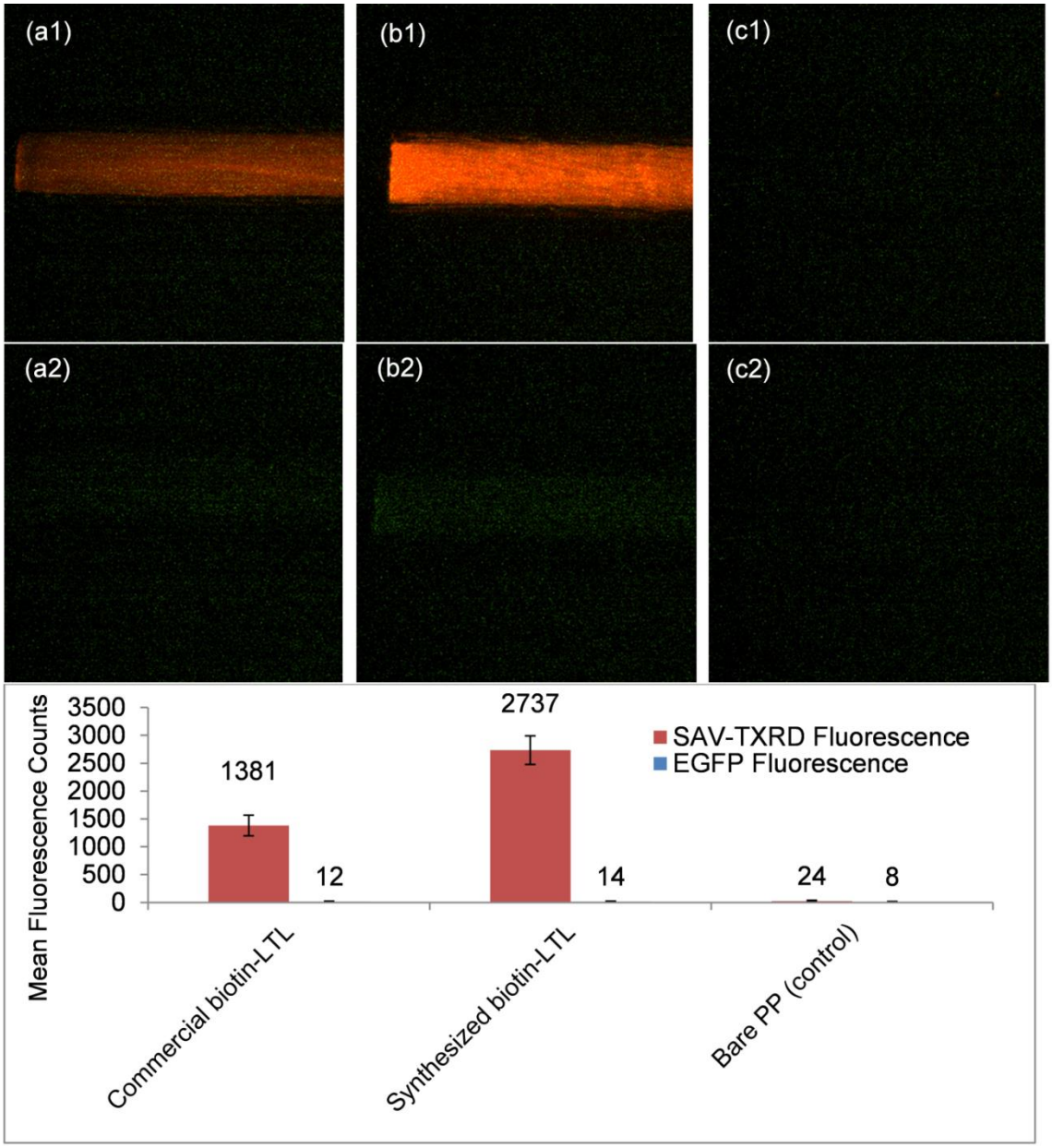

Figure 2.7 Fluorescence images of biotin-LTL functionalized PP C-CP fiber tips after the passage of 1.0 mL of *E. coli* cell lysate containing SAv-TR (0.5 g mL^{-1}, 8.3 nM) and EGFP (0.5 g mL^{-1}, 8.3 nM). Biotin-LTL solutions used for functionalization: (a) commercial biotin-LTL (15 g mL^{-1}, 5 M), (b) synthesized biotin-LTL (5 g mL^{-1}, 5 M), (c) No functionalization. Top row images show both red and green fluorescence, bottom row images only show green fluorescence. In all images, red fluorescence was normalized to fluorescence counts of 10-

3000, and green fluorescence was normalized to fluorescence counts of 10-100 for display.

Conclusions and Future Work

The potential utility of commercially available PEG-lipids as a general methodology to affect lipid tethered ligands (LTL) was demonstrated previously for the modification of PP C-CP fibers. It is felt that the method holds promise for functionalizing a wide range of hydrophobic chromatographic supports. The solid phase protein synthesis methodology described here was initially pursued as the presence of the phosphate group in most PEG-lipids makes them susceptible to chemical attack and degradation. Moreover, the synthetic method is viewed as a versatile means of preparing a wide diversity of LTLs, allowing the tailoring of the lipid anchor group composition, the coupling group (amide here), as well as the length of the PEG (or other moiety) linker group. Using FITC-LTLs as model ligands, the synthesized LTLs were found to adsorb more densely to the PP C-CP fiber surfaces, and were more resistant to solvent wash than the commercial LTLs. The synthesized LTLs showed better chemical stabilities than the commercial LTLs under acidic, basic, and neutral solvent conditions. The application of the LTL functionalization in affinity separations was demonstrated by employing the biotin-LTL functionalized PP C-CP fibers for the capture of streptavidin. The PP C-CP fibers functionalized with the synthesized biotin-LTL showed better performance than the commercial Biotin-LTL fibers for capturing SAv-TR from EGFP-spiked *E. coli* cell lysate.

Future efforts will look at the synthesis of LTLs with different head-group ligands for PP C-CP fiber functionalization. In comparison to traditional liquid phase synthesis, SPPS simplifies the overall synthesis procedure and reduces the time and cost of the synthesis. LTLs with a vast variety of ligands can be readily synthesized without large investments in infrastructure. As a result, various functionalities can be introduced to the PP C-CP fiber surface through LTL adsorption, yielding HPLC or SPE stationary phases for different types of separations. It is believed that the rapid mass transfer characteristic, excellent fluid transport property, and low cost of PP C-CP fibers, along with the simple and efficient LTL functionalization method, make LTL functionalized PP C-CP fiber stationary phase a promising choice in affinity separations across many size scales. More importantly, the LTL methodology is seen as a very attractive means of modifying a wide variety of hydrophobic supports such as polystyrene-divinylbenzene. It may also serve as a general-utility approach to surface functionalization across many areas of technological importance.

Acknowledgements

This material is based upon work supported by the National Science Foundation, Division of Chemistry, under grant CHE-1307078.

References

[1] Neue, U. D. *HPLC Columns: Theory, Technology, and Practice*; Wiley-VCH: New York, 1997.

[2] Neue, U. D.; VanTran, K.; Iraneta, P. C.; Alden, B. A. *J. Sep. Sci.* **2003**, *26*, 174-186.

[3] Chester, T. L. *Anal. Chem.* **2012**, *85*, 579-589.

[4] Gritti, F.; Guichon, G. *J. Chromat. A* **2012**, *1228*, 2-19.

[5] Kirkland, J. J.; Truszkowski, F. A.; Dilks, C. H.; Engel, G. S. *J. Chromatogr. A* **2000**, *890*, 3-13.

[6] Guichon, G.; Gritti, F. *J. Chromat. A* **2011**, *1218*, 1915-1938.

[7] Schuster, S. A.; Wagner, B. M.; Boyes, B. E.; Kirkland, J. J. *J. Chromat. A* **1315**, *1315*, 118-126.

[8] Svec, F.; Hubert, C. G. *Anal. Chem.* **2006**, *78*, 2101-2107.

[9] Jungbauer, A.; Hahn, R. *J. Sep. Sci.* **2004**, *27*, 767-778.

[10] Arrua, R. D.; Talebi, M.; Causon, T. J.; Hilder, E. F. *Anal. Chim. Acta* **2012**, *738*, 1-12.

[11] Carta, G.; Jungbauer, A. *Protein Chromatography: Process Development and Scale-Up*; Wiley-VCH: Weinheim, 2010.

[12] Jungbauer, A. *J. Chromatogr. A* **2005**, *1065*, 3-12.

[13] Marcus, R. K. *J. Sep. Sci.* **2008**, *31*, 1923-1935.

[14] Marcus, R. K. *J. Sep. Sci.* **2009**, *32*, 695-705.

[15] Marcus, R. K.; Davis, W. C.; Knippel, B. C.; LaMotte, L.; Hill, T. A.; Perahia, D.; Jenkins, J. D. *Journal of Chromatography A* **2003**, *986*, 17-31.

[16] Nelson, D. M.; Marcus, R. K. *Anal. Chem.* **2006**, *78*, 8462-8471.

[17] Stanelle, R.; Mignanelli, M.; Brown, P.; Marcus, R. K. *Anal Bioanal Chem* **2006**, *384*, 250-258.

[18] Fornea, D. S.; Wu, Y.; Marcus, R. K. *Anal. Chem.* **2006**, *78*, 5617-5621.

[19] Burdette, C. Q.; Marcus, R. K. *Analyst* **2013**, *138*, 1098-1106.

[20] Manard, B. T.; Marcus, R. K. *J. Am. Soc. Mass Spectrom.* **2012**, *23*, 1419-1423.

[21] Brown, P. J.; Marcus, K. R.; Webb, C. K.; Sinclair, K.; Stevens, K.; Fuller, L.; Nelson, D. M.; Stanelle, R. D. In *231st ACS National Meeting*; American Chemical Society: Atlanta, GA, United States, 2006, p POLY-277.

[22] Wang, Z.; Marcus, R. K. *J. Chromatogr. A* **2014**, *1351*, 82-89.

[23] Randunu, K. M.; Dimartino, S.; Marcus, R. K. *J. Sep. Sci.* **2012**, *35*, 3270-3280.

[24] Randunu, K. M.; Marcus, R. K. *Anal Bioanal Chem* **2012**, *404*, 721-729.

[25] Randunu, K. M.; Marcus, R. K. *Biotechnol. Prog.* **2013**, *29*, 1222-1229.

[26] Burdette, C.; Marcus, R. K. *J. Am. Soc. Mass Spectrom.* **2013**, *24*, 975-978.

[27] Manard, B. T.; Marcus, R. K. *Anal. Methods* **2013**, *5*, 3194-3200.

[28] Karian, H. *Handbook of polypropylene and polypropylene composites, revised and expanded*; CRC press, 2003.

[29] Kim, E. S.; Lee, C. H.; Kim, S. H. *J. Appl. Polym. Sci.* **2009**, *112*, 3071-3078.

[30] Dias, A. J.; McCarthy, T. J. *Macromolecules* **1985**, *18*, 1826-1829.

[31] Avny, Y.; Rebenfeld, L. *J. Appl. Polym. Sci.* **1986**, *32*, 4009-4025.

[32] Dave, J.; Kumar, R.; Srivastava, H. C. *J. Appl. Polym. Sci.* **1987**, *33*, 455-477.

[33] Bui, L. N.; Thompson, M.; McKeown, N. B.; Romaschin, A. D.; Kalman, P. G. *Analyst* **1993**, *118*, 463-474.

[34] Herrera-Alonso, M.; McCarthy, T. J.; Jia, X. *Langmuir* **2006**, *22*, 1646-1651.

[35] Jia, X.; Herrera-Alonso, M.; McCarthy, T. J. *Polymer* **2006**, *47*, 4916-4924.

[36] Schadock-Hewitt, A. J.; Marcus, R. K. *J. Sep. Sci.* **2014**, *37*, 495-504.

[37] Schadock-Hewitt, A. J.; Pittman, J. J.; Christensen, K. A.; Marcus, R. K. *Analyst* **2014**, *139*, 2108-2113.

[38] Schadock-Hewitt, A. J.; Marcus, R. K. *J. Sep. Sci.* **2014**, *37*, 2595-2602.

[39] Gerlt, J. A. In *The Enzymes*; David, S. S., Ed.; Academic Press: 1992; Vol. Volume 20, p 95-139.

[40] Kim, J. H.; Chin, J. *J. Am. Chem. Soc.* **1992**, *114*, 9792-9795.

[41] Florián, J.; Warshel, A. *J. Phys. Chem. B* **1998**, *102*, 719-734.

[42] Bryson, D. I.; Zhang, W.; Ray, W. K.; Santos, W. L. *Mol. BioSyst.* **2009**, *5*, 1070-1073.

[43] Kim, Y.-W.; Grossmann, T. N.; Verdine, G. L. *Nat. Protoc.* **2011**, *6*, 761-771.

[44] El-Faham, A.; Albericio, F. *Chem. Rev.* **2011**, *111*, 6557-6602.

[45] Culf, A. S.; Ouellette, R. J. *Molecules* **2010**, *15*, 5282-5335.

[46] Jullian, M.; Hernandez, A.; Maurras, A.; Puget, K.; Amblard, M.; Martinez, J.; Subra, G. *Tetrahedron Lett.* **2009**, *50*, 260-263.

[47] Ahn, D.-R.; Yu, J. *Bioorg. Med. Chem.* **2005**, *13*, 1177-1183.

[48] Song, A.; Wang, X.; Zhang, J.; Mařík, J.; Lebrilla, C. B.; Lam, K. S. *Bioorg. Med. Chem. Letts.* **2004**, *14*, 161-165.

[49] Hood, C. A.; Fuentes, G.; Patel, H.; Page, K.; Menakuru, M.; Park, J. H. *J. Peptide Sci.* **2008**, *14*, 97-101.

[50] Schadock-Hewitt, A. J.; Marcus, R. K. *Langmuir* **2016**, *31*, 10418-10425.

[51] Shaw, W. H. R.; Walker, D. G. *J. Am. Chem. Soc.* **1956**, *78*, 5769-5772.

CHAPTER III

BIOTIN FUNCTIONALIZED POLY(ETHYLENE TEREPHTHALATE) CAPILLARY-CHANNELED POLYMER FIBERS AS HPLC STATIONARY PHASE FOR AFFINITY CHROMATOGRAPHY

Introduction

Capillary-channeled polymer (C-CP) fibers have been under investigation and development as stationary phase for high performance liquid chromatography (HPLC) separations in this laboratory for over ten years [1-8]. C-CP fibers are made of polypropylene (PP), poly (ethylene terephthalate) (PET) or polyamide (nylon), providing a range of potential surface chemistries that are stable in a wide range of pH [4]. They are unique in shape, with eight capillary channels extending the whole length of the fiber [1]. This unique shape gives them ~3x greater surface area than that of circular cross-section fibers with the same nominal diameter. When packed into a column, C-CP fibers self-align, minimizing twisting and crimping and yielding (effectively) a monolith of 1-5 m open, parallel channels. As a result, C-CP fiber columns exhibit excellent fluid transport properties. A traditional-sized HPLC column packed with C-CP fibers can be operated at high linear velocity (> 100 mm s^{-1}) and low backpressure (< 2000 psi). In comparison to the size of a protein, the surface of C-CP fibers is non-porous thus high speed separations can be undertaken without significant van Deemter C-term broadening [7-9]. The high mass transfer efficiency of C-CP

fiber-packed HPLC columns provides particular promise for the high throughput and yield requirements of preparative protein separations [10].

Life is driven by the interactions among biomolecules such as proteins, with the extremely high specificity of biomolecule interactions maintaining the essential function in living cells. Affinity chromatography, which was first described in the late 60s [11], is one of the most powerful tools in protein separations. The mechanism of affinity chromatography is based on ligands coupled on a solid support that selectively capture a specific protein from a protein mixture, such as cell lysate. C-CP fibers, including nylon, PP and PET, have been used for protein separations in different modes such as reversed phase (RP) [12], ion-exchange (IEC) [13], hydrophilic interaction (HIC) [12-14], and affinity chromatography [15,16]. The two principle means of coupling a capture ligand to a chromatographic support are adsorption and covalent coupling [17,18] .Marcus *et al*. demonstrated that PP C-CP fibers modified by the simple adsorption of recombinant protein A were capable of capture and recovery of immunoglobulin G (IgG) [15]. A recent study showed that PP C-CP fibers could be modified by surface adsorption of head group-functionalized poly(ethylene glycol) (PEG)-lipids and used for affinity chromatography [16]. In this case, biotin head-group PEG-lipids could effectively isolate Texas Red-labeled streptavidin spiked into a cell lysate. Simple adsorption of selective ligands onto C-CP fibers which are already formed into column/tip formats is a highly convenient methodology. However, the possible drawbacks of surface

modification by physical adsorption include limited ligand densities and the leakage of ligand during the separation process. Hence, other approaches, such as chemical surface modification of C-CP fibers, needs to be investigated in order to overcome the potential drawbacks of physical modification.

The surface modification of polymeric materials has been studied for decades. There are numerous reports of the modification of PP, PET and nylon [18,19]. For example, Yang *et al.* grafted D-gluconamidoethyl methacrylate (GAMA) on PP membrane surfaces by UV-induced polymerization to improve the hydrophilicity and biocompatibility of PP [20]. Jia *et al.* showed that a nylon surface could be modified by targeting the amide group to introduce different functionalities [21,22]. Different from the case of bead-format columns that are assembled by “filling” of the container, it is easier to pack C-CP fibers into the HPLC column before chemical modification as the fibers may become fragile or twisted during the modification process [23]. The reaction conditions for the modification of PP and nylon materials are usually chemically harsh and not compatible with the modification of polymeric stationary phases *in situ*. As such, it is reasonable to look to the modification of PET as a basic approach to achieve greater selectivity on C-CP fibers. Specifically, the ester group on PET is susceptible to attack under mild reaction conditions, making it a better choice of stationary phase in terms of on-column modification. There is an extensive literature describing the chemical modification of PET [18,23]. Surface modification of PET includes chemical modification by hydrolysis [24,25],

aminolysis [23,25,26] and reduction [25]. Some other modification techniques are ion beam bombardment [27], plasma [28], laser [29], and air-corona treatment [30], UV-induced graft polymerization [6,31], and diffusion of poly(ethylene oxide) [32]. Among these techniques, aminolysis of the PET surface by treatment of multifunctional amines was chosen for this study because it is compatible with on-column modification and easily performed on an HPLC system. During the surface aminolysis process, a primary amine was introduced to affect a chemically reactive PET surface for the covalent attachment of affinity ligands.

In this study, a microbore HPLC column packed with PET C-CP fibers was sequentially functionalized to create a biotinylated surface as depicted schematically in Fig. 1. The PET fibers were initially aminated by treatment with ethylenediamine (EDA). The resultant amine density was determined by a simple ninhydrin assay. A hydrophilic spacer (9 atom length) and D-biotin were then covalently attached to the amine groups on the surface of the fibers. The coupling strategy of solid phase peptide synthesis (SPPS) was employed for the attachment of ligands [33]. The common biotin-streptavidin affinity pair was used as a demonstration of the basic methodology, wherein biotin was the immobilized ligand. The subsequent streptavidin binding homogeneity and binding capacity were studied by breakthrough curve experiments and frontal analysis. The biotin functionalized PET C-CP fiber column was shown to be able to affinity capture streptavidin in mixture with enhanced green fluorescent protein (EGFP), with little non-specific binding of EGFP occurring. The capturing of streptavidin from *E. coli*

cell lysate was also successfully performed. It is believed that this general methodology for surface amination of PET fibers, followed by the covalent ligand attachment holds a great deal of promise as the C-CP stationary phases are developed for protein therapeutics and downstream processing applications.

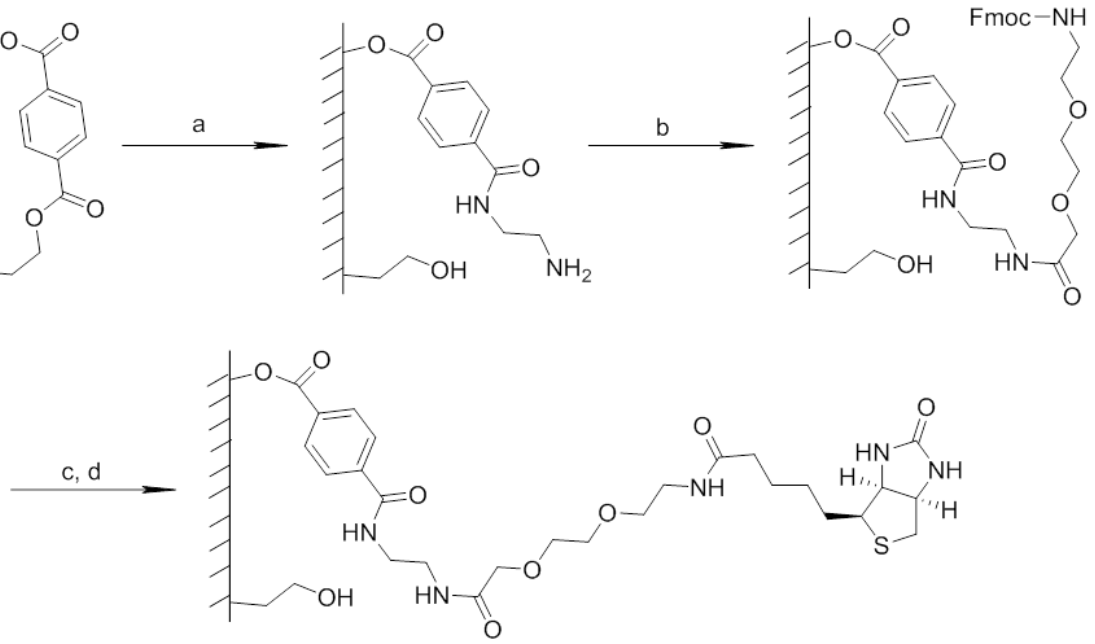

Figure 3.1 Scheme of surface functionalization of PET C-CP fibers. All reactions took place after C-CP PET fibers were packed in microbore columns. Reagents and conditions: (a) Ethylenediamine, 0.1 mL min^{-1}, 3 – 12 min; (b) Fmoc-8-amino-3,6-dioxaoctanoic acid, HCTU, DIPEA, DMF, 0.2 mL min^{-1}, 2h; (c) 25% piperidine in DMF, 0.2 mL min^{-1}, 30min; (d) D-biotin, HCTU, DIPEA, DMF, 0.2 mL min^{-1}, 2h.

Experimental Methods

Chemicals and materials

Unless otherwise specified, chemicals were purchased from commercially available sources and used without further purification. Dimethylformamide

(DMF), Dimethyl Sulfoxide (DMSO), N,N-Diisopropylethylamine (DIPEA), ninhydrin and piperidine were purchased from VWR (Atlanta, GA). Ethylenediamine (EDA), isopropanol, pyridine, propionic acid, sodium propionic and 2-methoxyethanol were purchased from Sigma-Aldrich (St. Louis, MO). Fmoc-8-amino-3,6-dioxaoctanoic acid, 1-[Bis-(dimethylamino)-methylene]-5-chloro-1H-benzotriazolium hexafluorophosphate 3-oxide (HCTU) and D-biotin were purchased from Chem-Impex International, Inc. (Wood Dale, IL). Ethanol was purchased from EMD (HPLC grade, 190 proof, Billerica, MA). Streptavidin-Texas Red (SAV-TXRD) was obtained from SouthernBiotech (Birmingham, AL). Streptavidin (SAV) was purchased from Leinco Technologies, Inc. (St. Louis, MO). Enhanced green fluorescent protein (Sequence for EGFP found in p3051 retrovirus vector was amplified by PCR) was provided by the group of G. Chumanov (Dept. of Chemistry, Clemson University, Clemson, SC). The cell lysate of *E. coli* (NEB 5-alpha *E. coli*) was obtained from the group of K. Christensen (Dept. of Chemistry, Clemson University, Clemson, SC). *E.coli* were grown in 1 L of Luria-Bertani broth at 37 ºC to an O.D. of 0.8. The cells were pelleted at 13,000x g for 10 minutes. The cell pellet was then re-suspended in PBS. This cell slurry was then disrupted and centrifuged at 30,000x g for 30 minutes to pellet out cell debris and producing a cleared lysate. Deionized water was prepared by Milli-Q water system. PBS buffer was prepared by dissolving NaCl (8.0g), KCl (0.2g), Na_2HPO_4 (1.44g) and KH_2PO_4 (0.24g) in deionized water

to a final volume of 1.0 L. The pH of PBS buffer was adjusted to 7.4. PBST buffer was prepared by adding 1.0 mL of Tween-20 in 1.0 L of PBS buffer (pH 7.4).

Preparation of PET C-CP fiber microbore column

The method for packing C-CP fiber microbore columns was previously described by Marcus, *et al*. [12,34]. PET C-CP fibers were obtained from the Clemson University School of Materials Science and Engineering on spools measuring more than 1000 m in length [35], with fiber sizes equivalent to 3 denier per filament (dpf). In this study, 450 PET fibers were pulled through two types of ~0.8 mm i.d. polymer casings to form the microbore columns; fluorinated ethylene propylene (FEP, 0.8 mm i.d., Cole Palmer, Vernon Hills, IL) tubing for experiments where fiber imaging was employed and polyether ether ketone (PEEK, 0.762 mm i.d., IDEX Health & Science LLC, Oak Harbor, WA) tubing for flow-through columns. After packing, the columns were connected to an HPLC pump (Shimadzu LC-10AT, Kyoto, Japan) and washed with ACN then deionized water until a stable baseline was observed on the UV-Vis absorbance detector (216 nm). Once assembled and cleaned, the microbore columns could be stored in ambient conditions and cut to appropriate lengths prior to surface modification.

Instrumentation

PET microbore column cleaning and modifications were performed using a Shimadzu LC-10AT pump (Kyoto, Japan) to deliver the solvents at a well-controlled rate. The UV-Vis absorbance data for the ninhydrin experiments to

determine primary amine concentrations on the fibers were taken from a Genesys 10S UV-Vis spectrometer (Thermo Fisher Scientific Inc., Sunnyvale, CA). The fluorescence data and images were generated on an Olympus IX71, 2×/0.08 UPlanFI (infinity corrected) objective (Olympus, Center Valley, PA). The fluorescence excitation was achieved by a Xe arc lamp with a filter (excitation: 575nm; emission: 624 nm; Chroma, Bellows Falls, VT). The fluorescence images were taken by an Ocra-ER (Hamamatsu) CCD camera. The fluorescence data was processed using Slidebook 5.0 (Denver, CO). The streptavidin loading characteristics were determined through breakthrough curve (frontal analysis) experiments which were performed on a Dionex Ultimate 3000 HPLC system with a LPG-3400SD pump, a WPS-3000TSL autosampler, a VWD-3400 RS UV–Vis absorbance detector and a FLD-3100 fluorescent detector (Thermo Fisher Scientific Inc., Sunnyvale, CA). Likewise, the same system was employed for the affinity separations.

Modification of C-CP PET microbore column

As depicted in Fig. 1, the creation of the biotinylated PET C-CP fiber surfaces occurred in a series of fairly straight forward steps.

a. Aminolysis of PET fiber surface - Prior to the exposure to the EDA modification solution, the columns were washed with DMF at a flow rate of 0.75 mL min^{-1} for 10 min to remove water residue. Neat EDA was then introduced in the column at a flow rate of 0.5 mL min^{-1}. The flow rate was reduced to 0.1 mL min^{-1} once the entire column was filled with EDA (when the

strong basic liquid was detected at the outlet of the column). The EDA exposure times were varied from 3 – 12 min to affect different degrees of aminolysis, following which the column was washed with DMF (0.75 mL min^{-1}, 15 min).

b. Determination of amine density on EDA-treated Fibers - The ninhydrin test method to determine the total amine content on the modified fibers was previously described [36,37]. PET fibers were recovered from 50 mm of a native PET column, a 3 min-EDA treated PET column, a 6 min-EDA treated PET column and a 12 min-EDA treated PET column. Each fiber sample was placed into a test tube containing 0.5 mL of 10% isopropanol, 0.5 mL of 10% pyridine and 1.0 mL of the ninhydrin solution composed of 2.325 mL propionic acid, 12.5 mL 2-methoxyethanol, 5.045 g sodium propionate, and 0.5 g ninhydrin, with the total volume adjusted to 25 mL with deionized water. The test tubes were sealed and heated in a boiling water bath for 30 min. After removal and cooling, 10 mL of 50% ethanol was added to each test tube, the tube was shaken, then left to sit for 15 min. The mixture solution in each test tube was diluted to 25 mL with deionized water prior to the absorbance measurement. The known concentration of 6-aminohexanoic acid solution was analyzed following the same procedure as a calibrant. A ninhydrin test containing no fibers or 6-aminohexanoic acid was used as blank. The concentration of amine was quantified by the absorbance measurements of diluted ninhydrin test solutions performed at 570 nm. All experiments were performed in triplicate.

c. Attachment of spacer arm and biotin on fiber surface – Fmoc-8-amino-3,6-dioxaoctanoic acid (116mg, 0.3 mmol), HCTU (124 mg, 0.3 mmol) and DIPEA (105 µL, 0.6 mmol) in 3 mL DMF was circulated through the EDA-treated PET columns at a flow rate of 0.2 mL min^{-1} for 2h. The columns were then washed sequentially with DMF (0.75 mL min^{-1}, 15 min) to remove the reaction solution, 25% piperidine in DMF (0.2 mL min^{-1}, 30 min) to de-protect the amine group on spacer, and DMF (0.75 mL min^{-1}, 15 min) to remove piperidine. D-biotin (74 mg, 0.03 mmol), HCTU (124 mg, 0.3 mmol) and DIPEA (105 µL, 0.6 mmol) in 3 mL 50/50 DMF/DMSO was circulated through each column at a flow rate of 0.2 mL min^{-1} for 2h. The column was then washed with DMSO at a flow rate of 0.75 mL min^{-1} for 20 min and 0.5 mL min^{-1} for 30 min. The biotin-functionalized PET C-CP columns were washed with deionized water at 1.0 mL min^{-1} for 30 min before further study. The resulting columns are designated hereafter as biotin-PET-3, biotin-PET-6, and biotin-PET-12, based on the time period of the initial aminolysis step.

Results and Discussions

Functionalization of PET C-CP microbore column

The surface of PET C-CP fibers was aminated *in situ* by treatment with EDA as depicted in Fig. 1 and described above. During this process, the ester bond on the PET surface was aminolyzed and the primary amine was introduced

[38]. EDA was chosen as the amination reagent because longer multifunctional amines were reported to be entropically prone to forming a ring structure by reaction at both amine ends with the polymer ester groups, which results in low primary amine densities on the polymer surface [25]. Shorter amines, such as ammonia and hydrazine, are not compatible with “on-column modification” since they are either unstable or must be used with an aqueous solution. Any latent water in the presence of the aminolysis reactions may cause hydrolysis of polymer without introducing primary amines, thus DMF was used as the wash solutions before and after EDA treatment.

The method for functionalizing the aminated PET fiber surfaces was adopted from standard solid phase peptide synthesis (SPPS) [33,39]. SPPS was first described by R. B. Merrifield in the 1960s [40]. After being developed over half a century, SPPS has been demonstrated as a general, yet effective method of coupling a large number of different ligands to amine groups [33,41-47]. Application of the SPPS coupling strategy in surface functionalization leads to the possibility of introducing a wide variety of ligands onto the EDA-treated PET C-CP fiber surfaces for future protein separations. 8-amino-3,6-dioxaoctanoic acid was coupled to the amine-rich surface of the PET fibers as a hydrophilic spacer. This 9-atom length spacer extends the ligand away from the hydrophobic surface of PET toward the hydrophilic mobile phase solution, facilitating the binding of the ligand to the target protein. HCTU was used as coupling reagent due to its high efficiency in SPPS coupling reactions [48]. D-biotin was attached on the terminal

amine group of the spacer after the protecting group (Fmoc) was removed. The D-biotin functionalized PET C-CP column was washed with DMSO, DMF and water to remove non-covalently bonded (e.g., adsorbed) biotin.

Amine density determination of EDA-treated PET C-CP column

Before attachment of the spacer-arm and biotin functionality, the density of the generated amines on the EDA treated PET fiber surface was determined by the ninhydrin reaction [36]. In order to investigate the homogeneity of aminolysis, fiber samples were taken from the top (near the inlet of EDA flow), middle, and bottom portions (near the outlet of EDA flow) of the column. The results presented in Fig. 2 indicate that longer amounts of EDA treatment time yield higher degrees of aminolysis, as reflected in the higher amine group densities on the PET C-CP fiber surfaces. All of the EDA-treated fibers retained their physical integrity and did not break apart within the columns (which would produce severe pressure drops and flow inhomogeneities). When treated outside of the column, the 3 and 6 min EDA-treated fibers had equivalent or similar mechanical strength as native PET fibers, with the 12 min treated fibers showing some brittleness. The treatment of the fibers *in situ* reflected no physical ill-effects. No significant backpressure increases (<10% increase) were observed for the EDA-treated columns under chromatographic conditions in comparison to native PET columns, which implies that there would be no loss in the excellent fluid transport features of C-CP fiber columns.

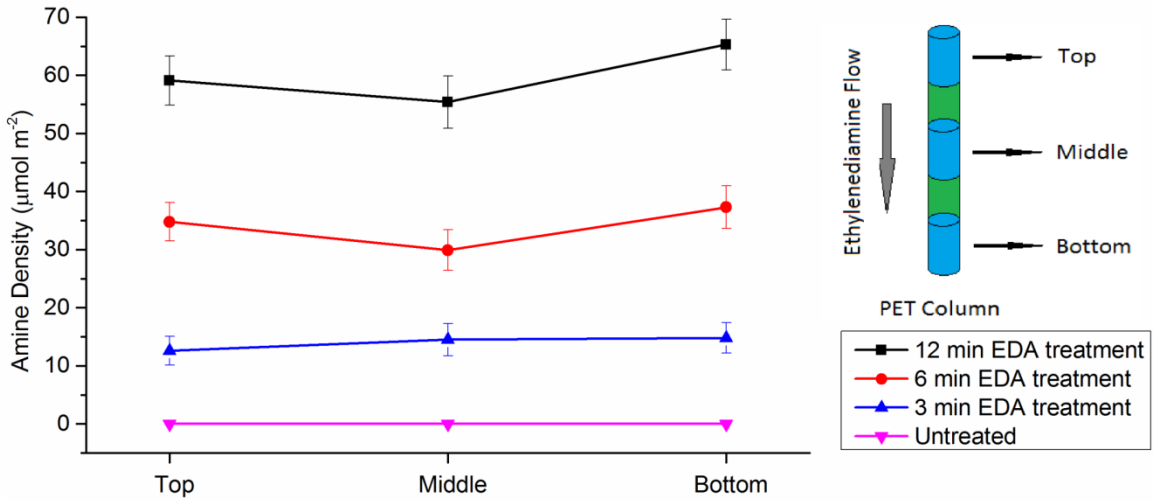

Amine Density (μmol m^{-2})	Top	Middle	Bottom
Untreated	0	0	0
3 min EDA treatment	12.6 ± 2.5	14.5 ± 2.8	14.8 ± 2.6
6 min EDA treatment	34.8 ± 3.3	29.9 ± 3.5	37.3 ± 3.7
12 min EDA treatment	59.1 ± 4.2	55.4 ± 4.5	65.3 ± 4.4

Figure 3.2 Amine density on EDA-treated PET fiber surface (μmol m^{-2}). Top portion of column reflects the column segment that was close to the inlet of EDA flow, with the bottom portion representing the portion nearest the column outlet. Aminated PET fibers were pulled out from the column for ninhydrin tests.

During the process of aminolysis, EDA was introduced into column by a HPLC pump. In order to maximize the homogeneity of aminolysis, the mobile phases and their flow rates were carefully controlled. The times of EDA treatment over the entire length of column should be the same no matter how close the fiber was to the inlet or outlet of the column. As seen in Fig. 2, there is no significant difference in amine density among the top, middle and bottom portions of the EDA-treated columns. However, the degree of aminolysis, at the outlet of

the columns is slightly higher than the middle and top portions of the columns when the EDA treatment time was 6 or 12 min. This is interpreted to some level of fronting as the high linear velocity (6.54 - 32.7 mm s^{-1}) may limit the exposure/interaction time of the solution-surface interactions.

A comparison of the amine surface densities among various amine-functionalized materials illustrates the very high efficiency of the EDA C-CP fiber amination process. As presented in Table 1, the densities generated for the 6- and 12- minute exposure times here are significantly higher than most of the reported values, but lower than ammonia-functionalized particulate poly(glycidyl methacrylate-co-ethylene dimethacrylate)-based polymers where amine was attached on every monomer of glycidyl group[49-53]. The BET surface area of PET C-CP fibers are determined to be from the order of 0.3 m^2 g^{-1} to 3 m^2 g^{-1} depending on the experiment conditions in the BET analysis. Since BET analysis requires sample degasing at raised temperatures, the pore sizes and specific surface area of organic polymer fibers may change during the degasing process. As the degasing temperature increased, the BET specific surface area decreased. The lowest amine densities, which are based on the highest BET specific surface area, are presented in Table 1.

Table 3.1 Comparison of amine surface density for the aminated C-CP fibers, nylon 6 C-CP fibers, and other chromatographic stationary phases.

Substrate	Amine density	References
Aminated PET C-CP fiber (3 min EDA treatment)[a]	≥ 13.9 μmol m^{-2}	
Aminated PET C-CP fiber (6 min EDA treatment)[a]	≥ 34.0 μmol m^{-2}	
Aminated PET C-CP fiber (12 min EDA treatment)[a]	≥ 60.0 μmol m^{-2}	
Ammonia-functionalized particulate poly(glycidyl methacrylate-co-ethylene dimethacrylate)-based polymers	172 μmol m^{-2}	[49]
Amine-functionalized cycloolefin polymer	20.1 μmol m^{-2}	[50]
Amine-functionalized silica nanoparticles	10.1 μmol m^{-2}	[51]
Amine-functionalized silica	6.64 μmol m^{-2}	[52]
3-Aminopropyl-functionalized silica gel	1.81 μmol m^{-2}	[53]
3-(Diethylenetriamino)propyl-functionalized silica gel	2.60 μmol m^{-2}	[53]
3-(Ethylenediamino)propyl-functionalized silica gel	2.80 μmol m^{-2}	[53]

a - Results are average amine density of top, middle and bottom portions of aminated PET fibers

Fluorescence imaging of PET C-CP columns after SAV-TXRD binding

While the density and homogeneity of the active amine groups sets the basis for the further ligand attachment, it is the distribution of the ligands and the capture protein that are of ultimate importance. Thus the distribution of the SAV-TXRD along the column length must be determined. For the imaging experiments, PET C-CP fibers were packed in FEP tubing as it is optically clear and allows for

the fluorescence imaging of bound SAV-TXRD on the fiber surface while still in the column. After being fully functionalized and cleaned, the PET C-CP column was mounted on the HPLC. SAV-TXRD was loaded onto the columns as 3.0 mL of a 5.0 μg mL^{-1} PBST solution passed through the test columns. The PBST buffer (0.1% Tween-20 in PBS buffer) was used to minimize non-specific binding of protein to the C-CP fiber surface [16]. A native PET C-CP column and a biotin washed PET C-CP column (D-biotin (74 mg, 0.03 mmol) in 3 mL 50/50 DMF/DMSO was circulated through the column at a flow rate of 0.2 mL min^{-1} for 2h) were used as controls, with the biotin-PET-6 column evaluated for the protein binding homogeneity. Fig. 3 clearly shows that the biotin-functionalized PET C-CP fiber surface has much higher fluorescence intensity than the biotin washed fiber surface and the native fiber surface after passage of SAV-TXRD solution and the distribution of that binding seems to be relatively uniform on this 5 mm wide image. The overall binding characteristics illustrate two very important aspects. First, biotin, in the presence of Tween-20, either does not bind to the native PET surface, or if it does, is not situated in a manner that SAV binding can occur. Second, SAV-TXRD in PBST does not have an affinity for the native PET surface, though in aqueous buffer solutions without the surfactant the interactions are quite strong (requiring >30% organic mobile phases for elution).

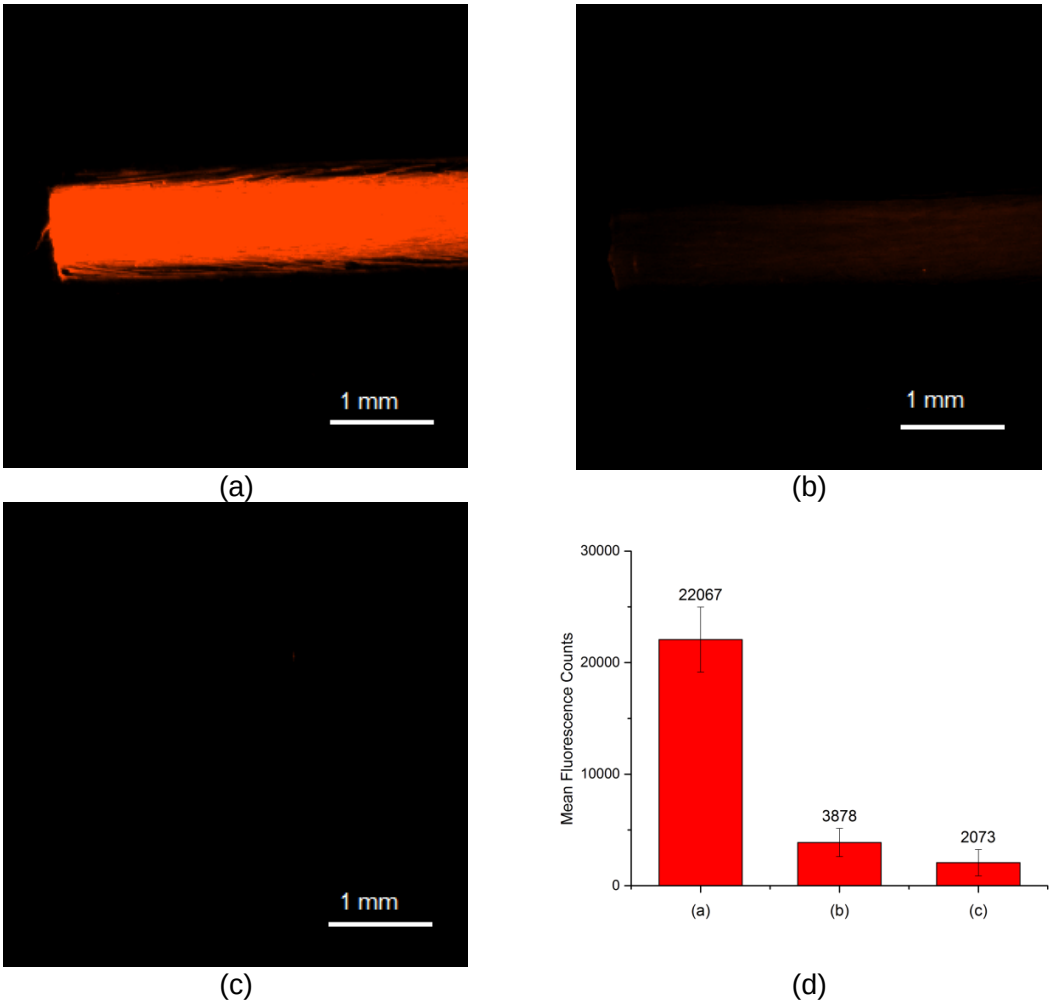

Figure 3.3 Fluorescence images of PET C-CP fibers after loading of 3.0 mL of 5.0 µg mL^{-1} of SAV-TXRD in a) biotin-PET-6 column (6 min EDA treatment); b) biotin washed PET column (no covalent attachment); c) native PET column. d) mean fluorescence intensities of each fiber (calculated from the mean fluorescence counts of fiber surface in images). All experiments were performed in triplicate.

Streptavidin binding capacity on functionalized PET C-CP columns

There are two key aspects in the practical evaluation of protein binding to a particular stationary phase, the accessible ligand density and the limiting kinetics in accessing those sites on the timeframe of a given separation. The streptavidin binding capacities of the biotin functionalized PET C-CP fiber columns (biotin-PET-3, biotin-PET-6, and biotin-PET-12) were determined through breakthrough curve experiments and frontal analysis [54,55]. A breakthrough curve plot consists of the relative concentration (detector response (C)) as a function of loading volume/time versus the maximum signal realized for the solute in the initial probe solution (C_o); C/C_0 as a function of volume (mL) of the mobile phase passed through the adsorbent (stationary phase). The starting point of the curve has a relative concentration of zero which indicates that all of the solute is retained; saturation is identified as the breakthrough curve reaches the maximum value of the feed concentration. The data extracted from the breakthrough curve is treated by an approach known as frontal analysis, providing the loading capacity for that phase under the specific conditions of solute concentration, solvent composition, and volume flow rate.[55]

Presented in Fig. 4a are the resultant breakthrough curves for the loading of SAV from a 1.0 g mL^{-1} solution in PBST at a flow rate of 1.0 mL min^{-1}; equivalent to a linear velocity of U = 65.4 mm s^{-1}. As depicted in the figure, the biotin-PET-12 showed the highest binding capacity as the point of C/C_o = 0.5 occurs at the highest loading volume, equating to an average fiber loading

density of 0.97 mg m^{-2} (based on the highest BET specific surface area of 3 m^2 g^{-1} of the fibers) or 1.84 mg mL^{-1} (based on column volumes), for triplicate columns/loadings. Biotin-PET-6 and biotin-PET-3 have binding capacities of 0.35 mg m^{-2} (0.67 mg mL^{-1}) and 0.063 mg m^{-2} (0.12 mg mL^{-1}), respectively. Clearly, the amount of captured SAV increases with the EDA exposure time. Indeed, the relative loading amounts of SAV on the biotinylated biotin-PET-12 are greater than biotin-PET-6 and biotin-PET-3 would be expected based on the results of the surface amine determinations. Specifically, while the biotin-PET-12 has ~2x more amine groups (to which biotin can be coupled), the eventual SAV loading is ~3x higher. This suggests that more primary amine groups are available on PET fiber surface for spacer and biotin attachments. In other words, the column with more EDA treatment carries a higher density of biotin after full functionalization, which is more favorable for affinity chromatographic separations. It should be pointed out that in all cases the molar amounts of spacer and biotin used in the functionalization reactions were in excess (~10x more) compared with the number of amines on PET fiber surface (based on the results from ninhydrin tests). The relative shapes (steepness) of the breakthrough curves suggest that the actually loading of SAV onto the high-density surface is indeed slower than for the low-density modifications. Fig. 4b shows that SAV bound to the Biotin-PET columns at the same speed at the beginning of SAV loading when the Biotin-PET columns were free of SAV. As loaded SAV increased, the binding of SAV to the Biotin-PET columns slowed down then reached zero (saturation).

The time, from when the binding of SAV started to slow down to when the binding sites on the Biotin-columns were saturated by SAV, increased with the EDA treatment time of the columns. The results suggested that when the bound amount of SAV on the Biotin-PET columns were low, the binding was only limited by the affinity between SAV and biotin, which is reflected from the same initial binding speeds on all columns. As the amount of bound SAV on the Biotin-PET surfaces increased, the binding was starting to be limited by the steric hindrance from the bound SAV. The Biotin-PET-12 column bound the highest amount of SAV in all Biotin-PET columns thus the longest saturating time was needed. It need to be pointed out that in the routine applications of analytical scale HPLC, the amount of loaded analyte is usually much lower than the column maximum capacities. Hence, long saturation time on the Biotin-PET-12 column does not limit its performance.

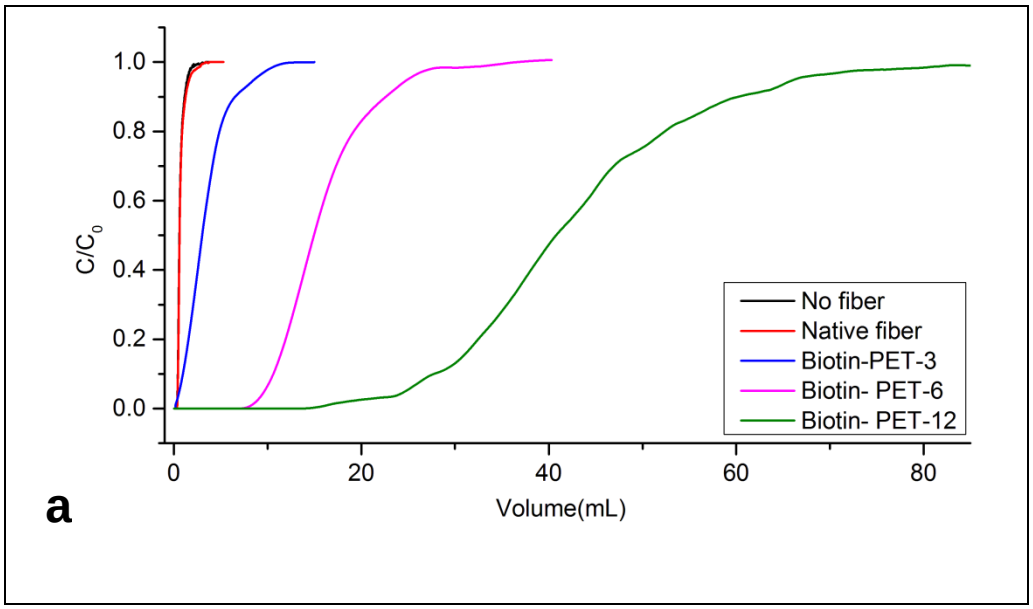

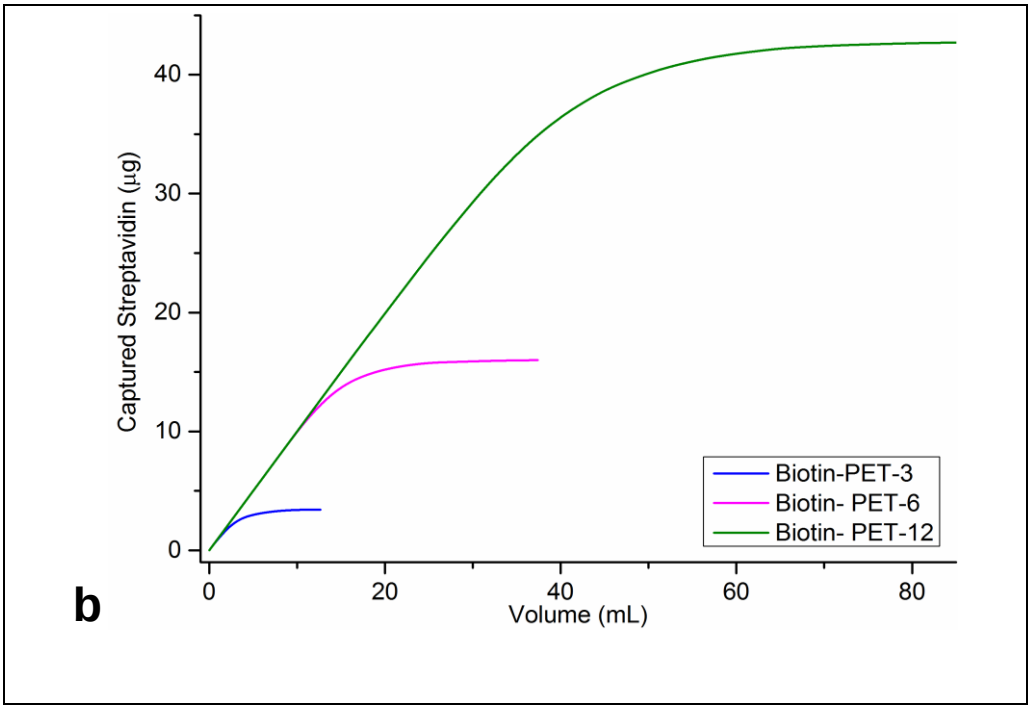

Figure 3.4 (a) Streptavidin breakthrough curves on PET C-CP fiber columns. (b) Streptavidin bound on PET C-CP fiber columns Chromatographic condition: biotin-PET-3, -6, and -12 columns (50 mm long, 0.762 mm i.d.), mobile phase: 1.0 µg mL^{-1} streptavidin in PBST buffer; flow rate: 1.0 mL min^{-1}; UV absorbance wavelength: 216 nm.

Streptavidin binding homogeneity of biotin-functionalized PET C-CP fiber columns

As might be discerned from the basic mechanisms laid out in Fig. 1, higher degrees of aminolysis results in more degradation of fiber physical structure. This negative effect is seen in the breakthrough curves presented in Fig. 5, which reflect the loading of each of the three EDA surface treatment times (followed by biotinylation) for columns cut into three equal-length segments. The breakthrough curves of the biotin-PET-3 fiber column and biotin-PET-6 fiber column indicate that the loading capacity is invariant with the position of the

segment in the modification process; i.e. the complete surface modification is uniform across the column length. On the other hand, the column with the longest EDA treatment time (biotin-PET-12), has the lowest homogeneity of binding among all modified columns. Specifically, the loading capacity in the top portion (nearest the inlet) is significantly below those of the middle and bottom portion of the column. It is concluded that a degree of degradation of fibers, has resulted from long EDA treatment time, that impairs the homogeneity of streptavidin binding of biotin functionalized PET C-CP fiber column. Based on the results from these breakthrough curve experiments, biotin-PET-6 fiber column was chosen for further study as it demonstrated a reasonable streptavidin binding capacity of 0.35 mg m^{-2} without sacrifice of binding homogeneity. Clearly, depending on the type of separation being performed, if absolute binding capacity were the driving force, the longer exposure time would be employed.

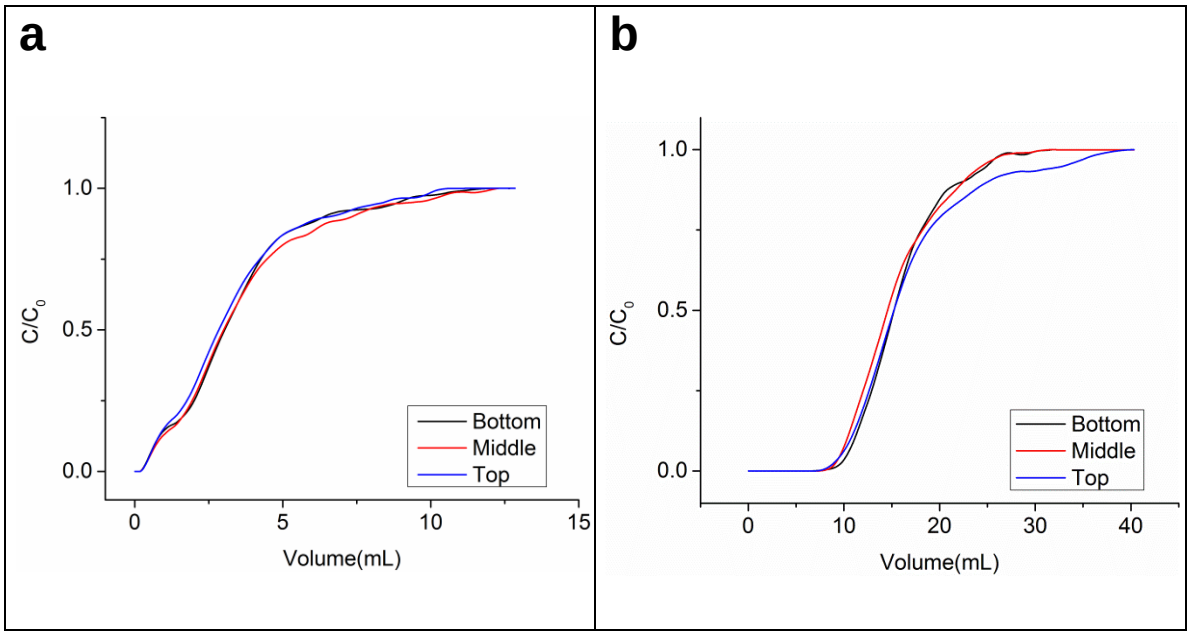

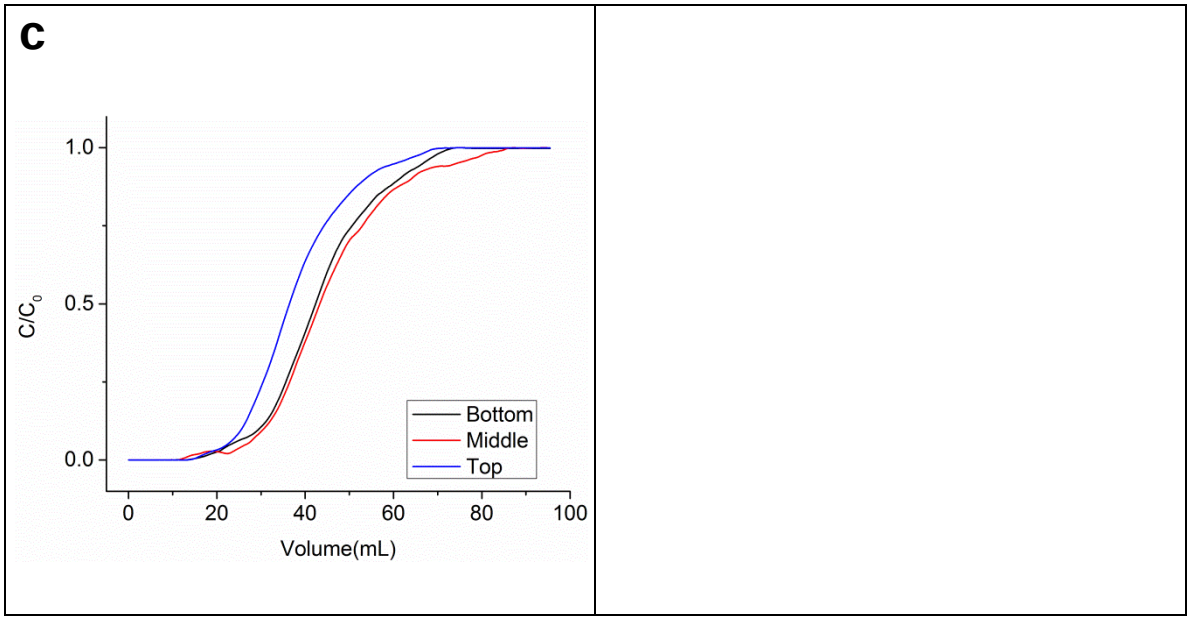

Figure 3.5 Streptavidin breakthrough curves at different positions of biotin functionalized PET fiber columns. a) biotin-PET-3; b) biotin-PET-6; c) biotin-PET-12. After full functionalization, the 300 mm PET C-CP fiber column was cut into 50 mm segments and used for breakthrough curve experiments. Chromatographic conditions: biotin-PET-3, -6, and -12 columns (50 mm long, 0.762 mm i.d.), mobile phase: 1.0 µg mL^{-1} streptavidin in PBST buffer; flow rate: 1.0 mL min^{-1}; UV absorbance wavelength: 216 nm.

Streptavidin binding specificity of biotin functionalized PET C-CP fiber columns

The purpose of any affinity phase is to isolate the target species of interest from a matrix of relevance, to the exclusion of non-desirable matrix species. To test streptavidin specificity of the biotin-functionalized PET C-CP fiber column, a mixture of SAV-TXRD and EGFP was used as the test pair in both PBS and cell lysate matrices. EGFP is a mutant of green fluorescent protein (GFP) that exhibits bright green fluorescent [56,57], thus providing two proteins which exhibit very different spectrochemical responses. Specifically, SAV-TXRD has the

greatest response at a 595 nm/615 nm excitation/emission combination, which EGFP performs best at 488 nm/509 nm. In the absence of any chemical modifications of the PET fiber surfaces, both of these proteins have a strong binding affinity in aqueous buffer solutions. The fibers were employed in 50 mm-long column formats to assess the relative retention of the two proteins, introduced in a PBST matrix as well as a cell lysate of *E. coli* (NEB 5-alpha *E. coli*). While the former can be considered a fairly pristine matrix, the spiking of the two proteins into the cell lysate introduces a wealth of potential complications in terms of the chemical complexity as well as the viscous nature of the lysate. To introduce a greater challenge in terms of potential competition for surface sites, the EGFP was introduced at a 10-fold excess over the SAV-TXRD; 2.0 M vs 0.2 M.

Table 3.2 Concentrations of SAV-TXRD and EGFP after passing through 50 mm PET C-CP fiber columns (Initial concentrations: SAV-TXRD = 0.2 μM, EGFP = 2.0 μM).

Sample matrix	Column	Concentration of SAV-TXRD (μM)	Concentration of GFP (μM)
PBST buffer	No fiber	0.20±0.001	2.0±0.005
	Native PET	0.20±0.01	2.0±0.02
	Biotin-PET-6	≤0.0030	2.0±0.01
Cell lysate	No fiber	0.20±0.009	2.0±0.004
	Native PET	0.19±0.009	1.9±0.008
	Biotin-PET-6	0±0.004	1.9±0.01

The chromatograms of Fig. 6 display the selectively of the biotin-PET-6 fiber column towards the capture of SAV-TXRD in the presence of a 10x excess of EGFP as they are introduced in a PBST matrix. The respective traces depict one of three separate measurements. In the top row, the transients represent the baseline case wherein the PEEK columns are empty; without any C-CP fiber packing. In the second row, the columns consist of native (i.e., not functionalized) PET fiber packing. As can be seen, the presence of PBST, there is not decrease in the respective protein's fluorescence response, indicating that there is no protein retention. The bottom row reflects the selective capture of SAV-TXRD as the transient never deviates from the background levels, while the signal for the EGFP is unperturbed. Table 2 presents the quantitative results of these experiments. Presented are the corresponding SAV-TXRD and EGFP concentrations based on the integrated fluorescence intensities for triplicate injections. As can be seen, in every case, the EGFP is totally un-retained as there is total recovery of that proteins fluorescence signal. In the case of the target SAV-TXRD, there is no retention observed for the open and native-PET fiber columns. In contrast, there is *at least* 99% retention of the target protein on the biotinylated C-CP fiber surface. Beyond demonstration of the chromatographic selectivity, the extremely high level of reproducibility, must be noted. This is particularly impressive as each experiment represents a separate biontin-PET-6 column. Also of note is the time-scale of the experiments,

reflecting ~10 s transients. Here, it is seen that the mobile phase-surface mass transfer kinetics are indeed quite favorable.

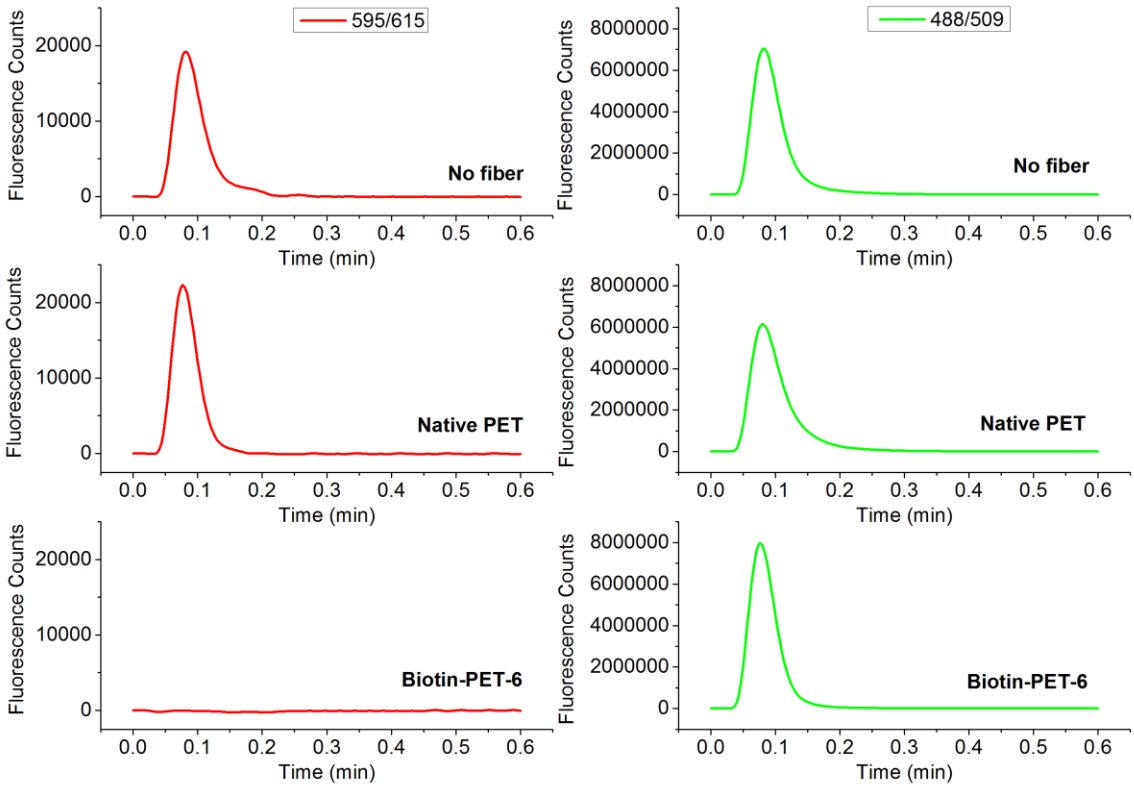

Figure 3.6 Chromatograms of SAV-TXRD capture from a mixture solution of SAV-TXRD and EGFP. Chromatographic condition: biotin-PET-6 column (50 mm long, 0.762 mm i.d.), mobile phase: PBST buffer; flow rate: 1.0 mL $^{-1}$min; sample: PBST solution of 0.2 μM SAV-TXRD and 2.0 μM EGFP; injection volume: 5.0 μL; detection wavelength: 595 nm excitation/615 nm emission for SAV-TXRD, 488 nm excitation/509 nm emission for EGFP.

To further study the capability of capturing streptavidin from a complex matrix, SAV-TXRD was captured from E. coli cell lysate. Here again, SAV-TXRD and EGFP were spiked into the sample at the 0.2 and 2.0 M levels. The traces in Fig 7 follow the same format as Fig. 6, with the inclusion of the native

fluorescence of the lysate constituents included in each chromatogram as a reference point. As can be seen, there is appreciable background fluorescence at the SAV-TXRD excitation/emission combination. As the respective proteins are added to the mixture, the traces reflect the total fluorescence signal. As seen in Fig. 6, there is no difference between the two proteins' fluorescent signals for empty and native-PET columns. On the other hand, introduction of the mixture onto the biotin-PET-6 fiber-packed columns results in a fluorescence signal that is indistinguishable from the lysate background at the 595 nm/615 nm channel. Table 2 presents the quantitative statistics for the SAV-TXRD and EGFP for triplicate experiments/columns. Based on the respective fluorescence responses, >99% of the SAV-TXRD has been retained from the lysate-based matrix, while at the same time, the non-specific hold-up at the EGFP channel was less than <5%. It cannot be concluded here whether the slightly lower fluorescence intensity in this case is due to the in-excess EGFP or other lysate components.

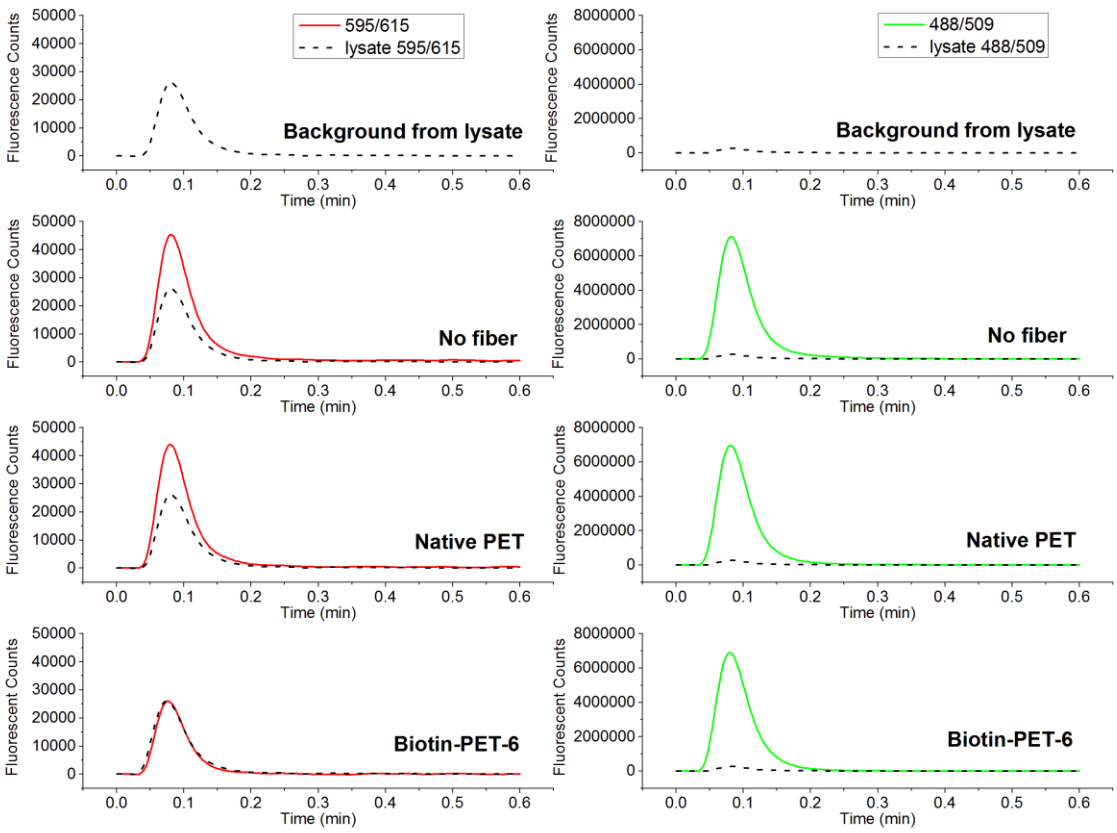

Figure 3.7 Chromatograms of SAV-TXRD capture from E. coli cell lysate containing SAV-TXRD and EGFP. Chromatographic condition: biotin-PET-6 column (50 mm long, 0.762 mm i.d.), mobile phase: PBST buffer; flow rate: 1.0 mL min^{-1}; sample: 0.2 μM SAV-TXRD and 2.0 μM EGFP in E. coli cell lysate; injection volume: 5.0 μL; detection wavelength: 595 nm excitation/615 nm emission for SAV-TXRD, 488 nm excitation/509 nm emission for EGFP.

Conclusions

Previous studies have demonstrated the practical advantages of the C-CP fiber columns in terms of the separation of proteins in terms of high throughput and yields. While the diversity of base polymers presents a certain amount of versatility with regards to the modes of separation, higher levels of selectivity

would serve to complement the physical attributes of the phases. In this study, PET C-CP fibers in HPLC column were treated with EDA to yield a primary amine-rich surface. This is a well-known methodology in the textile industry that can be used to advantage in further ligand binding strategies. Surface amine densities (13.9 – 60.0 mol m^{-2}) were found to be higher than other chromatographic phases reported in the literature or commercially available. A hydrophilic spacer and D-biotin were covalently attached to the EDA-treated PET fiber surface. All stationary phase modifications were performed on-column and controlled by an HPLC pump. Streptavidin binding capacities of biotin-functionalized PET C-CP columns were determined to be from 0.063 mg m^{-2} to 0.97 mg m^{-2} based on the time of EDA treatment. A biotin-PET-6 fiber column (6 min EDA treatment) was found to have a streptavidin binding capacity of 0.35 mg m^{-2} with good binding homogeneity over the entire column length. Biotin-PET-6 fiber column was also capable of capturing streptavidin from E. coli cell lysate with high binding specificity and >99% efficiency.

The SPPS coupling has been studied for more than 50 years and has been demonstrated to covalently attach thousands of ligands, including a variety of affinity ligands that were used in chromatographic separations of protein, to the amine groups on solid supports. The stationary phase functionalization method presented here combines the EDA modification of the PET C-CP fiber surface and the affinity ligand attachment using coupling strategy of solid phase peptide synthesis. The results of this initial proof of concept work demonstrated

the potential of a novel chromatography stationary phase for affinity separations. The possible limitation of the functionalization method is attachment of the ligand that has multiple chemical reactive groups and some of the groups might be indispensable for affinity targeting. In this case, orthogonal protection and de-protection strategies of reactive groups on ligands need to be investigated in the future study. Not limited for affinity chromatography, the future study of PET C-CP fibers will also look at the other chromatography mode. For example, attachment of iminodiacetic acid for immobilized metal affinity chromatography (IMAC), or attaching ion exchangers on stationary phase for ion exchange chromatography (IEC), which are all commonly used in protein downstream processing. The great fluid transport efficiency of PET C-CP fiber is quite attractive in terms of large sized column in preparative chromatography and the format of solid phase extraction (SPE) tip. The inexpensiveness of PET C-CP fiber and the low-cost, simple functionalization method bring functionalized PET C-CP fiber a great promise in bioanalytical applications.

Acknowledgements

This material is based on work supported by the National Science Foundation Division of Chemistry under Grant No. CHE-1307078. L.J. would like to thank Abby Schadock-Hewitt for helpful discussions regarding breakthrough curve experiments and frontal analysis.

References

[1] Marcus, R. K.; Davis, W. C.; Knippel, B. C.; LaMotte, L.; Hill, T. A.; Perahia, D.; Jenkins, J. D. *J. Chromatogr. A* **2003**, *986*, 17-31.

[2] Nelson, D. K.; Marcus, R. K. *J. Chromatogr. Sci.* **2003**, *41*, 475-479.

[3] Fornea, D. S.; Wu, Y.; Marcus, R. K. *Anal. Chem.* **2006**, *78*, 5617-5621.

[4] Nelson, D. M.; Marcus, R. K. *Anal. Chem.* **2006**, *78*, 8462-8471.

[5] Nelson, D. M.; Marcus, R. K. *Protein Peptide Lett.* **2006**, *13*, 95-99.

[6] Pittman, J. J.; Klep, V.; Luzinov, I.; Marcus, R. K. *Anal. Methods* **2010**, *2*, 461-469.

[7] Marcus, R. K. *J. Sep. Sci.* **2008**, *31*, 1923-1935.

[8] Marcus, R. K. *J. Sep. Sci.* **2009**, *32*, 695-705.

[9] Wang, Z.; Marcus, R. K. *J. Chromatogr. A* **2014**, *1351*, 82-89.

[10] Randunu, K. M.; Marcus, R. K. *Biotechnol. Progr.* **2013**, *29*, 1222-1229.

[11] Cuatrecasas, P.; Wilchek, M. *Biochem. Biophys. Res. Commun.* **1968**, *33*, 235-239.

[12] Randunu, K. M.; Marcus, R. K. *Anal. Bioanal Chem.* **2012**, *404*, 721-729.

[13] Stanelle, R. D.; Straut, C. M.; Marcus, R. K. *J. Chromatogr. Sci.* **2007**, *45*, 415-421.

[14] Stanelle, R.; Marcus, R. K. *Anal. Bioanal. Chem.* **2009**, *393*, 273-281.

[15] Schadock-Hewitt, A. J.; Marcus, R. K. *J. Sep. Sci.* **2014**, *37*, 495-504.

[16] Schadock-Hewitt, A. J.; Pittman, J. J.; Christensen, K. A.; Marcus, R. K. *Analyst* **2014**, *139*, 2108-2113.

[17] Mallik, R.; Hage, D. S. *J. Sep. Sci.* **2006**, *29*, 1686-1704.

[18] Goddard, J. M.; Hotchkiss, J. H. *Prog. Polym. Sci.* **2007**, *32*, 698-725.

[19] Tavakoli, M. In *Surfaces and Interfaces for Biomaterials*; Vadgama, P., Ed.; Woodhead Publishing: 2005, p 719-744.

[20] Yang, Q.; Xu, Z.-K.; Dai, Z.-W.; Wang, J.-L.; Ulbricht, M. *Chem. Mater.* **2005**, *17*, 3050-3058.

[21] Herrera-Alonso, M.; McCarthy, T. J.; Jia, X. *Langmuir* **2006**, *22*, 1646-1651.

[22] Jia, X.; Herrera-Alonso, M.; McCarthy, T. J. *Polymer* **2006**, *47*, 4916-4924.

[23] Chen, W.; McCarthy, T. J. *Macromolecules* **1998**, *31*, 3648-3655.

[24] Dave, J.; Kumar, R.; Srivastava, H. C. *J. Appl. Polym. Sci.* **1987**, *33*, 455-477.

[25] Bui, L. N.; Thompson, M.; McKeown, N. B.; Romaschin, A. D.; Kalman, P. G. *Analyst* **1993**, *118*, 463-474.

[26] Avny, Y.; Rebenfeld, L. *J. Appl. Polym. Sci.* **1986**, *32*, 4009-4025.

[27] Bertrand, P.; De Puydt, Y.; Beuken, J. M.; Lutgen, P.; Feyder, G. *Nucl. Instrum. Meth. B* **1987**, *19–20, Part 2*, 887-890.

[28] Wang, J.; Feng, D.; Wang, H.; Rembold, M.; Thommen, F. *J. Appl. Polym. Sci.* **1993**, *50*, 585-599.

[29] Arenholz, E.; Heitz, J.; Wagner, M.; Bäuerle, D.; Hibst, H.; Hagemeyer, A. *Appl. Surf. Sci.* **1993**, *69*, 16-19.

[30] Strobel, M.; Lyons, C. S.; Strobel, J. M.; Kapaun, R. S. *J. Adhes. Sci. Technol.* **1992**, *6*, 429-443.

[31] Yao, Z. P.; Rånby, B. *J. Appl. Polym. Sci.* **1990**, *41*, 1459-1467.

[32] Desai, N. P.; Hubbell, J. A. *Macromolecules* **1992**, *25*, 226-232.

[33] Kim, Y.-W.; Grossmann, T. N.; Verdine, G. L. *Nat. Protoc.* **2011**, *6*, 761-771.

[34] Stanelle, R.; Mignanelli, M.; Brown, P.; Marcus, R. K. *Anal. Bioanal. Chem.* **2006**, *384*, 250-258.

[35] Brown, P. J.; Marcus, K. R.; Webb, C. K.; Sinclair, K.; Stevens, K.; Fuller, L.; Nelson, D. M.; Stanelle, R. D. In *231st ACS National Meeting*; American Chemical Society: Atlanta, GA, United States, 2006, p POLY-277.

[36] Knott, J.; Rossbach, V. *Angew. Makromol. Chem.* **1980**, *86*, 203-213.

[37] Schadock-Hewitt, A. J.; Pittman, J. J.; Stevens, K. A.; Marcus, R. K. *J. Appl. Polym. Sci.* **2013**, *128*, 1257-1265.

[38] Phaneuf, M. D.; Deutsch, E. R.; LoGerfo, F. W.; Quist, W. C.; Bide, M. J.; Zhong, T. *AATCC Rev.* **2005**, *5*, 39-43.

[39] Bryson, D. I.; Zhang, W.; Ray, W. K.; Santos, W. L. *Mol. BioSyst.* **2009**, *5*, 1070-1073.

[40] Merrifield, R. B. *J. Am. Chem. Soc.* **1963**, *85*, 2149-2154.

[41] Lam, K. S.; Salmon, S. E.; Hersh, E. M.; Hruby, V. J.; Kazmierski, W. M.; Knapp, R. J. *Nature* **1992**, *358*, 434.

[42] Lescrinier, T.; Hendrix, C.; Kerremans, L.; Rozenski, J.; Link, A.; Samyn, B.; Van, A. A.; Lescrinier, E.; Eritja, R.; Van, B. J.; Herdewijn, P. *Chem. Eur. J.* **1998**, *4*, 425-433.

[43] Tan, D. S.; Foley, M. A.; Stockwell, B. R.; Shair, M. D.; Schreiber, S. L. *J. Am. Chem. Soc.* **1999**, *121*, 9073-9087.

[44] Roque, A. C. A.; Taipa, M. Â.; Lowe, C. R. *J. Mol. Recognit.* **2004**, *17*, 262-267.

[45] Song, A.; Wang, X.; Zhang, J.; Mařík, J.; Lebrilla, C. B.; Lam, K. S. *Bioorg. Med. Chem. Lett* **2004**, *14*, 161-165.

[46] Ahn, D.-R.; Yu, J. *Bioorg. Med. Chem.* **2005**, *13*, 1177-1183.

[47] Jullian, M.; Hernandez, A.; Maurras, A.; Puget, K.; Amblard, M.; Martinez, J.; Subra, G. *Tetrahedron Lett.* **2009**, *50*, 260-263.

[48] Hood, C. A.; Fuentes, G.; Patel, H.; Page, K.; Menakuru, M.; Park, J. H. *J. Pept. Sci.* **2008**, *14*, 97-101.

[49] Paredes, B.; Suárez, E.; Rendueles, M.; Villa-García, M. A.; Díaz, J. M. *J. Chem. Technol. Biotechnol.* **2001**, *76*, 1171-1178.

[50] Gandhiraman, R. P.; Volcke, C.; Gubala, V.; Doyle, C.; Basabe-Desmonts, L.; Dotzler, C.; Toney, M. F.; Iacono, M.; Nooney, R. I.; Daniels, S.; James, B.; Williams, D. E. *J. Mater. Chem.* **2010**, *20*, 4116-4127.

[51] Lu, H.-T. *Colloid J.* **2013**, *75*, 311-318.

[52] Soto-Cantu, E.; Cueto, R.; Koch, J.; Russo, P. S. *Langmuir* **2012**, *28*, 5562-5569.

[53] 2014, h. w. s. c. u.-s. h. A. J.

[54] Andrzejewska, A.; Kaczmarski, K.; Guiochon, G. *J. Chromatogr. A.* **2009**, *1216*, 1067-1083.

[55] Vera-Avila, L. E.; Gallegos-Perez, J. L.; Camacho-Frias, E. *Talanta* **1999**, *50*, 509-526.

[56] Ormö, M.; Cubitt, A. B.; Kallio, K.; Gross, L. A.; Tsien, R. Y.; Remington, S. J. *Science* **1996**, *273*, 1392-1395.

[57] Stauber, R.; Horie, K.; Carney, P.; Hudson, E.; Tarasova, N.; Gaitanaris, G.; Pavlakis, G. *Biotechniques* **1998**, *24*, 462-471.

CHAPTER IV

POLYETHYLENIMINE MODIFIED POLYETHYLENE TEREPHTHALATE CAPILLARY CHANNELED-POLYMER (C-CP) FIBERS FOR ANION EXCHANGE CHROMATOGRAPHY OF PROTEINS

Introduction

The development and use of protein therapeutics is experiencing phenomenal growth[1]. Over the last decade, the productivity of the protein upstream processes have been greatly improved, further relegating downstream processing as the bottleneck limiting the throughput of current bio-manufacturing [2-5]. The development of high efficiency, low-cost stationary phases for protein separation on the analytical and preparative scales thus continues to be an area of high interest. Capillary channeled polymer fibers (C-CP fibers) have been extensively studied in this laboratory for bio-macromolecule separations [6,7]. C-CP fibers are manufactured by melt-extruding commodity polymers, such as polyester (PET), polyamide (nylon 6) or polypropylene (PP) [8]. These base polymers provide chemical and physical stability over a wide range of the chromatographic conditions used in protein separations. C-CP fibers are unique in shape, with eight capillary channels extending to the whole length of the fiber that gives the fiber ~3X larger surface area then the circular cross-sectional fibers with the same diameters (30 – 50 μm) [8]. When packed in columns, C-CP fibers

self-align and yield a monolith-like structure with 1-5 μm open, parallel channels. These channels provide C-CP fiber packed columns excellent fluid transportation property and low mass transfer resistance, in comparison to the traditional monolithic columns and microsphere packed columns [9]. This allows for the direct loading of complex and viscous feedstock, such as cell fermentation broths, for target molecule capture. It is believed that the high column permeability, low mass transfer resistance and the low cost of the C-CP fiber chromatography columns make them promising choices for fast protein separations at various scales [7,9].

C-CP fiber-packed columns have been used for protein separations in different chromatographic modes, including reversed-phase (RP), ion-exchange (IEC), and hydrophilic-interaction (HIC) as dictated by the surface chemistry of the native fibers. In that regard, and of relevance here, nylon 6 has a polyamide backbone, with end groups that vary in ionic character as a function of pH. As such, that material has been applied previously for HIC, mixed-mode, and cation exchange (CEX) protein separations [10-12]. However, the binding selectivity of the native C-CP fibers limits the development of the practical applications of C-CP fiber chromatography media. Therefore, various surface modification strategies, including physical adsorption and covalent coupling chemistries, have been shown to provide C-CP fibers with a variety of practical functionalities. For example, very robust adsorption of protein A to the surface of PP C-CP fibers has been demonstrated for IgG capture [13]. Likewise, a completely new family

of ligands has been developed based on the high affinity for aliphatic chains for the hydrophobic PP fiber surfaces. Lipid tethered ligands (LTLs) having a variety of capture head groups readily adsorb at room temperature, and are immune from elution/leakage from the column under any sort of conditions common to biomolecule separations [13-16]. An example of covalent coupling involves the use of ethylenediame as a means of activating PET C-CP fibers, yielding a surface rich with primary amines. These amines are then readily modified with capture ligands such as biotin for protein affinity separations [14].

Ion-exchange chromatography is a widely used technique in the bio-separations, including protein downstream processing, because of the use of solvent conditions to do not affect large amounts of protein denaturation [17,18]. Bio-molecules have ionizable chemical moieties that retain them on the charged IEC stationary phase. When the environmental conditions are changed (e.g.,pH, ionic strength), the retained bio-molecules are sequentially eluted from the stationary phase and the separation is then realized. An amine-rich polymer, polyethylenimine (PEI), has been widely used in the chemical modifications of chromatography stationary phases for anion exchange (AEX) separation due to its low-cost and easy availability. PEI has been adsorbed on inorganic supports, including silicas [19,20], zirconia [21,22], graphite [23], and hydroxyapatite [24], followed by cross-linking for ion-exchange chromatography. On organic supports, PEI is usually reacted with surface anchor groups and covalently bound onto the surface. PEI has been used for the modifications of monoliths [25,26], cryogels

[27,28], membranes [29], polymer resins [30], and open-tubular capillaries [31,32] for protein separations.

In this study, PEI has been used for the surface modification of PET C-CP fibers to affect an AEX stationary phase. 1,4-Butanediol diglycidyl ether (BUDGE) was used to cross-link the PEI entities, creating better-ordered and greater density phases[30]. While the primary goal of the effort was to affect greater selectivity than previous found with nylon 6, the on-column modification could not compromise the hydrodynamic advantages inherent to the C-CP fiber format. The accessible amine densities, column permeability, protein dynamic binding capacity, protein IEC performance of the PEI-modified PET C-CP fiber columns were investigated as a function of different surface modification conditions. To the best of our knowledge, this is the first study of using PEI modification of PET to affect a stationary phase medium for AEX protein separations. The results presented here suggest that there is a great deal of practical advantage to combining the enhanced selectivity and capacity of the PEI phase and the previously demonstrated throughput and yield characteristics of C-CP fiber columns [7,33].

Experimental Methods

Materials

Unless otherwise specified, chemicals were purchased from commercially available sources and used without further purification. Polyethylenimine (PEI, MW 10000, 99%) was purchased from Polysciences, Inc (Warrington, PA). Dimethyl sulfoxide (DMSO, ACS grade), pyridine (99%), Tris base (99.8%) were purchased from VWR (Atlanta, GA). 1,4-Butanediol diglycidyl ether (BUDGE, 95%) and all proteins were purchased from Sigma-Aldrich (St. Louis, MO). All HPLC solvents were purchased from EMD (Billerica, MA). Deionized water (DI-H_2O) was obtained from a Milli-Q water system.

Preparation of PET C-CP fiber microbore columns

The C-CP fiber microbore columns were prepared following previously reported methods [9,34]. PET C-CP fibers were obtained from the Clemson University School of Materials Science and Engineering. In this study, 450 PET fibers were pulled through polyether ether ketone tubing (PEEK, 0.762 mm i.d., IDEX Health & Science LLC, Oak Harbor, WA). After packing, the columns were mounted on a Dionex Ultimate 3000 HPLC system (LPG-3400SD Quaternary pump, MWD-3000 UV–Vis absorbance detector, Thermo Fisher Scientific Inc., Sunnyvale, CA) and washed with acetonitrile then deionized water until a stable baseline was observed at 216 nm. Once assembled and cleaned, the microbore

columns could be stored in ambient conditions and cut to appropriate lengths prior to surface modifications.

Single modification of PET C-CP microbore column with polyethylenimine

PET C-CP fibers were packed in columns before modifications. It is easier to pack the fibers before modifications as the fibers may become twisted or folded during the modification process, which would result in inhomogeneous column packing after the fact. Before modifications, PET C-CP columns were mounted on a HPLC pump and washed with DMSO at 0.5 mL min^{-1} for 10min. The columns were then placed in a column heater assembly and connected to a syringe pump that contained the reactive PEI solution. The column heater was set to 100 °C, and solutions of 15% PEI in DMSO were continuously pumped through the columns at a flow rate of 0.6 ml h^{-1} for 2h, 3h or 4h. As such, the surface modification chemistries were varied from 1 – 4 h. The resulting columns were designated as PET-PEI-2h, PET-PEI-3h, and PET-PEI-4h. After the modifications, the columns were brought up to ambient temperature and mounted on the HPLC to be washed with DMSO and water until a stable baseline at 216 nm was observed; reflective of removal of unreacted/unbound PEI.

Multiple modification repetitions of PET C-CP fibers with polyethylenimine and 1,4-Butanediol diglycidyl ether

Before modifications, PET C-CP columns were mounted on a HPLC pump and washed with DMSO at 0.5 ml min^{-1} for 5 min. Different from the simple modification described above, the inclusion of BUDGE cross-linking and multiple repetitions were undertaken under static conditions. In the initial PEI modification step, 10 column volumes (CV) of 15% PEI in DMSO were pumped through the column. Then, the columns were sealed at both ends and placed in an oven at 100 °C for 20 min. After the initial PEI modification, the columns were cooled to room temperature and washed with DMSO at 0.5 ml min^{-1} for 5 min. For the BUDGE modification, 10 CV of 15% BUDGE in DMSO were pumped through the column, the columns re-sealed, and placed in an oven at 100 °C for 20 min. The columns were washed with DMSO at 0.5 ml min^{-1} for 5 min between each modification to remove the unreacted PEI or BUDGE. For the column designated PET-B-P #1, the column was first modified by PEI, followed by BUDGE cross-linking, and an additional PEI application. For the column designated PET-B-P #2, BUDGE and PEI modifications were repeated once beyond that of PET-B-P #1. Finally, for the column designated PET-B-P #3, the BUDGE and PEI modifications were repeated twice beyond that of PET-B-P #1.

After each of modification procedures were completed, the columns were mounted on the HPLC and washed with DMSO and water until a stable baseline absorbance values at 216 nm were observed. Columns were stored under ambient condition with a DI-H_2O fill and sealed with end caps.

Characterization of the modified PET C-CP fibers

The ninhydrin test method was used to determine the primary and secondary amine density on the fiber surfaces as previously described [12,14,35]. Each fiber sample (5-6 mg) was placed into a test tube containing 0.5 ml of 10% isopropanol, 0.5 ml of 10% pyridine and 1 ml of the ninhydrin solution composed of 2.325 mL propionic acid, 12.5 ml 2-methoxyethanol, 5.045 g sodium propionate, and 0.5 g ninhydrin, with the total volume adjusted to 25 mL with deionized water. The test tubes were sealed and heated in a boiling water bath for 30 min. After removal and cooling, 10 mL of 50% ethanol was added to each test tube. The tube was shaken and then left to sit for 15 min. The mixture solution in each test tube was diluted to 25 mL with deionized water prior to the absorbance measurement. The PEI solutions with known concentrations were analyzed following the same procedure and used as calibrants. A ninhydrin test containing no fibers or PEI was used as the blank. The concentration of the PEI was quantified by the absorbance measurements of diluted ninhydrin test solutions performed at 570 nm.

A field emission scanning electron microscope (Hitachi, SU6600, Japan) was used to examine the microscopic morphology of the fibers. The SEM was set to Variable Pressure (VP) mode at 30 Pa. The accelerating voltage was set to 15 kV. An atomic force microscope (AIST-NT SmartSPM 1000, AIST-NT, USA) in AC mode was used to examine the surface morphology of the fibers. The AIST-NT Control software was used to generate the AFM images. The Plane Level function in the software was applied to all AFM images.

Liquid Chromatography

All chromatography experiments were performed on a Dionex Ultimate 3000 HPLC system. The column hydrodynamic properties were determined using DI-H_2O as the mobile phase at different flow rates. The column permeability was calculated by equation 4.1.[28,36]

$$\frac{\Delta P}{L} = \frac{u\mu}{k_w} \qquad \text{(Equation 4.1)}$$

where ΔP represents the column backpressure (Pa), L for the column length (m), u for the linear velocity of the mobile phase (m s^{-1}), μ for the mobile phase viscosity (Pa s) and k_w the column hydraulic permeability.

The dynamic binding capacity (DBC) of the column was determined by load/elution experiments using BSA as the model protein[30]. After equilibration with buffer A (20 mM Tris-HCl buffer, pH = 7.5), the column was loaded with different concentrations of BSA in buffer A at a constant flow rate until a consistent absorbance value for the eluate was achieved, reflecting column saturation. Buffer A was then applied to the column until the absorbance at 280 nm of the eluent returned to baseline, effectively indicating that no non-bound protein existed in the column. Buffer B (1 M NaCl in Buffer A) was then applied to the column for BSA elution. The DBC was calculated based on the integrated absorbance value elution peak as compared calibration curves prepared from injections of BSA without a column present in the system. The response curves

were generated with BSA dissolved in 90:10 ACN:H_2O (RP solvent) and 1 M NaCl in Tris buffer (AEC solvent).

The relative chromatographic performance of the columns was evaluated by injection of a three-protein mixture (BSA, hemoglobin and lysozyme) at different flow rates, with the same gradient programs/rates of buffer A and B. The chromatograms were recorded as the optical absorbance at 280 nm.

Results and Discussions

There have been a number of reports on the use of small-molecule amines to activate and further introduce functionalities to PET surfaces [37-39]. To that end, we have recently reported use of ethylenediamine (EDA) to introduce functional ligands on PET C-CP fiber stationary phase [14], eventually adding biotin ligands to the surface. In that work, amine densities ranging from 13.9 – 60.0 μmol m^{-2} were realized in the initial activation step. In this study, we chose the polymeric amine (PEI) instead of small molecule amines (EDA) for the PET fiber modifications for a number of practical reasons. First, PEI contains primary amines, secondary amines and tertiary amines, while the surface affected by EDA contains only primary amines. Secondary and tertiary amines have better ion-exchange capacity than primary amines [40,41]. In other words, PEI should be a better ion-exchange ligand than EDA. Second, small molecule amines, including EDA, used to modify PET cause structural damage and

mechanical strength loss in the fiber due to the breakage of the ester backbone of the base polymer [37]. In the PEI modification, the polyamines react with multiple ester bonds of the PET (Fig. 1). In this case, the broken ester bonds are *de facto* cross-linked by the polymeric structure of PEI. As a result, the mechanical strength loss from the PEI modification is minimum or negligible [39]. Finally, EDA modification reactions occur not only on the surfaces of the PET fibers, but also in the bulk structure as the small molecules can diffuse through the polymer matrix pore structure and free volume. The created amines in the bulk structure are not accessible by proteins as the average pore size is on the order of 4 nm [42]. On the other hand, PEI (MW 10,000 Da) is excluded from the pore structure, as well as the fiber free volume. The PEI modification only occurs on the surfaces of the PET fibers, resulting in ion-exchangers with better accessibility for proteins. For these reasons, the combined PEI-BUDGE strategy is expected to be a very favorable approach for the modification of PET C-CP fibers to affect AEX stationary phases for protein separations.

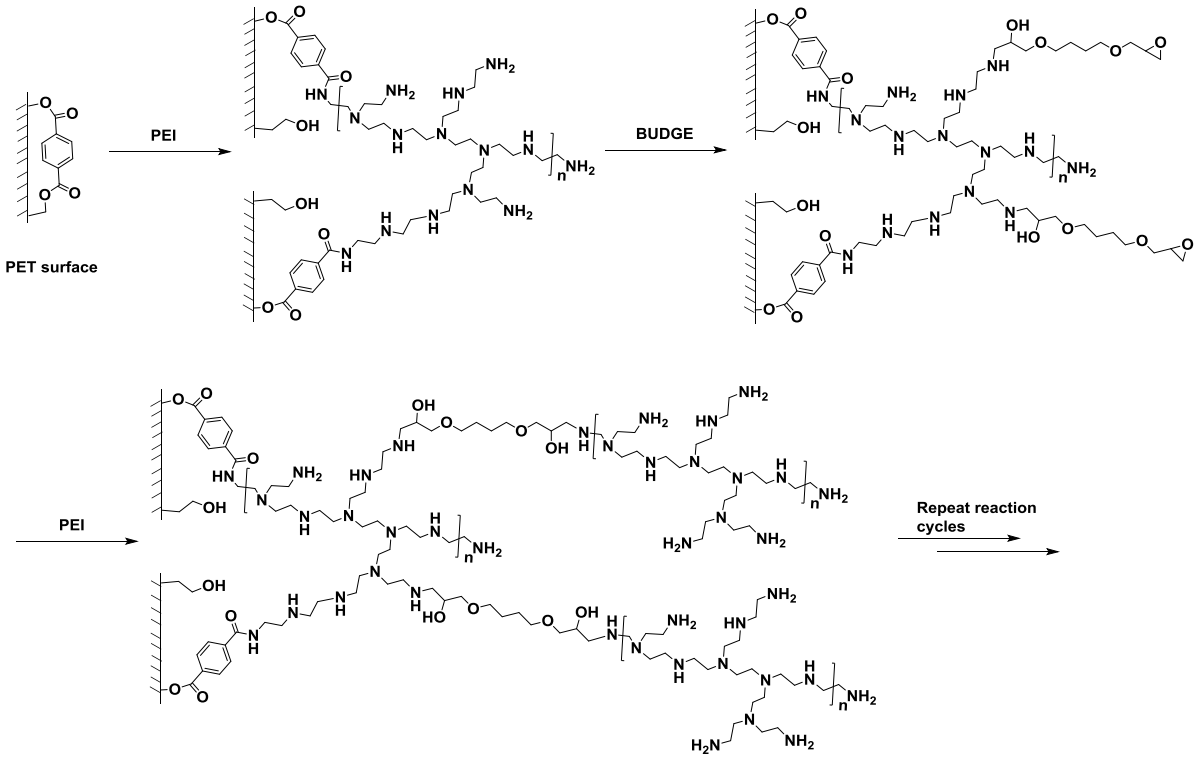

Figure 4.1 Illustrative scheme of surface modifications of PET C-CP fibers (details in text). All reactions took place after PET C-CP fibers were packed in microbore columns.

As reflected in Fig. 1, BUDGE treatment of the PEI-modified PET fibers partially converts the primary amines to secondary amines, and secondary amines to tertiary amines [43,44]. Thus the BUDGE treatment should increase the ion-exchange capacity of the PEI, without altering the net charge. In these experiments, excess amounts of BUDGE were applied in each step, with the unreacted BUDGE in the solution phase washed away. Any partially-reacted BUDGE, with an unreacted oxirane, remains on the PET fiber surfaces (Fig. 1). When a subsequent PEI modification is applied, the PEI reacts with the remnant

oxiranes, increasing the PEI density on the PET surfaces. As implied in the figure, the PEI-BUDGE reaction cycles can be repeated multiple times.

Characterization of PEI- and BUDGE-modified surfaces

The ninhydrin reaction is an effective means to quantify primary and secondary amines in solution and on fiber surfaces [12]. While the most desirable form of amine for AEX separations are tertiary amines, these are not quantifiable. Based on the assumption that the 1°/2°/3° ratio in PEI is 25/50/25 (provided by Polysciences, Inc Warrington, PA), the ninhydrin test should provide a reflection of the 3° species. (As described above this value is still an underestimate as the BUDGE treatment favors an over production of tertiary species versus the other forms.) The results of the ninhydrin determinations are presented in Table 1 as a function of the surface modification conditions. As would be expected, increased reaction times for the straight PEI treatments result in higher densities of 1° and 2° amines, though the effect is not linear across the intermediate (3 h) reaction time. This would seem to suggest that the formation of the PEI layer on PET does not follow a simple kinetic mode. The upper density value of ~143 μmol g^{-1} (48 μmol m^{-2}) is very much in line with the direct EDA treatment of PET [14], which only produces primary amines, and ~2X the primary amine density present as end groups for native nylon 6 C-CP fibers [12].

Table 4.1 Figures of merit for PEI and PEI-BUDGE modified C-CP fiber surfaces and columns.

Stationary phases	1° / 2° amine density (μmol g^{-1})[a]	1° / 2° amine density (μmol m^{-2}) [a,b]	Permeability (10^{-11} m^2)	Q_m (mg mL^{-1})[c]	R^2
Native PET	ND	ND	1.35	0.41	0.9630
PET-PEI-2h	74.8 ± 5.2	24.9 ± 1.7	1.33	1.99	0.9887
PET-PEI-3h	97.4 ± 14.9	32.5 ± 4.6	1.11	2.28	0.9863
PET-PEI-4h	142.7 ± 8.7	47.6 ± 2.9	0.98	2.35	0. 9843
PEI-B-P #1	111.4 ± 5.2	37.1 ± 1.7	1.05	7.15	0.9791
PEI-B-P #2	135.7 ± 10.4	45.2 ± 3.5	0.79	8.54	0.9852
PEI-B-P #3	154.9 ± 17.4	51.6 ± 5.8	0.66	8.32	0.9814

ND – Not detected
[a] – molar concentration based on PEI molecular weight of 10,000 Da
[b] – areal density based on fiber specific surface area of 3 m^2 g^{-1}
[c] – based on fitting of breakthrough data to a simple Langmuir isotherm

When considering the alternating PEI-BUDGE treatments, one would expect that the sequential layers would indeed provide greater primary and secondary amine densities, though with the caveat that there should be some disproportional towards tertiary amines as noted above. The results presented in Table 1 point to an interesting situation where the initial step does indeed yield greater ninhydrin accessible 1°/2° amines, but the successive treatments do not yield appreciable greater densities than the extended period treatments with neat PEI. The PEI density differences indicate that the PEI attachment efficiency of the PEI-BUDGE double modification is higher than the PEI single modification,

which is attributed to the BUDGE cross-linking. Interestingly, each additional PEI-BUDGE cycle adds an equivalent amount of detectable amine density. While seemingly a more complex process, the sequential modification cycles occur over a time frame of 80 min for the PEI-B-P #3, whereas the longest neat PEI treatment takes 4 h. It would seem reasonable, based on the chemistry taking place in the course of the BUDGE cross-linking step, this process should result in a higher density of tertiary amines than the simple PEI treatment of PET, which should be reflected in higher dynamic binding capacities.

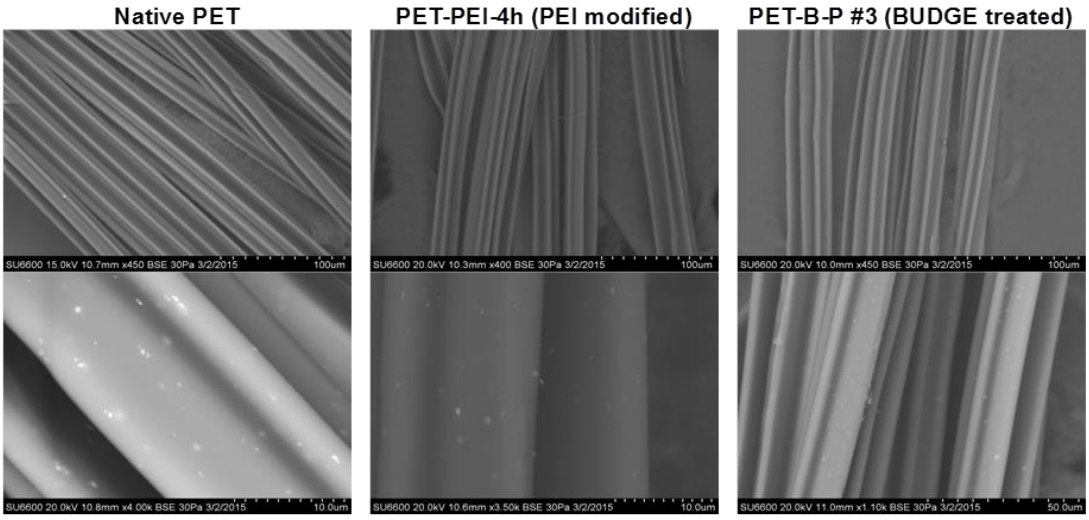

Figure 4.2 SEM images of native and modified PET C-CP fibers.

Column permeability

One of the advantages of using C-CP fiber as liquid chromatography stationary phase is the excellent permeability. This high permeability, coupled with very efficient solute mass transport from the mobile-to-stationary phases

permits high velocity analytical protein separations and high throughput downstream processing[7,9]. These advantages could certainly be compromised in the course of any on-column surface modification. Figure 2 shows SEM images of the native PET, and the PET-PEI-4h and PET-B-P #3 fibers that have recovered from the columns following chemical processing. Equally as important, there does not appear to be any deformation of the channels due to the 100 °C processing temperatures. This observation is perhaps surprising given the fact that the glass transition temperature is about 75 °C[45]. To further examine the potential surface morphology changes caused by the modifications, the fibers were probed via AFM. As shown in Fig 3, the nanometer-scale vertical resolution of AFM indeed reveals substantial changes on the 1 μm^2 fiber plane. Without any modification (Fig. 3a), the native PET C-CP fiber surface is seen to be relatively smooth and flat, with the variations of the surface features being ~$\pm$0.5 nm (the 20 nm vertical scale in that figure is due to a tilt of the fiber surface on the AFM stage). The surfaces of the PEI- and PEI-BUDGE-modified surfaces (Figs. 3b and c, respectively) show dramatically increased surface topography than the PET C-CP fibers.

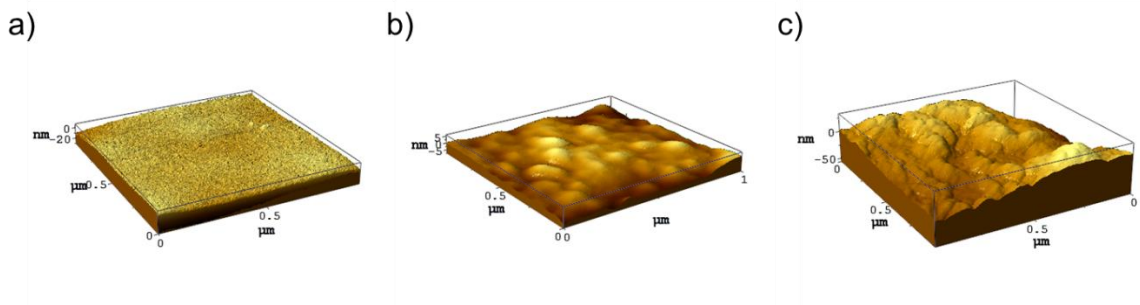

Figure 4.3 AFM images of native and modified PET C-CP fiber surfaces. (a) Native PET C-CP fiber surface, (b) PET-PEI-4h fiber surface, (c) PET-B-P #2 fiber surface.

Whilst the micrometer scale channel characteristics of the fibers appear to be unperturbed, this is no guarantee that the flow characteristics of the C-CP fiber columns are not compromised based on the passage of somewhat viscous solutions at elevated temperatures. Regions of polymer coagulation and solidification would not be unexpected, or at minimum there may be some increase in operating backpressures resulting from the added polymer layers (effectively increasing the fiber diameters) or presenting some resistance to liquid flow. Figure 4 depicts the responses of backpressures of the PET C-CP fiber packed columns at different mobile phase linear velocities. The good linear relationship between the column backpressures and the mobile phase linear velocities indicates negligible fiber compression or other bed perturbation across the linear velocity range of about 44 – 526 cm min^{-1} (equating to volume flow rates of 0.1 – 1.2 mL min^{-1}). In comparison to the native PET column, the increasing slopes of the responses reflect decreases in permeability for all PEI or

PEI-BUDGE modified columns (Table 1). In the PEI modified columns, the columns with longer modification time have lower permeability, which would reflect thicker polymer coatings. In the PEI-BUDGE modified columns, the columns with more reaction cycles have lower permeability, as would be expected. In general, the on-column modifications affected here do not appear to appreciably degrade the hydrodynamic characteristics of the C-CP fiber columns, as high throughput can be achieved at pressures easily maintained by standard HPLC systems.

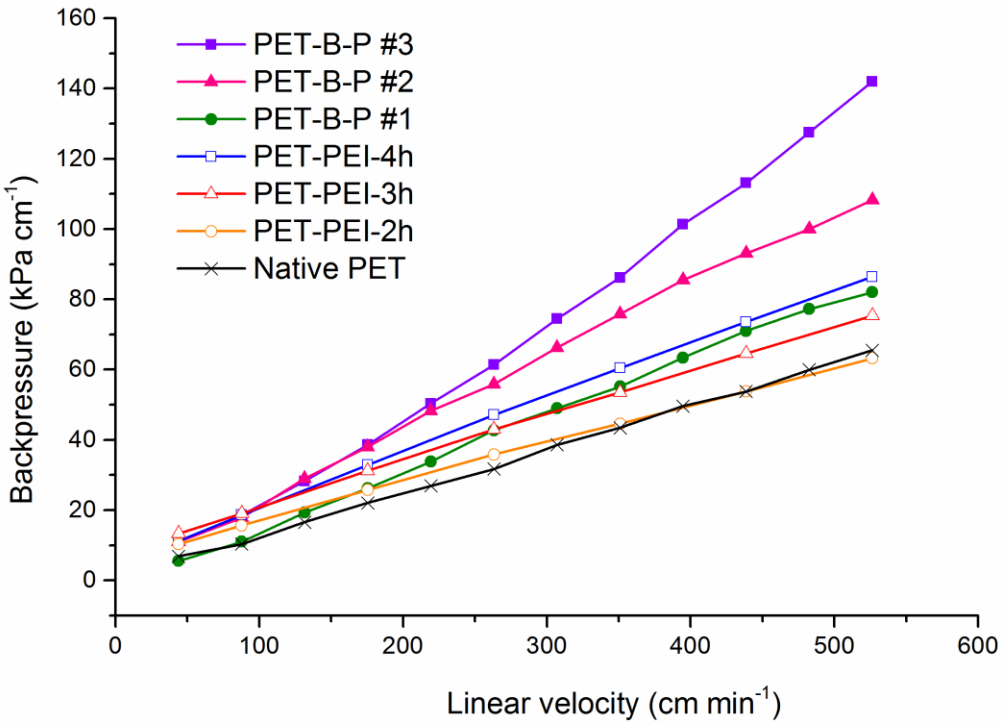

Figure 4.4 Resultant column back-pressures as a function of mobile phase flow rate. Mobile phase: DI-H_2O.

Protein binding capacity

Native PET C-CP fiber packed columns have been studied for RP protein separations. During the PEI modification, the hydrophobic surfaces of the PET fibers are covered by the branched polymer ion-exchangers, resulting in more hydrophilic and positively-charged surfaces. Based on the chemical nature of virtually all protein IEC phases, the retention/elution processes are mixed-mode in nature as the solute-stationary phase interactions have some component of hydrophobic (non-ionic) character. It is therefore instructive to assess the potential extent of these interactions in the modification of PET with PEI. BSA was used here as the model protein for chromatography studies. Figure 5 shows the protein load/elution transients under reversed phase and ion-exchange elution conditions for the native PET and a PET-PEI-4h column. BSA (1 mg mL^{-1}) in Tris-HCl buffer was loaded on each column until saturation was achieved. The protein was then eluted with a) 90:10 ACN:H_2O (RP) or b) 1 M NaCl in Tris-HCl buffer (pH 7.5) (AEC). Under reversed phase conditions, the native PET column yielded a detectable elution peak, while no elution was observed from the PEI-modified PET column. Under ion-exchange elution conditions, the PEI-modified PET column yields a clear elution peak, while no virtually elution peak was observed from the native PET column. The other PEI-BUDGE modified PET fiber columns behave in the same manner as the example here. This relatively simple experiment clearly shows that the BSA interactions with native PET are predominately hydrophobic in nature, with the interactions with the PEI phase being ionic in nature.

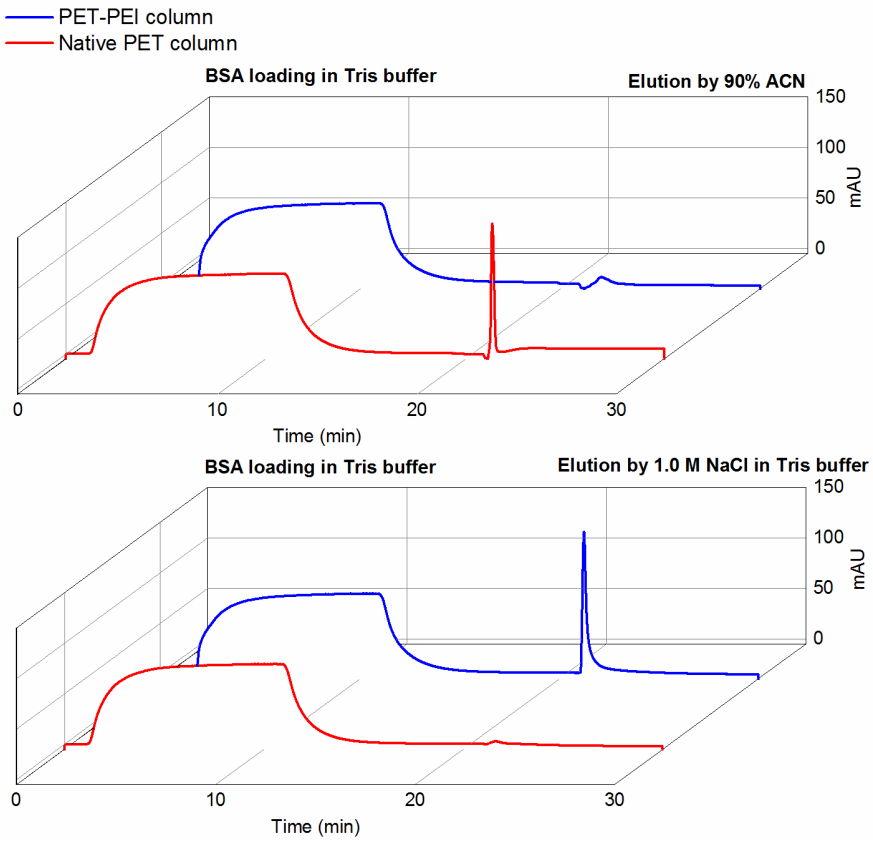

Figure 4.5 BSA loading and elution transients under reversed phase and anion-exchange elution conditions. Columns: Native PET C-CP fiber and PET-PEI-4h. Flow rate: 1 mL min^{-1}. Protein feedstock: 1 mg mL^{-1} BSA in 20 mM Tris-HCl buffer, pH 7.5. Elution buffer a) 90:10 ACN:H_2O (RP elution) and b) 1 M NaCl in 20 mM Tris-HCl buffer, pH 7.5 (AEC elution).

The protein binding capacity of the modified PET C-CP fiber columns was through dynamic load/elution experiments (as illustrated in Fig. 5), and creation of isotherms. BSA (0.1 – 1 mg mL^{-1}) in Tris-HCl buffer (20 mM, pH 7.5) was loaded onto columns at a flow rate of 1 mL min^{-1} (438 cm min^{-1}) until saturation was achieved as judged by the measured absorbance at 280 nm. The columns were then washed with Tris-HCl buffer until the absorbance at 280 nm returned

to baseline values. The elution buffer (1 M NaCl in 20 mM Tris-HCl, pH 7.5) was introduced onto the column until complete elution was achieved. The amount of protein retained on the columns was calculated based on the integrated absorbance of the elution peak and comparisons to calibration curve responses. Previous studies have shown that under dynamic (flow) conditions, the binding capacity of C-CP fiber columns is best modeled according to a Langmuir adsorption isotherm [33]. Figure 6 depicts the dynamic loading characteristics for the native PET and different PEI modification conditions, as a function of loading BSA concentrations (analogous to the measured equilibrium concentration in a static loading experiment). The data was fit to the Langmuir model (Equation 4.2),

$$q = \frac{Q_m c}{K_d + c} \qquad \text{(Equation 4.2)}$$

where c stands for the load concentration of the protein, q for the loading capacity of the column at the protein concentration c, Q_m for the maximum DBC at infinite protein loading concentration and K_d for the dissociation constant. As can be seen, the respective data sets for the different modification conditions are well approximated by the Langmuir fits. Also clear, the data fit into three distinct groups; the native PET, neat PEI-modified PET, and the sequential PEI-BUDGE treatments.

The Q_m values that were obtained from the Langmuir equations are listed in Table 1. The DBC of the native PET C-CP fibers was not detectable under IEC elution conditions as suggested from the response in Fig. 5, and so its value

represents the same injection conditions but with the RP elution solvent. The 0.41 mg mL^{-1} binding capacity value here is not unreasonable versus the DBC for BSA on nylon 6 C-CP fibers of 0.31 mg mL^{-1} obtained via frontal analysis of breakthrough curves [33]. This value is considered to be the DBC baseline based on the binding kinetics (flow rate) and formation of a monolayer of protein on the available fiber surface. Clearly, a dramatic increase in dynamic binding capacity is realized with the simple PEI modification, with the Q_m values increasing with modification time. The ~5X increase in binding capacity upon the initial PEI modification clearly points to the improved enthalpic interactions between the BSA and the aminated surface versus the native PET. Based on the relative permeability of these two columns, there would appear to be no appreciable differences in the stationary phase surface areas. Nor would one expect a kinetic advantage in solute/surface transport and binding kinetics. Referring again to studies of BSA on nylon 6 [33], where the primary reactions are with amine end groups, what is seen here is dramatically enhanced capacity due to the presence of tertiary amines in the PEI case. It is not surprising that the extent of the Q_m value increases for PEI-modified PET columns do not follow the ~2x increase seen in the results of the ninhydrin tests as a function of PEI reaction time. Increased PEI layer thickness is reflected in the lower column permeabilities with reaction time. The ninhydrin results reflect the ability of the small molecule to permeate into the polymer layer, whereas there will not likely be substantial protein ingress. Likewise, there is no guarantee that the number of tertiary

amines increases in direct proportion to the primary and secondary species. Ultimately, the relatively straightforward chemistries here provide substantial increases in dynamic binding capacity under AEX elution conditions.

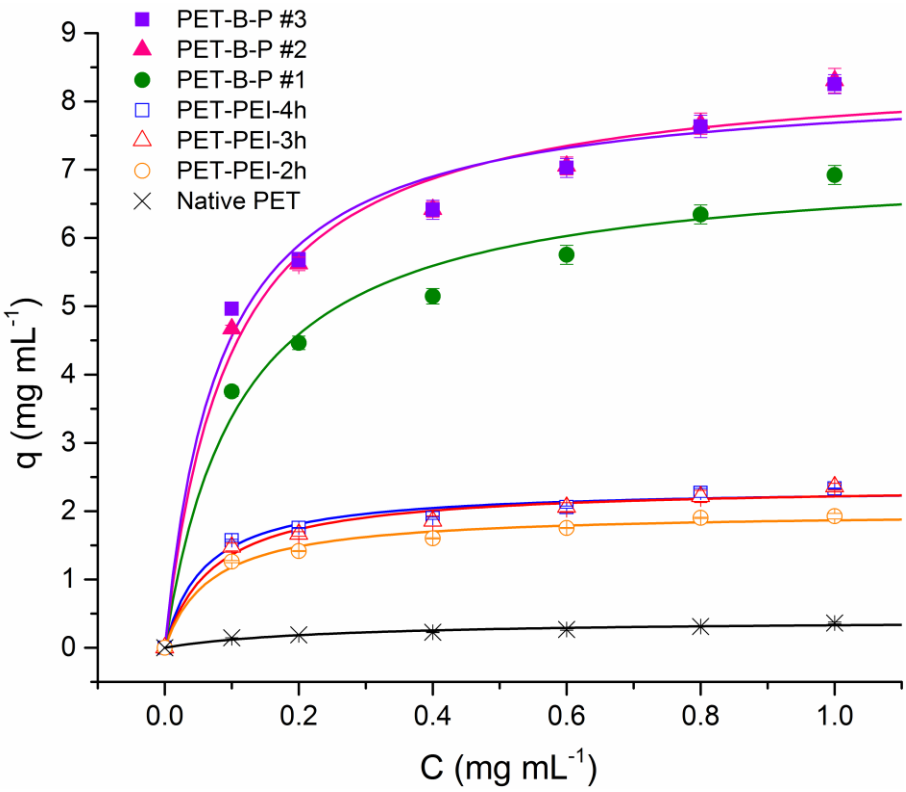

Figure 4.6. Effect of the BSA concentration on the dynamic loading for the native PET, PEI-modified, and PEI-BUDGE-modified PET C-CP fiber columns at a flow rate of 1 mL min^{-1}. Lines reflect the fitting to a Langmuir isotherm model to generate dynamic binding capacities.

When BUDGE crosslinking was used in the PEI modification process, the Q_m values of the columns dramatically increase. The Q_m values of the PEI-BUDGE double modified PET columns are about 4 times greater than the neat-PEI modified columns. Clearly reflected in the AFM micrographs of Fig. 3 and the permeability values of Table 1, the thickness and surface area of the polymer

films are far greater for the PEI-BUDGE system, even though the overall reaction times are far less for the BUDGE system. In comparison, the ninhydrin-based 1°/2° amine densities are not appreciably different in the two cases of the most extensive modifications. As noted previously, the BUDGE modification should yield a higher fraction of 3° amines than the 25:50:25 distribution expected for PEI. Thus it is concluded that the BUDGE modification provides greater capacity through the generation of high tertiary amine densities, that due to the observed topology changes are more accessible by the BSA solutes. This point is made most definitively in comparing the capacities of PET-PEI-4h and PEI-B-P#1, where the former has ~25% higher 1°/2° amine densities, comparable column permeabilities, and yet a factor-of-3 lower BSA binding capacity. As a final note, there is no increase in the DBC values between the PEI-B-P #2 and #3 conditions, as might be expected based on the results of the ninhydrin test. In this instance, it is believed that the there is limited protein ingress to the polymer layer, as well as perhaps constriction within the column structure as reflected in the reduced column permeability. Literally, as fibers come into contact with one another, the solvent/solute do not have access to the fiber surfaces [9,33]. Based on Stoke's radius of BSA (3.48 nm) and the surface area of PET fiber (3 m^2 g^{-1}), the maximum binding capacity of BSA on PET fibers is ~6.65 mg g-1. This number is under the assumption that: (1) PET surface is fully covered by BSA molecules, (2) the size of BSA molecules do not change during binding. (3) there is no protein-protein interaction (no multiple layer of protein adsorption). The

highest BSA binding capacity on PET-PEI/BUDGE phase is 8.54 mg mL^{-1}, which equivalent to ~13 mg g^{-1}. This number is larger than the theoretical maximum binding capacity is due to multiple reasons including (1) PET surface area changed after surface medication, (2) BSA size changes after adsorption, (3) multiple layers of BSA adsorption due to protein-protein interactions.

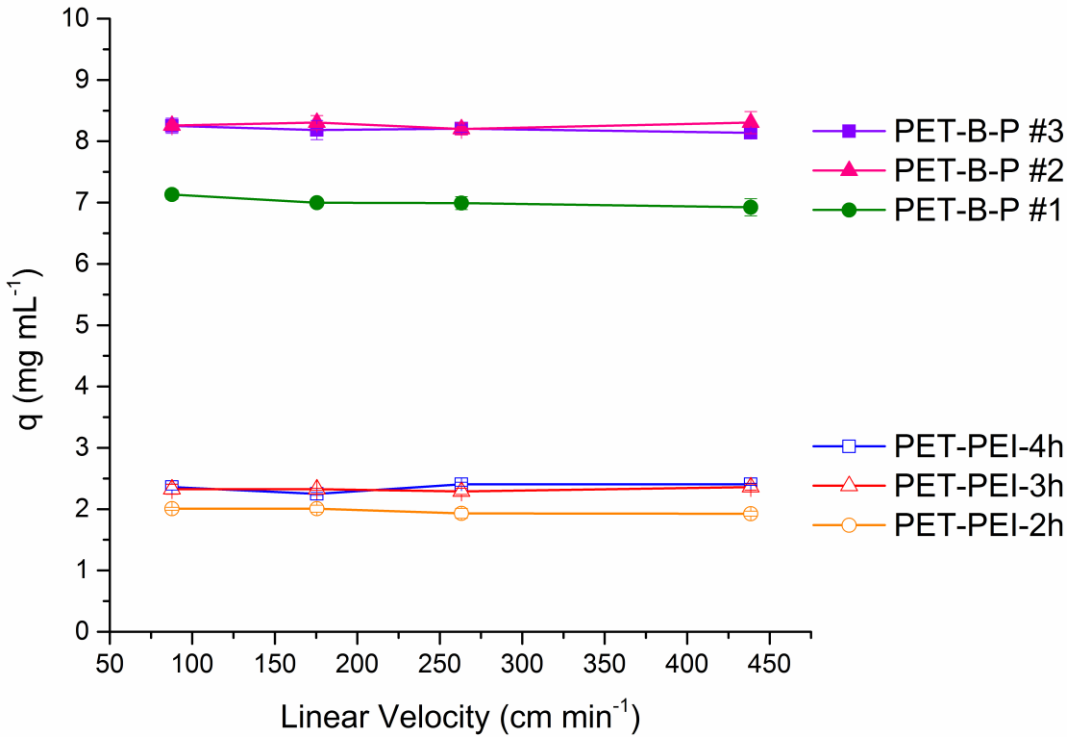

Figure 4.7 Effect of the load linear velocity on the dynamic loading capacity of BSA on PEI-modified, and PEI-BUDGE-modified PET C-CP fiber columns. The BSA loading concentration was 1 mg mL^{-1}.

In the area of downstream processing, the concepts of throughput and yield are of greater importance than the equilibrium binding capacity of a given phase [18]. In this regard, it is important to understand potential tradeoffs

between linear velocity and the load characteristics. A primary advantage of using C-CP fiber columns for protein separations is the low mass transfer resistance of the bed. Figure 7 shows the DBCs of the modified PET C-CP fiber columns at different feed rates for a BSA feed concentration of 1 mg mL^{-1}. By changing the flow rates from ~88 cm min^{-1} to ~438 cm min^{-1} (equivalent to volume flow rates of 0.2 – 1 mL min^{-1} for these columns), there were no significant changes on the DBC values for any of the modified columns. The results suggest that fast protein separations can be achieved on the PEI-modified PET C-CP fiber columns by increasing the flow rate without losing column capacity.

PEI has been employed for the modification of other polymer-based chromatography media for anion exchange protein separations (Table 2). On a bed-volume basis, the protein binding capacity of the modified PET C-CP fiber columns are comparable to the PEI modified cryogel bed, such as resin particle fabricated cryogel monoliths (2.8–11.7 mg mL^{-1}) [27] and nanoparticle coated cryogel monoliths (2.4–11.2 mg mL^{-1})[28], but lower than PEI modified PMA-EDMA monoliths (14.3 mg mL^{-1}) [25]. It is not surprising that the polymer bead media, PGMA-DVB-PEI_{600} resin, provide a much higher capacity (11–26 mg mL^{-1}) than the modified C-CP fibers due to the large specific surface area of the resins [30]. It is also not a surprise that the permeability of the modified PET C-CP fiber media is over 10 times higher than the other literature reported PEI modified media. With the excellent column permeability, the binding capacity of the

modified PET C-CP fiber media was determine at a very high linear velocity (~438 cm min^{-1}), while the DBC values of the literature reported media were determined at relatively low linear velocities (6 – 8 cm min^{-1}). The moderate binding capacity at high flow rates indicates that C-CP fiber media indeed holds promise for high-throughput protein separations.

Table 4.2 Comparison of figures of merit for different PEI protein separation phases.

Stationary phases	DBC or Q_m (mg mL^{-1})	Flow rate DBC/Q_m determination (cm min^{-1})	Permeability k_w (10^{-11} m^2)	Pressure drop (kPa cm^{-1}); 50 cm min^{-1}
PET-B-P (this study)	7.1–8.5	440	0.79 – 1.05	10
Nanoparticle coated and PEI modified cryogel monoliths [24]	2.8–11.7	6	1.86 – 2.88×10^{-2}	NP
Resin particle fabricated and PEI modified cryogel monoliths [25]	2.4–11.2	8	0.75– 1.34×10^{-2}	NP
PEI modified PMA-EDMA monoliths [22]	14.3	6	NP	800
PGMA-DVB-PEI_{600} Resin [28]	11–26	6	NP	400–800

NP: Not provided

Rapid separation of proteins as a function of linear velocity

A consideration in the development of any sort of surface modification strategy, addressed from the process perspective above, is the role of column throughput (linear velocity) on chromatographic efficiency. One must consider any detrimental effects that may results in the creation of polymeric layers as stationary phases. To this end, the PET-B-P #2 column was tested for protein separations at different flow rates. Figure 8 shows the chromatograms of separations of synthetic protein mixture containing lysozyme, hemoglobin, and BSA (0.3 mg/mL for each protein), under the same gradient conditions. In this

demonstration, the elution gradient program remained fixed as a function of elution volume across the various flow rates, rather than a time-based gradient. For each chromatogram, the linear velocity and gradient time are presented. On a constant volume basis, the chromatograms are virtually superimposable, even though the linear velocities are increased from 55 to 438 cm min^{-1} (equivalent to volume flow rates of 0.125 – 1 mL min^{-1}). The only differences are the reduced absorbance values that come about due to the solute dilution with increasing flow rates. The creation of the PEI-BUDGE polymer layer does not impart any sort of mass transfer limitation on the C-CP fiber packed columns, as rapid protein separations can be achieved at increasing flow rates, without suffering from peak broadening.

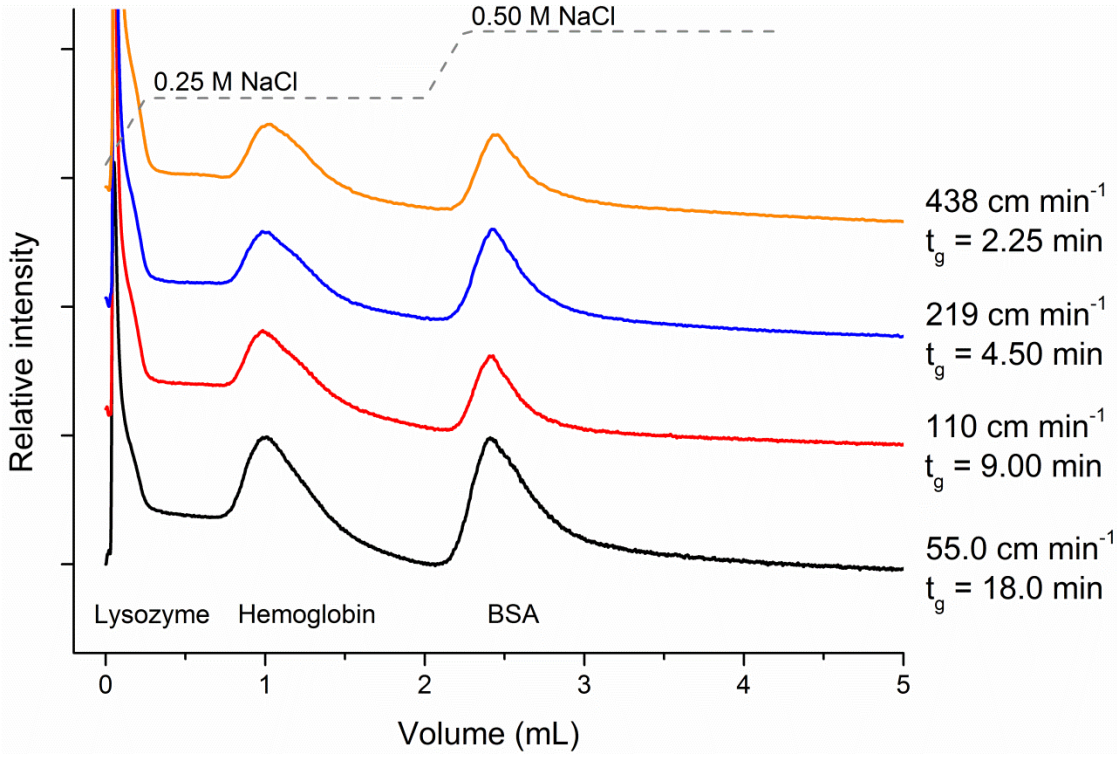

Figure 4.8 Chromatograms for the AEC separation of lysozyme, hemoglobin and BSA (left to right) on PET-B-P #2 at four different flow rates. Separations were carried out with buffer A (20 mM Tris-HCl, pH 7.5) and buffer B (1 M NaCl in buffer A). The gradient was performed from 0% to 25% buffer B across the initial 0.25 mL volume, kept at 25% B for 1.75 mL, then buffer B was increased from 25% to 50% across a 0.25 ml volume and kept at 50% for a total of 2.0 ml.

The qualitative aspects of the separations in Fig. 8 are very interesting from the perspective of previous mixed-mode separations on native nylon 6 C-CP fibers [11,12]. In that system, lysozyme is highly retained as the surface is composed on primary amine end groups and am

ides in the polymer backbone. Here, lysozyme is nearly un-retained, coming off very early in the gradient. The elution order of this C-CP PEI-BUDGE surface here is very much like that reported by Tan et al. on a PEI-modified monolithic column for the same three proteins [25]. Importantly, while the elution volumes of the two separations are comparable (2.5 mL for BSA on the C-CP fibers and ~8 mL for the monolith), the linear velocity of the C-CP fiber column is 438 cm min^{-1}, while the monolith operates at 24 cm min^{-1}. In both cases, though, the columns show no mass transfer limitations over the operable ranges.

Conclusions

Previous studies had shown the potential advantages of using native C-CP fiber packed media for reversed phase and mixed-mode protein separations. In this study, PET C-CP fibers were treated in a relatively straightforward manner

with PEI to generate polyamine layers on the fiber surfaces. BUDGE was used to cross-link the PEI on the fiber surfaces and further increase the PEI density. The extent of the surface modification was monitored to a first approximation via the ninhydrin test of primary and secondary amines. The modified fiber-packed columns were tested for protein anion exchange chromatography in terms of column permeability, protein binding capacity and chromatographic efficiency in fast protein separations. While the neat PEI modifications improved the binding capacity toward BSA versus PET, the cross-linking step substantially improved the binding capacity. This improvement is attributed to the formation of a greater density polymer coating and higher fractions of tertiary amines versus primary and secondary ones. Dynamic binding capacities were found to be invariant with linear velocity, up to values of 440 cm min^{-1}. The AEC separation of a synthetic three-protein mixture confirmed that the formation of the polymer PEI-BUDGE layer did not inhibit the mass transfer kinetics, allowing for separations at the highest linear velocity without compromise in chromatographic quality. It is believed that the PEI-BUDGE-modified PET C-CP fibers have a great potential for high-throughput analytical protein separations and downstream processing.

Acknowledgement

This material is based upon work supported by the National Science Foundation Division of Chemistry under grant CHE-1307078.

References

[1] Fekete, S.; Guillarme, D. *Trends Analyt. Chem.* **2014**, *63*, 76-84.

[2] Gottschalk, U. *Biotechnol. Progr.* **2008**, *24*, 496-503.

[3] Wurm, F. M. *Nat. Biotechnol.* **2004**, *22*, 1393-1398.

[4] Gottschalk, U. *BioPharm. Int.* **2005**, *18*, 42-58.

[5] Thömmes, J.; Etzel, M. *Biotechnol. Progr.* **2007**, *23*, 42-45.

[6] Nelson, D. M.; Marcus, R. K. *Anal. Chem.* **2006**, *78*, 8462-8471.

[7] Randunu, K. M.; Marcus, R. K. *Biotechnol. Progr.* **2013**, *29*, 1222-1229.

[8] Marcus, R. K.; Davis, W. C.; Knippel, B. C.; LaMotte, L.; Hill, T. A.; Perahia, D.; Jenkins, J. D. *J. Chromatogr. A* **2003**, *986*, 17-31.

[9] Randunu, K. M.; Dimartino, S.; Marcus, R. K. *J. Sep. Sci.* **2012**, *35*, 3270-3280.

[10] Stanelle, R. D.; Marcus, R. K. *Anal. Bioanal. Chem.* **2009**, *393*, 273-281.

[11] Stanelle, R. D.; Straut, C. A.; Marcus, R. K. *J Chromatogr. Sci.* **2007**, *45*, 415-421.

[12] Schadock-Hewitt, A. J.; Pittman, J. J.; Stevens, K. A.; Marcus, R. K. *J. Appl. Polym. Sci.* **2013**, *128*, 1257-1265.

[13] Schadock-Hewitt, A. J.; Marcus, R. K. *J. Sep. Sci.* **2014**, *37*, 495-504.

[14] Jiang, L.; Schadock-Hewitt, A. J.; Zhang, L. X.; Marcus, R. K. *Analyst* **2015**, *140*, 1523-1534.

[15] Schadock-Hewitt, A. J.; Marcus, R. K. *J. Sep. Sci.* **2014**, *37*, 3595-3602.

[16] Schadock-Hewitt, A. J.; Marcus, R. K. *Langmuir*, *submitted for publication*.

[17] Jungbauer, A. *J. Chromatogr. A* **2005**, *1065*, 3-12.

[18] Carta, G.; Jungbauer, A. *Protein Chromatography: Process Development and Scale-Up*; Wiley-VCH: Weinheim, 2010.

[19] Vanecek, G.; Regnier, F. E. *Anal. Biochem.* **1982**, *121*, 156-169.

[20] Kopaciewicz, W.; Regnier, F. E. *J. Chromatogr. A* **1986**, *358*, 107-117.

[21] McNeff, C.; Carr, P. W. *Anal. Chem.* **1995**, *67*, 3886-3892.

[22] Hu, Y.; Carr, P. W. *Anal. Chem.* **1998**, *70*, 1934-1942.

[23] Knox, J. H.; Wan, Q. H. *Chromatographia* **1996**, *42*, 83-88.

[24] Murakami, Y.; Sugo, K.; Hirano, M.; Okuyama, T. *Talanta* **2011**, *85*, 1298-1303.

[25] Wang, M.; Xu, J.; Zhou, X.; Tan, T. *J. Chromatogr. A* **2007**, *1147*, 24-29.

[26] Lin, H.; Ou, J.; Tang, S.; Zhang, Z.; Dong, J.; Liu, Z.; Zou, H. *J. Chromatogr. A* **2013**, *1301*, 131-138.

[27] Tao, S.-P.; Wang, C.; Sun, Y. *J. Chromatogr. A* **2014**, *1359*, 76-83.

[28] Wang, C.; Dong, X.-Y.; Jiang, Z.; Sun, Y. *J. Chromatogr. A* **2013**, *1272*, 20-25.

[29] Liu, G.; Dotzauer, D. M.; Bruening, M. L. *J. Membr. Sci.* **2010**, *354*, 198-205.

[30] Zhang, R.; Li, Q.; Gao, Y.; Li, J.; Huang, Y.; Song, C.; Zhou, W.; Ma, G.; Su, Z. *J. Chromatogr. A* **2014**, *1343*, 109-118.

[31] Zhang, X.; Yang, J.; Liu, S.; Lin, X.; Xie, Z. *J. Sep. Sci.* **2011**, *34*, 3383-3391.

[32] Aydogan, C.; Cetin, K.; Denizli, A. *Analyst* **2014**, *139*, 3790-3795.

[33] Wang, Z.; Marcus, R. K. *Biotechnol. Progr.* **2015**, *15*, 97-109.

[34] Stanelle, R. D.; Mignanelli, M.; Brown, P.; Marcus, R. K. *Anal. Bioanal. Chem.* **2006**, *384*, 250-258.

[35] Knott, J.; Rossbach, V. *ANGEW MAKROMOL CHEM* **1980**, *86*, 203-213.

[36] Rendueles de la Vega, M.; Chenou, C.; Loureiro, J. M.; Rodrigues, A. E. *Biochem. Eng. J.* **1998**, *1*, 11-23.

[37] Bide, M.; Zhong, T.; Ukponmwan, J.; Phaneuf, M.; Quist, W.; LoGerfo, F. *AATCC Rev.* **2003**, *3*, 24-28.

[38] Chen, W.; McCarthy, T. J. *Macromolecules* **1998**, *31*, 3648-3655.

[39] Avny, Y.; Rebenfeld, L. *J. Appl. Polym. Sci.* **1986**, *32*, 4009-4025.

[40] Neue, U. D. *HPLC Columns: Theory, Technology, and Practice*; Wiley-VCH: New York, 1997.

[41] Cunico, R. L.; Gooding, K. M.; Wehr, T. *Basic HPLC and CE of Biomolecules*; Bay Bioanalytical Laboratory: Richmond, CA, 1998.

[42] Wang, Z.; Marcus, R. K. *J. Chromatogr. A* **2014**, *1351*, 82-89.

[43] Goyal, R.; Bansal, R.; Tyagi, S.; Shukla, Y.; Kumar, P.; Gupta, K. C. *Mol. Biosyst.* **2011**, *7*, 2055-2065.

[44] Swami, A.; Kurupati, R. K.; Pathak, A.; Singh, Y.; Kumar, P.; Gupta, K. C. *Biochem. Biophys. Res. Commun.* **2007**, *362*, 835-841.

[45] Zhang, Y.; Zhang, J.; Lu, Y.; Duan, Y.; Yan, S.; Shen, D. *Macromolecules* **2004**, *37*, 2532-2537.

CHAPTER V

COMPARISON OF ANALYTICAL PROTEIN SEPARATION CHARACTERISTICS FOR THREE AMINE-BASED CAPILLARY-CHANNELED POLYMER (C-CP) STATIONARY PHASES

Introduction

The breadth and scope of protein separations is incredibly diverse. Analytical-scale protein separations are essential in almost all forms of “omics”, biomarker identification, and clinical diagnostics. Common to each of these applications are aspects of small quantities/volumes of protein and the need for high chromatographic resolution/peak capacity, and to lesser extents speed and compatibility with some form of post column detection method. Protein separations are performed on numerous platforms including high performance liquid chromatography (HPLC), capillary electrophoresis (CE), two-dimensional electrophoresis, and various formats of solid phase extraction [1]. There is also the realm of separations in downstream processing as needed in the manufacture of protein therapeutics. In 1982, human insulin received U.S. approval as the first genetically engineered protein-based drug [2]. The sales of biologics has grown from 20 billion dollars in 2000 (10% of the global drugs market) to 159 billion dollars in 2014 (29% of the global drugs market) [3]. In 2014, the Center for Drug Evaluation and Research approved 11 biologics (27% of FDA total approvals), which increased from just 2 (7%) in 2013 and 6 (15%) in

2012 [4,5]. The performance metrics for downstream processing differ from analytical separations. In downstream processing, the throughput, yield, and purity of the process are primary drivers, with operational overhead (primarily back pressure) and column lifetimes being lesser concerns [6,7].

When considering the liquid chromatography (LC) separation of proteins on either the analytical or preparative scales, the choice of the support/stationary phase sets the basis for overall kinetics of the separation process. Different from the case of “small molecule” separations, the slow diffusion of proteins limits the timescale over which efficient separation can take place as well as the fraction of the stationary phase that can be accessed in the process. Beyond kinetic considerations, the support must be chosen to provide a suitable substrate for the desired stationary phase (ligand) modifications as well as to physically and chemically withstand the separation conditions. Traditional small diameter, highly porous silica HPLC support phases are excellent for small organic molecule separations because of the large surface area and ability to generate highly uniform beds. However, these supports suffer from several drawbacks when they are applied to protein separations [8,9]. Due to the large size of proteins, proteins diffuse slowly into and out of the pores of silica beads, results in peak broadening and tailing. Also, due to the complexity of the biological samples, pore clogging is a common problem. For these reasons, a great deal of effort is placed in the use of superficially porous silica phases as means of enhancing the kinetics of protein separations [10,11]. In terms of the chemistry

of the base material, some protein separation modes (e.g., ion exchange), require changing of the mobile phase pH across a broad range of values. Silica-based materials are generally not stable under basic conditions. Finally, biomolecule separations are subject to non-ideal, if not irreversible, interactions with residual surface silanol groups.

Polymer-based support/stationary phases, such as monoliths, polymer bead and fiber-packed beds have been employed for diverse protein separations across the analytical and preparative scales [9,12,13]. As a general rule, polymeric phases possess diametrically opposite physical and chemical attributes to silica phases. That is, the traits that make them inferior performers towards small molecule separations are very favorable in terms of protein chromatography. Polymeric phases tend to be non-porous with respect to the ingress of proteins, while also exhibiting a high level of column permeability. While the first attribute limits the binding capacity of the phases, the latter suggests high levels of throughput. In addition, the diversity of available polymer chemistries provides both a level of robustness as well as versatility towards the coupling of selective stationary (ligand) phases.

Capillary-channeled polymer (C-CP) fibers have been extensively studied as protein separation media in this laboratory [14-16]. C-CP fibers are made via melt extrusion, with the most commonly used polymers including polypropylene (PP), polyester (PET) and polyamide (nylon 6). Their unique shape gives C-CP fibers ~3X more surface area than circular-shaped fibers with the same

diameters (30-50 µm). When packed into columns, C-CP fibers self-align, resulting in a monolith like structure with 1-5 µm diameter parallel channels. In comparison to the size of proteins, the C-CP fiber surface is non-porous, which reduces mass transfer resistance [15,17,18]. As a result, separations can be run at high linear velocity (100 mm s^{-1}) and low backpressure (<2000 psi), without sacrifices due to van Deemter C-term broadening.

The base polymer identity of C-CP fibers provides different surface chemistries, and thus protein separations are affected in different modes. PET and PP C-CP fibers have been used for reversed phase (RP) chromatography, due to their hydrophobic surfaces [14,19,20]. Nylon 6 C-CP fibers, with amine and carboxylic acids present on their surfaces have been used in mixed-mode ion-exchange [21] and hydrophobic interaction chromatography (HIC) separations [15]. The base chemistry of the C-CP fibers can be tailored by modifying the surface by adsorbing or covalently-coupling selective functional groups/molecules. For example, PP can be modified by adsorption of protein A to affect IgG capture [22]. A new approach, termed lipid tethered ligands (LTLs) [23-25], involves adsorption of hydrophobic lipid tails to anchor selective hydrophilic head groups to the PP fiber surface. Surface-modified PET C-CP fibers have been studied for affinity chromatography following activation via simple diamine chemistry [26]. Recently we reported the use of polyethylenimine (PEI)-modified PET C-CP fibers for weak anion exchange (WAX) separations of proteins [27]. The initial characterization was focused on the performance merits

of the materials in downstream processing scenarios. The PEI modified PET columns (PEEK, 0.762 mm i.d.) showed excellent column permeability of 0.66×10^{-11} to 1.33×10^{-11} m^2, with a BSA dynamic binding capacity of 2.35 mg mL^{-1}. When a cross-linker (1,4-butanediol diglycidyl ether) was used in the modification, the BSA binding capacity increased to 8.54 mg mL^{-1}. Fast protein separations were demonstrated on the PEI/BUDGE modified columns at high mobile phase linear velocity (up to 438 cm min^{-1}) without loss of resolution.

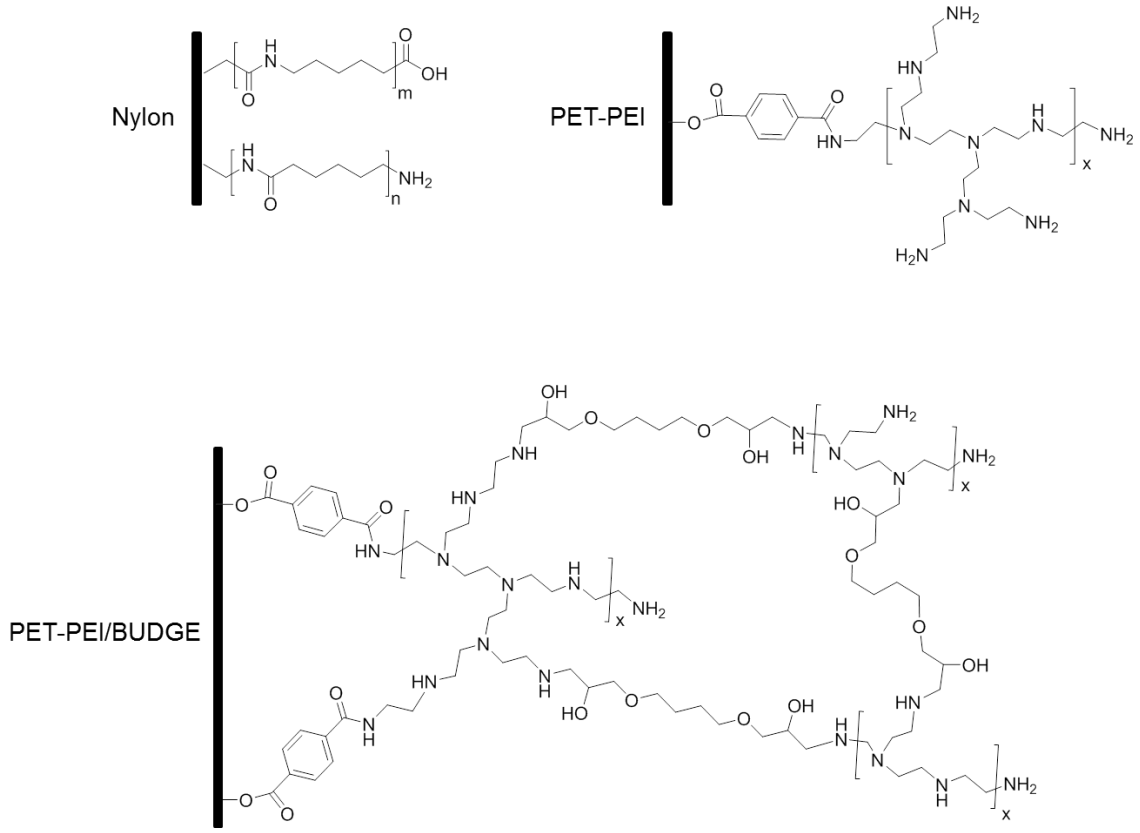

Figure 5.1 Representations of the chemical functionality of the surfaces of nylon 6, PET-PEI, and PET-PEI/BUDGE C-CP fibers.

While the PEI/BUDGE-modified PET column is believed to be promising in protein downstream processing, more work is needed in terms of the analytical characterization of that material. In that regard, we present here a comparison of the basic characteristics the of PEI/BUDGE system to that of PEI-modified PET and native nylon 6 C-CP fibers. As shown in Fig. 1 and Table 1, the three stationary phases have quite different types of amine functionality and density, which are evident in the ion exchange separation of a simple three-protein test suite. Indeed, differences are seen in both the enthalpic and kinetic aspects of the separations as changes are made in mobile phase velocities and gradient elution rates. Studies such as these not only improve the capabilities to use these materials, but also basic understanding towards the development of other modified C-CP fiber phases used for protein separations on the analytical and preparative scales.

Table 5.1 Figures of merit for native and modified C-CP fiber surfaces and columns.

Support/stationary phase	1° / 2° amine density (μmol g^{-1})	Permeability (10^{-11} m^2) [28]	Q_m (mg mL^{-1})[a]
Nylon 6	78.6 ± 1.2 [33]	1.30	0.31[b][32]
Native PET	ND	1.35	0.41 [28][b]
PET-PEI	142.7 ± 8.7 [28]	0.98	2.35 [28]
PEI-PEI/BUDGE	135.7 ± 10.4 [28]	0.79	8.54 [28]

ND – Not detected
[a] – Q_m is the maximum dynamic binding capacity at infinite protein loading concentration from fitting of breakthrough data to Langmuir isotherm
[b] – based on reversed phase mode

Experiment Procedure

Materials

Unless otherwise specified, chemicals were purchased from commercially available sources and used without further purification. Polyethylenimine (PEI, MW 10000, 99%) was purchased from Polysciences, Inc (Warrington, PA). Dimethyl sulfoxide (DMSO, ACS grade), pyridine (99%), and Tris base (99.8%) were purchased from VWR (Atlanta, GA). 1,4-butanediol diglycidyl ether (BUDGE, 95%) and all proteins were purchased from Sigma-Aldrich (St. Louis, MO). All HPLC solvents were purchased from EMD (Billerica, MA). Deionized water (DI-H_2O) was obtained from a Milli-Q water system.

Preparation of nylon 6 and PET C-CP fiber microbore columns

The methods of packing the C-CP fiber columns have been previously reported [14,20]. Nylon 6 and PET C-CP fibers were obtained from the Clemson University School of Materials Science and Engineering [28]. Either, 720 nylon 6 fibers or 450 PET fibers were pulled through polyether ether ketone tubing (PEEK, 0.762 mm i.d., IDEX Health & Science LLC, Oak Harbor, WA) in such a way that the fibers are aligned in a parallel fashion, with column interstitial fractions of $\varepsilon_i \approx 0.55$ as determined by the elution characteristics of proteins injected under non-retentive solvent conditions. After packing, the columns were connected to a Dionex Ultimate 3000 HPLC system (LPG-3400SD Quaternary pump and MWD-3000 UV–Vis absorbance detector, Thermo Fisher Scientific

Inc., Sunnyvale, CA) and washed successively with acetonitrile and DI-H_2O until a stable baseline was observed at 216 nm. Once assembled and cleaned, the microbore columns could be filled with DI-H_2O, capped, and stored at ambient conditions prior to surface modifications or protein separation.

Modification of PET C-CP microbore columns with polyethylenimine and BUDGE

The details of the modification procedures were reported previously [27]. In all instances, the fiber modifications are performed on-column using a standalone syringe pump to deliver the solutions. In this way, the physical structure of the column is established before the chemistries, rather than modifying the “loose” fibers and then packing the columns. PET C-CP columns were washed with DMSO at 0.5 mL min^{-1} for 10 min then PEI modification was affected by passing a 15% (w:v) solution of PEI in DMSO through the columns at a flow rate of 0.6 ml h^{-1} for 4h at 100 °C, using a column heater to control the column temperature. The resulting columns were designated as PET-PEI. After modification, the columns were equilibrated to ambient temperature and washed with ~ 200 CV of DMSO. The columns were then connected to the HPLC to be washed with ACN, and DI-H_2O to remove the unreacted chemicals on the fiber, until a stable absorbance baseline at 216 nm was observed in each case. For the PEI/BUDGE double modification (two complete cycles), 10 column volumes (CV) of 15% PEI in DMSO were first pumped through the column. Then, the columns were sealed at both ends and placed in an oven at 100 °C for 20 min. After the

initial PEI modification (and each of the subsequent treatments), the columns were cooled to ambient temperature and washed with DMSO at 0.5 ml min^{-1} for 5 min. The initial cross-linking was accomplished by pumping 10 CV of 15% BUDGE in DMSO (v:v) through the column, the columns re-sealed, and placed in an oven at 100 °C for 20 min. Unreacted PEI or BUDGE was removed by washing with DMSO at 0.5 ml min^{-1} for 5 min. The BUDGE and PEI modifications were repeated to effectively create a double layer of cross-linked PEI. The column were finally washed with ~200 CV of DMSO then connected to the HPLC and washed with ACN and DI-H2O until a stable absorbance baseline was observed at 216 nm in each case. The resulting columns were designated as PET-PEI/BUDGE. All columns were stored under ambient conditions with a DI-H_2O fill and sealed with end caps.

Liquid chromatography system

All chromatography experiments were performed on the Dionex Ultimate 3000 HPLC system using a UV-Vis detector at 280 nm. The relative chromatographic performance of the columns was evaluated by injection of a three-protein mixture (bovine serum albumin (BSA), hemoglobin and lysozyme) at different flow rates and gradient rates of buffer A (20 mM Tris-HCl buffer, pH = 7.5) and B (1 M NaCl in mobile phase A). The chromatograms were recorded as the optical absorbance at 280 nm. After each separation, buffer A was applied to the column until the absorbance at 280 nm of the eluent returned to baseline, effectively indicating that no non-bound protein existed in the column.

Results and Discussions

C-CP fiber media have been shown to provide fast protein separations at high linear velocities (upwards of 100 mm sec^{-1}) due to their high column permeability and lack of stationary phase mass transfer limitations. A more subtle result of the small diameter parallel channels formed in the column is an enhancement of the mobile phase-to-stationary phase mass transfer at high shear rates [29], as a result there is no penalty towards dynamic binding capacity at these velocities [30,31]. Beyond these kinetic aspects due to the fiber physical structure, it is the surface chemistry which determines the nature of the protein separation. Native nylon 6 C-CP fiber packed columns have been used for IEC and HIC protein separations [15,21,32]. Nylon fibers have three different functional groups on the surface as depicted in Fig. 1; amide, primary amine and carboxylic acid. The amine and carboxylic acid polymer end groups provide the electrostatic interaction sites for ion-exchange, while the amide moiety enhances the hydrophilicity of the nylon surface; reducing the hydrophobic interactions of proteins. The presence of both anion (amine) and cation (carboxylic acid) (i.e., zwitterionic) exchangers at neutral pH [33] yields a mixed-mode separation scenario, dependent upon the isoelectric point of the respective proteins (though this is an admitted oversimplification). In reality, these two functional groups lead to “weak” ion exchange capacities [34].

To further develop the potential of using C-CP fibers for IEC protein separations, native PET C-CP fibers have been chemically modified with PEI to yield polyamine surfaces [27]. Due to the large molecular size of PEI, the primary amines react with the esters on PET surfaces without entering the bulk structure, minimizing physical integrity loss of the fibers [35]. PEI has primary, secondary and tertiary amine groups with the approximate ratio of 1:2:1 (provided by the manufacturer), as illustrated in Fig. 1. While the primary amines may have strong binding to proteins, the secondary and tertiary amines provide better ion-exchange capacity [1,34]. BUDGE not only reacts with PEI to convert the primary amines to secondary amines and the secondary amines to tertiary amine, it cross-links the PEI to generate a more structured surface layer, as implied in Fig. 1 [36]. Two other important features are that the BUDGE processing allows for the addition of more PEI layers (greater loading), as well as effectively creating a hydrophilic barrier above the base polymer surface. In this regard, the level of hydrophobicity-driven protein retention should be reduced.

Comparison of fiber and column characteristics

Observed analytical separation characteristics are the product of the physical and chemical characteristics of the fiber support/stationary phases and the column packing/hydrodynamics. In this work, four basic fiber/column systems are compared: native nylon 6, native PET, PEI-modified PET, and the PEI/BUDGE-modified PET. Table 1 presents the essential characteristics of these fibers/columns. In the first column, the molar densities of primary and

secondary (1°/2°), as determined through Ninhydrin reactions, are presented (tertiary amines (3°) are not detected). As expected, no amines were detected on the native PET fibers. The initial PEI modification approximately doubles the density of the "accessible" amines over that of native nylon 6. The BUDGE modification (which should yield significantly more PEI on the surface) does not appreciably shift the amine distribution towards more 2° and 3° species. In addition, there is no way to judge the fraction of amines that are actually accessible by the Ninhydrin reagent.

The permeability of the columns is also presented. The interstitial fractions of C-CP fiber columns affect the hydrodynamics and resultant band broadening [37]. In this case, the native nylon 6 and PET columns have very similar permeability. Without considerations of the surface chemistry difference, they should have very similar peak characteristics. PEI and PEI/BUDGE modification of PET columns decreases the column permeability as the polymer layers are added to the fiber surfaces. Based on previous studies [16], it is expected that eluting proteins should change little in elution band widths based on the lower permeability.

The final points of comparison, certainly more important in terms of downstream processing, are the dynamic binding capacities of the respective C-CP fiber columns. The values were determined by dynamic loading – elution (recovery) studies [27]. A dramatic difference is seen between the native and modified fibers for the binding of BSA. In Table 1, the dynamic binding capacity

for BSA is very similar on both the native nylon 6 and PET surfaces (under reversed-phase conditions), while the PEI and PEI/BUDGE modifications increase the loadings appreciably, by approximately 20X in the latter case. This relationship seems reasonable if one assumes that proteins adsorb onto the surface in the native fibers, while the two modifications create greater surface area as seen in AFM imaging [27], and indeed may have some level of protein permeability within the PEI/BUDGE layers. This latter point might be expected to have implications in the chromatographic quality of analytical protein separations.

General assessment of retention

Different from either RP or HIC separations, the retention/elution behavior of proteins via IEC is dependent on a variety of experimental parameters that will affect the charge characteristics of both the stationary phase and the proteins of interest. To illustrate the basic differences of the native nylon 6, PET-PEI, and PET-PEI/BUDGE C-CP fiber-packed columns, single protein injections were performed under a fixed set of chromatographic conditions. BSA solution (3 µL, 1.0 mg mL^{-1} in Tris buffer) was injected on to each column under 100% of buffer A at a flow rate of 0.4 mL min^{-1}. The proteins was eluted with a 2 min gradient of 0-to-100% mobile phase B and the retention times/elution compositions recorded. As presented in Table 2, the BSA retention characteristics are statistically different for the three amine phases (single-protein injections were performed in triplicate on each column) . As mentioned previously, under the conditions of these separations, buffered at pH 7.5, the nylon 6 surface is zwitterionic, with

approximately the same number of anionic and cationic sites, with the PEI-based phases being cationized amines. Seen here is the fact that BSA experiences lesser amounts of electrostatic retention on nylon 6 than PEI. It is important to note that IEC is a displacement form of separation, and so the NaCl gradient can affect either cation or anion displacement with increasing salt content. Based on its pI of 4.7, BSA is charge-negative (net), but this does not explicitly mean that it is those species that are interacting with the stationary phase. In general, it would be expected that the interaction would be less extensive on the lower charge density (Table 1), zwitterionic surface.

Table 5.2 Elution times and corresponding mobile phase compositions for single-protein (BSA) injections on C-CP fiber columns.

Support/Stationary Phase	t_R (min)	%B
Native Nylon	2.21 ± 0.003	5.5 ± 2.5
PET-PEI	3.31 ± 0.006	60 ± 2.5
PET-PEI/BUDGE	3.14 ± 0.006	52 ± 2.5

The relative retentivity of BSA towards the PEI and PEI/BUDGE surfaces is similar, but is lesser on the BUDGE cross-linked phase. In this case, while it is PEI that molecule that is the WAX-active component, there are two chemical differences that explain the retention characteristics. First, the cross-linking of the PEI entities shifts the distribution among the types of amines more towards secondary and tertiary forms, away from greater fractions of primary amines [36,38] . In this way, the extent of the protein-amine interactions is reduced. A

second contribution may be seen in the fact that the BUDGE cross-linking creates a more dense PEI architecture, which also contains some of the hydrophilic character of the epoxide linkers. Finally, if one considers that BUDGE is the linker of the ligand PEI, the relative retention follows what was observed by Lenhoff and co-workers, that as ligand linker arms decrease in length, strong cation exchange is enhanced [39].

The protein recoveries were examined by injections of BSA and lysozyme as model proteins under non-retained condition. For each test, 3 μL of 1.0 mg mL^{-1} BSA or lysozyme was injected in to a 20 cm column at 100% mobile phase B. Same injections were performed without any columns installed and the elution peak was recorded as 100% recovery. The recoveries were determined by comparing to the elution peaks with and without column installed. The results are from the average of 5 injections and presented in table 3. The BSA and lysozyme recovery on the PET-PEI and PET-PEI/BUDGE columns are around 94% to 97%. Interestingly, BSA was loaded into the modified PET columns and eluted under reverse phase conditions in the previous study but no protein elution was observed.[27] The lack of fully recovery is possibly due to the hydrophobic nature of the base PET polymer surface which causes protein un-folding and strongly binds to the stationary phase. On native nylon column, 94% recovery of BSA and 90% recovery of lysozyme were obtained. Previous study showed that protein loading and elution could be performed on native nylon column under reversed phase conditions.[31] The protein binding on the native nylon is from the

combination of ionic interaction and hydrophobic interaction. As the ionic strength of the mobile phase increases, the hydrophobic interactions between proteins and the stationary phase increase which cause slightly reduced recovery.

Table 5.3 Protein recoveries on C-CP fiber columns.

Support/Stationary Phase	Recovery of BSA (%)	Recovery of Lysozyme (%)
Native Nylon	94 ± 2.1	90 ± 3.5
PET-PEI	96 ± 1.8	97 ± 1.4
PET-PEI/BUDGE	96 ± 1.4	94 ± 0.9

Analytical chromatography characteristics

A synthetic three-protein mixture of BSA, lysozyme and hemoglobin (0.25 mg mL^{-1}, each) was used to test the separation characteristics on PET-PEI, PET-PEI/BUDGE and native nylon 6 C-CP fiber-packed columns. Figure 2 shows the elution profiles for 3 µL injections of the protein mixture at flow rates from 0.25 mL min^{-1} to 1.0 mL min^{-1} (equivalent to linear velocities of 110 – 440 cm min^{-1}). In each separation, the gradient programs were kept the same on a volume-basis, thus normalizing the gradient composition as a function of flow rate. Note that the gradient programs differ between the PEI-modified and native nylon fibers, with those employed being found as optimal for each phase. For each of the fiber types, the elution profiles are almost superimposable on the volume basis as the peaks each elute in the same nominal position in the gradient program. The predominate effect is a compression of the peak shapes on the time basis,

as would be expected in the absence of mass transfer limitations. Essentially, fast protein separations can be realized on each of the columns by increasing flow rate, without sacrifice to the separation characteristics. The consistency reflects the low mass transfer resistance on C-CP fibers as well as a lack of enthalpic changes that would be reflected in the %B of protein elution.

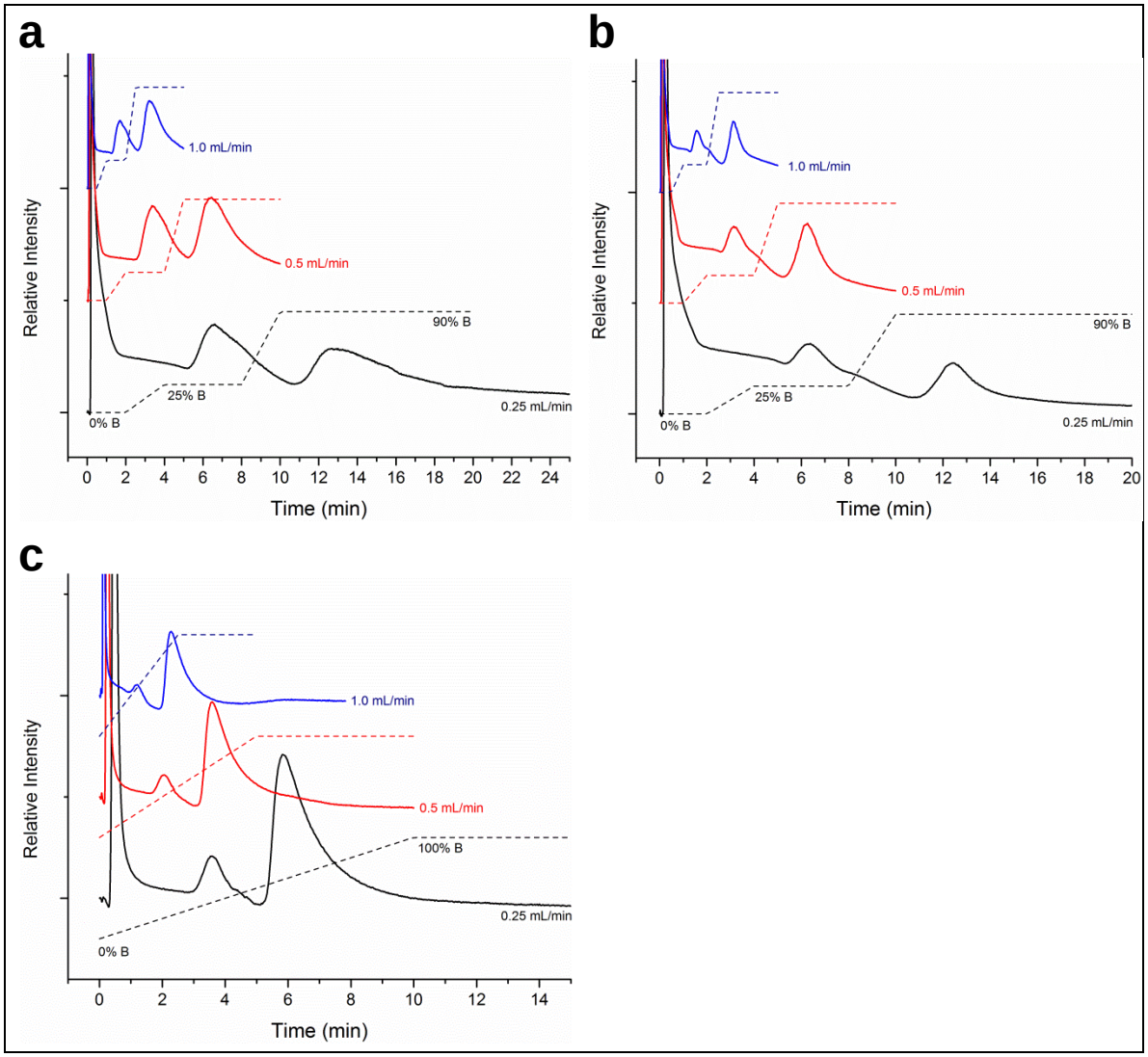

Figure 5.2 Chromatograms of the three-protein separations on a) PET-PEI, b) PET-PEI/BUDGE, and c) native nylon 6 C-CP fiber columns at different mobile phase flow rates while maintaining a constant volumetric gradient rate. Mobile phase A: 20 mM Tris-HCl buffer, pH 7.5. Mobile phase B: 1.0 M NaCl in mobile phase A.

A comparison of the retention characteristics among the fiber types point to significant differences in the surface chemistries of PET-PEI, PET-PEI/BUDGE, and nylon 6. Similar to the results of single protein (BSA) experiments, the

retention times (and thus %B) of hemoglobin and BSA on PET-PEI/BUDGE are slightly shorter than those on PET-PEI. Lysozyme is not retained to an appreciable extent on either modified PET as it is charge-positive at this near-neutral pH, having a pI of 11.35. As discussed above, the higher retention volumes observed for the PET-PEI phase are likely driven by a couple of chemical factors. Beyond the strength of the protein-surface interactions, comparison of the chromatograms from PET-PEI (Fig. 2a) and PET-PEI/BUDGE (Fig. 2b), reveals that the eluting peaks of hemoglobin and BSA from the PET-PEI/BUDGE column are narrower ($w_{1/2}$=1.21 min for hemoglobin, $w_{1/2}$=1.57 min for BSA, at 0.25 mL min^{-1}) than the corresponding peaks from PET-PEI ($w_{1/2}$=2.45 min for hemoglobin, $w_{1/2}$=3.93 min for BSA, at 0.25 mL min^{-1}), which results in higher resolution (R=2.55 for PET-PEI/BUDGE, R=1.12 for PET-PEI, at at 0.25 mL min^{-1}). In fact, the hemoglobin profile reveals the presence of a satellite peak, suggestive of a multiplicity of interactions. The peak broadening on PET-PEI column may be the results of the interaction between the protein and the base PET surface, which would be hydrophobic in nature. The increased hydrophobic interaction delays the protein elution from the stationary phases, which causes the peak broadening in ion-exchange mode. On PET-PEI/BUDGE fibers, cross-linking increases the surface density of PEI, providing better coverage and minimizing the interactions with the surface. Also, the hydrophillic BUDGE linker creates a barrier toward further surface interaction. Hence, the BUDGE treatment in the surface modifications improves the ion-exchange

protein separations on the PEI-modified PET C-CP fiber columns. Although the peak shapes and the separation resolutions from the PET-PEI/BUDGE are better the ones from the PET-PEI, all the peaks are suffering from broadening and strong tailing. The chromatograms in figure 2 indicate that there is no significant change of the peak shapes (on volume basis) at increased linear velocities, which suggest that the peak broadening is probably neither due to the longitudinal diffusion (the B term in Van Deemter equation) nor the mass transfer resistance (the C term in Van Deemter equation). Actually, the peak broadening and asymmetry is mainly from the non-ideal packing.[27] The C-CP column was packed by pulling the C-CP fiber bundles through the PEEK tube which results in irregular stacking of fiber wings along the column. Guiochon and co-workers reported that the heterogeneous packing of columns causes the heterogeneous radial distribution of the flow velocity, which results to the peak broadening and tailing.[40-42] Unlike the PEI-modified PET fibers, nylon 6 fibers have both anion- and cation-exchange sites on the surface, the proportion of which varies as a function of pH as depicted in the upper portion of Fig. 3. As a result, the elution order of the three proteins is different for nylon 6 (Fig. 2c) than from the PEI-modified PET. When the elution gradient is applied, hemoglobin elutes first (actually not retained), followed by BSA and lysozyme. The isoelectric points (pI) of BSA, hemoglobin, and lysozyme are 4.70, 6.80, and 11.35, respectively. The difference between the pI of each protein and the environmental pH reflects the magnitude of net charge of the proteins. (Of course pI reflects a global charge,

and not necessarily what is accessible for electrostatic interactions with the stationary phase.) As shown in Fig. 3, the pI of BSA is 2.60 units below the buffer pH (7.5), while the pI of lysozyme is 3.85 units above the buffer pH. This difference makes lysozyme significantly more retentive than BSA, though nylon carries more cationic sites than anionic sites (0.29 units difference, according to Fig. 3). The pI of hemoglobin is only 0.70 units below the buffer pH, thus it is relatively charge-neutral in comparison to a surface that is effectively charge-neutral at this pH. While electrostatic interactions can explain the retention of the proteins, the interactions are surely more complicated, including factors such as hydrophobic interactions.

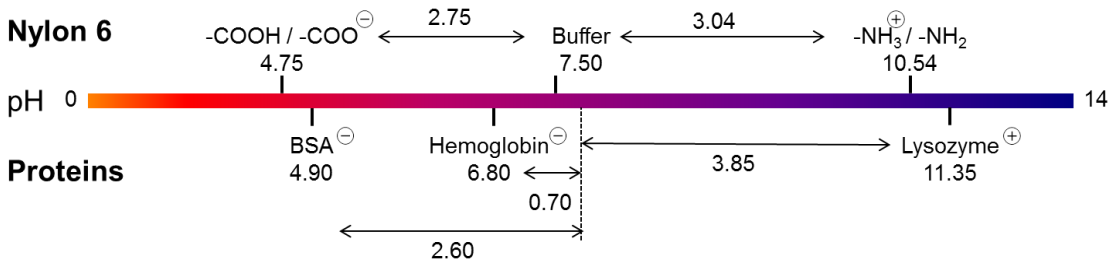

Figure 5.3 Comparison between the pI values of the surface functionality of nylon 6 fibers and the test proteins. The pK_a of the amine and acid functionalities on nylon 6 are calculated by Advanced Chemistry Development (ACD/Labs) Software V11.02 using N-(6'-Aminocaproyl)-6-aminocaproic acid as the model molecule.

One final point relative to the retention of the proteins on nylon 6 is reflective of the relatively low amine density of that surface (Table 1). As seen in Fig. 2c, the peak area of the BSA elution (2nd peak) is significantly lower than other two peaks. The reduced elution peak area for BSA is due to the fact that

some portions of the injected BSA co-elutes with the un-retained hemoglobin. The two distinct elution peaks of BSA on the nylon 6 column were also observed in the single-protein injection experiment. In this case, it seems clear that the lower density of amines on the nylon-6 surface, in combination with the low pI of BSA yield a very small binding capacity. As the result, some portions of the injected BSA were totally un-retained. In comparison, lysozyme, farther removed from its pI value is readily retained, much like hemoglobin and BSA on the PEI phases.

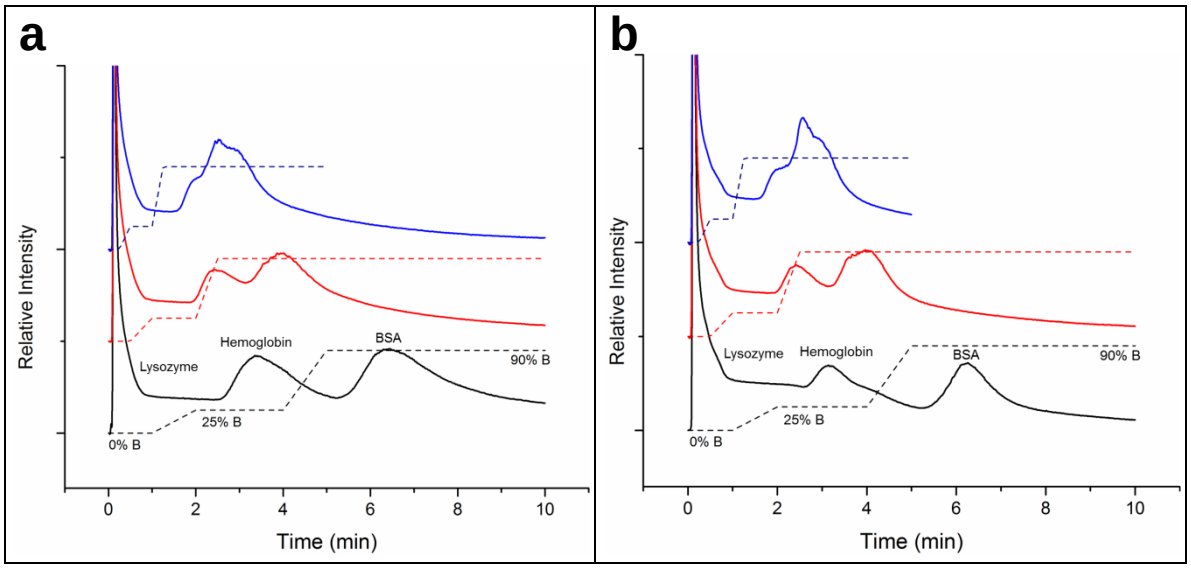

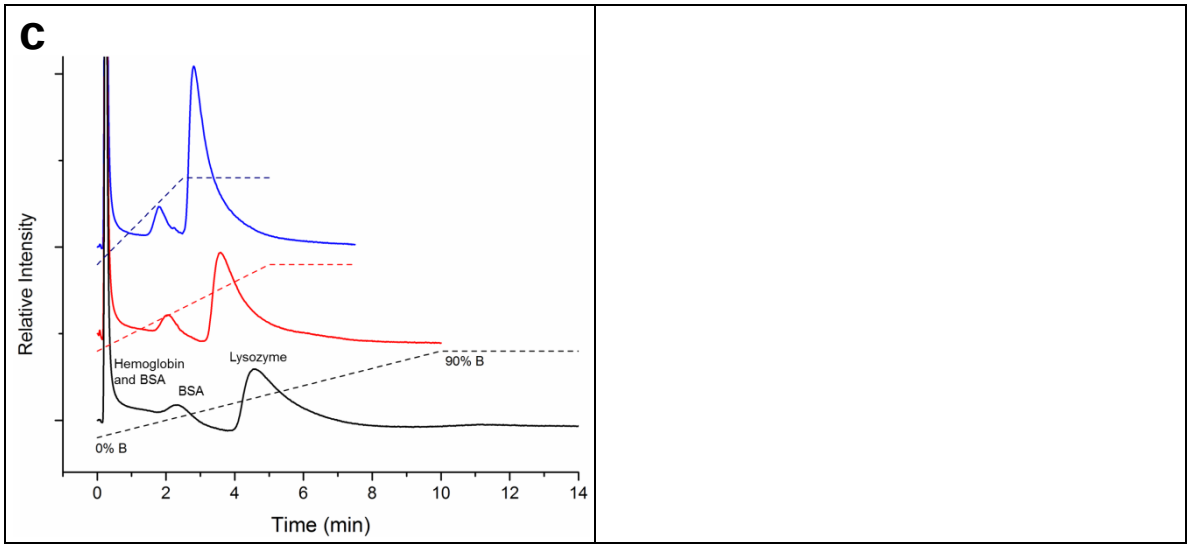

Figure 5.4 Chromatograms of the three-protein separations on a) PET-PEI, (b) PET-PEI/BUDGE, and c) native nylon 6 C-CP fiber columns at a constant mobile phase flow rate and different gradient rates. Bottom separation in each case reflects the "optimized" gradient for each, with the others reflecting 2X increases in the gradient rate. Mobile phase A: 20 mM Tris-HCl buffer, pH 7.5. Mobile phase B: 1.0 M NaCl in mobile phase A.

While the kinetics of mass transport within a phase are revealed in experiments involving changes in linear velocity as depicted in Fig. 2, there is also a kinetic aspect to the adsorption/desorption processes. Figure 4 shows the elution profiles of the three proteins at same flow rates but with different gradient rates. In each case, the slowest gradient (bottom trace) represents the optimum gradient program for the respective phase, with the rates increased by a factor of 4 from bottom to top separations. There are significant differences in terms of both the peak resolution and recoveries between the PEI-modified and native nylon 6 C-CP fiber columns. In comparing the PET-PEI and PET-PEI/BUDGE responses (Figs. 4a and b), no appreciable differences are seen between the two

as higher gradient rates are applied. As expected, increases in the gradient rates (shorter times) lead to substantial sacrifices in the observed resolution for the modified fibers, with the latter showing somewhat better resolution. In the case of the PET-PEI separations, the resolution decreases from 1.36 to ~0.6 for the critical pair, while for the BUDGE-modified system it decreases from 2.1 to ~0.6. This general phenomenon stems from the fact that the proteins do not desorb at a finite mobile phase composition, but over some range as dictated by the multiplicity of potential protein-surface interactions. Therefore, as the rate is increased, the ranges “overlap” in time as reflected in chromatograms.

In the case of the nylon 6 column (Fig. 4c), the resolution does not visually appear to to suffer as much as the gradient is increased. In fact, different from the modified phases, the resolution shows no real degradation (admittedly, the gradients used for nylon 6 are much slower than explored for the modified fiber phases, which are optimized for the modified fiber phases). More pronounced, is a loss in protein recovery as reflected in the absorbance peak heights from the nylon column as the gradient time is increased. Quantitatively, the integrated peak areas decrease when the gradient time is increased. Related studies suggest that the losses of protein may be the result of protein unfolding on the stationary phase [38,43,44]. The hydrophobic interactions between the proteins and the native nylon fiber surface cause protein unfolding/denature, leading to potential irreversible binding as well as peak broadening, the extent of which increases with the protein residence time on-column [38]. Thus any advantage

expected from using slow gradients is lost in the case of nylon 6, in fact the resolution across this 4X difference in gradient rate does not change, ranging from 1.35 to 1.4. On the PET-PEI and PET-PEI/BUDGE, the peak profiles do not reflect protein unfolding or irreversible binding as witnessed by the uniform recoveries. Here, the ionic interactions dominate potential non-ionic (hydrophobic) interactions between proteins and stationary phase [27], resulting in favored desorption kinetics under ion-exchange chromatography conditions.

Conclusions

Previous studies have demonstrated that the use of a straight forward set of on-column chemistries can be affected to develop weak anion exchange surfaces on polyester C-CP fibers [27]. The PEI and PEI/BUDGE-modified PET C-CP fiber packed columns were demonstrated to have high dynamic binding capacities, with the latter showing ~20X improvements over non-modified fibers. In this work, the analytical separation characteristics of these amine-based phases are compared to a native nylon 6 C-CP fiber packed for the ion-exchange protein separation of a synthetic three protein mixtures. The native nylon 6, with amines and carboxylic acid end groups as the electrostatic ligands, was used to separate the protein mixture under mixed-mode chromatography. Under the constant volumetric gradient rate, all columns in this study were capable of performing fast protein separations by increasing the flow rate without a loss of resolution. The BUDGE treatment not only increases the binding capacity of the

columns, but also improves the separation quality (peak width and separation resolution) on shorter gradient time scales. At this level of investigation, the PEI-modifications do not seem to impart any sort of kinetic limitations. Studies of the role of gradient rates and the protein recoveries reflect the fact that there is a level of irreversible binding and band broadening on the nylon 6 columns with longer gradients that is not seen for the PEI-modified fibers. Thus the PEI-modified PET C-CP fibers, particularly when incorporating the BUDGE cross-linking step offer specific advantages in preparative separations without sacrifice in the favorable mass transport characteristics that allow for high throughput analytical-scale separations. In the other hand, the native nylon C-CP fiber column has different protein retention characteristics than the modified PET C-CP fiber columns. The nylon C-CP fiber column, combines with the modified PET C-CP fiber columns, provide more selectivity to protein separations thus increase the chance for the proteins to be separated. The major defects of the C-CP fiber columns in this study are the peak broadening and tailing which are the results of irregular column packing. Future study will look at improving the peak shape by modifying the column packing method. The reaction conditions (such as the reaction time, temperature, etc.) will also be investigated to affect the surface chemistry and morphology of the C-CP fibers. We will study the native nylon and modified PET C-CP fiber columns on the applications of the separations of more complex protein mixtures, such as cell lysate. The PEI modifications yield PET C-CP fiber amine-rich surfaces which are chemically reactive and can be further

functionalized. Various ion-exchange ligands and affinity ligands can be covalently attached to PEI modified PET fiber surfaces. The PEI modifications on PET C-CP fibers provide opportunities to use the functionalized C-CP fibers for various protein separations.

Acknowledgements

This material is based upon work supported by the National Science Foundation Division of Chemistry under grant CHE-1307078.

References

[1] Cunico, R. L.; Gooding, K. M.; Wehr, T. *Basic HPLC and CE of Biomolecules*; Bay Bioanalytical Laboratory: Richmond, CA, 1998.

[2] *FDA drug bulletin* **1982**, *12*, 18-19.

[3] Sackman, J. E.; Kuchenreuther, M. J. *BioPharm International* **2015**, *28*.

[4] Mullard, A. *Nat. Rev. Drug. Discov.* **2015**, *14*, 77-81.

[5] Research, C. f. D. E. a.; January ed.; www.fda.gov/drugs: www.fda.gov/drugs, 2015.

[6] Wurm, F. M. *Nat. Biotechnol.* **2004**, *22*, 1393-1398.

[7] Gottschalk, U. *Biotechnol. Progr.* **2008**, *24*, 496-503.

[8] Tanaka, N.; Kobayashi, H.; Nakanishi, K.; Minakuchi, H.; Ishizuka, N. *Anal. Chem.* **2001**, *73*, 420 A-429 A.

[9] Zou, H.; Huang, X.; Ye, M.; Luo, Q. *J. Chromatogr. A* **2002**, *954*, 5-32.

[10] Kirkland, J. J.; Truszkowski, F. A.; Dilks, C. H.; Engel, G. S. *Journal of Chromatography A* **2000**, *890*, 3-13.

[11] Schuster, S. A.; Wagner, B. M.; Boyes, B. E.; Kirkland, J. J. *J. Chromatogr. A* **2013**, *1315*, 118-126.

[12] Sun, G.-Y.; Shi, Q.-H.; Sun, Y. *J. Chromatogr. A* **2004**, *1061*, 159-165.

[13] Nelson, D. K.; Marcus, R. K. *J. Chromatogr. Sci.* **2003**, *41*, 475-479.

[14] Nelson, D. M.; Marcus, R. K. *Anal. Chem.* **2006**, *78*, 8462-8471.

[15] Stanelle, R.; Marcus, R. K. *Anal Bioanal Chem* **2009**, *393*, 273-281.

[16] Randunu, K. M.; Marcus, R. K. *Analytical and bioanalytical chemistry* **2012**, *404*, 721-729.

[17] Marcus, R. K. *Journal of separation science* **2008**, *31*, 1923-1935.

[18] Wang, Z.; Marcus, R. K. *J. Chromatogr. A* **2014**, *1351*, 82-89.

[19] Marcus, R. K.; Davis, W. C.; Knippel, B. C.; LaMotte, L.; Hill, T. A.; Perahia, D.; Jenkins, J. D. *J. Chromatogr. A* **2003**, *986*, 17-31.

[20] Stanelle, R.; Mignanelli, M.; Brown, P.; Marcus, R. K. *Analytical and bioanalytical chemistry* **2006**, *384*, 250-258.

[21] Stanelle, R. D.; Straut, C. M.; Marcus, R. K. *J. Chromatogr. Sci.* **2007**, *45*, 415-421.

[22] Schadock-Hewitt, A. J.; Marcus, R. K. *Journal of separation science* **2014**, *37*, 495-504.

[23] Schadock-Hewitt, A. J.; Pittman, J. J.; Christensen, K. A.; Marcus, R. K. *Analyst* **2014**, *139*, 2108-2113.

[24] Schadock-Hewitt, A. J.; Marcus, R. K. *Journal of separation science* **2014**, *37*, 3595-3602.

[25] Jiang, L.; Schadock-Hewitt, A. J.; Marcus, R. K. *Analyst* **2015**, *140*, 1523-1534.

[26] Jiang, L.; Marcus, R. K. *Analytical and bioanalytical chemistry* **2015**, *407*, 939-951.

[27] Jiang, L.; Marcus, R. K. *J. Chromatogr. A*, *submitted for publication*.

[28] Brown, P. J.; M., M.; Sinclair, K.; Tucker, E.; Inam, A. In *Southeast Regional Meeting of the American Chemical Society* 2004.

[29] Leveque, M. *Ann. Mines.* **1928**, *13*, 284.

[30] Randunu, K. M.; Marcus, R. K. *Biotechnol. Prog.* **2013**, *29*, 1222-1229.

[31] Wang, Z.; Marcus, R. K. *Biotechnol. Progr.* **2015**, *15*, 97-109.

[32] Schadock-Hewitt, A. J.; Pittman, J. J.; Stevens, K. A.; Marcus, R. K. *J. Appl. Polym. Sci.* **2013**, *128*, 1257-1265.

[33] Lewis, D. M. In *Synthetic Fibre Materials*; Brody, H., Ed.; Longman Group: Essex, UK, 1994.

[34] Neue, U. D. *HPLC Columns: Theory, Technology, and Practice*; Wiley-VCH: New York, 1997.

[35] Avny, Y.; Rebenfeld, L. *J. Appl. Polym. Sci.* **1986**, *32*, 4009-4025.

[36] Zhang, R.; Li, Q.; Gao, Y.; Li, J.; Huang, Y.; Song, C.; Zhou, W.; Ma, G.; Su, Z. *J. Chromatogr. A* **2014**, *1343*, 109-118.

[37] Randunu, J. M.; Dimartino, S.; Marcus, R. K. *Journal of separation science* **2012**, *35*, 3270-3280.

[38] Kopaciewicz, W.; Rounds, M. A.; Regnier, F. E. *Journal of chromatography* **1985**, *318*, 157-172.

[39] DePhillips, P.; Lagerlund, I.; Farenmark, J.; Lenhoff, A. M. *Anal. Chem.* **2004**, *76*, 5816-5822.

[40] Farkas, T.; Sepaniak, M. J.; Guiochon, G. *J. Chromatogr. A* **1996**, *740*, 169-181.

[41] Farkas, T.; Guiochon, G. *Anal. Chem.* **1997**, *69*, 4592-4600.

[42] Miyabe, K.; Guiochon, G. *J. Chromatogr. A* **1999**, *857*, 69-87.

[43] Goheen, S. C.; Hilsenbeck, J. L. *J. Chromatogr. A* **1998**, *816*, 89-96.

[44] Lu, X. M.; Figueroa, A.; Karger, B. L. *J. Am. Chem. Soc.* **1988**, *110*, 1978-1979.

CHAPTER VI

MICROWAVE-ASSISTED GRAFTING POLYMERIZATION OF NYLON 6 CAPILLARY-CHANNELED POLYMER FIBERS FOR ION EXCHANGE PROTEIN SEPARATION: I. WEAK CATION-EXCHANGE

Introduction

In recent years, macromolecular therapeutics have played increasingly important roles in the pharmaceutical industry [1,2]. Protein-based drugs are the most common of these macromolecular drugs. The manufacture of protein therapeutics involves two major operations, upstream processing (i.e., production via cell culturing/fermentation) and downstream processing (i.e., purification/recovery). Upstream processing has been largely improved over the last two decades [3,4], while the downstream processing continues to be the rate limiting step in protein drug production [3,5,6]. Chromatographic separation is the bottle-neck of the downstream processing due to its high costs and time consumption. Thus there is a continuous interest in the development of stationary phases that can provide high-throughput, cost-effective protein separations [7,8].

Traditional liquid chromatography (LC) stationary phases are composed of highly porous, micro-sphere packed-bed support phases. While the majority of supports are silica-based, polymeric materials find application due to their

chemical robustness [9]. Currently, use of sub-2 μm diameter silica supports dominates the realm of “small molecule” separations [10,11]. However, the application of such supports in protein separations suffers from the slow solute diffusion into and out the pores, limitations of flow rate and backpressure, and the pore clogging due to the complexity of the production mixtures. To this end, there has been a resurgence of interest in the use superficially porous silica support phases [12,13]. Additionally, alternative support phases, such as monoliths, membranes and fibers, have been developed for protein separations[14-18]. Capillary-channeled polymer (C-CP) fibers have been under study in this laboratory towards applications in protein analytics and downstream processing[19-24]. The C-CP fiber-packed bed presents a number of physical advantages over porous microsphere-packed beds. The combination of a virtually non-porous fiber structure and high permeability allows for analytical separations that can be run at high mobile phase linear velocity (100 mm s^{-1}) while maintaining low column backpressure (< 2000 psi) [25,26]. Short inter-fiber diffusion distances combine with the lack of porosity to minimize the mass transfer resistance of proteins, allowing for very high processing throughput [27]. C-CP fibers are melt-extruded from commodity polymers such as polyamide (nylon 6), polyester (PET) and polypropylene (PP). The low-cost of the C-CP fibers makes them an attractive candidate in terms of implementation on the industrial-scale.

The different surface chemistries provided by the base C-CP fiber phases allows for protein separations under reversed-phase (RP), hydrophobic interaction (HIC), and ion-exchange (IEX) modes [20,21,28,29]. Just as in the case of poly(styrene-divinylbenzene) (PS-DVB) bead phases [9,30,31], there exists a rich tool box of surface modification chemistries to effect greater chromatographic efficiency and selectivity. Several surface modification strategies have been pursued on C-CP fibers to affect greater efficiency/selectivity, with the caveat that retention of the basic hydrodynamic properties was essential. For example, simple amination of the PET surface has allowed creation of a biotinylated surface for affinity separations [32] and the creation of polymeric polyethyleneimine (PEI) phases for weak anion exchange protein separations [33,34]. A new class of surface functionalizing agent, ligand tethered lipids (LTL), was developed for surface functionalization of PP C-CP fibers for protein extractions and separations [35,36]. These modification strategies introduce different types of surface chemistries on C-CP fiber phase and expand the potential applications of C-CP fiber phase.

In terms of the ability to mitigate any decomposition/deactivation of product proteins, ion exchange-based separations are extremely attractive [8]. Unfortunately, hydrophobic interactions between proteins and no-polar support phases lead to separations that are actually mixed-mode in nature [9,37,38]. Hydrophobic interactions can cause proteins to de-nature during separations, lead to low protein recoveries, and peak tailing in chromatograms. Therefore,

hydrophilic supports such as acrylates are common in IEX protein separations [39]. Among the types of C-CP fiber materials, nylon 6 is the most hydrophillic. Based on the acid/base character depicted below for the natural carboxylic acid and primary amine end groups,

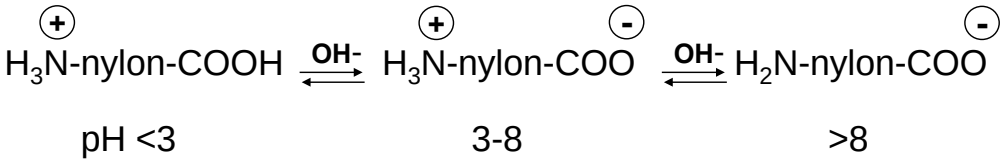

native nylon 6 C-CP fibers have been used in IEX protein separations [29,40]. However, the low density of these ion-exchange ligands limits the performance of the material in protein separations [34]. Thus additional surface modifications on the native nylon 6 C-CP fibers are needed to improve the chromatography properties of this phase.

Presented here is a proof-of-concept in the modification of nylon 6 C-CP fibers used in weak cation exchange (WCX) protein separations, without sacrificing the nature of the hydrophilic surface or the column hydrodynamics. As-extruded fibers were functionalized via a microwave-assisted grafting polymerization. Acrylic acid was polymerized and grafted onto the native nylon 6 C-CP fibers as the functional ligands. The modified fiber (nylon-COOH) packed columns exhibit significantly-increased protein dynamic binding capacity. Protein recoveries and the reproducibility of the modification were investigated on the nylon-COOH fibers. Finally, fast protein separations were demonstrated on the nylon-COOH fiber phase. The microwave-assisted modification is a versatile

method to introduce various functional ligands onto the nylon C-CP fiber phase, thus it greatly expands and improves the application of nylon 6 C-CP fiber phase for analytical and preparative protein separations.

Experimental Methods

Chemicals and Instrumentation

Unless otherwise specified, chemicals were purchased from commercially available sources and used without further purification. Nylon 6 C-CP fibers were obtained from the Material Science and Engineering department, Clemson University. Acrylic acid (99.5%) and potassium persulfate (KPS) (99%) were purchased from Alfa Aesar (Haverhill, MA). Activated alumina powder was purchased from Polysciences, Inc. (Warrington, PA). All HPLC solvents were purchased from EMD (Billerica, MA). All other chemicals and all proteins were purchased from Sigma-Aldrich (St. Louis, MO). Deionized water (DI-H_2O) was secured from a Milli-Q water system. The protein loading/elution characterization and chromatographic protein separations were performed on a Dionex Ultimate 3000 HPLC system, LPG-3400SD Quaternary pump, and MWD-3000 UV–vis absorbance detector (Thermo Fisher Scientific Inc., Sunnyvale, CA). A Rheodyne model 8125 low dispersion injector with a 5 µL injection loop was used for protein sample injections. The microwave-assisted polymerizations were performed in a

Sunbeam SBM7700W microwave oven, without any modifications of the commercial unit.

Microwave-assisted nylon C-CP fiber surface modification

The surface grafting polymerization method was modified from an earlier-reported method [41]. All DI-H_2O used in the modification reactions was purged with nitrogen for 30 min to remove oxygen prior to use. The acrylic acid was filtered through an activated alumina bed to remove remnant stabilizing agents before use. The modification solution was prepared by dissolving acrylic acid (2.0 mL, 29 mmol) and potassium persulfate (100 mg, 0.37 mmol) in 20 mL DI-H_2O. The native nylon 6 C-CP fibers were removed from the fiber spool and placed on a dying fork. For each modification reaction, 720 fibers of ~35 cm length were used. The fibers were rinsed with excess amounts of DI-H_2O, methanol, and then DI-H_2O again, to remove any chemical residues left from the fiber extrusion process. The fibers were placed into the modification solution in a 50 mL beaker. All fibers must be immersed in the solution and suspended in the solution. The beaker was then put in the microwave oven. Due to the small scale of the reaction, another beaker containing 30 mL water was also placed in the microwave oven as a heat sink for better control and reproducibility of the experiments. The microwave reaction was run at 100 W for 10 min. After reaction, the fibers were removed from the beaker immediately and washed with excess amounts of DI-H_2O until no homopolymer parciptates were visible on the fibers. A control experiment was run with the fibers submerged in neat DI-H_2O

instead of in the modification solution to assess any thermal or microwave-induced decomposition.

Preparation of the C-CP fiber columns

The C-CP fiber columns were packed following the previously-reported procedure [26]. In this study, the native and modified nylon 6 fibers were pulled through polyether ether ketone tubing (PEEK, 0.762 mm i.d., IDEX Health & Science LLC, Oak Harbor, WA). After packing, columns were mounted on the HPLC system and washed with DI-H_2O at 0.2 mL min^{-1} for 12 h to remove any non-covalently bound chemicals (initiators, homopolymers) from the fibers. Once cleaned, the fiber-packed columns could be cut to appropriate length (20 cm, in this study) and stored in ambient conditions.

Characterization of the modified nylon 6 C-CP fibers

The scanning electron microscope (SEM) images were taken at the Clemson University Electron Microscopy Laboratory, using a Hitachi SU6600 system operating in the variable pressure mode, with a 20 kV accelerating voltage. The attenuated total reflection-Fourier transform infrared spectroscopy (ATR-FTIR) was performed on a Thermo-Nicolet Magna 550 FITR in the Analytical Testing Lab of Material Science & Engineering department, Clemson University. The ligand densities of native and modified nylon C-CP fibers were determined by acid-base titration. Native and modified fibers were washed in 100 mM HCl solution for 1 min, and then large amounts of DI-H_2O to remove

residual HCl from the fibers. The fibers were then washed with acetone to remove water, and dried under mild mechanical vacuum for 20 hours at room temperature to remove residual solvent. The dried fibers, were weighed, placed in DI-H_2O, and were titrated with standardized 0.1142 M NaOH solution and phenolphthalein used as the end-point indicator.

Liquid chromatography

All experiments were performed on a Dionex Ultimate 3000 HPLC system. The dynamic loading capacity (DLC) of the columns was determined through breakthrough (frontal) analysis as described previously [22], using lysozyme as the test protein. After the column was cleaned and equilibrated with 20 mM phosphate buffer (pH=6.5, designated as buffer A), lysozyme at the chosen concentration in the buffer was introduced to the column. UV absorbance at 280 nm was monitored as a means of detecting breakthrough and quantifying the amount of protein retained on-column. When the UV absorbance of the eluting solution reached a plateau, indicating column saturation, buffer A was then applied on the column to remove non-bound protein. When the absorbance returned to the original baseline, buffer B (1.0 M NaCl in buffer A) was introduced to the column to affect protein elution. The amount of lysozyme retained was determined by integration of the breakthrough curve (equal area method).[42] A blank experiment was performed using an empty PEEK tubing to determine the system hold-up volume/time. The DLC at 10% breakthrough was calculated at the point that the absorbance of the eluting solution reached 10% of its maximum

absorbance (plateau). If needed, based on the amount of protein eluted, column regeneration was performed by washing the column with 100 mM NaOH solution for 10 min.

The analytical quality of the protein separations was determined using gradient separations (from 100% buffer A to 50% buffer B) of a four-protein mixture. For each separation experiment, 5 μL of the protein mixture containing myoglobin, α-chymotrypsinogen A, cytochrome C and lysozyme (0.25 mg mL^{-1} each) was injected and the chromatogram was recorded at 216 nm. The gradient baseline absorbance was obtained by running the gradient with no protein injected. The absorbance baseline was subtracted from protein separation chromatograms.

Results and Discussions

Microwave-assisted nylon surface polymerization modification

Different methods have been reported in the literature for the modification nylon materials. Some of the modification methods target activation of the amide groups [43,44], unfortunately resulting in cleavage of the amide bond and causing inevitable physical damage to the nylon bulk structure. Such a decrease of mechanical strength to the C-CP fibers used here would result in breakage in the column packing process. The other principal type of modification introduces the target species onto the nylon surface via polymerization of a monomer containing the desired functional groups [41,45]. Radical polymerization

reactions are usually induced by UV light, conventional heating, plasma or microwave energy [41,45,46]. UV light treatment is a straight forward, easily controlled approach, but is not applicable on large quantities of material or on materials that have non-uniform shapes, such as C-CP fibers. The conventional heating method requires mixing or stirring of the materials in the reactive solution. Such an approach on C-CP fibers would results in folding and twisting, greatly reducing the homogeneity of the fiber column packing if not prohibiting it all together. Plasma beam treatments are difficult to impart on non-uniform surfaces and cause severe degradation of the polymers and decreased their mechanical properties due to oxidative damage [45,47]. Finally, microwave-irradiation is a well-established technique and its application to surface polymerization has been widely investigated [48-51]. Microwaves consist of electromagnetic radiation that has frequencies of 300 MHz to 300 GHz, corresponding to wavelengths of ~1 m to 1 mm, which can penetrate through many materials. The majority of microwave sources that are used for industrial and domestic purposes operate at a frequency of 2.45 GHz, corresponding to the wavelength of ~12 cm. In comparison to conventional heating methods, microwave irradiation offers many advantages including non-contact heating, rapid heating, high levels of temperature homogeneity, selective heating (some materials absorb more microwave radiation than others) and low energy cost. Non-thermal “microwave effects” that enhance the reactions may exist, but the exact mechanisms are still under discussion [52-54].

In this study, native nylon 6 C-CP fiber surfaces were functionalized by radical grafting polymerization as depicted below, with KPS used as the radical initiator. The mechanisms of KPS decomposition and KPS-initiated grafting polymerization have been discussed [41,55].

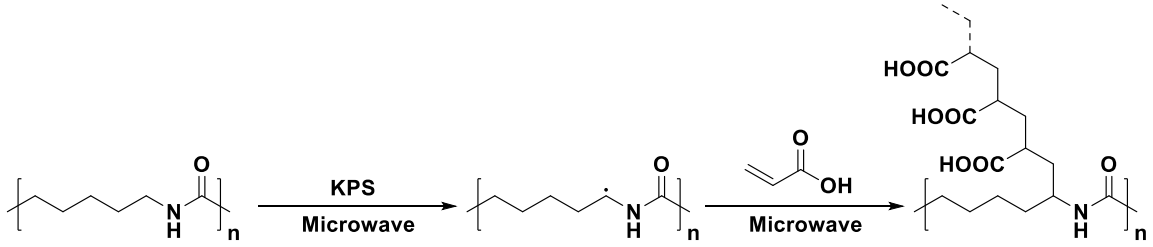

The power of the domestic microwave oven used for the modification reaction was set at 100 W, the lowest power option on that particular unit. The scale of the reaction (20 mL) in this study is quite small in comparison to the heating capacity of the domestic microwave oven. As such, an additional beaker containing 30 mL of water was placed in the microwave oven as a “heat sink”. Without the “heat sink”, the reaction mixture heats too quickly. In such cases, large amounts of air bubbles and homopolymer precipitants are formed after 5 min of microwave reaction and the modifications lack reproducibility. With the heat sink, the reaction is run for 10 min with greatly improved reproducibility. It is believed that using a more controllable microwave reactor, such as employed in the organic synthesis community would improve the modifications. However, the less expensive domestic microwave oven is sufficient for the proof-of-concept study of using the nylon-COOH C-CP fiber phase for protein separations.

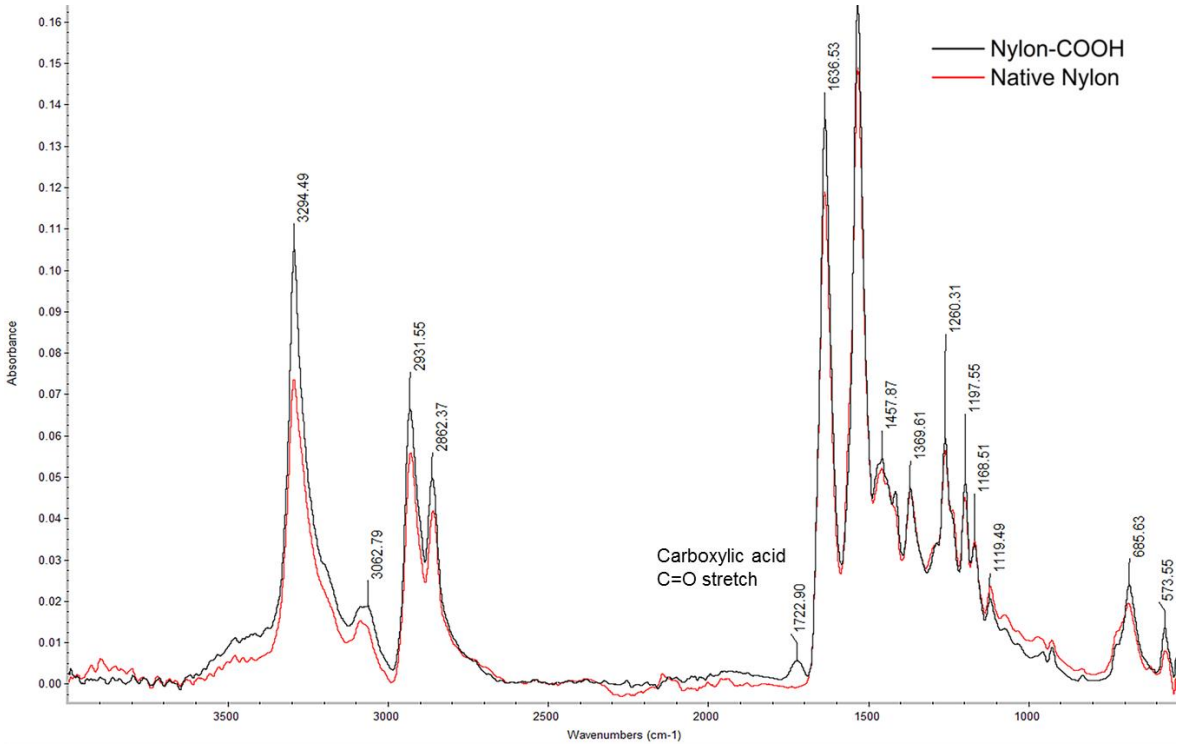

Figure 6.1 ATR-FTIR spectrum of the native and modified nylon C-CP fibers.

The acrylic acid-functionalized nylon fibers (Nylon-COOH) were characterized using ATR-FTIR and compared to the native nylon 6 starting material (Fig. 1). The spectra are virtually identical except one key feature. The peak at 1722.9 cm^{-1} in the Nylon-COOH case corresponds to the carbonyl (C=O) stretch associated with a carboxylic acid, indicating the presence of those new groups on the nylon-COOH fiber surfaces, which were not apparent in the spectrum of the native nylon 6. The fact that the other spectral features are not changed reflects the fact that the polymer backbone is not perturbed by the modification process.

As noted previously, the driving force for these efforts was the desire to attain high densities of carboxylic acid WCX groups on the already-hydrophilic nylon 6 support. Earlier efforts in assessing the end group densities on nylon 6 were based on the classic ninhydrin reaction, which actually measures primary and secondary amine densities, which should equate nominally with the carboxylic acid values as there are no 2° amines in the nylon system. Here, a simple acid/base neutralization titration has been applied to specifically quantify the –COOH densities. Those determinations yield values of 28 ± 9 μmol g^{-1} of fiber for the native nylon 6 and 575 ± 7 μmol g^{-1} for the nylon-COOH, an ~20X increase following the microwave-enhanced grafting method. The –COOH value here is a factor of ~2.5X less than obtained for the same fiber using the ninhydrin test, which is not out of line given the uncertainties of that method. In comparison to other polymer-based WCX phases, density of the nylon-COOH is higher than the carboxylic acid functionalized poly(glycidyl methacrylate-co-ethylene dimethacrylate) beads (-COOH density 400 μmol g^{-1}) [56] and chloroacetic acid modified polymeric monolith (-COOH density 351 μmol g^{-1}) [57]. To better classify the nylon-COOH ligand density versus other WCX phases, it is better to express that value on a surface area basis; 821 ± 10 μmol m^{-2}. In terms of a surface area basis, this is a very high density of surface ligand, in comparison to a surface functionalized silica gel developed for protein separations, which has a carboxylic acid density of 568 μmol m^{-2} [58]. It must be emphasized that, based

on the virtual non-porosity of the C-CP fibers, that all of the surface ligand are accessible, versus those that might in within porous structures.

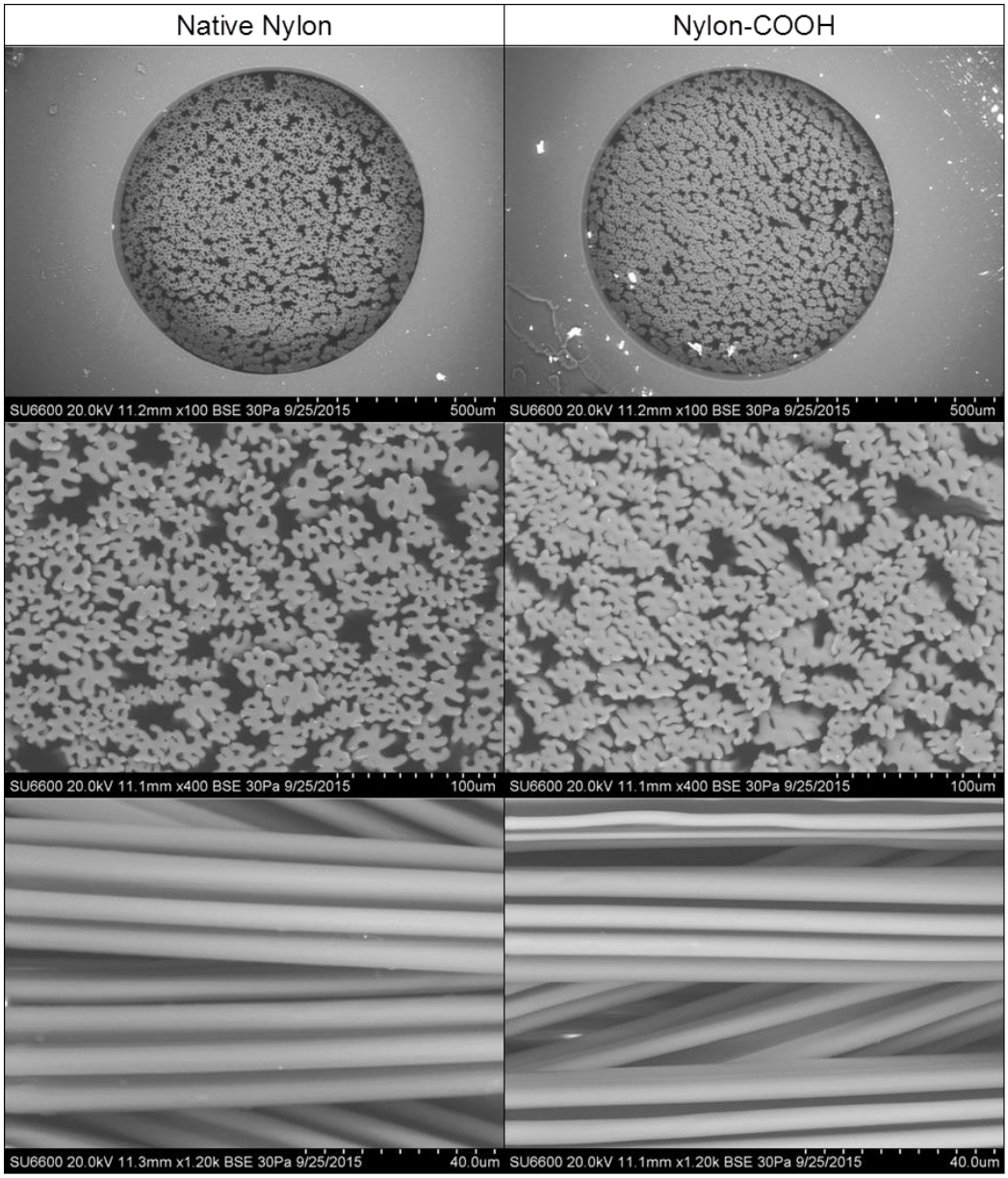

Figure 6.2 SEM images of the (left) native nylon C-CP fiber and (right) nylon-COOH C-CP fiber and column cross-sections.

As stated previously, it is imperative that any modification process not lead to sacrifices in the hydrodynamic efficiency of the C-CP fiber columns. SEM imaging of the fibers provides some evidence of potential macroscopic changes as seen in Fig. 2. The images of the column cross sections of the native nylon 6 and nylon-COOH (Figs., 2a and b, respectively) suggest that the modified fibers are packed more tightly (i.e., their fiber diameters have increased), even though the number of the fibers is the same in both columns. This point is more readily seen in the magnified views of Figs. 2c and d. In the chromatography experiments, the back-pressure of using nylon-COOH column is ~4× higher than using native nylon column (though still comparatively low). One might question whether the increased thickness is simply the result of swelling in the hot water, microwave modification step. In fact, micrographs of control samples of the nylon 6, microwaved in DI-H_2O instead of the modification solution, showed no difference in SEM images in comparison to the native fibers. Hence, the increase in fiber thickness following modification appears to be due to the added polyacrylic acid layer from the grafting polymerization. As a final assessment of potential damage/change during the microwave modification process, side-on SEM images (Figs. 2e and f) indicate no macro-damage to the fiber channel structures. These findings support the desired outcome that the grafting polymerization is a non-destructive surface modification method.

Table 6.1 Dynamic loading capacity (DLC) of lysozyme on nylon-COOH column at different protein loading concentrations.

Loading Concentration (mg mL^{-1})	Native nylon DLC @50% BT (mg g^{-1})	Native Nylon DLC @50% BT (mg mL^{-1})	Nylon-COOH DLC @50% BT (mg g^{-1})	Nylon-COOH DLC (mg mL^{-1})		
				@10% BT	@50% BT	10%/50% Ratio
0.05	0.63±0.44	0.37±0.26	19.13±0.18	9.21±0.08	10.65±0.10	0.86
0.1	1.81±0.02	0.7±0.01	20.11±0.02	9.18±0.02	11.19±0.01	0.82
0.2	0.87±0.19	0.52±0.11	20.56±0.01	9.44±0.01	11.44±0.01	0.82
0.4	0.81±0.27	0.48±0.16	21.07±0.38	9.71±0.21	11.73±0.21	0.83
0.6	1.24±0.47	0.74±0.28	22.22±0.03	10.37±0.02	12.37±0.02	0.84
0.8	0.94±0.67	0.56±0.40	22.28±0.04	10.40±0.03	12.40±0.02	0.84
1.0	1.66±0.10	0.99±0.06	22.60±0.89	10.52±0.47	12.58±0.50	0.84

Dynamic loading capacity

The DLC of the native and modified nylon 6 C-CP fiber phases were determined by breakthrough experiments using lysozyme as the model protein. Preliminary assessment of the throughput and yield characteristics of the C-CP fiber phases were done with the same lysozyme/nylon 6 system [22]. Under buffer conditions of pH 6.5, the carboxylic acid on the native nylon (as the end groups) and nylon-COOH fiber phase carry negative charges. Lysozyme has the isoelectric point of ~11.3 and so has a net positive charge in the buffer, thus it interacts with the native and modified nylon fiber phases via electrostatic

interactions. Various concentrations (0.05 – 1.0 mg mL^{-1}) of lysozyme solutions were loaded onto the fiber columns at a flow rate of 0.4 mL min^{-1} ($U_o \cong 29.2$ mm s^{-1}). Increasing the ionic strength of the buffer (1.0 M NaCl) elutes the lysozyme from the fiber phases following each loading. Representative breakthrough curves (UV absorbance at 280 nm) are shown in Fig. 3. Plotting on a time axis depicts the expected temporal response; as the concentration is increased, breakthrough occurs at shorter times/volumes. Frontal analysis of the breakthrough data in terms of the absolute amounts of protein allows calculation of the dynamic binding capacities presented in Table 1, in terms of the mass of lysozyme per unit fiber mass (mg g^{-1}) and bed volume (mg mL^{-1}). The DLC of nylon fiber phase varies from about 0.4 – 1 mg mL^{-1} on the native nylon to about 10 – 12 mg mL^{-1} on the nylon-COOH. There is a good bit of scatter in the native nylon 6 data as the absolute difference between the breakthrough volumes in those cases is very close to the actual column breakthrough (hold-up) volume. On the other hand, the precision of replicate loadings is much better for the nylon-COOH phase as the absolute values are much higher. There is a very slight (positive) dependence on the binding capacity for the modified surfaces versus the load concentrations, conforming to the upper-concentration regions of what would be expected to be a Langmuir or Langmuir-linear isotherm [23,33,42]. It is easy to conclude that the 12X increase in DLC is attributed to the added acrylic acid (-COOH) ligands following modification.

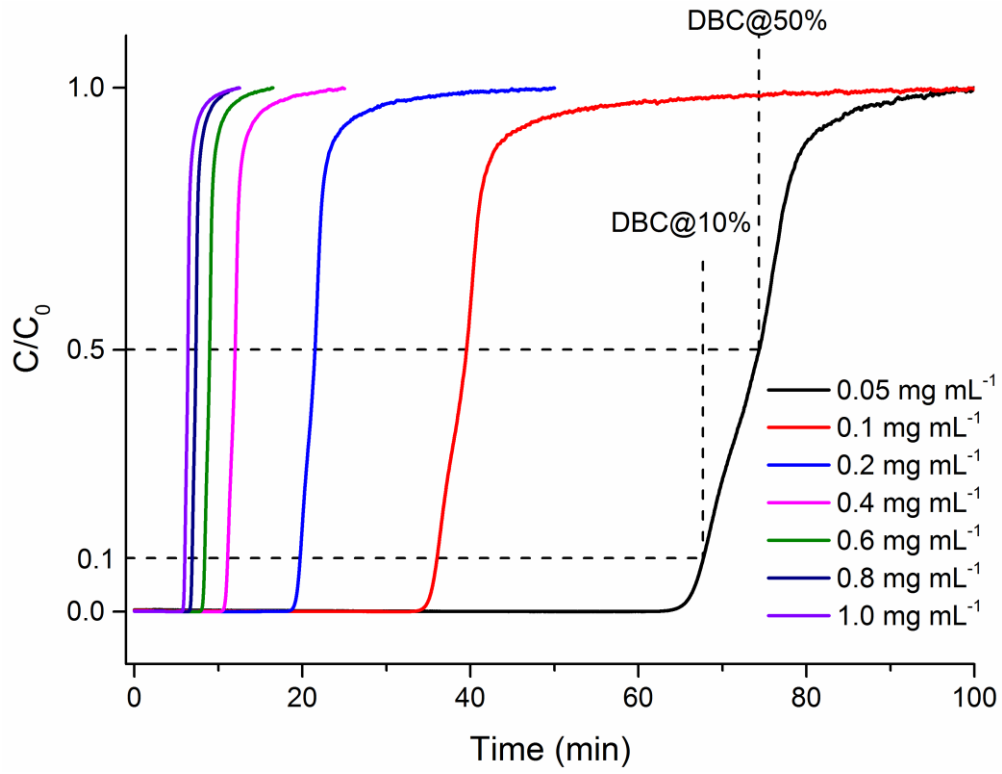

Figure 6.3 Lysozyme loading breakthrough curves on the nylon-COOH C-CP fiber column at constant mobile phase linear velocity and various protein loading concentrations. The breakthrough curves are plotted on the time basis. (Column length: 200 mm, I.D.: 0.762 mm. Loading buffer: lysozyme in 20 mM phosphate buffer, pH 6.5. Flow rate: 0.4 mL min^{-1}. Detection: 280 nm)

Any situation wherein large increases in capacity are realized brings along natural questions as to potential perturbations of the loading/elution kinetics. One useful metric towards this regard is the ratio between the 10% and 50% breakthrough (BT) volumes obtained through frontal analysis. These values reflect the amount of bound lysozyme at the point when the lysozyme concentration of the eluent reaches 10% and 50% of the maximum (solution) concentration. The ratio of the DLC at 10% to the DLC at 50% reflects the

sharpness of the breakthrough curve. In these lysozyme loading experiments, the ratios on the nylon-COOH column range from 0.82 – 0.86, indicative of the high efficiency of mass transfer on the nylon-COOH phase. There is no significant change in the 10%/50% BT ratio across the protein feed concentration changes, which would be expected in a diffusion-limited loading situation. This reflects the convective-diffusion driven solute transport that takes place in the C-CP fiber beds [27]. Overall, the protein DLC of a separation media at low protein feeding concentrations (e.g., 0.05 mg mL^{-1}) is especially important for industrial applications, since many of the desired proteins can be present at low concentrations in cell lysate media. This high loading capacity is complemented by the efficient adsorption kinetics, suggesting that the nylon-COOH phase holds great potential to be used for large-scale protein extraction and purification.

As described previously, downstream processing continues to be a limiting factor in the production of bio-therapeutics. The advantages of operating a separation under conditions which affect high throughput (T) and yield (Y) are ultimately desirable, these are some of the most outstanding attributes of C-CP fiber phases [22,23]. Figure 4 presents representative lysozyme breakthrough curves on the nylon-COOH column at various flow rates/linear velocities. In this experiment, the lysozyme load concentration was kept at a constant value of 1 mg mL^{-1}. The breakthrough curves are plotted on the basis of the load solution volume to better-reveal any kinetic limitations. As seen in the scale expansion, there is a very slight bias in the volume equating to the 50% load, with the

slowest application yielding an ~4% higher binding capacity than the highest velocity, though the latter occurred at a 10× higher velocity/shorter time scale. Thus, a vast improvement in T is observed. It is also interesting to note that the volume displacement at the 10% breakthrough between the different velocities and the 50% level are virtually the same, thus the mass transfer/adsorption kinetics are not sacrificed at the higher linear velocities. Only in the case of the highest linear velocity (73 mm s^{-1}) does it appear that mass transfer limitations are occurring, as the slope of the total breakthrough curve begins to decrease. The negligible difference on DLC at various linear velocities indicates the low mass transfer resistance of the nylon-COOH phase at high flow rates, thus fast protein loading/elution can be realized to improve the throughput of protein separations.

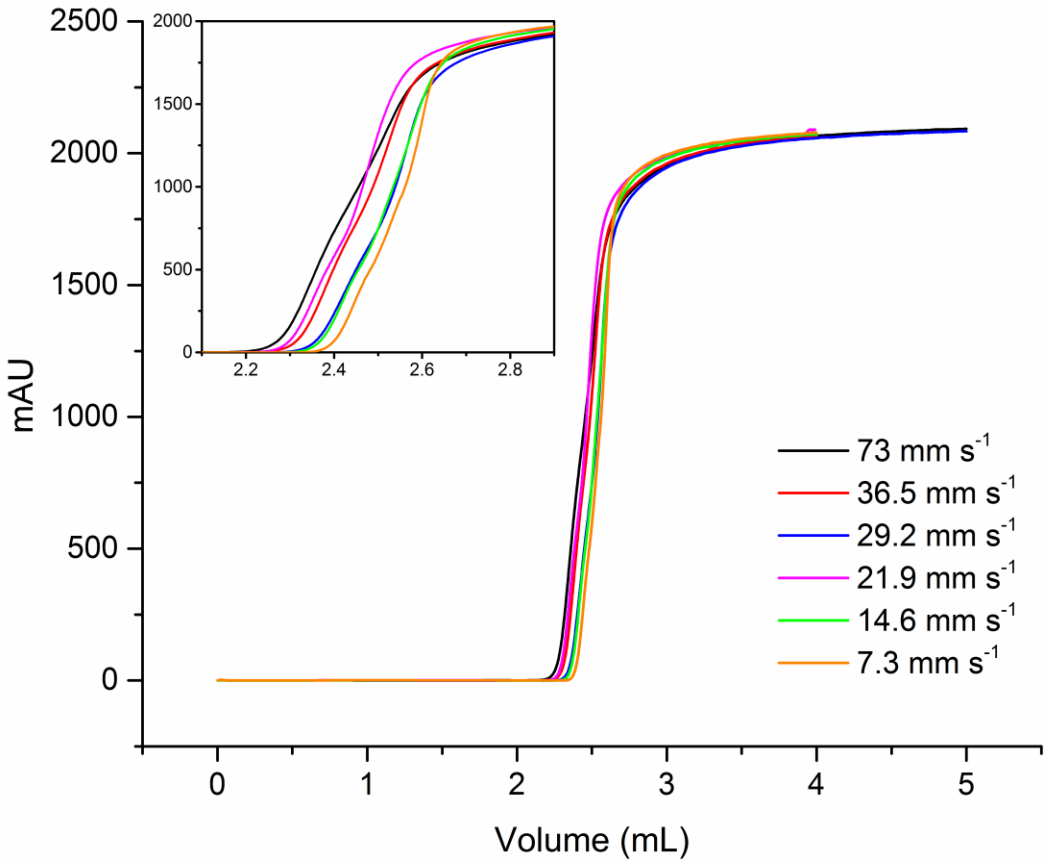

Figure 6.4 Lysozyme loading breakthrough curves on the nylon-COOH C-CP fiber column at constant protein loading concentration and various mobile phase linear velocities. The breakthrough curves are plotted on the volume basis. (Column length: 200 mm, I.D.: 0.762 mm. Loading buffer: 1 mg mL^{-1} lysozyme in 20 mM phosphate buffer, pH 6.5. Detection: 280 nm)

Consistency of the protein loading and elution

The ability to consistently recycle columns after saturation is a key attribute in terms of practical column lifetime. In many instances, some form of clean-in-place (CIP) step is required, both to remove undesirable contaminants such as host cell proteins (in downstream processing) as well as "unrecovered" target proteins in analytical separations. More so than in analytical-scale

separations, the ability to maintain consistent, high efficiency is challenging in preparative-scale applications where complete column saturation may occur. This is of course the case in the dynamic loading studies employed here, and so an evaluation of column stability/reproducibility was performed. After an initial cleaning using a 100 mM NaOH solution, 10 complete load/elute cycles were executed without any CIP performed in between. The subsequent load/elute transients are presented in Fig. 5, stacked from first-to-last from the bottom-to-top. As seen in each case, the nylon-COOH fiber bed is saturated. The consistency shown here is quite impressive in terms of both the load and elution steps, with the differences in load masses (via breakthrough volumes) differing by only 0.2 %RSD (n = 10) and the recoveries (via the integrated areas under the curve) by only 0.3 %RSD (n = 10). As an extension, though not needed here, the same experiment was repeated 6 additional times, with 10 min. 100 mM NaOH CIP exposures between each. Here again, there was no loss in binding capacity or recovery efficiency. This bares testament to the chemical robustness of the acrylic acid overlayer and the physical robustness of the base nylon fibers towards use for downstream processing applications.

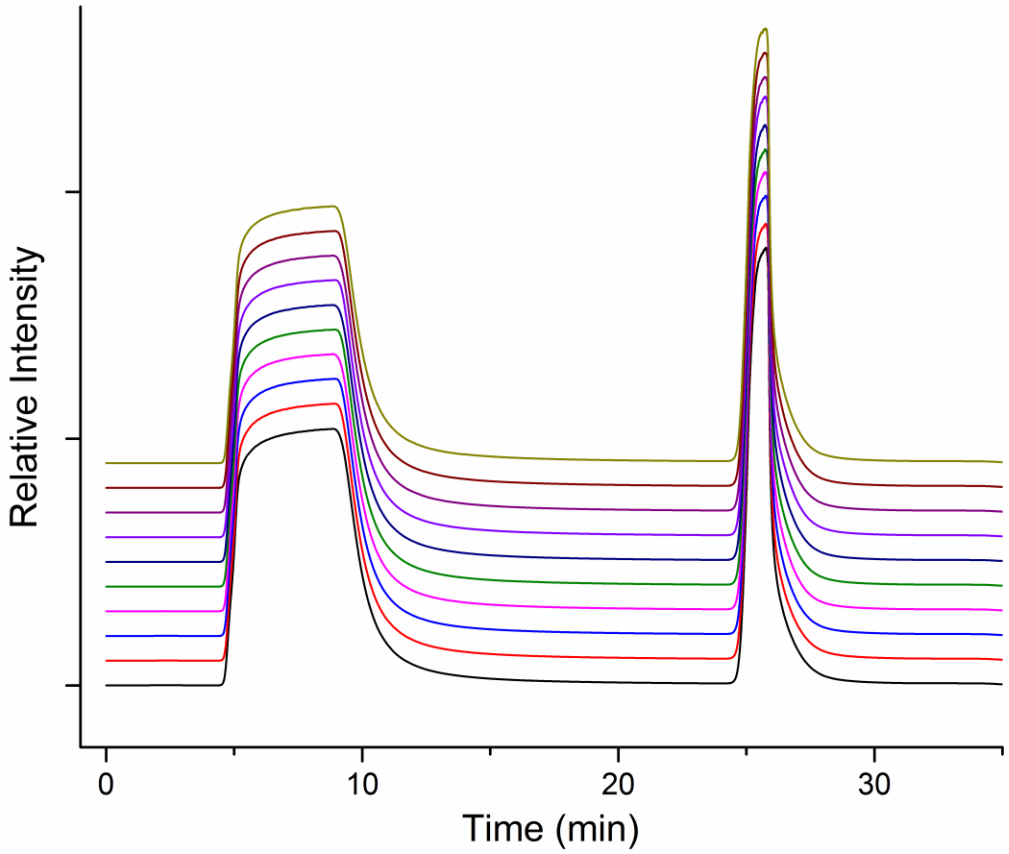

Figure 6.5 Chromatographs of 10 continuous lysozyme loading/elution cycles on the nylon-COOH C-CP fiber column without column regeneration in between. (Column length: 200 mm, I.D.: 0.762 mm. Loading buffer: 1 mg mL^{-1} lysozyme in 20 mM phosphate buffer, pH 6.5. Flow rate: 0.5 mL min^{-1}. Detection: 280 nm)

Batch-to-batch reproducibility of the modification process

It is a natural concern, due to the fact that the microwave modification reactions were not well controlled, that the batch-to-batch reproducibility would be suspect when using a simple domestic microwave oven. Different from commercial units designed for organic synthesis, the operational aspects of these units are not held to high rigor or precise control. To test the reproducibility

of the polymerization process, columns were made once a week for 5 consecutive weeks. Shown in Fig. 6 are the load/elute transients for those 5 columns (1.0 mg mL^{-1} lysozyme loading concentration at 0.5 mL min^{-1}), directly overlaid to emphasize the quality of the processing. The consistency shown here is very impressive in terms of both the load and elution steps, with the differences in load masses differing by only 3 %RSD (n = 5) and the recoveries by only 2 %RSD (n = 5). The overall performance of these columns is equivalent, though there are very slight differences seen in the transition regions of the breakthrough curves as seen in the insert of the figure. Since all of the columns were manually assembled following the microwave modifications, the variation due to the column packing is likely a contributing factor in the shapes of breakthrough curves. It is believed that these variations can be overcome by optimizing the column packing method and using better, controllable microwave reactors.

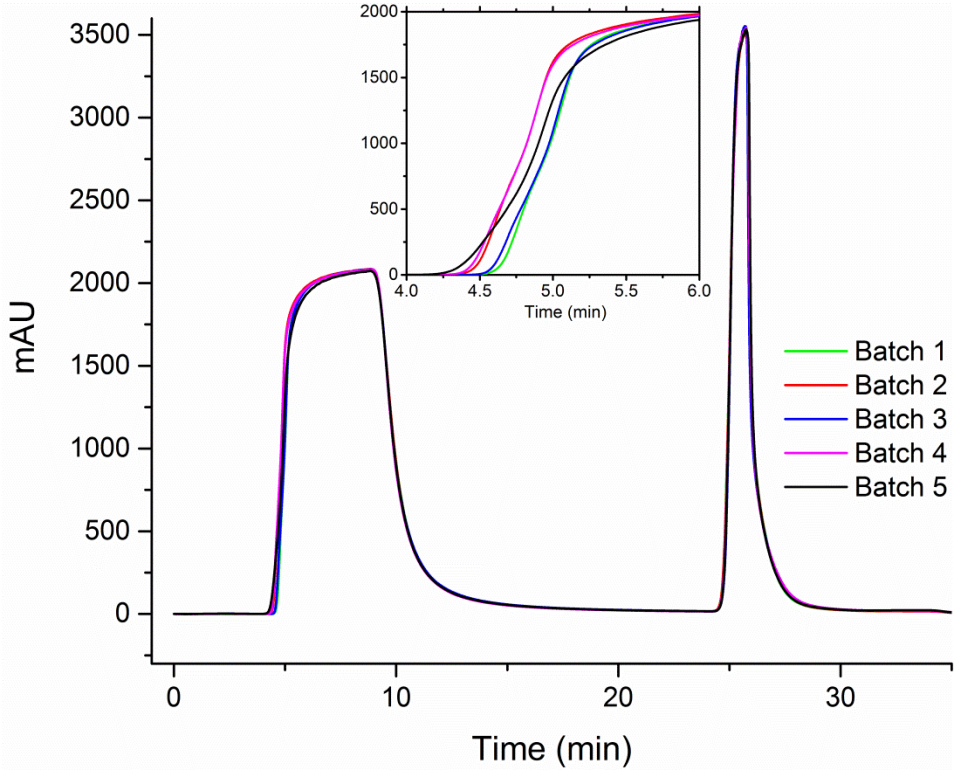

Figure 6.6 Chromatographs of lysozyme loading/elution on 5 nylon-COOH C-CP fiber columns that were prepared in different weeks. (Column length: 200 mm, I.D.: 0.762 mm. Loading buffer: 1 mg mL^{-1} lysozyme in 20 mM phosphate buffer, pH 6.5. Flow rate: 0.5 mL min^{-1}. Detection: 280 nm)

Rapid protein separation

While the load/elute studies readily demonstrate the enhanced loading capacity of the nylon-COOH phase versus native nylon 6, it would be equally desirable to have that phase be viable for analytical protein separations. The primary metrics here are the capacity to adequately separate the mixture components (an enthalpic quality) while also providing very high throughput (an entropic quality). Protein separations were evaluated at linear velocities of 7.3

and 36.5 mm s^{-1} for a four-protein (myoglobin, α-chymotrypsinogen A, cytochrome C and lysozyme) mixture using a more or less generic NaCl gradient. The chromatograms of the separations are showed in Fig. 7. The top set of chromatograms (Fig. 7a) reflects the protein separations on the native nylon 6 fiber phase. The native nylon has carboxylic acid end groups, however their low density leads to poor retention and broad elution peaks.[34] The cytochrome C component (2) is split into two peaks, the first peak co-eluted with the non-retained myoglobin (1) and the second co-eluting with chymotrypsinogen-A (3) as confirmed by single component injections. Meanwhile, the lysozyme peak (4) exhibits severe tailing and poor recovery. Use of the lower linear velocity (dashed line) provides little significant improvement. The same gradient separations were performed on the nylon-COOH column, as in the case of the nylon 6. The four proteins were well separated on the nylon-COOH column (Fig. 7b), with the hydrophilic myoglobin still remaining unretained. The other proteins show well-behaved responses, with high recoveries. The increase on the mobile phase linear velocity (5×) did not impair the baseline separation. Consistent with previous protein separations on C-CP fiber phases [20,21], increases in linear velocity do not diminish the resolution, with a tendency for the proteins to elute with at a slightly lower solvent strength. In these instances, the apparent loss of recovery (based on lower absorbance signals) is due to solute dilution per unit time and sometime constant bias in the optical detection system. Clearly the

nylon-COOH fiber phase provides a much-improved platform for high-throughput WCX protein separations.

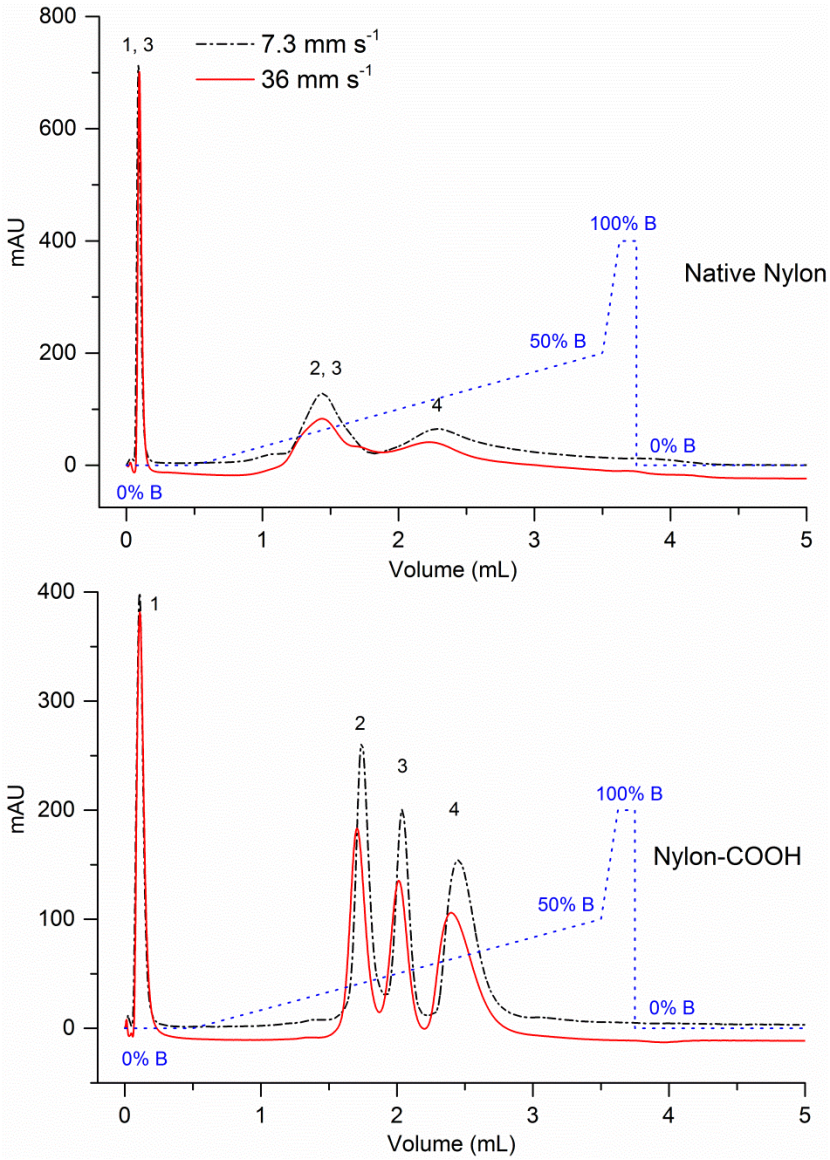

Figure 6.7 Separations of (1) myoglobin, (2) α-chymotrypsinogen A, (3) cytochrome C and (4) lysozyme on the native and nylon-COOH C-CP fiber columns at different linear velocities.

Conclusions

This proof-of-concept study demonstrates the feasibility and demonstrative advantages of the nylon-COOH C-CP fiber phase for protein separations. The native nylon C-CP fibers were functionalized with acrylic acid via a microwave-assisted grafting polymerization. Acid/base titrations reveal increased ligand density (-COOH, 575 ± 7 μmol g^{-1}) on nylon C-CP fibers after functionalization. The resulting nylon-COOH fiber packed column showed 12× increased protein dynamic binding capacity versus native nylon fibers, with values that are nearly independent to the mobile phase linear velocity. Excellent recovery of lysozyme was demonstrated on the nylon-COOH fiber phase under ion-exchange elution conditions. The intra- and inter-batch reproducibility was found to be 0.3 % and 3%. Fast protein separations were demonstrated on the nylon-COOH fiber phase, and the separation resolution was not affected by increasing the mobile phase linear velocity.

Acrylics are a very versatile family of monomers. A large number of acrylic monomers that contain different functional ligands is industrially available. Implementation of a similar modification route would allow the functionalization of the nylon 6 C-CP fibers with a variety of acrylic monomers such as (3-acrylamidopropyl)trimethylammonium chloride for strong anion exchange, N-[3-(dimethylamino)propyl]acrylamide for weak anion exchange, 3-allyloxy-2-hydroxy-1-propanesulfonic acid for strong cation exchange and allyl glycidyl ether for epoxide coupling chemistry. Although more study of the modification

conditions and the protein separations on nylon C-CP fiber stationary phase is still needed, the results from this study suggest that the nylon C-CP fiber modified by microwave-assisted grafting polymerization has a great potential for protein separations on the analytical and preparative scales.

Acknowledgements

This study is supported by the National Science Foundation Division of Chemistry under grant CHE-1307078.The authors appreciate the help from Dr. Qian Haijun (Clemson University Electron Microscope Facility) on SEM instrumentation and Ms. Kim Ivey (Analytical Testing Lab, Materials Science & Engineering, Clemson University) on ATR-FTIR instrumentation.

References

(1) Fekete, S.; Guillarme, D. *Trends. Analyt. Chem.* **2014**, *63*, 76-84.

(2) Gottschalk, U. *Biopharm. Int.* **2005**, *18*, 42-58.

(3) Wurm, F. M. *Nat. Biotechnol.* **2004**, *22*, 1393-1398.

(4) Gronemeyer, P.; Ditz, R.; Strube, J. *Bioengineering* **2014**, *1*, 188-212.

(5) Gottschalk, U. *Biotechnol. Progr.* **2008**, *24*, 496-503.

(6) Thömmes, J.; Etzel, M. *Biotechnol. Progr.* **2007**, *23*, 42-45.

(7) Ladisch, M. R. *Bioseparations Engineering: Principles, Practice, and Economics*; Wiley-Interscience: New York, 2001.

(8) Carta, G.; Jungbauer, A. *Protein Chromatography: Process Development and Scale-Up*; Wiley-VCH: Weinheim, 2010.

(9) Neue, U. D. *HPLC Columns: Theory, Technology, and Practice*; Wiley-VCH: New York, 1997.

(10) Walter, T. H.; Andrews, R. W. *Trends. Analyt. Chem.* **2014**, *63*, 14-20.

(11) Fekete, S.; Schappler, J.; Veuthey, J.-L.; Guillarme, D. *Trends. Analyt. Chem.* **2014**, *63*, 2-13.

(12) Kirkland, J. J.; Truszkowski, F. A.; Dilks, C. H.; Engel, G. S. *J. Chromatogr. A* **2000**, *890*, 3-13.

(13) Schuster, S. A.; Wagner, B. M.; Boyes, B. E.; Kirkland, J. J. *J. Chromatogr. A* **2013**, *1315*, 118-126.

(14) Svec, F.; Frechet, J. M. J. *Anal. Chem.* **1992**, *64*, 820-822.

(15) Ghosh, R. *J. Chromatogr. A* **2002**, *952*, 13-27.

(16) Marcus, R. K. *Journal of separation science* **2008**, *31*, 1923-1935.

(17) Arrua, R. D.; Talebi, M.; Causon, T. J.; Hilder, E. F. *Anal. Chim. Acta* **2012**, *738*, 1-12.

(18) Tanaka, N.; McCalley, D. V. *Anal. Chem.* **2016**, *88*, 279-298.

(19) Marcus, R. K.; Davis, W. C.; Knippel, B. C.; LaMotte, L.; Hill, T. A.; Perahia, D.; Jenkins, J. D. *J. Chromatogr. A* **2003**, *986*, 17-31.

(20) Nelson, D. M.; Marcus, R. K. *Anal. Chem.* **2006**, *78*, 8462-8471.

(21) Randunu, K. M.; Marcus, R. K. *Analytical and bioanalytical chemistry* **2012**, *404*, 721-729.

(22) Randunu, K. M.; Marcus, R. K. *Biotechnol. Prog.* **2013**, *29*, 1222-1229.

(23) Wang, Z.; Marcus, R. K. *Biotechnol. Progr.* **2015**, *15*, 97-109.

(24) Schadock-Hewitt, A. J.; Marcus, R. K. *Journal of separation science* **2014**, *37*, 495-504.

(25) Wang, Z.; Marcus, R. K. *J. Chromatogr. A* **2014**, *1351*, 82-89.

(26) Stanelle, R. D.; Mignanelli, M.; Brown, P.; Marcus, R. K. *Analytical and bioanalytical chemistry* **2006**, *384*, 250-258.

(27) Randunu, J. M.; Dimartino, S.; Marcus, R. K. *Journal of separation science* **2012**, *35*, 3270-3280.

(28) Stanelle, R.; Marcus, R. K. *Analytical and bioanalytical chemistry* **2009**, *393*, 273-281.

(29) Stanelle, R. D.; Straut, C. M.; Marcus, R. K. *J. Chromatogr. Sci.* **2007**, *45*, 415-421.

(30) Chambers, T. K. F., James. *J. Chromatogr. A* **1998**, 139-147.

(31) Yang, Y.-b. H., Kervin.Kindsvater, John. *J. Chromatogr. A* **1996**, *723*, 1-10.

(32) Jiang, L.; Marcus, R. K. *Analytical and bioanalytical chemistry* **2015**, *407*, 939-951.

(33) Jiang, L.; Jin, Y.; Marcus, R. K. *J. Chromatogr. A* **2015**, *1410*, 200-209.

(34) Jiang, L.; Marcus, R. K. *Analytical and bioanalytical chemistry* **2015**, 1-11.

(35) Jiang, L.; Schadock-Hewitt, A. J.; Zhang, L. X.; Marcus, R. K. *Analyst* **2015**, *140*, 1523-1534.

(36) Schadock-Hewitt, A. J.; Pittman, J. J.; Christensen, K. A.; Marcus, R. K. *Analyst* **2014**, *139*, 2108-2113.

(37) DePhillips, P.; Lenhoff, A. M. *J. Chromatogr. A* **2001**, *933*, 57-72.

(38) Gu, B.; Li, Y.; Lee, M. L. *Anal. Chem.* **2007**, *79*, 5848-5855.

(39) Hunter, A. K.; Carta, G. *J. Chromatogr. A* **2000**, *897*, 81-97.

(40) Schadock-Hewitt, A. J.; Pittman, J. J.; Stevens, K. A.; Marcus, R. K. *J. Appl. Polym. Sci.* **2013**, *128*, 1257-1265.

(41) Zhao, Q.; Gu, X.; Zhang, S.; Dong, M.; Jiang, P.; Hu, Z. *Surf. Coat. Technol.* **2014**, *240*, 197-203.

(42) Trang, H. K.; Schadock-Hewitt, A. J.; Jiang, L.; Marcus, R. K. *J. Chromatogr. B* **2016**, *1015*, 92-104.

(43) Xu, F. J.; Zhao, J. P.; Kang, E. T.; Neoh, K. G.; Li, J. *Langmuir* **2007**, *23*, 8585-8592.

(44) Herrera-Alonso, M.; McCarthy, T. J.; Jia, X. *Langmuir* **2006**, *22*, 1646-1651.

(45) Deng, J.; Wang, L.; Liu, L.; Yang, W. *Prog. Polym. Sci.* **2009**, *34*, 156-193.

(46) Choi, H.-S.; Kim, Y.-S.; Zhang, Y.; Tang, S.; Myung, S.-W.; Shin, B.-C. *Surf. Coat. Technol.* **2004**, *182*, 55-64.

(47) Bhattacharya, A.; Misra, B. N. *Prog. Polym. Sci.* **2004**, *29*, 767-814.

(48) Zhang, C.; Liao, L.; Gong, S. *Green Chem.* **2007**, *9*, 303-314.

(49) Sinnwell, S.; Ritter, H. *Aust. J. Chem.* **2007**, *60*, 729-743.

(50) Hoogenboom, R.; Schubert, U. S. *Macromol. Rapid Commun.* **2007**, *28*, 368-386.

(51) Wiesbrock, F.; Hoogenboom, R.; Schubert, U. S. *Macromol. Rapid Commun.* **2004**, *25*, 1739-1764.

(52) Kappe, C. O.; Pieber, B.; Dallinger, D. *Angew. Chem. Int. Ed.* **2013**, *52*, 1088-1094.

(53) Dudley, G. B.; Stiegman, A. E.; Rosana, M. R. *Angew. Chem. Int. Ed.* **2013**, *52*, 7918-7923.

(54) Sosnik, A.; Gotelli, G.; Abraham, G. A. *Prog. Polym. Sci.* **2011**, *36*, 1050-1078.

(55) Hunkeler, D. *Macromolecules* **1991**, *24*, 2160-2171.

(56) Gong, B.; Ke, C.; Geng, X. *Analytical and bioanalytical chemistry* **2003**, *375*, 769-774.

(57) Wei, Y.; Huang, X.; Liu, R.; Shen, Y.; Geng, X. *Journal of separation science* **2006**, *29*, 5-13.

(58) Zhao, K. L.; Song, C.; Wang, F.; Bai, Q. *Chin. Chem. Lett.* **2012**, *23*, 305-308.

CHAPTER VII

MICROWAVE-ASSISTED GRAFTING POLYMERIZATION MODIFICATION OF NYLON 6 CAPILLARY-CHANNELED POLYMER FIBERS FOR ION EXCHANGE PROTEIN SEPARATIONS: II – STRONG CATION EXCHANGE

Introduction

Ion-exchange chromatography (IEC) is based on the electrostatic interaction between charged analytes and opposite-charged ligands on the chromatography support phase. The separation takes place as analytes making up the mixture have different affinities to the ligands and thus are eluted from stationary phase at different times/solvent compositions. IEC is especially popular in biomolecule separations, such as analytical and preparative protein separations [1]. The complicated nature of proteins results in relatively weak interactions with ion-exchangers in comparison hard inorganic ions. As such, proteins can be separated and eluted under “soft” solvent conditions where protein denaturation is minimal [2]. The commonly used chromatography support phases include silica-based materials and organic polymers. However, silica-based phases suffer from chemical and physical deterioration at desirable biological pH conditions [3]. Moreover, in the case of IEC, where alkaline buffers are typically used in elution or column regeneration, organic polymer phases offer superior robustness over silica-based materials. The commonly used synthetic polymeric stationary phases, such as polystyrene-divinylbenzene beads

(PS-DVB) and polyacrylamide (PAM) gel, remain inert across a wide range of pH conditions [2,4].

Beyond chemical effects, peak tailing and slow separation of macromolecules are problematic on porous particulate-packed columns due to the high mass transfer resistance as they diffuse through the pores. Superficially porous silica microspheres are composed of non-porous cores and thin porous outer shells (0.1 – 1 μm). The superficially porous silica bead-packed columns are capable of fast separation of macromolecule at relatively high mobile phase velocities [5,6]. Monolithic columns have attracted a lot of attention on protein separations along these lines since they were introduced in 1990s [7,8]. Use of polymeric monoliths provide high mass transfer efficiencies along with the chemical robustness desirable for protein IEC separations[2]. The large through-pores and channels in monolithic columns enable them to perform fast protein separations at high flow rate and low backpressure while maintaining high mass transport efficiencies.

Capillary-channeled polymer (C-CP) fibers have been studied in this laboratory as a support/stationary phase for protein separations [9-11]. C-CP fibers are 30 – 50 μm in diameter, with 8 axial capillary channels on their surface running along the length of the fiber. Once packed in a column format, C-CP fibers self-align and form flow-through channels that allow efficient, high permeability fluidic transport. The short inter-fiber separations result in very rapid, solution-surface mass transfer. The relatively non-porous (in comparison to the

size of proteins) surface of C-CP fibers eliminates van Deemter C-term broadening at linear velocities of up to 100 mm s^{-1} [12]. The low-cost, high permeability, low mass transfer resistance and very high protein throughput of these materials bodes well for both analytical and preparative-scale protein separations. However, low equilibrium protein binding capacities, due to low specific surface areas (1 - 5 m^2 g^{-1}) and relatively low native surface ligand densities, may limit some applications of the C-CP fibers [11,13].

C-CP fibers are made via melt extrusion of commonly used polymers including polypropylene (PP), polyester (PET) and polyamide (nylon 6). PP and PET C-CP columns have been studied for reversed phase protein separations [11,12,14]. Due to its lower degree of hydrophobicity than PP and PET, nylon 6 C-CP fibers have been studied as a hydrophobic interaction chromatography (HIC) and mixed-mode (RP and IEC) stationary phases for protein separations [15,16]. Beyond the basic chemistries present on the surface of C-CP fibers, a good deal of effort has been placed into improving the selectivity available of the fiber separations. Adsorption chemistries have been employed to anchor ligands on PP fiber surfaces. Protein A-modified PP C-CP columns are easily manufactured, having high levels of chemical robustness and excellent throughput and yield for the capture of immunoglobulin G (IgG) [17,18]. A totally new approach to adsorptive modification involves the use of lipid tethered ligands (LTLs) to affect affinity separations [19,20]. Amine coupling chemistry has been performed on PET C-CP fibers to affect the surface chemistry to increase the

protein binding capacity [21,22]. In the case of ion-exchange chromatography where high and low pH buffers were used, the chemical stability of PET is a concern relative to column lifetime [23]. Surface hydrophobicity of the base polymer also plays an important role on protein separation. Proteins tend to non-specifically bind to hydrophobic surfaces, leading to peak tailing and low recovery [24,25]. As such, nylon 6 would be least prone to non-specific retention, so long as a suitable chemical modification could be implemented to achieve the desired selectivity.

Several nylon surface functionalization methods have been reported in the literature [26-28], unfortunately they usually cause structural damage to the bulk material structure; i.e. the physical structure of fibers is compromised. In the case of using nylon 6 C-CP fibers as chromatographic stationary phases, high densities of ligands need to be affected on the nylon surface without compromising the fiber structure. Previously, we reported a proof-of-concept study on the surface modification of nylon 6 C-CP fibers for weak anion exchange (WAX) separations of proteins[29]. Native fibers were functionalized with poly-acrylic acid via a microwave-assisted grafting polymerization of acrylic acid. In comparison to the native nylon 6 fibers, the modified fibers (nylon-COOH), showed an ~20× increase in –COOH ligand density and ~12× increase of lysozyme binding capacity. Better protein separations were also realized on the nylon-COOH fibers than native nylon fibers. Despite the promising results, further study is necessary to better understand how the reaction conditions affect

the ligand density and the protein separation performance on the nylon C-CP phase.

In this study, native nylon C-CP fibers are functionalized with acrylamido-2-methylpropanesulfonic acid (AMPS) by microwave-assisted grafting polymerization. In this way, sulfonate groups common to strong cation exchange (SCX) populate the fiber surface. The resultant nylon-SO_3H fibers are characterized by FT-IR and scanning electron microscopy (SEM), with the density of the added $–SO_3H$ ligands determined by acid-base titration. Various reaction conditions, including monomer and initiator concentrations, were evaluated. These parameters were not investigated in the original description of the methodology [29]. Protein separation qualities and dynamic loading capacities were examined on the modified fibers. Very fast protein separations under high mobile phase linear velocities (up to 110 mm s^{-1}) were performed, with the column re-equilibrium characteristics probed in terms of using the modified nylon C-CP column as the second dimensional phase in 2D HPLC separations. It is believed that the microwave-assisted grafting polymerization holds promise for creation of phases for both analytical and preparative scale separations, with the promise of further diversification of the potential C-CP fiber surface modalities.

Experimental methods

Chemicals and instruments

Unless otherwise specified, chemicals were purchased from commercially available sources and used without further purification. Nylon 6 C-CP fibers were obtained from the Material Science and Engineering Department of Clemson University. Potassium persulfate (KPS) (99%) was purchased from Alfa Aesar (Haverhill, MA). 2-Acrylamido-2-methylpropanesulfonic acid (AMPS, 99%) and all HPLC solvents were purchased from EMD (Billerica, MA). All other chemicals and all proteins were purchased from Sigma-Aldrich (St. Louis, MO). Deionized water (DI-H_2O) was prepared using an in-house Milli-Q water system.

All chromatography experiments were performed on a Dionex Ultimate 3000 HPLC system (LPG-3400SD Quaternary pump, MWD-3000 UV–vis absorbance detector, Thermo Fisher Scientific Inc., Sunnyvale, CA). A Rheodyne model 8125 low dispersion injector with either a 3 or 5 μL injection loop used for protein sample injections. The microwave-assisted polymerizations were performed in a household-type Sunbeam SBM7700W microwave oven, without any modifications of the commercial unit.

Microwave-assisted nylon 6 C-CP fiber surface modification

The details of the modification have been reported in literature [29]. All DI-H_2O used in the modification reactions was purged with nitrogen for 30 min prior to use to remove oxygen. The native nylon 6 C-CP fibers were removed from the

fiber spool and placed on a dying fork. For each modification reaction, 720 fibers of ~35 cm length were used. The fibers were cleaned with excess amounts of DI-H_2O, methanol, and DI-H_2O again, to remove chemical residues left from fiber extrusion process. The modification solution was prepared by dissolving the desired amounts of AMPS and potassium persulfate in 20 mL of deoxygenated DI-H_2O. The fibers were then placed into the modification solution in a 50 mL beaker. The fibers were immersed and uniformly suspended in the solution. The beaker was then put in the microwave oven along with another beaker containing 30 mL of tap water as a "heat sink" [29]. The microwave reaction was run at 100 W for 10 min. After reaction, the fibers were removed from the beaker immediately and washed with excess amounts of DI-H_2O until no visible homopolymer residues were seen on the fibers. The modified nylon C-CP fibers are referred to as "nylon-SO_3H". In order to assess any physical perturbations to the fibers due to microwave irradiation and hot water exposure, control experiments were run in DI-H_2O instead of the modification solution.

Preparation of C-CP fiber columns

The column packing technique used in this study has been reported in literature [14]. Native nylon 6 and nylon-SO_3H C-CP fiber bundles were pulled through polyether ether ketone tubing (PEEK, 0.762 mm i.d., IDEX Health & Science LLC, Oak Harbor, WA) by a fishing line. After packing, the columns were washed with phosphate buffer (10 mM, pH = 6.5) at 0.2 mL min^{-1} for 12 h to remove any non-covalently bound chemicals (such as initiators, homopolymers)

from the fiber. After cleaning on the HPLC, the columns were cut from both ends to achieve the desired length. The columns were capped and stored at room temperature.

Characterization of the modified nylon C-CP fibers

The attenuated total reflection-Fourier transform infrared spectroscopy (ATR-FTIR) was run on a Thermo-Nicolet Magna 550 FT-IR in the Analytical Testing Laboratory of the Clemson University Material Science and Engineering Department. Nylon fiber samples were cleaned with water, methanol and acetone, and then dried under vacuum for 12 h prior to FT-IR analysis. Scanning electron microscope (SEM) images were taken in the Electron Microscopy Laboratory, Clemson University using Hitachi SU6600 instrument operating in the variable pressure mode, and a 20 kV accelerating voltage. Fiber column cross sections were obtained by filling with water and freezing in liquid nitrogen before cutting to minimize fiber movement during cutting process.

The ligand densities of native nylon 6 and nylon-SO_3H C-CP fibers were determined by acid-base titration. Native and modified fibers were washed with 100 mM HCl solution for 1 min, and then with large amounts of DI-H_2O to remove HCl residue on fibers. The fibers were then washed with acetone to remove the water, and dried under vacuum (an Edwards 1.5 vacuum pump was used) for 20 hours at room temperature. The dried fibers were titrated with standardized NaOH solution (0.1142 M) with phenolphthalein as the indicator.

The hydrodynamic permeability of the fiber columns was determined by running phosphate buffer (20 mM, pH = 6.5) in the columns at different flow rates. The backpressure and corresponded mobile phase linear velocity were recorded and the permeability was calculated (Eq. 1)

$$\frac{\Delta P}{L} = \frac{u\mu}{k_w} \quad (1)$$

where ΔP represents the column pressure drop (Pa), L is the column length in meters, u is the linear velocity of the mobile phase (m s^{-1}), μ is the mobile phase viscosity (Pa s) and k_w is the column permeability [30,31]. The viscosity of 20 mM phosphate buffer was obtain from [32,33].

Liquid chromatography

All experiments were performed on a Dionex Ultimate 3000 HPLC system. Phosphate buffer (20 mM, pH = 6.5) was prepared and designated as buffer A. To buffer A, 1 M NaCl was added and the resulting buffer was designated as buffer B.

The dynamic loading capacity (DLC) of the column was determined by protein breakthrough experiments. In the experiments, lysozyme in buffer A was loaded in the column until the UV absorbance at 280 nm reached plateau, indicating the saturation of the column. To remove the loaded protein, buffer B was then applied on the column until the absorbance reached the original baseline. The DLC data was calculated from the breakthrough curves through

frontal analysis [18]. If needed, column regeneration was performed by washing the column with a 100 mM NaOH, 1M NaCl solution for 10 min.

For the protein separation experiments, 5 μL of the protein mixture containing 0.1 - 0.25 mg mL^{-1} each of myoglobin, α-chymotrypsinogen A and lysozyme was injected. Gradient elution was performed from 100% buffer A to 100% buffer B. The chromatogram was recorded as the UV-vis absorbance at 216 nm.

Results and discussions

Surface modification of nylon 6 C-CP fibers.

The enthalpic aspects of polymer stationary phases are dictated by the corresponding surface chemistries. There are two basic approaches to affect the surface chemistry on polymeric stationary phases [34,35]. The most straightforward way is to prepare the polymer directly from the monomers containing functional ligands, or co-polymerizing these ligand monomers with other monomers that provide desired mechanical characteristics. However, this approach is limited in three ways: 1) Reaction conditions optimized for one polymer system cannot be directly used on other systems. When different ligand monomers are employed, re-optimization of the polymerization conditions is required to obtain the desired particle size, porosity, etc.; a time-consuming process [2,35,36]. 2) Changes in the solvent composition (make-up and counter-ions) can lead to large amounts of swelling and de-swelling of the stationary

phase bulk structure [37]. These changes reduce the reproducibility of separations and access to/from ligand sites. 3) A large portion of the functional ligands are in the polymer bulk structure and not accessible by macromolecular analytes in particular.

Another approach to introduce functional ligands “onto” polymer supports is to include a monomer bearing a reactive group, e.g., epoxide, ester and amine, in the base polymer as “anchors” to the surface. Thus, the support having the desired mechanical/physical attributes can be functionalized afterward by attaching ligands to the reactive groups [38]. Surface grafting is one means to introduce ligands onto the surface of base polymer materials [39,40]. The advantage of surface grafting is that high densities of ligand can be attached to the support and be accessible to macromolecular analytes. Surface grafting includes two categories: “grafting onto” and “grafting from”. The “grafting onto” method refers to attaching functional polymer chains from reaction solution onto the base polymer. However, the polymer chains are more thermodynamically favored in the solution phase rather than on the polymer surface. The attached polymer chains increase the steric hindrance for the subsequent grafting. As a result, the “grafting onto” approach is usually self-limiting with low grafting densities. The “grafting from” approach refers to “growing” functional polymer chains from the reactive groups on the base polymer surface. In the “grafting from” mechanism, the polymerization is initiated and propagated from the base

polymer surface, as such the method results in greater grafting densities than "grafting onto" method [41,42].

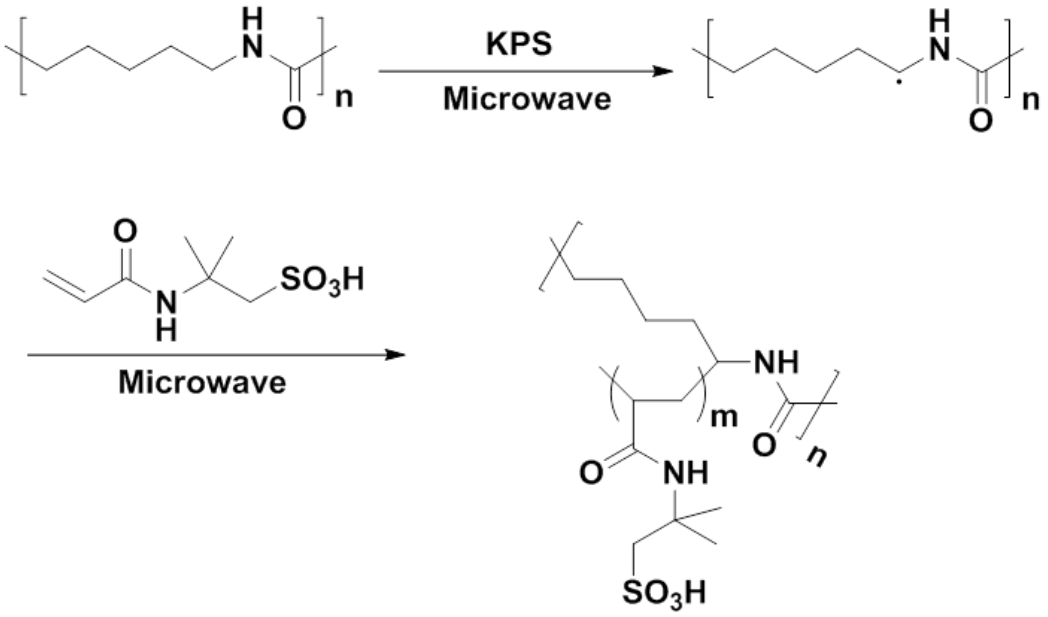

Figure 7.1 Reaction scheme of microwave-assisted grafting polymerization on nylon 6 C-CP fibers.

In this study, poly-AMPS was grafted from the nylon 6 C-CP fiber surface via a microwave-assisted radical polymerization using KPS as the initiator (Fig. 1). The mechanism of the reaction has been discussed [43,44]. Although thermo or UV radiation is commonly used for initiating grafting polymerization, they are not appropriate for this system. Their unique shape makes C-CP fibers unlikely to be uniformly illuminated by UV light. Conventional heating usually requires stirring the material that is being heated, twisting or folding the fibers and ultimately sacrificing the column packing uniformity. Microwave energy is

used in here because it is capable of homogeneous treatment of the C-CP fibers without disturbing the alignment of the fiber bundles. Under microwave irradiation, the persulfate initiator decomposes and forms persulfate radicals in solution. Persulfate radicals can also react with water to form hydroxyl radicals. These radicals initiate the acrylic monomer polymerization in the solution phase and on the nylon fiber surfaces. The preliminary research showed very good batch-to-batch reproducibility for the microwave-assisted grafting polymerization of carboxylic acid moieties on nylon 6 C-CP fibers [29].

Grafted ligand density

The concentrations of the reactants and the reaction conditions dictate the extent of the surface modification. Various monomer (AMPS) and initiator (KPS) concentrations were used for the grafting polymerization on nylon 6 C-CP fibers. When more than 30% (w/v) AMPS was attempted in the reaction, large amounts of homopolymer formed in the solution phase and it was very difficult to clean the fibers. The permeability of the resultant fiber packed columns was very low. Thus, it was not practical to use those columns for separation. AMPS concentrations lower than 7.5% resulted in minimal ligand grafting on fibers. It is well-known that initiators (KPS) not only initiate the polymerizations but react with other radicals [45], thus a balance must be achieved. With lower KPS concentrations, fewer grafting sites are seeded on the nylon surface thus low ligand densities would be expected, although higher degree of polymerization may occur on single polymer chain. Increases in the initiator concentration would

surely lead to greater opportunities for surface activation but also increasing the possibility of terminating the chain propagation, which results in low degrees of polymerization and low ligand densities. Studies by Zhang and co-workers had shown that ~0.5% KPS is sufficient to initiate grafting polymerization on nylon 66 surfaces [43].

Table 7.1. Reaction conditions and the resultant nylon C-CP fiber/column properties.

Stationary Phase	AMPS (w/v)	KPS (w/v)	Ligand Density (μmol g^{-1})	Permeability (10^{-12} m^2)	R^2
Native Nylon	N/A	N/A	28 ± 9	8.8	0.9947
Nylon-SO_3H #1	30%	0.125%	115 ± 12	0.59	0.9822
Nylon-SO_3H #2	30%	0.25%	317 ± 13	0.41	0.9785
Nylon-SO_3H #3	30%	0.50%	245 ± 21	0.59	0.9772
Nylon-SO_3H #4	15%	0.25%	132 ± 19	4.2	0.9892
Nylon-SO_3H #5	15%	0.50%	108 ± 5	3.2	0.9815
Nylon-SO_3H #6	7.5%	0.50%	50 ± 7	7.3	0.9942

The combinations of reactant concentrations and column characteristics are listed in Table 1. With the same reaction times, reaction volume and microwave power were applied, with the concentration of AMPS monomer varied from 7.5% - 30% (w/v) and the concentrations of the initiator varied from 0.125% - 0.5% (w/v). The sulfonic acid ligand densities determined through acid-base titration of the fibers for triplicate reactions are listed in Table 1. Without any modification, the native nylon fiber has a ligand density (-COOH in this case) of 28 μmol g^{-1}. The set of tradeoffs in terms of initiator is clearly demonstrated in

entries nylon-SO_3H #1-to-3 in the table for the fixed AMPS concentration of 30 % (w/v) (the maximum concentration of monomer to form a homogeneous solution). Doubling of the KPS concentration from 0.125 to 0.25 % yields an ~2.8X increase the surface ligand density to a maximum value of 317 μmol g^{-1}, while a further doubling of the KPS concentration actually results in a reduction in the surface density by ~25%. Use of lower AMPS concentrations below the highest practical concentration was investigated, yielding the expected results. In comparison to nylon-SO_3H #2, reducing the AMPS concentration by one-half to 15% at the optimum KPS (nylon-SO_3H #4) reduced the determined ligand density by approximately the same proportion. Increasing the KPS concentration from 0.25 to 0.5% to perhaps compensate for the loss (nylon-SO_3H #5) reduced the ligand concentration as it did at the higher AMPS concentration. A further decrease of the AMPS concentration to 7.5% (nylon-SO_3H #6) led to 50% loss of the ligand density, in comparison to nylon-SO_3H #5. The concentration of AMPS is clearly the limiting factor in the grafting polymerization reactions, while at the highest workable AMPS concentration (30%) the KPS concentration largely affects the ligand density.

The ligand densities of nylon-SO_3H fibers are similar to other SCX media. Polyester short-cut “winged” fibers were modified by surface-initiated atom transfer radical polymerization (SI-ATRP) for protein SCX separations and the ligand density were determined to be 50 - 400 μmol g^{-1} [46]. A monolithic cryogel material, prepared by copolymerization of 2-hydroxyethylmethacrylate (HEMA)

and glycidyl-methacrylate (GMA) and then treated with 3-mercaptopropane sulfonic acid for SCX separation, showed a sulfonic acid density of 530 μmol g^{-1} [47]. The porous resin beads, Fractogel® EMD SO_3^- (M), has a ligand density of 380 μmol g^{-1} [48]. It is important to note that those ligands exist on the surface of the C-CP fibers, as opposed to the latter porous media, where those ligands are not necessarily accessible to proteins. Specifically, for these C-CP fibers, the surface ligand density is ~0.01 μmol cm^2 and ~190 μmol mL^{-1} on a bed volume basis.

Characterization of the modified fibers

The native nylon 6 and modified fibers were examined by ATR-FTIR to assess the chemical functionality of their surfaces. As shown in Fig. 2a, the spectra across the suit of fibers (designated according to the compositions presented in Table 1) are virtually identical. The consistency among the various fibers suggests that the grafting polymerization conditions do not appreciable perturb the fibers' composition/structure. The most prominent transitions are consistent with the bulk nylon composition with the classic signature features being: 3300 cm^{-1} (N-H stretch), 2931 cm^{-1} (CH_2 asymmetric stretch), 2861 cm^{-1} (CH_2 symmetric stretch), and 1639 cm^{-1} (amide stretch). The sole spectral feature that differs between the native and modified fibers exists at a frequency of 1041 cm^{-1}, corresponding to S=O stretch associated with the $–SO_3H$ ligand present after AMPS modification. Scale expansion around that spectral region (Fig. 2b) provides spectroscopic confirmation of the titration-determined ligand

densities in Table 1. The magnitude of the S=O peak absorbance for the nylon-SO_3H #2 fiber is the highest, followed by those nylon-SO_3H #3 and #1. However, those same transitions show much lower absorbance values in the cases of nylon-SO_3H #4 and #5, even though they have similar densities to those of nylon-SO_3H #1. ATR-FTIR is a surface-sensitive method, but as an absorbance measurement is still sensitive to the path length over which the absorbers exist. In the case of the grafting polymerization, the ratio of the monomer to initiator also affects the length of the polymer chains. In this case, high AMPS concentrations yield long chains, while low concentrations populating many active surface sites, yield short chains. This assumption agrees with the column backpressure data that will be discussed later. Thus, while the number of absorbing ligands (based on titration) is similar between treatments #1, #4, and #5, the absorbance in the latter two is much lower due to shorter ligand chains.

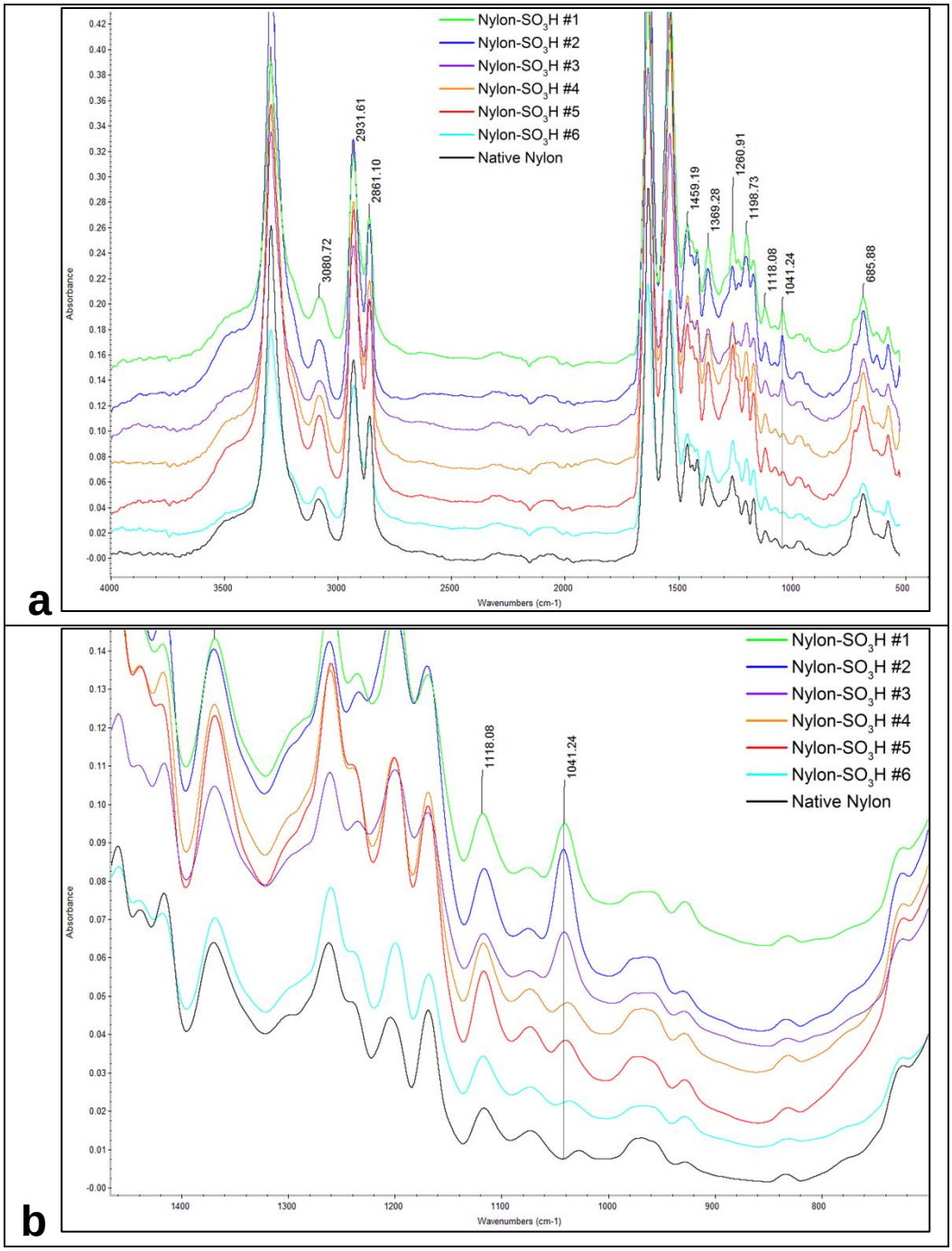

Figure 7.2 ATR-FTIR spectra of the native and modified nylon 6 C-CP fibers.

To investigate potential differences in fiber morphology, native and modified nylon fibers and fiber column cross-sections were examined by SEM (Fig. 3). Differences between the native and modified fibers could come about due to fiber swelling, creation of layers, or degradation of the bulk fiber structure. As was the case in the previous works in the microwave grafting of acrylic acid [29], the cross sectional micrographs reflect a tighter packing of the modified fibers versus the native nylon 6, even though the number of fibers is the same for all cases. The increased packing density after surface modification is due to the increase of fiber diameter, in other words, the thickness of the channel "walls" of the fibers. A control experiment was done by microwave heating of native nylon 6 fibers in water instead of modification solution. The control fiber column sample did not show any increase of packing density or fiber diameter, which indicates the increased thickness is due to the added poly-AMPS overlayer on fiber surface. While far from quantitative, the cross sections reflect the fact Nylon-SO_3H #2 fiber, having the highest grafted ligand density, has the highest packing density. Indeed, columns composed of fibers having the least number of ligand show lower packing densities. To the point of diagnosing any changes to the base fiber geometries, the side-on micrographs reveal that fibers' channel geometries are retained in the modification process.

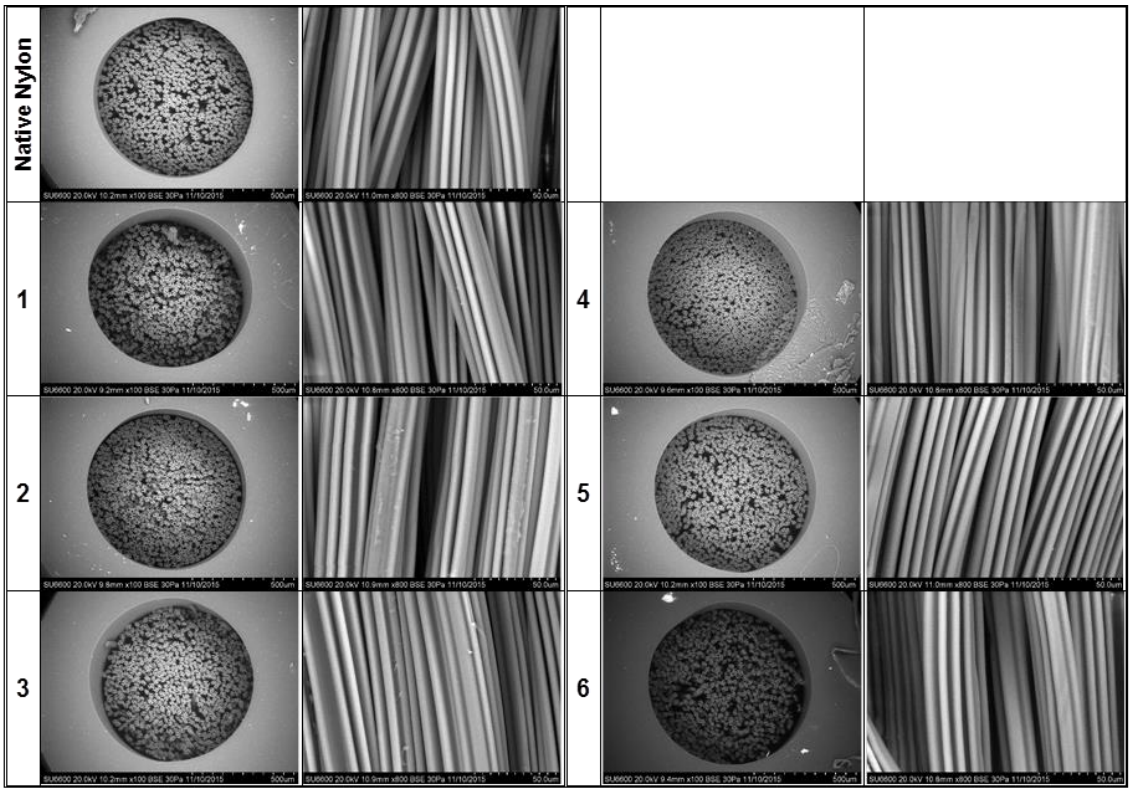

Figure 7.3 SEM images of native nylon 6 C-CP fibers and nylon-SO_3H C-CP fibers. Numbers correspond to the treatment procedure listed in Table 1.

Column permeability

As noted previously, while the goals of the microwave assisted grafting polymerization process are improved selectivity and capacity, they must be achieved without compromising the inherent hydrodynamic advantages of C-CP fiber columns. The ideal is to allow high linear velocities to be achieved at normal HPLC backpressures, while maintaining the requisite solute-surface interactions. The permeability of nylon-SO_3H columns was determined by pumping mobile phase through columns at different flow rates (linear velocities).

The relationship between column pressure drops (kPa cm^{-1}) and mobile phase linear velocity (using 20 mM potassium phosphate mobile phase) are plotted for the native nylon 6 and the modified C-CP fiber column suite in Fig. 4, with the calculated permeability values listed in Table 1. The ranges depicted here reflect the maximum operating pressure of ~7500 kPa for the 20 cm long columns employed here. The well-behaved linear fits depicted in Fig. 4, along with the goodness-of-fit (R^2 = 0.9772 – 0.9947) values in Table 1, indicate negligible stationary phase compression or bed perturbation. The native nylon 6 C-CP column showed the highest permeability of 8.8×10^{-12} m^2 while the nylon-SO_3H #2, having the highest ligand density, showed the lowest permeability of 4.1×10^{-13} m^2. As in the case of the ligand density values, two clear sets are apparent; those of the highest AMPS monomer concentration and the others. However, the column permeability does not have a simple inverse relationship with the ligand density. The columns composed of nylon-SO_3H #1, #4 and #5 are similar in ligand density but differ appreciably in their permeability. A possible explanation is that the surface ligand layer on nylon-SO_3H #1 extends further from the surface (longer ligand chains) than the nylon-SO_3H #4 and #5 fibers, and as such could lead to more swelling of the ligand layer in buffer solution and lowering the column permeability. This rationale, fewer ligand attachments but longer chains, is consistent with what was proposed as the reason for the apparent lower number density in the ATR-FTIR spectra and the pressure changes during salt

gradients. Such a situation would also be expected to have ramifications in the protein loading capacity of the various treatments.

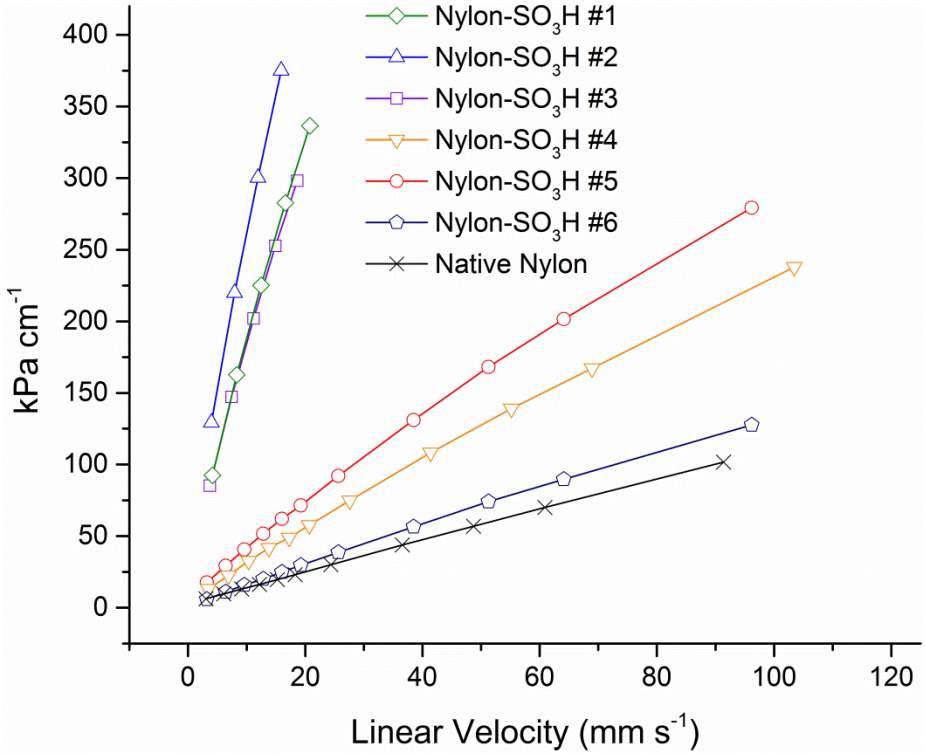

Figure 7.4 Column backpressure as a function of mobile phase linear velocity. Mobile phase: 20 mM phosphate buffer, pH 6.5.

Lysozyme loading capacity

The protein dynamic loading capacity (DLC) of the nylon C-CP fiber columns was determined by breakthrough experiments with lysozyme as the model protein. Various concentrations (0.1 – 1 mg mL^{-1}) of lysozyme in buffer A (20 mM phosphate, pH 6.5) were fed into columns at 0.2 mL min^{-1} (~15 mm s^{-1} linear velocity) until the absorbance at 280 nm reached plateau, indicating the

saturation of the column by lysozyme. Elution of the bound protein was done by passing buffer B (1 M NaCl in buffer A) though the column. The determined DLC values are shown in Fig. 5. Without surface modification, the native nylon 6 C-CP fiber column has a lysozyme DLC of about 1 mg mL^{-1} bed volume. The grafting polymerization modification greatly enhances the DLC on the same number of nylon fibers, up to ~13 mg mL^{-1}. However, high ligand densities as determined by titration do not necessarily yield higher protein loading capacity, with the same two general groups seen as had segregated themselves in the FT-IR and permeability characteristics. Slight differences are seen within the groups. Nylon-SO_3H #1 has the highest DLC but its ligand density is appreciably lower than the nylon-SO_3H #2 and #3 columns (Table 1). It needs to be emphasized that acid-base titrations determine all ligands that are accessible to the solvent, including ligands not accessible by proteins. By the same token, the spatial distribution of ligands can be such that a given protein molecule surely covers multiple surface ligands, thus a one-to-one correlation cannot be realized. In essence, higher numbers of ligands are wasted.

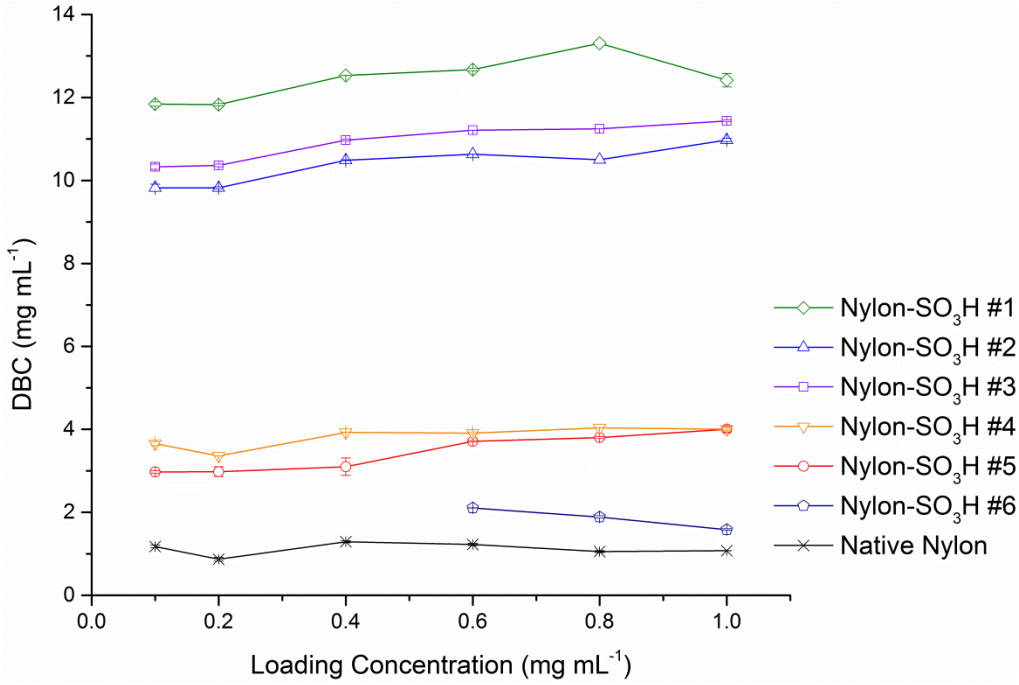

Figure 7.5 Effect of the lysozyme concentration on the dynamic loading capacity for the native nylon and nylon-SO_3H fiber columns. Note that errors bars for triplicate determinations are within the many of the data symbols. (Column length: 200 mm, I.D.: 0.762 mm. Loading buffer: lysozyme in 20 mM phosphate buffer, pH 6.5. Flow rate: 0.2 mL min^{-1}).

Comparison of the loading capacity of nylon-SO_3H #1 to those of nylon-SO_3H #4 and #5 presents another set of situations. Based on the titration-based ligand densities, these should have similar protein capacities. What is seen is a dramatic depression in the latter two cases. This mismatch agrees with the observation in the FTIR spectra and permeability of nylon-SO_3H #4 and #5, where it was suggested that those ligands are more surface-bound, and not extending from the surface. As such, they would be less efficient in effectively acting as interaction sites for protein solutes.

As a final note, for all nylon-SO_3H columns, there is virtually no concentration dependence of the dynamic loading capacity on the lysozyme feed concentration. Variations in the feed concentration by 10X (from 0.1 to 1.0 mg mL^{-1}) effects the DLC by ≤10 %. This response reflects the fact that the loading is not diffusion-controlled. The consistent protein DLC at low protein feed concentrations is especially important for industrial applications, since most of the desired proteins present in cell lysate exist at low concentrations. In addition to the previously demonstrated throughput and yield characteristics of the nylon 6 C-CP fiber phase [49], the nylon-SO_3H phase holds a great potential to be used for preparative-scale protein extraction and purification.

Protein separation characteristics

Ultimately, whether operating in the analytical or preparative modes, chromatographic efficiency becomes a prominent figure of merit when evaluating chromatographic phases. Previous efforts in IEC protein separations on nylon 6 C-CP fibers had shown that ammonium chloride was the preferred eluent phase in terms of separation quality (resolution, peak capacity, etc.)[13,16]. The native surface, though has limited capacity. For the sake of a preliminary comparison, separations of a three-protein mixture containing myoglobin, α-chymotrypsinogen A and lysozyme were performed on the native nylon 6 and modified nylon-SO_3H columns. While further optimization regarding eluent salt and buffer composition are in order, a simple NaCl salt gradient has been employed here. Representative chromatograms for the separation are presented in Fig. 6. All

chromatograms were subjected to absorbance baseline subtractions based on the same gradients without protein sample injection. These qualitative comparisons among the separations provide insights to the system. First, common to all of the columns, myoglobin is only minimally retained on the columns. This is due to the fact that pI of the protein (6.8 – 7.3) dictates that it is close to charge neutral in the pH=6.5 buffer. It is also comparatively hydrophilic in nature, and so is not retained to an appreciable extent on the nylon 6 and nylon-SO_3H surfaces. It is clear, though, that myoglobin exhibits peak tailing with the lowest peak height and largest peak width for the fibers having the highest –SO_3H densities (nylon-SO_3H #2), reflecting some amount of ionic interactions. Second, the addition of –SO3H groups to the nylon surfaces all lead enhanced retention (longer retention times) for α-chymotrypsinogen A, meaning greater Na^+ concentrations are required to displace the protein. This is not surprising from the simple point of view that the surface ligand in nylon 6 is low density –COOH as opposed to the high density sulfonate groups of the modified fibers. Third, AMPS modification significantly increased the protein retention time and the separation resolution on nylon fiber columns. It is believed that the increase of protein retention and resolution is due to the added AMPS cation-exchange ligands. Nylon-SO_3H #5 gives the best protein separation resolution among all modified columns.

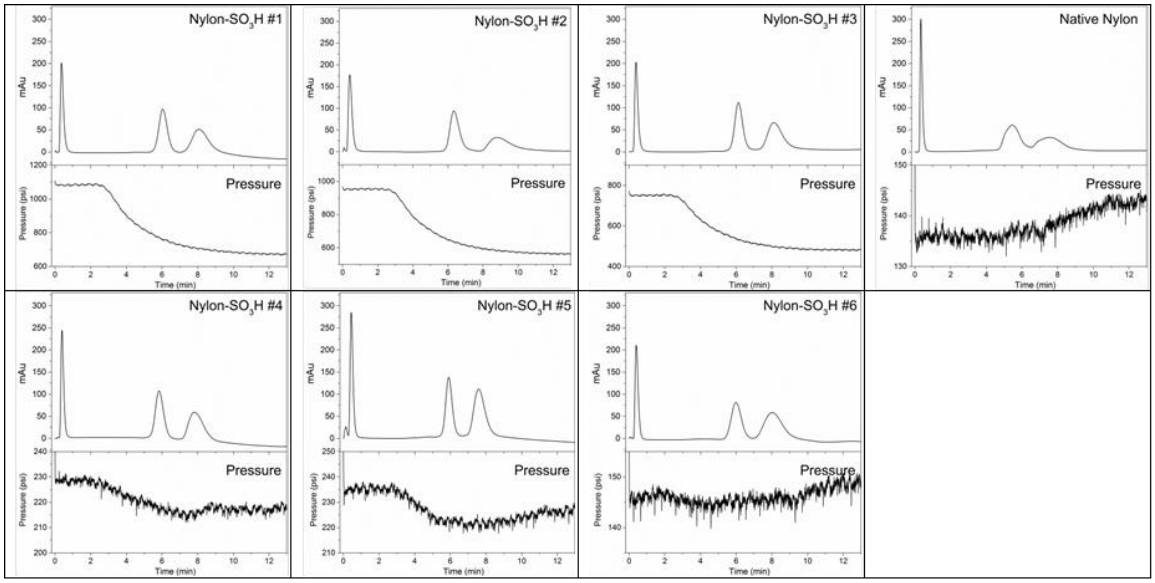

Figure 7.6 Chromatograms of the separation of myoglobin, α-chymotrypsinogen A and lysozyme (left to right) on different nylon-SO_3H columns. Separations were carried out with buffer A (20 mM phosphate, pH 6.5) and buffer B (1 M NaCl in buffer A). The gradient was performed from 0% to 100% buffer B in 10 min. (Column length: 150 mm, I.D.: 0.762 mm. Flow rate: 0.2 mL min^{-1}).

The columns modified by 30% AMPS (#1, #2, and #3) showed longer protein retention times and peak broadening than nylon-SO_3H #5, which is probably due to the increased mass transfer resistance with the higher ligand densities. The high columns pressures (750 – 1100 psi) and the large pressure change during salt gradient (~400 psi decrease) on nylon-SO3H #1, #2 and #3 indicate the presence of thick layers of poly(AMPS) on the fiber surfaces. This assumption agrees with the large –SO_3H peaks on FTIR spectra of nylon-SO_3H #1, #2 and #3. Thick ligands layers lead to the increased mass transfer resistance thus increase the protein retention. Nylon-SO_3H # 1 #4 and #5 have

very similar ligand density but largely differs on column pressures. During the modification of nylon-SO_3H #1, the high AMPS concentration (30%) with low initiator concentration (0.125%) lead to limited grafting sites on nylon surface but with long grafted poly(AMPS) chains. For nylon-SO_3H #4 and #5, lower AMPS concentration (15%) and higher initiator concentrations (0.25% - 0.5%) lead to more grafting sites on fiber surfaces with shorter poly(AMPS) chains. This assumption agrees with the differences of the column pressure decreases while larger pressure decrease on nylon-SO_3H #1 but smaller pressure decrease on nylon-SO_3H #4 and #5, indicating the difference on ligand chain length. Due to low ligand density, nylon-SO_3H #6 showed negligible column pressure change during salt gradient. Native nylon showed column pressure increase (~ 10 psi) because of the increase of mobile phase viscosity with increase of salt concentration.

Table 7.2 Comparison of protein separations and recovery yield on nylon C-CP columns

Stationary Phase	Chy-A			Lyso			Resolution
	t_R (min)	$W_{1/2}$ (min)	Recovery (%)	t_R (min)	$W_{1/2}$ (min)	Recovery (%)	
Native Nylon	5.4	0.95 ± 0.05	62 ± 19	7.6	1.5 ± 0.08	49 ± 15	1.00 ± 0.08
Nylon-SO_3H #1	6.04 ± 0.01	0.53 ± 0.01	84 ± 2	8.12 ± 0.02	1.07 ± 0.04	81 ± 2	1.54 ± 0.03
Nylon-SO_3H #2	6.29 ± 0.03	0.57 ± 0.01	72 ± 2	8.84 ± 0.06	1.35 ± 0.01	76 ± 3	1.57 ± 0.01
Nylon-SO_3H #3	6.16 ± 0.02	0.47 ± 0.01	81 ± 3	8.12 ± 0.04	0.95 ± 0.01	82 ± 1	1.63 ± 0.04
Nylon-SO_3H #4	5.84 ± 0.02	0.52 ± 0.01	81 ± 1	7.86 ± 0.03	0.95 ± 0.01	88 ± 1	1.60 ± 0.02
Nylon-SO_3H #5	5.90 ± 0.04	0.40 ± 0.01	83 ± 3	7.58 ± 0.04	0.72 ± 0.02	86 ± 3	1.79 ± 0.02
Nylon-SO_3H #6	5.98 ±0.02	0.65 ± 0.01	73 ± 1	8.08 ± 0.04	1.19 ± 0.04	77 ± 3	1.34 ± 0.04

The protein recovery on the modified nylon fiber columns are determined by injecting α-chymotrypsinogen A and lysozyme samples at non-retaining condition (100% mobile phase B) and comparing the integrated peak area with protein injections without columns. All columns were washed with 100 mM NaOH, 1 M NaCl solution then with 70% method solution, eliminating any bound protein due to ionic interaction or hydrophobic interaction, prior to recovery determination experiments. A previous study showed the lysozyme recovery on native nylon fiber is ~90%, when 1 mg mL^{-1} lysozyme sample were used for study [50]. In this study, 3 µL of 0.1 mg mL-1 protein samples were injected to the columns. It needs to be noted that the injected amount of protein (0.3 µg) is only 0.03% – 0.2 % of the total protein binding capacity of the columns, thus trace level of non-specific binding should be seen. Generally speaking, the recovery of α-chymotrypsinogen A and lysozyme is similar on single columns. The recovery of lysozyme on nylon columns are shown in table 2. Nylon-SO_3H # 4 and #5

showed the highest lysozyme recovery yield of 88% and 86% which is probably resulted from the high density of short chain ligands which provides good hydrophilic barriers. Nylon-SO_3H #1 and #3 showed slight lower lysozyme recovery (81% and 82%) than #4 and #5, and nylon-SO_3H #2 showed even lower recovery (76%). The increased length of ligand chains decreases the mass transfer efficiency thus impairs protein recovery. In the experiments, severe peak tailing of lysozyme was seen on nylon-SO_3H #2 which has the highest ligand density. The protein recovery on Nylon-SO_3H #6 is lower than nylon-SO_3H #4 and #5, due to its low ligand density. Native nylon showed the lowest protein recovery of (50 – 60%) due to the hydrophobic interaction between native nylon and proteins. The larges errors of the recovery on native nylon are due to the fast saturation of hydrophobic interaction sites on native nylon fibers during the three parallel experiments, thus the recovery significantly increased as more protein been injected.

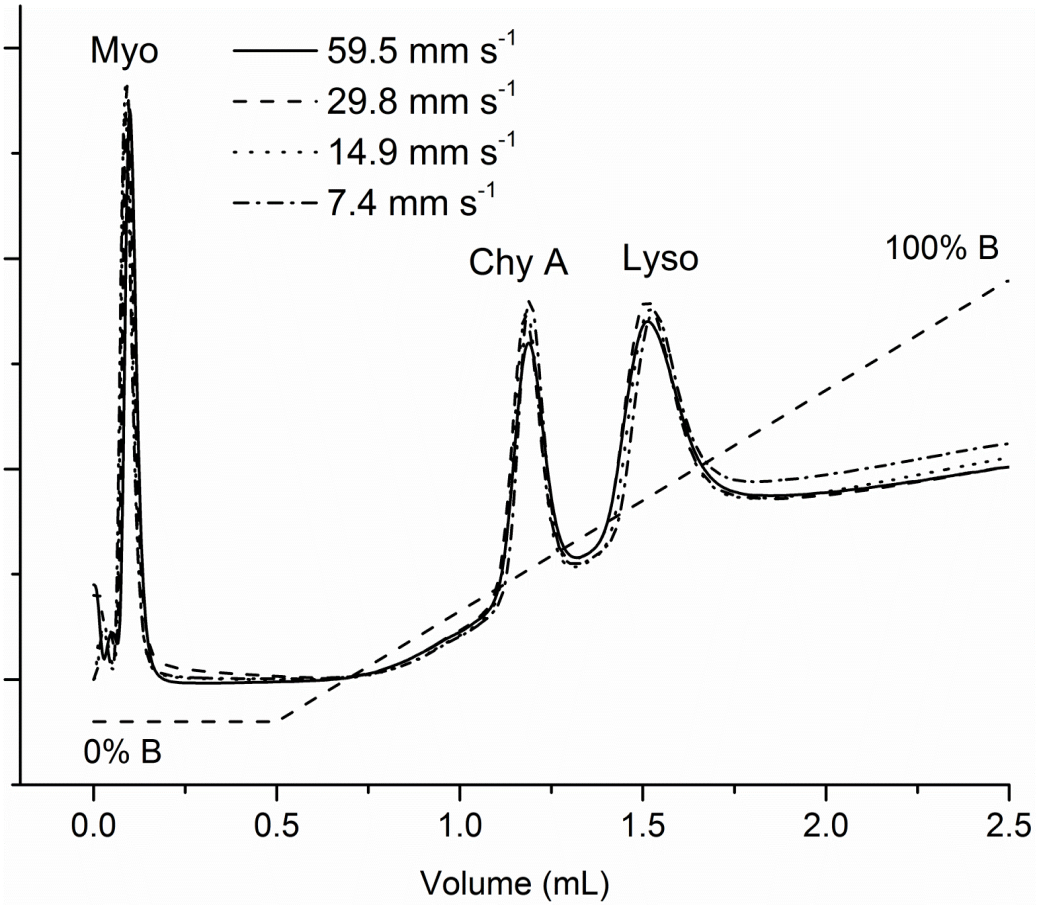

Figure 7.7 Chromatograms for the separation of myoglobin, α-chymotrypsinogen A and lysozyme (left to right) on nylon-SO_3H #5 at four different flow rates. Separations were carried out with buffer A (20 mM phosphate, pH 6.5) and buffer B (1 M NaCl in buffer A). The gradient was performed from 0% to 100% buffer B for a total volume of 2.0 mL.

Based on the higher quality of the separation on the nylon-SO_3H #5 column, separations of the three-protein suite at flow rates varying from 0.1 to 0.8 mL min^{-1} (7.4 – 59.5 mm s^{-1}) were performed across a gradient of 100% buffer A to 100% buffer B (0 to 1 M NaCl). The gradient rate was held constant across a total volume of 2.0 mL. Plotting of the chromatograms as a function of elution

volume (Fig. 7) allows for an assessment of potential kinetic (predominately van Deemter C-term) limitations. There is no significant change of elution volume or peak shapes as the flow rate is increased by a factor of 8×. The independence of the separation quality to such variations in flow rate reflects the excellent protein adsorption/desorption kinetics on nylon-SO_3H column. The lack of broadening has practical implications as the protein separation time on the nylon-SO_3H column is reduced from 20 to 2.5 min; a tremendous improvement in throughput without sacrifice in performance.

To complement the ability to achieve high throughput at high linear velocities, there must also be a capacity to maintain quality over many cycles. Previous studies on the nylon-COOH columns showed excellent protein recovery and protein loading/elution consistency (~0.3 %RSD, n=10) on one column and across replicate columns (~ 3 % RSD, n=5) [29]. In this study, the consistency of the separation on the nylon-SO_3H#5 column was investigated. Separations of myoglobin, α-chymotrypsinogen A and lysozyme were performed 35 times without column regeneration in between. The variation in the retention time and peak area for α-chymotrypsinogen A were 0.4 %RSD and 4 %RSD, respectively. The corresponding precision of the more highly retained lysozyme were 0.2 %RSD and 5 %RSD. In fact, the fluctuations in the elution peak area are due to integration errors from baseline shifts caused by gradient jitter. The small %RSD on retention time indicates good protein recovery and consistency of the separations on nylon-SO_3H columns.

To further investigate the ability to affect rapid separations on nylon-SO_3H columns, a matrix of high linear velocities and various gradient rates was evaluated for the 3-protein suite. Chymotrypsinogen A and lysozyme were chosen as the critical pair. The flow rates used were 0.5, 1.0, and 1.5 mL min^{-1}, which correspond to the linear velocities of 36.5, 73.0 and 110 mm s^{-1}. (It is important to note that the column backpressure at the highest linear velocity is <1000 psi for the 20 cm column.) The gradient times studied ranged from from 0.5 to 3 min. The resolution ($R_s = 1.18\Delta t_R / (w_{1/2(1)} + w_{1/2(2)})$) and the peak capacity ($PC = t_G/w$) for the separations are presented in Figs. 8a and b, respectively. For the longer gradient times, the resolution difference among various flow rates is not significant. On the other hand, as gradient time decreases (faster gradients), flow rate has much more profound effects. Specifically, high linear velocities that affect the narrowest peaks, yield much higher resolution. In fact, at the shortest gradient time (0.5 min), the critical pair is not at all resolved at the lowest linear velocity. Here, the driving forces in determining resolution are quite apparent. Under conditions of slow gradients, the differences in component retention times (Δt_R) dominate, but for fast gradients, peak width (w) dominates.

In the case of gradient separations, a more practical metric of separation throughput is the peak capacity. This is particularly true in characterizing the second dimension of two-dimensional LC separations, where the time to affect that separation is limited. As seen in Fig. 8b, the ability to operate C-CP fiber columns at high linear velocities to affect more narrow peaks is quite clear. As

exhibited for many phases, the peak capacity increases with the gradient time. Under the supposition of uniform peak widths, the peak capacity should loosely increase proportionally with $t_G^{1/2}$. This trend is roughly followed in Fig. 8b. What is not typical is the fact that the PC values for the nylon-SO_3H#5 C-CP fiber columns increase with mobile phase linear velocity. Within a, given linear velocity data set, the peak width decreases with shorter gradient time (faster gradient). This is a direct reflection of a lack of any van Deemter C-term broadening. As protein elution occurs over a range of solvent strengths, it would be expected that the time-breadth of the elution of each protein would limit the peak width that can be obtained and the peak capacity would reach a plateau. It was found that at the highest mobile phase linear velocity studied (110 mm s^{-1}), 30 s of column re-equilibrium time between separations is sufficient to produce repeatable chromatograms.

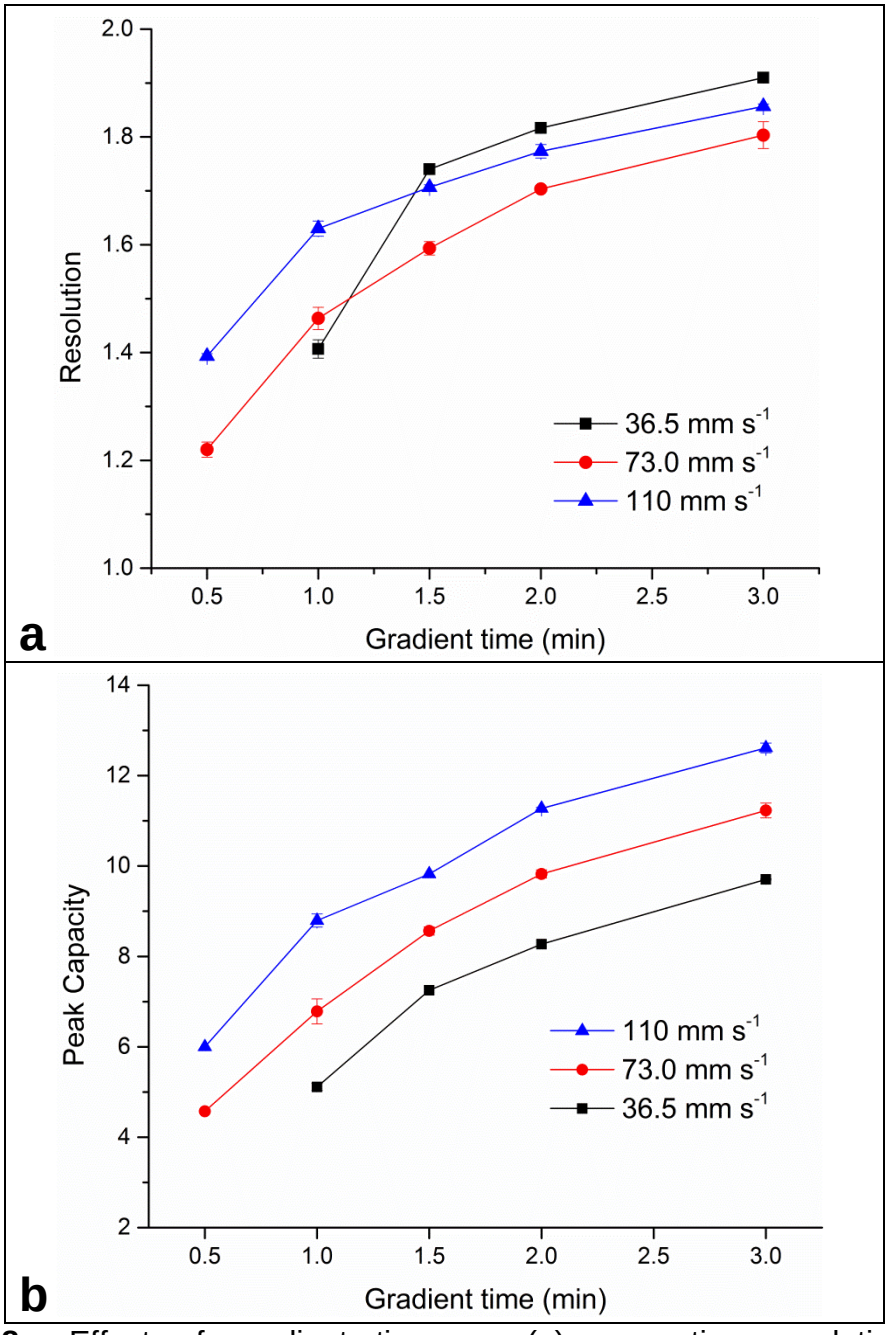

Figure 7.8 Effect of gradient time on (a) separation resolution of α-chymotrypsinogen A and lysozyme (b) peak capacity on nylon-SO_3H #5 column at various flow rates.

In comprehensive two dimensional LC separations (2D-LC), the total separation time is determined by the numbers of fractions injected into second dimension separation and the time that second dimension separation takes. The second dimension separation must be as fast as possible with adequate resolving power while the first dimension separation should be slow down to match up the second dimension separation time and frequency. Hence, the second dimension separation is a key factor that limits the total separation time of 2D LC. The capability of performing fast protein separation and column re-equilibrium (total time under 2 min) and the consistency of the separations suggest that nylon-SO_3H fiber phase is promising to be applied as the second dimension separation media in 2D LC separations.

Conclusions

Nylon 6 C-CP fibers were functionalized with sulfonic acid by a microwave-assisted grafting polymerization of 2-acrylamido-2-methylpropanesulfonic acid (AMPS) to yield a strong cation exchange (SCX) phase for protein separations. A simple domestic microwave oven was used to induce the polymerization. The native nylon 6 and modified fibers were characterized by FTIR, SEM and acid-base titration. The highest values of ligand density were 317±13 μmol g^{-1}, obtained under conditions of 30% AMPS and 0.25% potassium persulfate (w/v). The protein dynamic loading capacity of the nylon C-CP columns was increased from ~1 mg mL^{-1} on native nylon column to ~12 mg

mL^{-1} on the nylon-SO3H column. In comparison to native nylon fibers, the modified nylon fibers showed higher protein separation resolutions. The nylon-SO_3H #5, which was modified with 15% AMPS and 0.5% KPS, showed the highest protein separation resolution among all the modified fibers. Protein separations at different flow rates were demonstrated on the nylon-SO_3H#5 column. The separation time can be reduced by increasing flow rates without Van Deemter C term broadening. Very fast gradient separation (30 s) under higher mobile phase linear velocity (110 mm s^{-1}) was demonstrated on nylon-SO_3H column and shows that nylon-SO_3H column is promising to be used as the second dimension in 2D HPLC separation where the fast separations are required.

The large number of commercially available acrylic monomers makes the microwave-assisted grafting polymerization a very versatile but simple method to offer nylon C-CP fibers different types of surface chemistry. Future studies will focus on further optimization of the modification recipe to improve the protein separation, recovery, and binding capacity. The columns packed with modified nylon fibers at various packing densities will be studied to achieve high protein binding capacity while maintaining high column permeability. Not only the cation-exchange groups, but also many other functional groups such as anion exchange groups, epoxides, iminodiacetic acid and affinity ligand can be used to affect the nylon 6 fiber surface chemistry, providing more opportunities of applying C-CP fiber phases in protein separations.

Acknowledgement

This study is supported by the National Science Foundation Division of Chemistry under grant CHE-1307078. The authors appreciate the assistance of Dr. Qian Haijun (Clemson University Electron Microscope Facility) on the SEM instrumentation and Ms. Kim Ivey (Analytical Testing Lab, Materials Science & Engineering, Clemson University) on the ATR-FTIR instrumentation.

References

[1] Fekete, S.; Guillarme, D. *Trends. Analyt. Chem.* **2014**, *63*, 76-84.

[2] Gottschalk, U. *Biopharm. Int.* **2005**, *18*, 42-58.

[3] Wurm, F. M. *Nat. Biotechnol.* **2004**, *22*, 1393-1398.

[4] Gronemeyer, P.; Ditz, R.; Strube, J. *Bioengineering* **2014**, *1*, 188-212.

[5] Gottschalk, U. *Biotechnol. Progr.* **2008**, *24*, 496-503.

[6] Thömmes, J.; Etzel, M. *Biotechnol. Progr.* **2007**, *23*, 42-45.

[7] Ladisch, M. R. *Bioseparations Engineering: Principles, Practice, and Economics*; Wiley-Interscience: New York, 2001.

[8] Carta, G.; Jungbauer, A. *Protein Chromatography: Process Development and Scale-Up*; Wiley-VCH: Weinheim, 2010.

[9] Neue, U. D. *HPLC Columns: Theory, Technology, and Practice*; Wiley-VCH: New York, 1997.

[10] Walter, T. H.; Andrews, R. W. *Trends. Analyt. Chem.* **2014**, *63*, 14-20.

[11] Fekete, S.; Schappler, J.; Veuthey, J.-L.; Guillarme, D. *Trends. Analyt. Chem.* **2014**, *63*, 2-13.

[12] Kirkland, J. J.; Truszkowski, F. A.; Dilks, C. H.; Engel, G. S. *J. Chromatogr. A* **2000**, *890*, 3-13.

[13] Schuster, S. A.; Wagner, B. M.; Boyes, B. E.; Kirkland, J. J. *J. Chromatogr. A* **2013**, *1315*, 118-126.

[14] Svec, F.; Frechet, J. M. J. *Anal. Chem.* **1992**, *64*, 820-822.

[15] Ghosh, R. *J. Chromatogr. A* **2002**, *952*, 13-27.

[16] Marcus, R. K. *Journal of separation science* **2008**, *31*, 1923-1935.

[17] Arrua, R. D.; Talebi, M.; Causon, T. J.; Hilder, E. F. *Anal. Chim. Acta* **2012**, *738*, 1-12.

[18] Tanaka, N.; McCalley, D. V. *Anal. Chem.* **2016**, *88*, 279-298.

[19] Marcus, R. K.; Davis, W. C.; Knippel, B. C.; LaMotte, L.; Hill, T. A.; Perahia, D.; Jenkins, J. D. *J. Chromatogr. A* **2003**, *986*, 17-31.

[20] Nelson, D. M.; Marcus, R. K. *Anal. Chem.* **2006**, *78*, 8462-8471.

[21] Randunu, K. M.; Marcus, R. K. *Analytical and bioanalytical chemistry* **2012**, *404*, 721-729.

[22] Randunu, K. M.; Marcus, R. K. *Biotechnol. Prog.* **2013**, *29*, 1222-1229.

[23] Wang, Z.; Marcus, R. K. *Biotechnol. Progr.* **2015**, *15*, 97-109.

[24] Schadock-Hewitt, A. J.; Marcus, R. K. *Journal of separation science* **2014**, *37*, 495-504.

[25] Wang, Z.; Marcus, R. K. *J. Chromatogr. A* **2014**, *1351*, 82-89.

[26] Stanelle, R. D.; Mignanelli, M.; Brown, P.; Marcus, R. K. *Analytical and bioanalytical chemistry* **2006**, *384*, 250-258.

[27] Randunu, J. M.; Dimartino, S.; Marcus, R. K. *Journal of separation science* **2012**, *35*, 3270-3280.

[28] Stanelle, R.; Marcus, R. K. *Analytical and bioanalytical chemistry* **2009**, *393*, 273-281.

[29] Stanelle, R. D.; Straut, C. M.; Marcus, R. K. *J. Chromatogr. Sci.* **2007**, *45*, 415-421.

[30] Chambers, T. K. F., James. *J. Chromatogr. A* **1998**, 139-147.

[31] Yang, Y.-b. H., Kervin.Kindsvater, John. *J. Chromatogr. A* **1996**, *723*, 1-10.

[32] Jiang, L.; Marcus, R. K. *Analytical and bioanalytical chemistry* **2015**, *407*, 939-951.

[33] Jiang, L.; Jin, Y.; Marcus, R. K. *J. Chromatogr. A* **2015**, *1410*, 200-209.

[34] Jiang, L.; Marcus, R. K. *Analytical and bioanalytical chemistry* **2015**, 1-11.

[35] Jiang, L.; Schadock-Hewitt, A. J.; Zhang, L. X.; Marcus, R. K. *Analyst* **2015**, *140*, 1523-1534.

[36] Schadock-Hewitt, A. J.; Pittman, J. J.; Christensen, K. A.; Marcus, R. K. *Analyst* **2014**, *139*, 2108-2113.

[37] DePhillips, P.; Lenhoff, A. M. *J. Chromatogr. A* **2001**, *933*, 57-72.

[38] Gu, B.; Li, Y.; Lee, M. L. *Anal. Chem.* **2007**, *79*, 5848-5855.

[39] Hunter, A. K.; Carta, G. *J. Chromatogr. A* **2000**, *897*, 81-97.

[40] Schadock-Hewitt, A. J.; Pittman, J. J.; Stevens, K. A.; Marcus, R. K. *J. Appl. Polym. Sci.* **2013**, *128*, 1257-1265.

[41] Zhao, Q.; Gu, X.; Zhang, S.; Dong, M.; Jiang, P.; Hu, Z. *Surf. Coat. Technol.* **2014**, *240*, 197-203.

[42] Trang, H. K.; Schadock-Hewitt, A. J.; Jiang, L.; Marcus, R. K. *J. Chromatogr. B* **2016**, *1015*, 92-104.

[43] Xu, F. J.; Zhao, J. P.; Kang, E. T.; Neoh, K. G.; Li, J. *Langmuir* **2007**, *23*, 8585-8592.

[44] Herrera-Alonso, M.; McCarthy, T. J.; Jia, X. *Langmuir* **2006**, *22*, 1646-1651.

[45] Deng, J.; Wang, L.; Liu, L.; Yang, W. *Prog. Polym. Sci.* **2009**, *34*, 156-193.

[46] Choi, H.-S.; Kim, Y.-S.; Zhang, Y.; Tang, S.; Myung, S.-W.; Shin, B.-C. *Surf. Coat. Technol.* **2004**, *182*, 55-64.

[47] Bhattacharya, A.; Misra, B. N. *Prog. Polym. Sci.* **2004**, *29*, 767-814.

[48] Zhang, C.; Liao, L.; Gong, S. *Green Chem.* **2007**, *9*, 303-314.

[49] Sinnwell, S.; Ritter, H. *Aust. J. Chem.* **2007**, *60*, 729-743.

[50] Hoogenboom, R.; Schubert, U. S. *Macromol. Rapid Commun.* **2007**, *28*, 368-386.

[51] Wiesbrock, F.; Hoogenboom, R.; Schubert, U. S. *Macromol. Rapid Commun.* **2004**, *25*, 1739-1764.

[52] Kappe, C. O.; Pieber, B.; Dallinger, D. *Angew. Chem. Int. Ed.* **2013**, *52*, 1088-1094.

[53] Dudley, G. B.; Stiegman, A. E.; Rosana, M. R. *Angew. Chem. Int. Ed.* **2013**, *52*, 7918-7923.

[54] Sosnik, A.; Gotelli, G.; Abraham, G. A. *Prog. Polym. Sci.* **2011**, *36*, 1050-1078.

[55] Hunkeler, D. *Macromolecules* **1991**, *24*, 2160-2171.

[56] Gong, B.; Ke, C.; Geng, X. *Analytical and bioanalytical chemistry* **2003**, *375*, 769-774.

[57] Wei, Y.; Huang, X.; Liu, R.; Shen, Y.; Geng, X. *Journal of separation science* **2006**, *29*, 5-13.

[58] Zhao, K. L.; Song, C.; Wang, F.; Bai, Q. *Chin. Chem. Lett.* **2012**, *23*, 305-308.

CHAPTER VI

SUMMARY AND FUTURE WORK

The research in this dissertation presented using surface modifications of capillary-channeled polymer (C-CP) fibers and using surface modified C-CP fiber columns for protein separation. C-CP fiber is a cost-efficient base material of liquid chromatography for protein separation. C-CP fiber packed column is capable of fast protein separation under high flow rate without high column pressure. Different surface modification strategies have been studied on C-CP fibers to affect their surface chemistry. In chapter II, lipid tethered ligand (LTL) is synthesized and used to introduce biotin functionality onto PP C-CP fiber surface. In chapter III, an easy but effective method is introduced to functionalize PET C-CP fiber surface. PET surface is covalently bound with biotin ligand with a hydrophilic spacer arm in between. In chapter IV, PET surface is modified with cross-linked polyethylenimine for weak anion exchange chromatography. In chapter V, three amine-based C-CP fiber phases (Native nylon 6, PEI modified PET and PEI/BUDGE modified PET) are compared interms of protein separation characteristics. In chapter VI, a weak cation exchange liquid chromatography stationary phase (nylon-COOH) was prepared by grafting polyacrylic acid on to native nylon 6 capillary-channeled polymer (C-CP) fibers via a microwave-assisted radical polymerization.In chapter VII, native nylon C-CP fibers were modified with 2-acrylamido-2-methylpropanesulfonic acid (AMPS) via the

microwave-assisted grafting polymerization to affect a strong cation exchange stationary phase. The surface functionalization methods that are discussed in this dissertation can effectively introduce various ligands onto C-CP fiber surface and largely expand the applications of C-CP fiber columns. The results showed in this dissertation suggest that C-CP fibers have a great potential to be high-throughput protein separation media.

To further improve the protein separation on C-CP fibers, some future study will be proposed in this chapter.

Improve C-CP Fiber Column Packing

In this dissertation, C-CP fibers are manually pulled through PEEK tubing and packed to columns. The small variations from person to person will result in large column to column packing variations. When fibers are pulling through tubing, the friction force between fibers and tubing wall makes fibers getting stretched. The degree of stretching is depending on how much force a person used pulling the fibers. The pulling forces are varied from person to person. For the same person, the pulling force may vary from batch to batch. To further improve the column to column reproducibility, a new method of packing is proposed here.

Firstly, C-CP fiber bundles are stretched by a constant force. When stretched, each C-CP fibers become thinner and the diameter of the whole

bundle is reduced. Secondly, PEEK tubing is slide onto the C-CP fibers bundle. Due to reduced fiber bundle diameter, the friction force from sliding tubing on fibers is minimal. After the tubing are slide on fibers and kept in place, release the fibers from stretching. Fibers are then shrined to the original diameter while they are in the tubing. A machine assisted, semi-automatic or fully automatic packing process is preferred. The ratio of tubing inner diameter to the number of fibers, the force of stretching fibers and the force of sliding tubing need to be investigated for the optimal fiber column packing reproducibility.

One of the main challenges of improving the C-CP fiber column efficiency is to reduce the A term of van Deemter plot, packing homogeneity. When packed in a column, C-CP fibers stacked with each other, resulting in 1 – 5 μm inter fiber channels. However, due to the mis-stacking of some of the fiber “wings”, large but irregular sized channels (>10 μm) may form and cause regional non-uniformed packing. The mis-stacking of the fibers may result from the fiber twisting during packing process. To solve this problem, fibers should be packed into tubing without any stretching or twisting. Using heat shrinkable tubing provides a possible solution. Heat shrinkable tubing can is capable of “shrink to fit”. When being heated, it can shrink to a reduced inner-diameter. Certain number of C-CP fibers can be placed in to heat shrinkable tubing, and then the tubing with fibers in it can be placed into an oven for homogenous heating. After heating, the tubing will be shrunk to match with the diameter of the fiber bundle, resulting in a tight packing of fibers without any twisting or stretching. The

material of the shrinkable tubing needs to be capable of withstanding high pressure for HPLC use. The ratio of recovered tubing inner diameter to the number of fibers that are packed, as well as the shrinking temperature and the shrinking time need to be carefully tuned for optimal column packing.

Improving LTL Functionalization on Polypropylene C-CP Fibers

Lipid tethered ligands (LTL) have been shown to be a very effective method to functionalize polypropylene C-CP fiber surface. Structurally optimized LTL has been synthesized and shown to be superior to the commercially available LTLs, in terms of chemical stability, adsorption to PP and resistance to aqueous buffer wash. However, due to lack of covalent attachments, the surface adsorbed LTL may not be robust on PP surface when organic solvent is used is separation process, which results in shortened column life time and ligand leaching in to eluted protein. To further improve the surface modification of LTL, a new design of LTL structure is proposed here (figure 8.1)

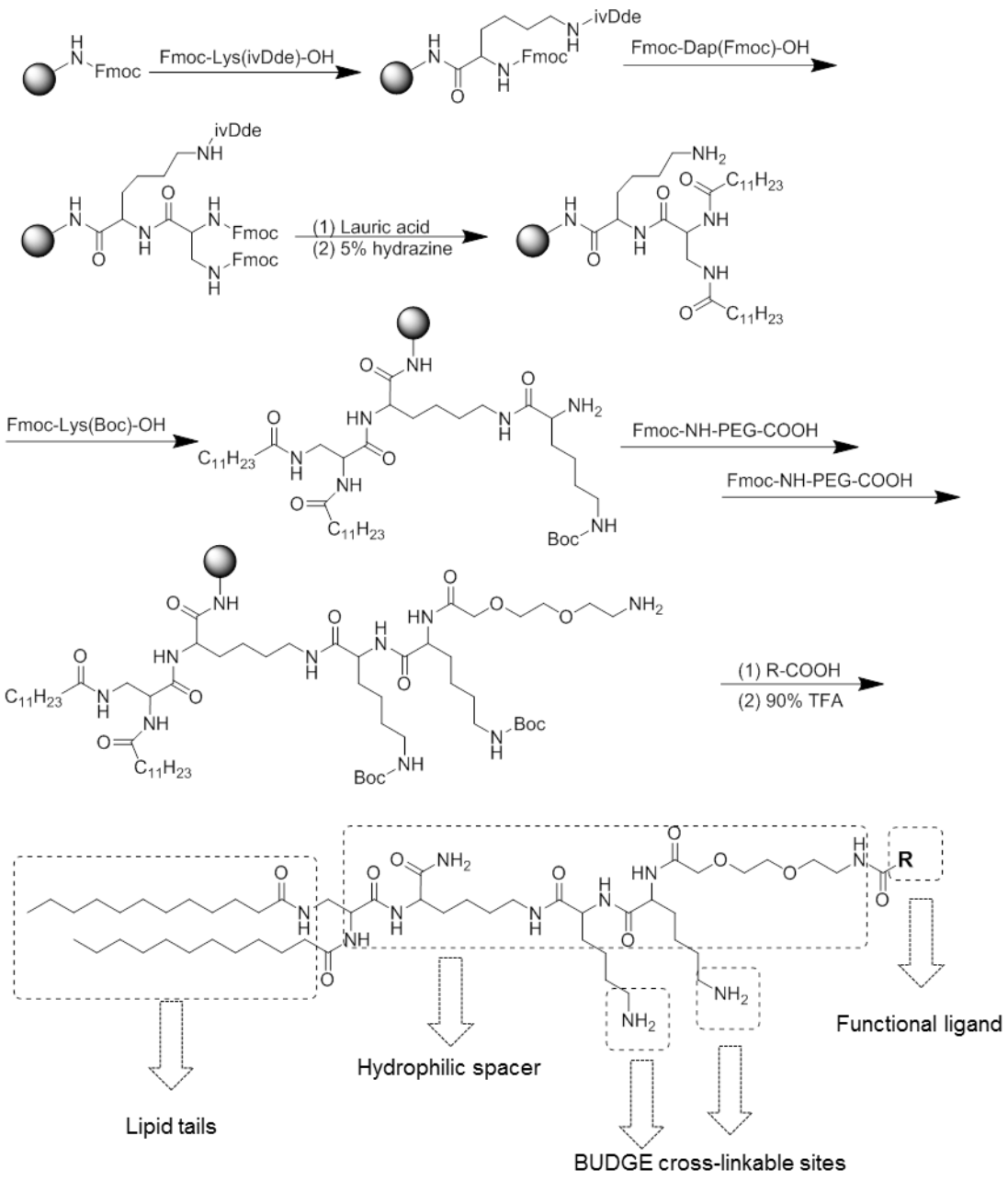

Figure 8.1 Synthesis of cross-linkable lipid tethered ligand (LTL) (R = Ligand)

The new LTL is named cross-linkable LTL (cLTL). In comparison to the structure of the original LTL, cLTL has two lysine residues being connected between the lipid tails and the hydrophilic spacer. These two lysine residue

provide two free primary amine groups after the cLTL is cleaved from resins. After applying with the cLTL solution, PP fibers were treated with 1,4-Butanediol diglycidyl ether (BUDGE). The free amine groups on cLTL are readily reacted with the epoxide of BUDGE so that cLTL are cross-linked on PP surface (Figure 8.2). The cross-linking will improve the stability of cLTL adsorption and resistance to solvent wash.

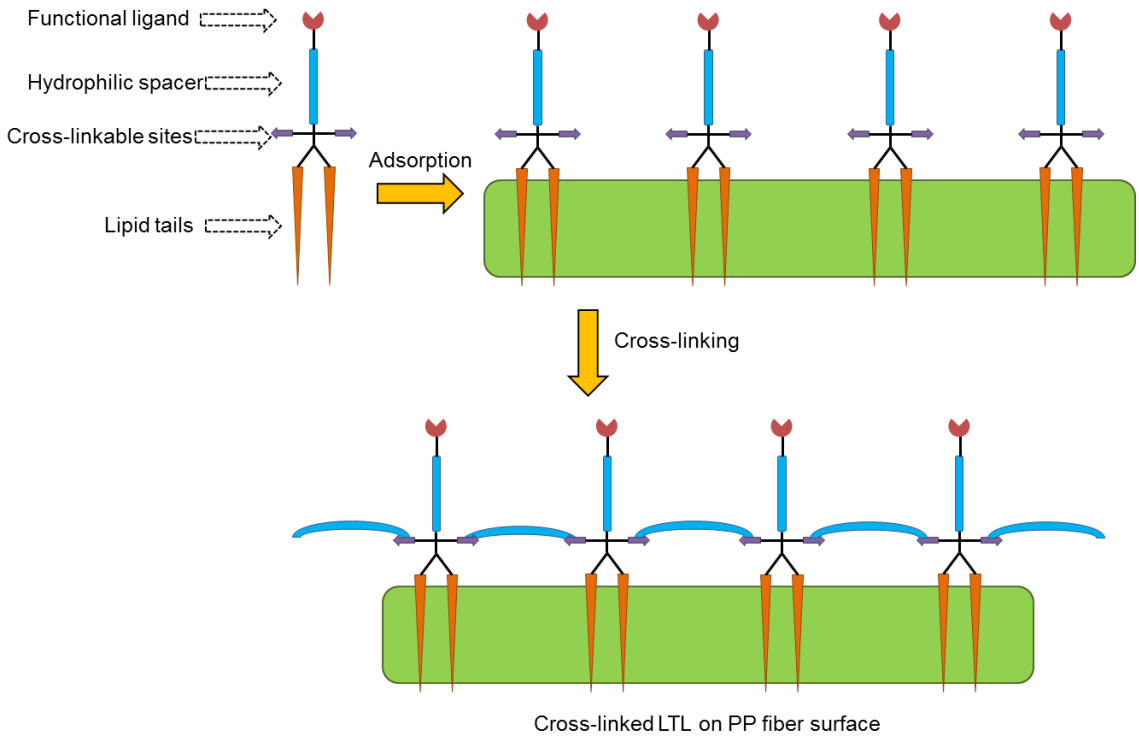

Figure 8.2 cLTL on PP surface is cross-linked by BUDGE

Comparing to the synthesis of the original LTL, the synthesis of cLTL only have two extra solid phase synthesis steps which should not significantly increase the time and labor cost of the solid phase synthesis. Future study will

include the synthesis of cLTL, study on the cross-linking reaction condition, testing the life time of the cross-linked cLTL functionalization on PP fiber surface.

Nylon C-CP Fiber Surface Modification for Various Separations

In chapter VI and VII, a microwave assisted grafting polymerization method is used to functionalize nylon-6 C-CP fibers surface for weak cation exchange and strong cation exchange. The functionalized nylon C-CP fiber column showed greatly improved protein separation performance, in terms of separation resolution, protein recovery yield and protein binding capacity. The future study is focused on investigation of the reaction conditions. Reaction conditions, including concentrations of reagents, ratio of monomer to initiator, reaction time, reaction temperature and the selection of microwave reactor, will greatly affect the surface morphology (pore size) and the thickness of modification layer. The reaction conditions need to be studied and optimized for fibers to achieve high protein binding capacity with high column permeability and fast mass transfer.

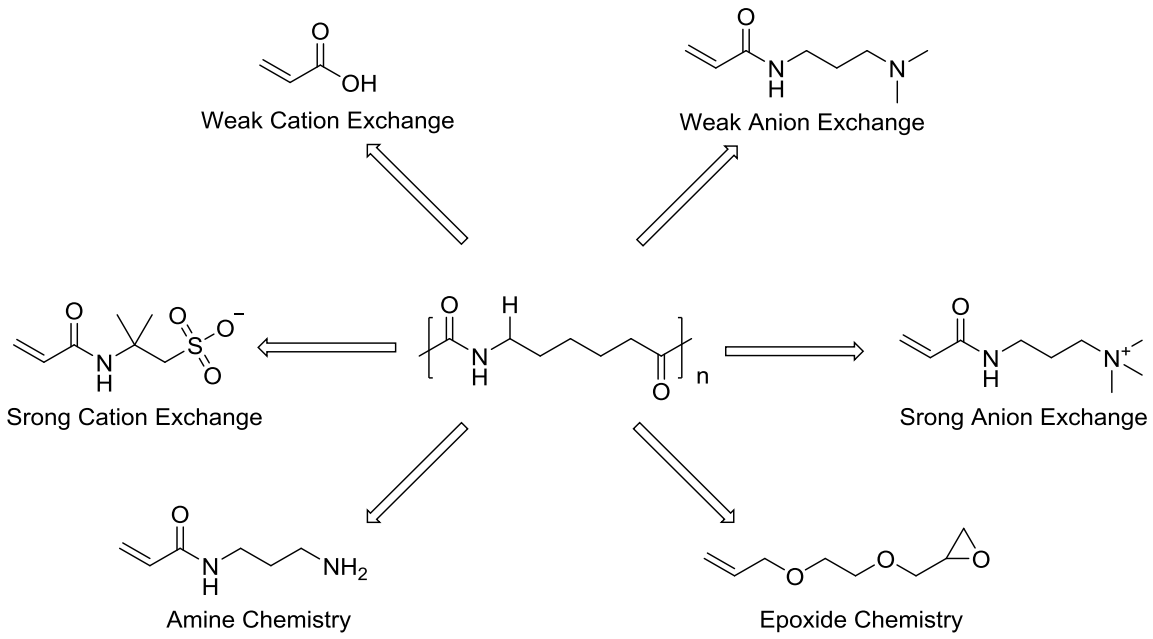

Figure 8.3 Overview of microwave assisted grafting polymerization of nylon 6 C-CP fibers for various applications.

More surface chemistry is available by using microwave assisted grafting modification. Figure 8.3 provides an overview of various polymerizable ligands that can be grafted onto nylon fiber. N-[3-(Dimethylamino)propyl]methacrylamide can be used for weak anion exchange. (3-Acrylamidopropyl)trimethylammonium can be used for strong anion exchange. In addition to that, high density of free amine can be attached on nylon fiber surface for amine chemistry. Ligands that are readily attachable with primary amine can be easily bound on nylon fiber surface. Epoxide chemistry, which is a very effective and versatile tool for functionalization, can also be introduced onto nylon C-CP fibers. Ligands with amine groups have high reactivity to epoxides so they can be easily covalently bound to epoxides. Protein ligands, such as protein A, can also be covalently

bound onto epoxide bearing nylon C-CP fiber. This microwave assisted grafting modification is a very promising method to functionalized nylon C-CP fibers for many applications including protein solid phase extraction and protein separation.

APPENDICES

Appendix A

Supporting material for Chapter II

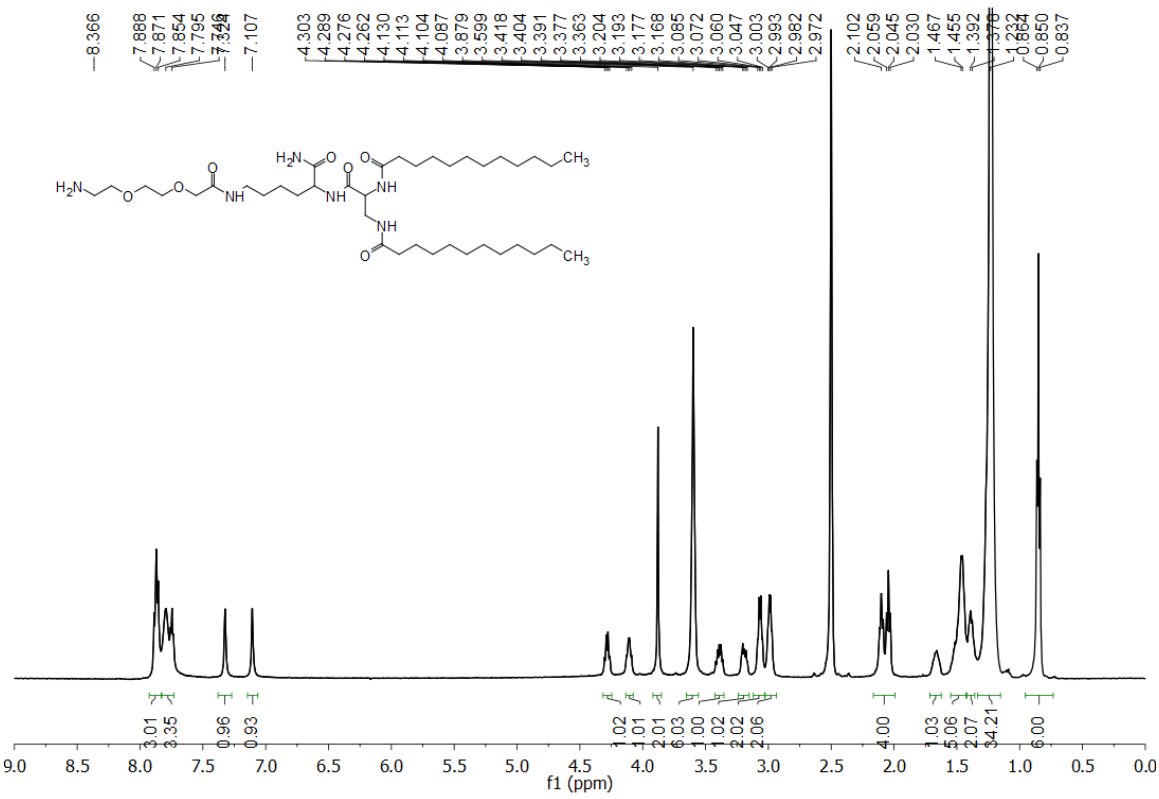

Fig. S1 ^{1}H NMR of **Amine-LTL**

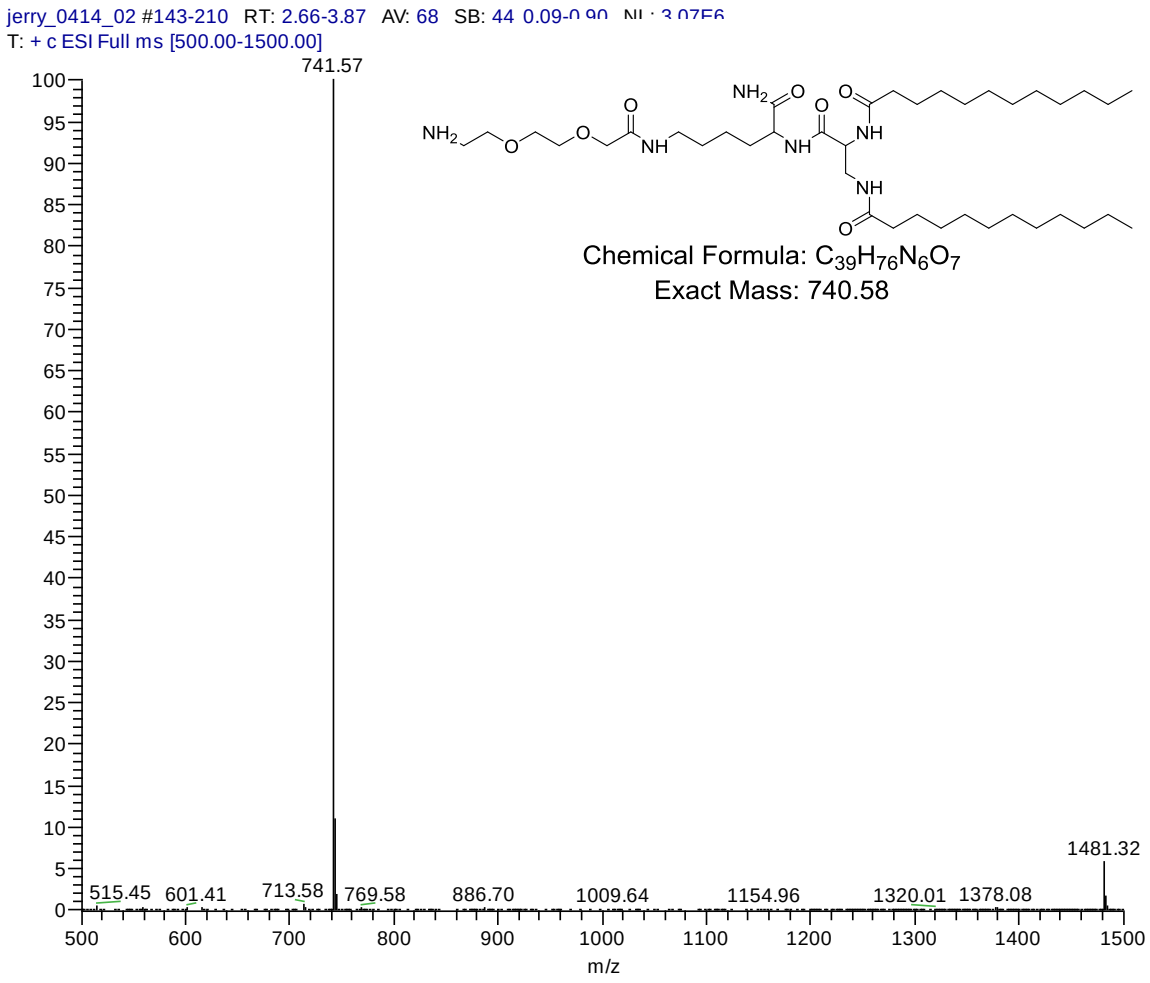

Fig. S2 ESI-MS of **Amine-LTL**

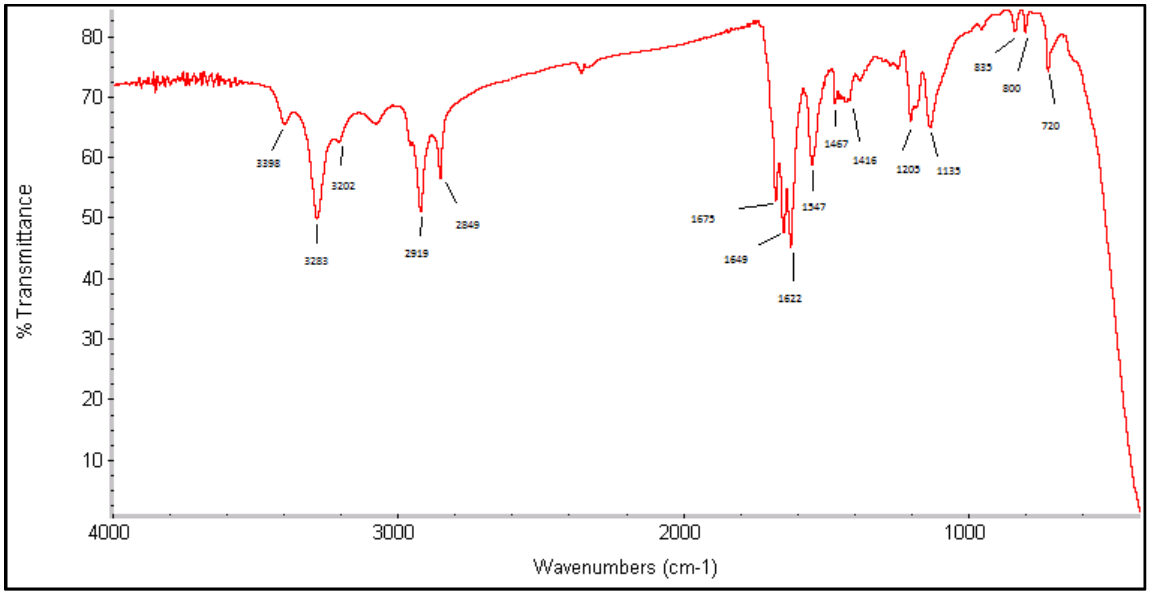

Fig. S3 FT-IR of **Amine-LTL**

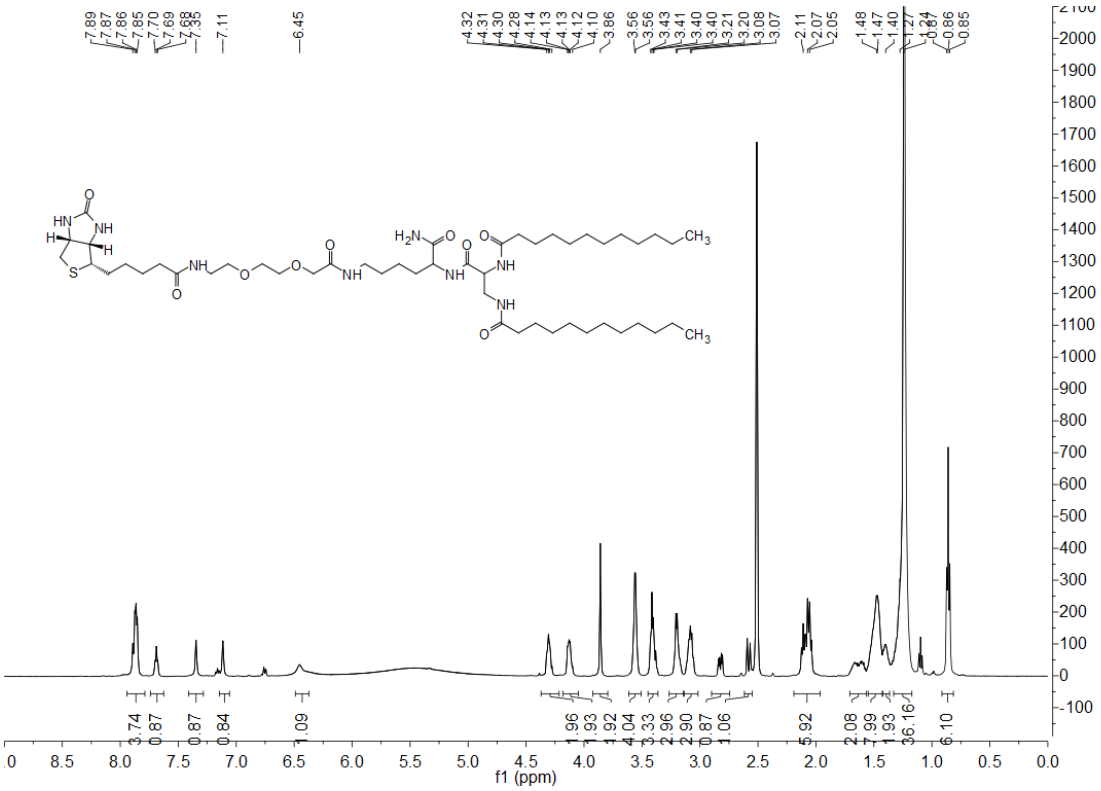

Fig. S4 ^{1}H NMR of **Biotin-LTL**

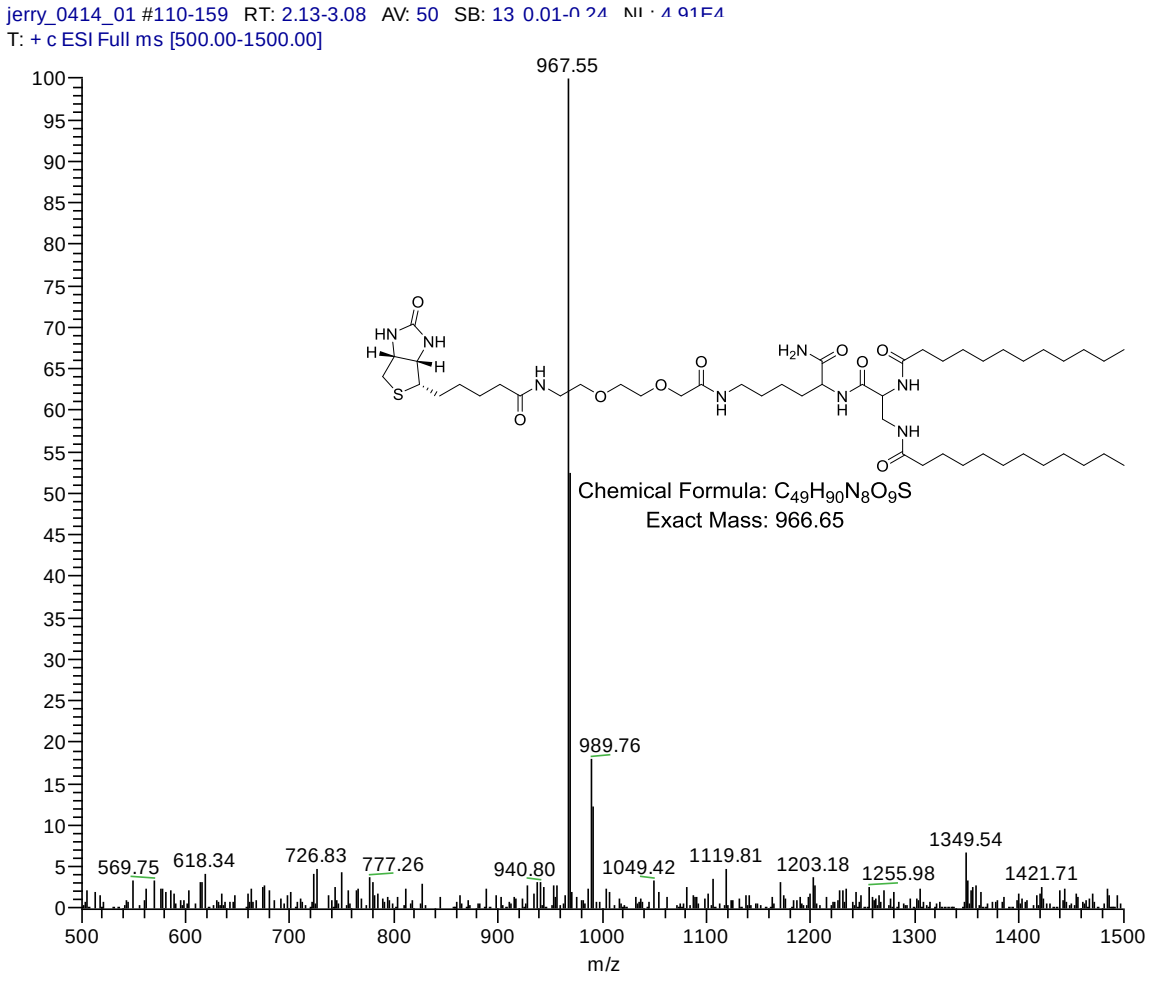

Fig. S5 ESI-MS of **Biotin-LTL**

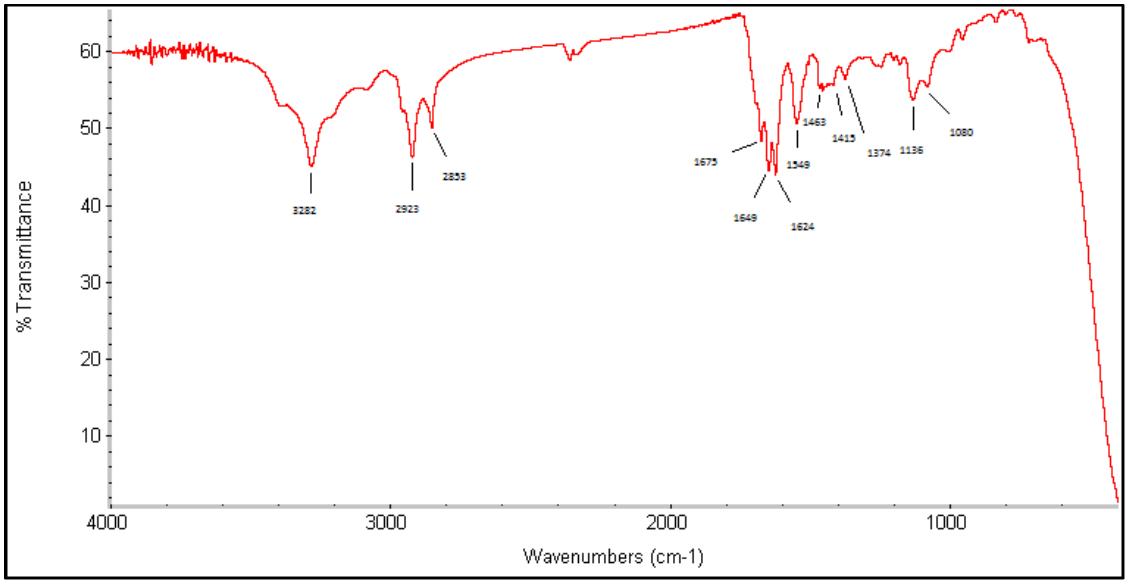

Fig. S6 FT-IR of **Biotin-LTL**

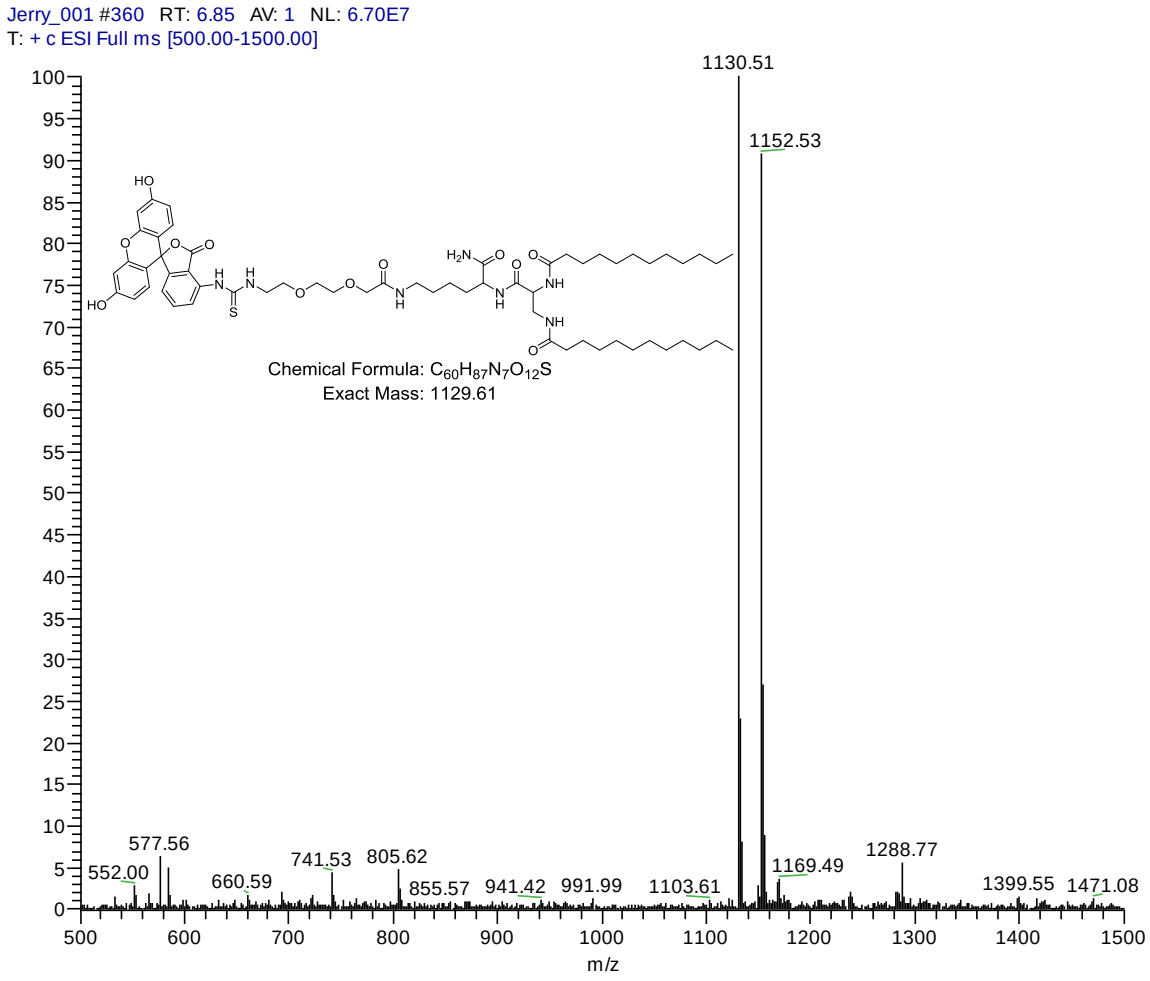

Fig. S7 ESI-MS of **FITC-LTL**

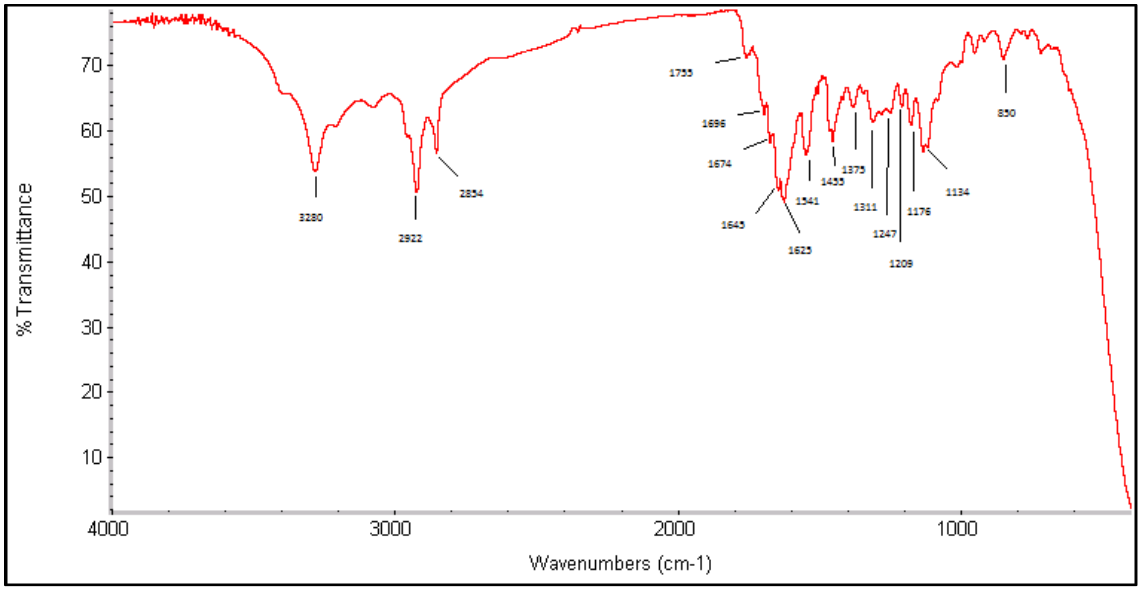

Fig. S8 FT-IR of FITC-LTL

Appendix B

Reuse Permission for Chapter III

SPRINGER LICENSE
TERMS AND CONDITIONS

Jun 14, 2016

This Agreement between Liuwei Jiang ("You") and Springer ("Springer") consists of your license details and the terms and conditions provided by Springer and Copyright Clearance Center.

License Number	3887780431291
License date	Jun 14, 2016
Licensed Content Publisher	Springer
Licensed Content Publication	Analytical and Bioanalytical Chemistry
Licensed Content Title	Biotin-functionalized poly(ethylene terephthalate) capillary-channeled polymer fibers as HPLC stationary phase for affinity chromatography
Licensed Content Author	Liuwei Jiang
Licensed Content Date	Jan 1, 2014
Licensed Content Volume Number	407
Licensed Content Issue Number	3
Type of Use	Thesis/Dissertation
Portion	Full text
Number of copies	1
Author of this Springer article	Yes and you are the sole author of the new work
Order reference number	
Title of your thesis / dissertation	SURFACE MODIFICATIONS OF CAPILLARY-CHANNELED POLYMER (C-CP) FIBER STATIONARY PHASES FOR PROTEIN SEPARATIONS
Expected completion date	Aug 2016
Estimated size(pages)	275
Requestor Location	Liuwei Jiang 102 Biosystem Research Complex 105 Collings Street CLEMSON, SC 29634 United States Attn: Liuwei Jiang
Billing Type	Invoice
Billing Address	Liuwei Jiang 102 Biosystem Research Complex 105 Collings Street CLEMSON, SC 29634 United States Attn: Liuwei Jiang
Total	0.00 USD
Terms and Conditions	

Appendix C

Reuse Permission for Chapter IV

ELSEVIER LICENSE
TERMS AND CONDITIONS

Jun 14, 2016

This Agreement between Liuwei Jiang ("You") and Elsevier ("Elsevier") consists of your license details and the terms and conditions provided by Elsevier and Copyright Clearance Center.

License Number	3887781147482
License date	Jun 14, 2016
Licensed Content Publisher	Elsevier
Licensed Content Publication	Journal of Chromatography A
Licensed Content Title	Polyethylenimine modified poly(ethylene terephthalate) capillary channeled-polymer fibers for anion exchange chromatography of proteins
Licensed Content Author	Liuwei Jiang,Yi Jin,R. Kenneth Marcus
Licensed Content Date	4 September 2015
Licensed Content Volume Number	1410
Licensed Content Issue Number	n/a
Licensed Content Pages	10
Start Page	200
End Page	209
Type of Use	reuse in a thesis/dissertation
Intended publisher of new work	other
Portion	full article
Format	both print and electronic
Are you the author of this Elsevier article?	Yes
Will you be translating?	No
Order reference number	
Title of your thesis/dissertation	SURFACE MODIFICATIONS OF CAPILLARY-CHANNELED POLYMER (C-CP) FIBER STATIONARY PHASES FOR PROTEIN SEPARATIONS
Expected completion date	Aug 2016
Estimated size (number of pages)	275
Elsevier VAT number	GB 494 6272 12
Requestor Location	Liuwei Jiang 102 Biosystem Research Complex 105 Collings Street CLEMSON, SC 29634 United States Attn: Liuwei Jiang

Appendix D

Reuse Permission for Chapter V

SPRINGER LICENSE
TERMS AND CONDITIONS

Jun 14, 2016

This Agreement between Liuwei Jiang ("You") and Springer ("Springer") consists of your license details and the terms and conditions provided by Springer and Copyright Clearance Center.

License Number	3887781018732
License date	Jun 14, 2016
Licensed Content Publisher	Springer
Licensed Content Publication	Analytical and Bioanalytical Chemistry
Licensed Content Title	Comparison of analytical protein separation characteristics for three amine-based capillary-channeled polymer (C-CP) stationary phases
Licensed Content Author	Liuwei Jiang
Licensed Content Date	Jan 1, 2015
Licensed Content Volume Number	408
Licensed Content Issue Number	5
Type of Use	Thesis/Dissertation
Portion	Full text
Number of copies	1
Author of this Springer article	Yes and you are the sole author of the new work
Order reference number	
Title of your thesis / dissertation	SURFACE MODIFICATIONS OF CAPILLARY-CHANNELED POLYMER (C-CP) FIBER STATIONARY PHASES FOR PROTEIN SEPARATIONS
Expected completion date	Aug 2016
Estimated size(pages)	275
Requestor Location	Liuwei Jiang 102 Biosystem Research Complex 105 Collings Street CLEMSON, SC 29634 United States Attn: Liuwei Jiang
Billing Type	Invoice
Billing Address	Liuwei Jiang 102 Biosystem Research Complex 105 Collings Street CLEMSON, SC 29634 United States Attn: Liuwei Jiang
Total	0.00 USD
Terms and Conditions	